

## Dynamic Controls on Sedimentology and Reservoir Architecture in the Alpine Foreland Basin

### *A Field Guide to the Eocene - Oligocene Grès d'Annot Turbidite System of SE France*

Philippe JOSEPH<sup>1</sup>, Yannick CALLEC<sup>2</sup> and Mary FORD<sup>3</sup>

<sup>1</sup> IFP Energies nouvelles, 1-4 avenue de Bois-Préau, 92852 Rueil Malmaison, France,  
email : philippe.joseph@ifpen.fr

<sup>2</sup> BRGM, Service CDG/CG, 3 avenue Claude Guillemin, 45060 Orléans Cedex 2, France

<sup>3</sup> CNRS-ENSG, Rue du Doyen Marcel Roubault, BP40, 54501 Vandoeuvre-lès-Nancy Cedex, France



## Reference

It is recommended that reference to all or part of this field guide should be made in one of the following ways:

JOSEPH P., CALLEC Y. & FORD M. (2012). *Dynamic Controls on Sedimentology and Reservoir Architecture in the Alpine Foreland Basin - A Field Guide to the Eocene - Oligocene Grès d'Annot Turbidite System of SE France*. IFP Energies nouvelles e-books. DOI : 10.2516/ifpen/2012001 <http://books.ifpenergiesnouvelles.fr>.

JOSEPH P., CALLEC Y. & DU FORNEL E. (2012). Saint Antonin. In: JOSEPH P., CALLEC Y. & FORD M. (2012). *Dynamic Controls on Sedimentology and Reservoir Architecture in the Alpine Foreland Basin - A Field Guide to the Eocene - Oligocene Grès d'Annot Turbidite System of SE France*. IFP Energies nouvelles e-books. DOI : 10.2516/ifpen/2012001 <http://books.ifpenergiesnouvelles.fr>.

## Table of contents

<b>Abstract.....</b>	<b>5</b>
<b>Field trip itinerary .....</b>	<b>6</b>
<b>Introduction.....</b>	<b>9</b>
<b>General geological context.....</b>	<b>10</b>
Structural setting.....	10
Geodynamic evolution.....	11
Lithostratigraphy .....	13
Chronostratigraphy .....	14
Structural evolution .....	15
Paleogeographic evolution of the Grès d'Annot sub-basins .....	18
Regional correlations .....	20
Gravity flow facies models.....	22
The turbiditic ramp model .....	24
<b>Saint Antonin.....</b>	<b>27</b>
General geological framework of the Saint Antonin syncline.....	27
Stop n° 1 : Saint Antonin section. Fan delta facies. ....	29
Stop n° 2 : Saint Antonin cemetery. Channelized conglomeratic system. ....	37
<b>Annot.....</b>	<b>39</b>
General geological framework of the Annot syncline.....	40
Stop n° 1 : Panorama from Plateau d'Educh.....	42
Stop n° 2 : Braux road. Confined lobes and interaction of turbiditic flows with topography.....	46
Stop n° 3 : Panorama of the Gastres megaslump.....	56
Stop n° 4 : Annot. Transit channels of Scaffarels - la Chambre du Roi. ....	57
3D reservoir and seismic modelling .....	65
<b>Chalufy.....</b>	<b>69</b>
General geological framework .....	69
Stop n° 1 : Panorama of Peymian. General architecture of the series. ....	69
Stop n° 2 : Panorama of Défens des Barres. Geometry of the onlap.....	74
Stop n° 3 : Detailed organisation of the Upper Sandbody – Interaction of gravity flows with the topography. ....	78
<b>The Barrême Syncline - a Piggy-back Basin .....</b>	<b>81</b>
Geological setting of the Barrême Syncline .....	82
Stop n°1 : The Nummulitic Trilogy of the Sauzeres section.....	87
Stop n°2 : The Grès de Ville Formation .....	90
Stop n°3 : The Clumanc Conglomerates. The Champ-Richard-Tréouiller Section .....	95
Stop n°4 : General view of the Château de Clumanc hill. Geometry of the synsedimentary fold in the Clumanc conglomerates.....	102
Stop n°4 : General view of the Château de Clumanc hill. Geometry of the synsedimentary fold in the Clumanc conglomerates.....	102
Stop n°5 : Saint-Lions Gilbert Delta. Evolution and Geometry of the Conglomérats de St-Lions .....	106
Stop n°6 : General view of the Senez town. The Grès de Senez.....	112
Stop n°7 : General View of the Roche Blanche. The Malvoisin anticline .....	115
Synthesis .....	118
<b>Bibliography .....</b>	<b>121</b>

## List of figures

Figure 1 : Itinerary of the field trip .....	7
Figure 2 : Regional structural map of SE France (modified from Puigdefàbregas <i>et al.</i> 2004). ....	10
Figure 3 : Location of outcrops of the Grès d'Annot and equivalent systems and of the cross section shown in Figure 9. ....	11
Figure 4 : Geodynamic evolution of the north western Mediterranean from the middle Eocene to the early Oligocene (Séranne 1999). ....	12
Figure 5 : Schematic lithostratigraphy of the Grès d'Annot Basin (Tertiary foreland basin) of SE France showing the Nummulitic trilogy (modified from Ravenne <i>et al.</i> 1987). ....	13
Figure 6 : Chronostratigraphic and biostratigraphic scales used in this guide (Joseph and Lomas 2004). ....	14
Figure 7 : Paleogene lithostratigraphy and biostratigraphy of the Alpes Maritimes and Provence (Sztrakos and du Fornel 2003). ....	15
Figure 8 : Schematic model of the principal structural and depositional elements of a wedge-top type foreland basin which represents many of the characteristics of the Grès d'Annot basin of SE France (Mutti <i>et al.</i> 2003). ....	15
Figure 9 : A balanced and sequentially restored NE-SW cross section through the Valensole basin in the west, the Digne fold and thrust belt, the Argentera massif and the Frontal Pennine Fault (Lickorish and Ford 1998). The cross section is located on Figure 2 et la Figure 3. ....	16
Figure 10 : Schematic models for the paleogeographic evolution of the Grès d'Annot basin during the Priabonian (units 1, 2 and A), early Rupelian (units B to G) and mid-Rupelian (Grès de Ville). ....	19
Figure 11 : SW-NE correlation profile across the sub-basins of Sanguinière and Annot-Grand Coyer (modified from du Fornel 2003). ....	21
Figure 12 : NW-SE oriented correlation profile across the southern sub-basins of Saint Antonin – Annot - Grand Coyer – Chalufy - Trois Evêchés (modified from du Fornel 2003). ....	21
Figure 13 : Principal transformation phases of a gravity flow during its displacement (Mutti 1992) and associated facies (with their equivalents in the classification of Lowe 1982: Facies R and S, and Bouma 1962: facies T). ....	22
Figure 14 : Correlation between the facies schemes of Lowe (1982), Bouma (1962) and Stow and Shanmugam (2000) in Shanmugam (2000). ....	23
Figure 15 : Evolution from slope to basin of an idealised turbidity current (Mutti 2003). ....	24
Figure 16 : Model of canyon-fed radial fan (a) and model of delta-fed turbiditic ramp (b) (Reading & Richards 1994). ....	24
Figure 17 : Turbiditic ramp model and associated facies (compiled by F. Gaumet). ....	25
Figure 18 : Schematic reconstruction of the Grès d'Annot depositional system at the beginning of the Oligocene (Joseph & Lomas 2004). ....	25
Figure 19 : Schematic representation of characteristic depositional geometries within the sub-basins of Saint Antonin – Annot - Grand Coyer - Chalufy within early Rupelian deposits (Units C, D and E). ....	26
Figure 20 : (a) Geological map of the Saint Antonin Syncline (Bodelle 1971) ; (b) Geological sections through the Saint Antonin Syncline (Campredon & Giannerini 1982), in du Fornel (2003). ....	28
Figure 21 : Location of the geological section of Saint Antonin on IGN 1/25000 map, with the elevations of the sedimentological section of Figure 22. ....	29
Figure 22 : Schematic sedimentological log of the Saint Antonin section (modified from du Fornel <i>et al.</i> 2004). ....	30
Figure 23 : Detailed sedimentological log of the lower part of the Saint Antonin section (description by E. du Fornel and S. Lesur) : stars indicate particularly interesting observations. ....	31
Figure 24 : Sigmoidal megaripples with shaly layers (Unit B : elevation 283 m). ....	34
Figure 25 : Sandy matrix supported conglomerates (Unit F : elevation 650 m). ....	35
Figure 26 : Clast supported conglomerate eroding a pebbly sandstone with pebbles organized in oblique stratifications (Unit C : elevation 360 m). ....	35
Figure 27 : Geometry and facies of sigmoidal bars generated by floods (Mutti <i>et al.</i> 1996, in du Fornel 2003). ....	36
Figure 28 : Conglomerates filling large erosive structures at Chamengearde. ....	36
Figure 29 : Large-scale clinoforms in Unit G (elevation 760 m) below the Saint Antonin village. ....	37
Figure 30 : Erosive conglomeratic lens in Unit G below the Saint Antonin cemetery. ....	37
Figure 31 : (a) Simplified geological map of the Annot syncline ; (b) Simplified structural section across the Annot syncline (modified from Callec 2004). ....	40
Figure 32 : Composite log of the Grès d'Annot in the Annot syncline (modified from du Fornel <i>et al.</i> 2004). ....	41
Figure 33 : Location of view points (1 : Plateau d'Educh ; 2 : Braux road ; 3 : Les Gastres ; 4 : Les Scaffarels), stops (C : Scaffarels - Chambre du Roi ; B : Route de Braux) and panorama of Annot – Les Scaffarels – La Chambre du Roi outcrops of Figure 51 (A-B-C-D-E-F). ....	42
Figure 34 : Panorama of the Annot Syncline viewed from Plateau d'Educh (view point 1 of Figure 33). ....	43
Figure 35 : Structural section across the Annot Syncline and restoration of the section to the end of Grès d'Annot sedimentation (modified from Ravenne <i>et al.</i> 1987). ....	43
Figure 36 : Geological map of the Annot Syncline (modified from Salles <i>et al.</i> , in revision). ....	44
Figure 37 : Sequential restoration of the AA' cross-section of Figure 36 (modified from Salles <i>et al.</i> , in revision). ....	45
Figure 38 : Panorama of Crête de la Barre (Unit B) along the Braux road (modified from Callec 2004). ....	46
Figure 39 : Evolutionary model of the Braux Paleofault (Tomasso & Sinclair 2004). ....	47



Figure 40 : Sedimentological log of Grès d'Annot at Crête de la Barre along the Braux road (data from IFP Energies nouvelles « Turbidites » consortium).....	49
Figure 41 : Low-density turbidites Tbc along the Braux road (elevation 15.5 m).....	50
Figure 42 : Apparent onlap with pinchout of fine-grained turbidites into Marnes Bleues along the Braux road (elevation 6 m).....	50
Figure 43 : Evolution of the apparent onlap angle $\beta$ (slope base trajectory) as a function of the paleoslope angle $\alpha$ and the respective basin aggradation rate $A_b$ and slope aggradation rate $A_s$ (in Smith & Joseph 2004).....	51
Figure 44 : Lateral evolution of a débrite interstratified in a turbidite along the Braux road, modified from Callec (2001) (M bed : elevation 83 m).....	51
Figure 45 : Megagrooves at the base of sandstone bed O (elevation 80 m).....	52
Figure 46 : Current directions in the upper member of Crête de la Barre (modified from Callec 2004) and evolution scheme of current lines and deposition regime of a turbidite flow approaching a slope (modified from Kneller & McCaffrey 1999).....	53
Figure 47 : Log signature of the section of Crête de la Barre (Braux road).....	55
Figure 48 : Panorama of the Gastres megaslump viewed from the Braux road (modified from Callec 2004).....	56
Figure 49 : Synsedimentary faults sealed by the conglomerate body of the Gastres megaslump.....	57
Figure 50 : Flute casts at the contact between Marnes Bleues and Grès d'Annot (Garambes section).....	57
Figure 51 : General panorama of the Annot – La Chambre du Roi outcrops (Joseph <i>et al.</i> 2000).....	58
Figure 52 : Detailed panorama of Les Scaffarels outcrops from view point 4 of Figure 33 (Joseph <i>et al.</i> 2000).....	60
Figure 53 : General correlation of Annot – La Chambre du Roi outcrops (Joseph <i>et al.</i> 2000).....	60
Figure 54 : 3D reconstruction of the Annot channelized transit system (Joseph <i>et al.</i> 2000).....	61
Figure 55 : Geometry of a channel in unit E (photo from McCaffrey & Kneller 2004 ; drawing from Callec 2001).....	62
Figure 56 : Internal deformation inside the coarse-grained infill of the channels of La Chambre du Roi.....	63
Figure 57 : Heterolithic layers in Les Scaffarels Ouest section (level 2).....	64
Figure 58 : Fence diagram view from the South of the 3D facies geocellular model.....	65
Figure 59 : Seismic modelling of the 3D facies model (512 Hz).....	67
Figure 60 : Seismic modelling of the 3D facies model (125 Hz).....	67
Figure 61 : Itinerary and simplified geological map of the Chalufy outcrops (modified from Joseph <i>et al.</i> 2000).....	70
Figure 62 : General overview of the Chalufy outcrops from Sommet de Peymian (Joseph <i>et al.</i> 2000).....	71
Figure 63 : General correlation of the Chalufy outcrops (Joseph <i>et al.</i> 2000).....	72
Figure 64 : Megachannel below Sommet de Denjuan (unit D).....	72
Figure 65 : Detail of the basal filling of the Chalufy megachannel (debris flow).....	73
Figure 66 : Panorama of Défens des Barres.....	74
Figure 67 : Reconstruction of the Défens des Barres fault, in Puigdefabregas <i>et al.</i> (2004).....	74
Figure 68 : Onlap of the Lower Sandstone body of Chalufy (unit C).....	75
Figure 69 : Detailed correlation of the Lower Sandstone body of Chalufy (unit C).....	75
Figure 70 : Hyperconcentrated deposit with dish structures in the Lower Sandbody of Chalufy (unit C).....	76
Figure 71 : Onlap of the Middle Sandbody of Chalufy (unit C').....	77
Figure 72 : Detail of synsedimentary folds (slump) at the onlap border of the Middle Sandbody (unit C').....	77
Figure 73 : Onlap of the Upper Sandbody of Chalufy (unit D).....	78
Figure 74 : Detailed correlation of the Upper Sandbody of Chalufy (unit D).....	79
Figure 75 : Facies of the Upper Sandbody of Chalufy (unit D).....	79
Figure 76 : Two types of onlap configuration of gravity deposits onto a pre-existing paleoslope.....	80
Figure 77 : Geological map of the Southern Subalpine Domain in SE France superimposed on a DEM image (IGN database). The Barrême syncline is located few kilometres east of the Digne Thrust Front.....	81
Figure 78 : Geological map of the Barrême Syncline. Taken from the French Geological Survey maps at a scale of 1 : 50 000-Digne n°944 and Moustiers-Ste-Marie n° 970 (BRGM Editions).....	83
Figure 79 : Schematic E-W section across Tertiary deposits of Barrême syncline in the northern Clumanc area (Callec, 2001).....	84
Figure 80 : Chronostratigraphic diagram of the whole Tertiary series of the Barrême Syncline.....	86
Figure 81 : General view of the western limb of the Barrême Syncline near les Sauzeres. Outcrop Boundaries for each formation of the Nummulitic Trilogy are distinguish along the hill flank of Buissière d'Entouart.....	87
Figure 82: Sedimentary log of the Sauzeres ravine from the Calcaires à Nummulites to the top of the Clumanc Conglomerates, showing lithostratigraphic divisions, biostratigraphic data and second and third order depositional sequences.....	89
Figure 83 : a – a – Geological map of the northern closure of the Barrême syncline in the Nummulitic Trilogy and the Clumanc Conglomerates.....	91
Figure 84 : Vertical facies evolution of the Grès de Ville on the D219 Sauzeres log.....	92
Figure 85 : The most important facies of the Grès de Ville characterised by wavy and storm influences. Each photograph is located on Figure 84.....	93
Figure 86 : Detail of the Grès de Ville lenticular body near spot height 1013m of the Buissière d'Entouart.....	94
Figure 87 : General view toward the south of the successive cuestas of the Clumanc Conglomerates . E-W cross-section highlighting the asymmetrical geometry of the syncline and the synsedimentary deformation with complex internal unconformities on the eastern limb of the syncline.....	95

Figure 88 : Map of the members of the Conglomérats de Clumanc Formation. Paleoflow rose diagrams for the Grès de Ville and the superposed Clumanc Conglomerate members. 1/ Grès de Ville ; 2/ gravity deposits ; 3/ Champ-Richar Member; 4/ Treouiller Member; 5/ Serre-Genestier and Château de Clumanc Members. ....	97
Figure 89 : Facies model of the alluvial system of the Conglomérats de Clumanc Series. Spatial repartition of the major sedimentary processes. ....	98
Figure 90 : Synthetic log of the Clumanc Conglomerates from Champ-Richard to Serre-Genestier hills. Depositional environments and sequential interpretations are given. Log 1 located in Figure 88. ....	99
Figure 91a et b : Major facies of the Conglomérats de Clumanc. ....	101
Figure 92 : General view toward the south of the Château de Clumanc hill. ....	102
Figure 93a, b : A- Map of the major surfaces in the Conglomérats de Clumanc. ....	104
Figure 94 : Sequential correlation between the eastern and western limbs of the syncline. Relationships with the synsedimentary fold, see Figure 93. ....	105
Figure 95 : Detailed geological map of the Saint-Lions area. ....	106
Figure 96 : North South profile through the St-Lions Tertiary exposures (view to the east) from the Cemetery to the Coulet Rouge. Major paleocurrent orientations shown by open arrows. ....	107
Figure 97 : Synthetic and composite log of the Saint-Lions Conglomerates. ....	108
Figure 98A : clast imbrication developed in foresets of the Saint Lions Gilbert Delta. B- Large conglomeratic foresets and rapid pinch-out to bottomsets. C- Shoreface deposits in the Sables Verts Member and the Conglomerates of Coulet Rouge. D-General view of the Gilbert delta. ....	110
Figure 99 : General view of the Gilbert delta (View to the SE) and geometric diagram of the Gilbert delta of Saint-Lions (Coulet Rouge member) with the overlying Biostrome. ....	111
Figure 100 : (a) General view to the north of the Senez cliffs. (b) Simplified geological map of the Senez area. ....	113
Figure 101 : General view of the left bank of l'Asse de Blieux River near the Senez Bridge. The Grès de Senez programmes to the north and is characterised by large oblique stratifications with a general regressive trend. ...	114
Figure 102 : Synthetic log of the Grès de Senez (Malvoisin section). ....	114
Figure 103 : Panoramic view of the Malvoisin anticline (view to the north). The synsedimentary fold was developed during deposition of the Grès de Senez and seems to die out during deposition of the Molasse Rouge. ....	115
Figure 104 : Progressive evolution of the depositional geometry of Grès de Senez and the Malvoisin Conglomerates in relationship with the genesis of the Malvoisin anticline. ....	116
Figure 105 : Folded slides in the Grès de Senez Formation along the N85 road. ....	117
Figure 106 : Chronology of tectonic events and depositional sequences during the Paleogene history of the Barrême Basin. ....	119
Figure 107 : Tectono-eustatic model for infill of a foreland basin (modified after Posamentier & Allen, 1993). ....	119

## Abstract

The Grès d'Annot system, deposited during the late Eocene and early Oligocene (Priabonian-Rupelian) in the Tertiary foreland basin of SE France, is an important example of a confined sand-rich turbidite system, offering spectacular exposures over an area of over 5000 km<sup>2</sup>.

The establishment of the clastic system is related to the development of the alpine foreland basin that started with a regional flexural basin in the Eocene, followed by the creation of synclinal depocentres due to gentle folding of the underlying Mesozoic succession above various décollement levels. A true piggy back basin developed at Barrême in the early Oligocene, where alluvial sedimentation was established sourced from the internal Alps, necessitating the termination of the Grès d'Annot depositional system and uplift of the internal fold and thrust belt.

During the late Eocene and the early Oligocene active thrusts, folds, oblique strike slip and normal faults as well as gravitational normal faults, generated a complex basin floor topography within the sub-basins of the alpine foredeep such as Peira Cava or Annot. In contrast to the original image of a sandy cone sourcing from a submarine canyon incised into the continental slope, the Grès d'Annot system is now thought of as an ensemble of shallow turbiditic ramps directly connected to fan deltas (Quatre Cantons, Saint Antonin), fed from the south by the massifs of Sardinia-Corsica and Maures-Esterels. On these ramps sediment transit was via a system of ephemeral, shallow channels that fed prograding elongated tongues : their activity was probably linked to the frequency of fluvial flood supply (hyperpycnal flows). Within the basin itself these evolved into non-confined turbidity currents that deposited sandy lobes in tabular beds.

The aim of this excursion is to study the organization of facies and stratigraphic architecture of the different elements of the Grès d'Annot depositional system. We will examine :

- (1) the different phases of infill of the confined Annot sub-basin in the south and their relationship to synsedimentary tectonics (in particular the Saint Benoit-Braux Fault system).
- (2) The dispersion of turbidites in planar sandy lobes to infill a basin floor topography in a more distal part of the basin (Chalufy).
- (3) The final phase of piggy-back basin evolution and the closure of the main turbidite basin corresponding to the arrival of the first erosional products from internal zones.

# **Field trip itinerary**

**(Itinerary in Figure 1)**

## **Day 1 :**

### **Saint Antonin : Fan delta feeder system of the Annot confined basin (Late Priabonian to early Rupelian)**

- Overall introduction to the structural setting, the global basin geometry, the lithostratigraphy and the sequence stratigraphy of the Grès d'Annot turbidite system in the framework of the Alpine Foreland Basin
- Vertical evolution and sequence organization of the 1000m thick series from turbidites to alluvial conglomerates (fan delta)
- Geometry, facies and heterogeneities of the channelized conglomeratic system

## **Day 2 :**

### **Annot : lower part of the Annot sub-basin (confined ponded trough)**

- Saint Benoit panorama : structural scheme and tectonic evolution of the syncline
- Sequence organization of the series and vertical and horizontal evolution of the net-to-gross
- Saint Benoit-Braux paleofault zone : trapping of the turbidite sedimentation
- Confined lobe deposits along the Braux road section (basal part of the system : ponding phase) and interaction of turbidity currents with basin floor topography
- Interpretation of the different facies in terms of depositional processes
- Gastres outcrops : large synsedimentary deformation (pebbly megaslump)

### **Annot : upper part of the Annot sub-basin (transit system)**

- Scaffarels panorama : global organization of the series
- Annot outcrops : depocenter migration of the coarse-grained turbidite channel system (spilling phase)
- Chambre du Roi outcrops : facies and 3D architecture of coarse-grained transit channels during downstream overflow of the system
- Well log and synthetic seismic signature of the reservoir facies and architecture
- Interpretation of these different facies in terms of depositional processes

## **Day 3 :**

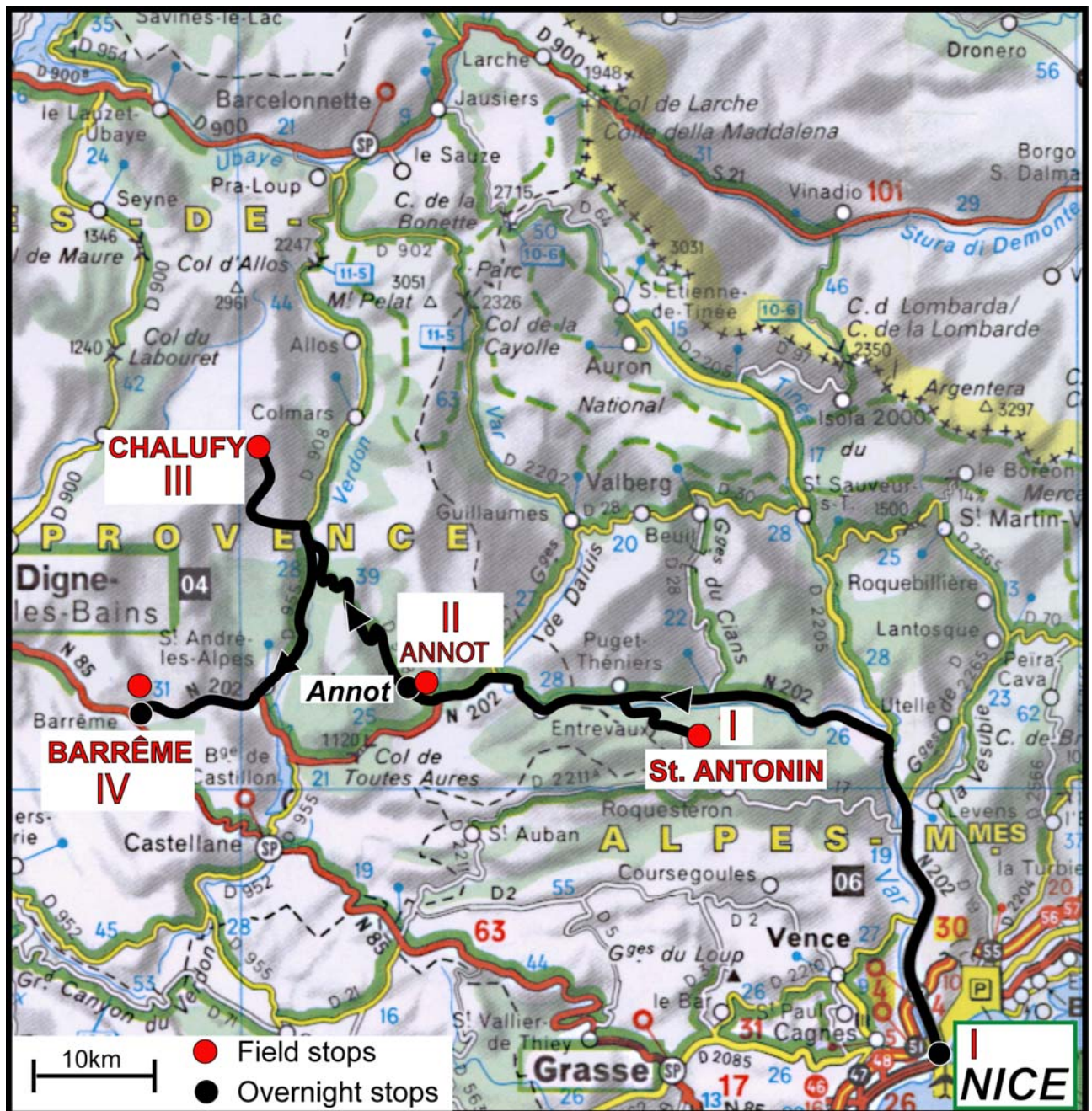
### **Chalufy : distal part of the Annot sub-basin and connection with the Trois Evéchés sub-basin (tabular sheet lobes)**

- Structural scheme and tectonic evolution of the sub-basin
- Chalufy outcrops : different modalities of onlap of the Grès d'Annot on the pre-existing tilted "Marnes Bleues" paleoslope and associated facies
- Facies and syn-sedimentary deformation on and around the paleoslope : interpretation in terms of depositional processes, impact on the heterogeneities and connectivity of the reservoirs
- Denjuan outcrops (if time) : large-scale erosional features due to the retrogressive connection to the Grand Coyer conduit
- Vertical and lateral evolution of the reservoir architecture, connectivity and net-to-gross from the central part to the border of the basin (4 km long transect) : correlation issues

## **Day 4 :**

### **Barrême : westernmost piggy-back sub-basin infilled during the middle Rupelian.**

- Shallow turbidite facies, recording wave influence
- Spatial organization and evolution of the series within the synclinal basin
- Synsedimentary folding - regional and local scales
- Relative roles of eustatic and tectonic controls.







## Introduction

For at least the last 150 years the exceptional exposures of the Grès d'Annot Formation have attracted the attention of both French and international geologists. Initially, interest was principally stratigraphic (time equivalence of continental and marine formations), then structural as significant horizontal displacement of alpine thrust sheets was demonstrated. Then in the 1950's and 60's major advances in understanding deep water sedimentation phenomena were made in the Grès d'Annot with the emergence of the notion of turbidite and its recognition in the field : it was at Peira Cava that Bouma in 1962 defined his famous turbidite sequence and that Lanteaume *et al.* (1967) described sedimentary structures created by turbidity currents. Based on the Annot exposures Stanley proposed the first canyon and submarine fan model in 1961.

In the 1980's research activity was relaunched due to petroleum exploration on continental margins and the emergence of seismic stratigraphy : the large scale internal organization of the Grès d'Annot was studied in order to help with interpretation of seismic profiles (Ravenne *et al.* 1987). In parallel, the influence of tectonic deformation on the evolution of paleotopography was demonstrated (Apps 1985, 1987; Elliott *et al.* 1985) and experimental studies of submarine avalanches allowed a better understanding of gravitational processes (Laval *et al.* 1988).

The discovery of numerous petroleum fields in the deep offshore and their exploitation led to a second renewal of research activity at the end of the 1990's : in the framework of industrial consortia several international teams carried out detailed studies of reservoir architecture in the Grès d'Annot in order to better characterise gravitational deposits, to model them in 3D and thus to provide guidelines for deepwater exploration. Principal results were presented at a research conference in Nice in 2001 and published in the related edited book (Joseph and Lomas 2004).

These recent studies have prompted a general questioning of the depositional model and its relation to tectonics. The Grès d'Annot is now considered as a type example of a sand-rich delta-fed ramp turbidite system (*sensu* Reading and Richards 1994). Its sedimentary architecture is the result of a close interaction between paleotopography created by syn-sedimentary alpine deformation and different types of gravitational flows (from debris flows to low density turbidites). This formation is frequently used as an analogue for deep water hydrocarbon reservoirs, most notably in the North Sea, Gulf of Mexico and offshore Brazil.

The results presented in this excursion are based on work carried out between 1997 and 2010 within the framework of the IFP Energies nouvelles (IFPEN) consortium 'Turbidites' and the theses of Yannick Callec (2001), Olivier Broucke (2003), Elodie du Fornel (2003) and Lise Salles (2010). The three latter theses have benefited from the financial support of Total. We thank all our colleagues at IFP Energies nouvelles, the Ecole de Mines of Paris, Géosciences Rennes, and industrial partners for their help in the lab and in the field.

The aims of this excursion are triple:

- to study the sequential organization at the fine and medium scales of a turbidite system, to discuss the interpretation of recognised genetic sequences in terms of sedimentary processes (hyperpycnal currents versus turbiditic surges), and to study the impact of syn-sedimentary tectonics on the architecture of these sequences,
- to study the distal to proximal evolution of this turbidite ramp system, from the feeder fan deltas to the distal deposits in nappes passing via the intermediate transit channels,
- to relate the sedimentological evolution of the whole system to different phases of deformation of the basin and to discuss the relative roles of eustatic and tectonic controls.

## General geological context

### Structural setting

The Grès d'Annot formation and its associated systems (Grès de Barrême, du Champsaur, du Dévoluy) crop out in south east France in the departments of Alpes Maritimes, Haute Provence and Hautes Alpes. From a structural point of view this area belongs to the Southern Subalpine chains, which are part of the alpine external fold and thrust belt. The principal structural elements are from west to east (and therefore from the most external to the most internal; Figure 2):

- The NE-SW trending fold and thrust belt known as the Digne fold and thrust belt (Digne Nappe) that links southward into the E-W trending Castellane arc ; these structures were employed from the late Eocene to the Pliocene above a décollement in Triassic evaporates (Ford and Lickorish 2004). The Digne nappe overthrusts the Mio-Pliocene infill of the autochthonous Valensole Basin. Estimates of the SW directed shortening from balanced cross sections are very variable from the 21,5 km of Lickorish and Ford (1998), 25 km from Ritz (1991), to the 65 km of Elliott *et al.* (1985).
- The Sub-briançonnais Embrunais-Ubaye nappes, that in the Oligocene transported various units of Cretaceous to Eocene age (Helminthoid Flysch, Black Flysch...), deposited further east, over the Digne fold and thrust belt. Minimum displacement is estimated to have been 50 km (Ford et al. 1999)
- The Briançonnais units of the internal Penninic zone, which overthrust the preceding units along the Frontal Pennine Fault (FPF, Figure 2).

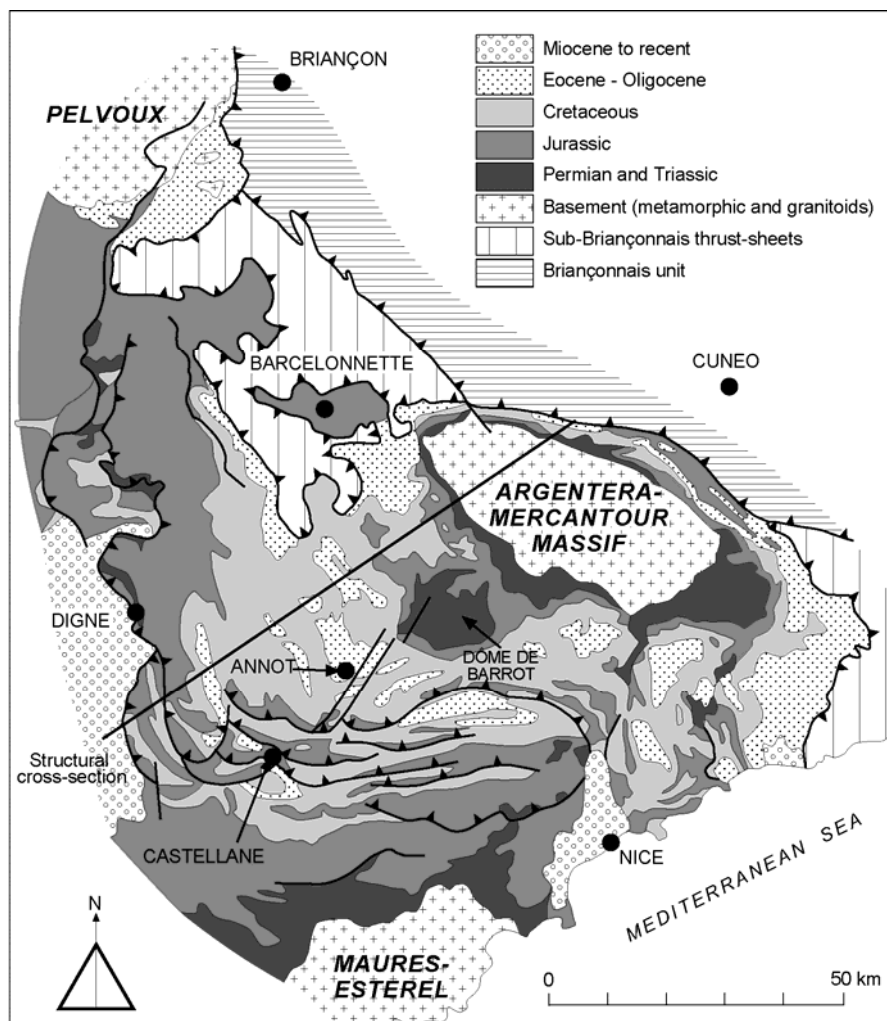


Figure 2 : Regional structural map of SE France (modified from Puigdefàbregas *et al.* 2004).

The Eocene-Oligocene series that will be studied during this excursion belongs to the first external unit, the parautochton or (Digne Nappe). They crop out in a series of isolated synclinal outliers, identified in Figure 3 with the name of their type locality.

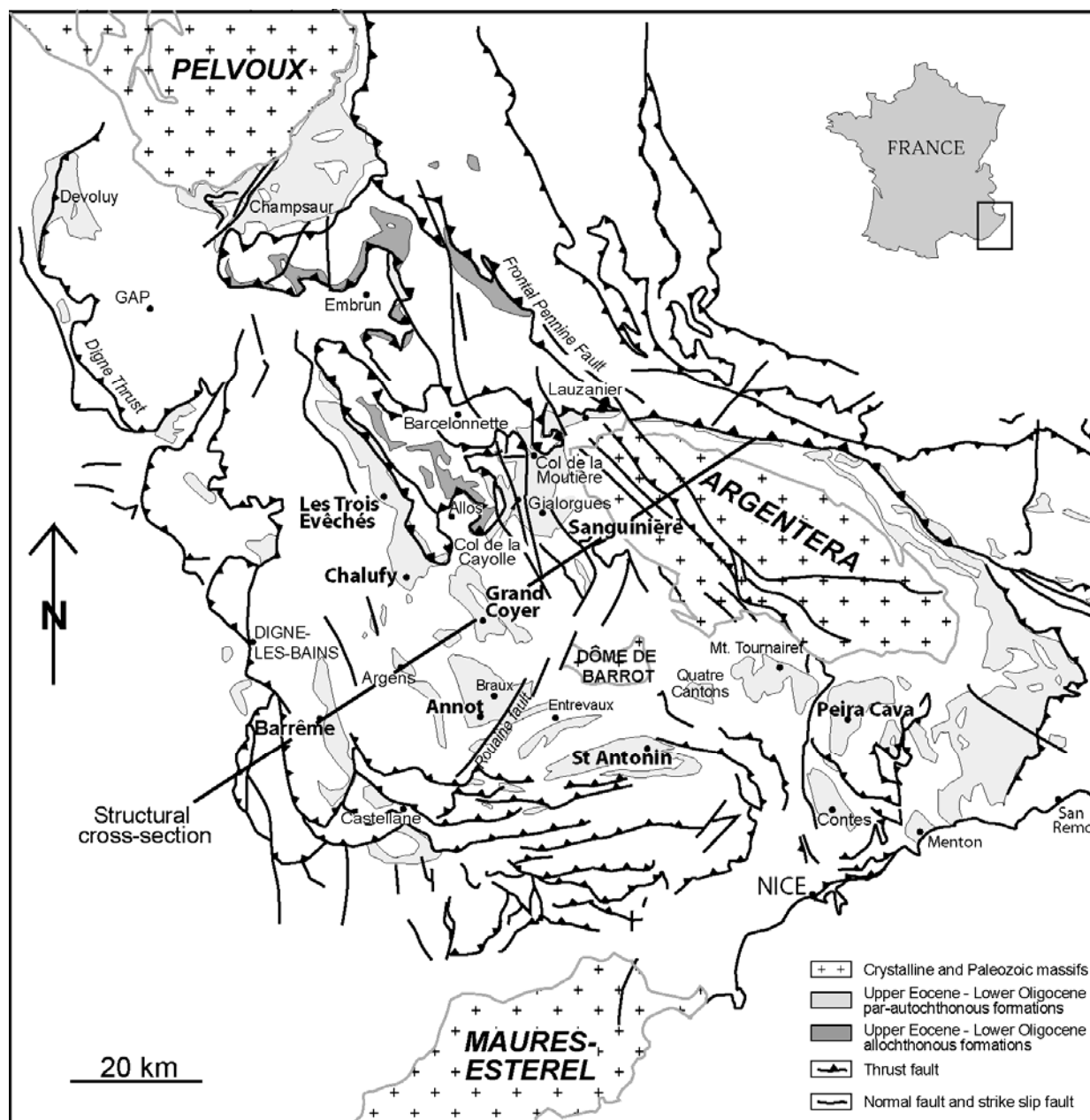


Figure 3 : Location of outcrops of the Grès d'Annot and equivalent systems and of the cross section shown in Figure 9.

### Geodynamic evolution

The Southern Subalpine Chains record a complex history involving the superposition of several orogenic events (Séranne 1999) :

- From end Cretaceous to middle Eocene (around 40 Ma), the northward displacement of the Iberian plate and associated Hercynian blocks (Balearics, Corsica, Sardinia, Calabria and Kabylies) induced collision with the European plate and formation of the Pyrenean orogenic belt (Figure 4a). The Languedoc-Provençal segment of the Pyrenees resulted from the collision of the Corsica-Sardinia block with Provence. Further south Tethyan oceanic crust of the African plate and its satellite Apulia was subducted NW below the Iberian plate along the Tethyan subduction zone. To the east the northward migration of Apulia initiated the Alpine orogen so that the European plate (including SE France) was subjected to regional flexural subsidence (initiation of the foreland basin).
- In late Eocene (Priabonian, 35 Ma, Figure 4b) an increase in NW directed oblique subduction generated an Andean type orogenic belt along the southern margin of the Iberian plate. This orogen,

named the East Iberian orogen by Apps et al. (2004) (to differentiate it from the contemporaneous Alpine orogen), uplifted the Corsica-Sardinia massifs and the reactivated Pyrenean-provençal structures in SE France (Maures Esterels). These uplifted regions became the principal source areas for the Grès d'Annot in the latest Eocene and early Oligocene. To the NE convergence of the Apulian and European plates entered the 'soft' collision phase as the thinned distal European passive margin entered the SE dipping subduction zone. Further north in the European foreland E-W extension generated the West European rift system (Rhine, Rhone, Limagne grabens). In southern France the Languedoc region was subjected to NE-SW sinistral strike-slip deformation.

- In the early Oligocene (Late Rupelian, 30 Ma, Figure 4c) two nearly simultaneous events led to the termination of the Grès d'Annot basin. (a) To the south, the SE-ward migration of the Tethyan subduction zone due to slab rollback generated backarc extension and calc-alkaline volcanism to create the Gulf of Lion. The SE-ward migration of the Corsica-Sardinia blocks cut off these sediment sources to the Grès d'Annot basin. Only the Maures-Esterels massif, which remained on the northern side of the Gulf of Lion, continued to supply sediment northward into the Barrême sub-basin (Grès de Ville). (b) To the east, the alpine collision reached its peak at 30 Ma. In the internal zones the end of rapid exhumation of high pressure and ultra high pressure rocks, the intrusion of granites and the creation of major topography are interpreted as due to slab breakoff (von Blanckenburg & Davies 1995). As convergence continued, the western Alpine arc was accentuated. Major uplift of internal zones caused the emplacement by gravity gliding of the internally derived Embrunais-Ubaye nappes outward across the Alpine foreland.

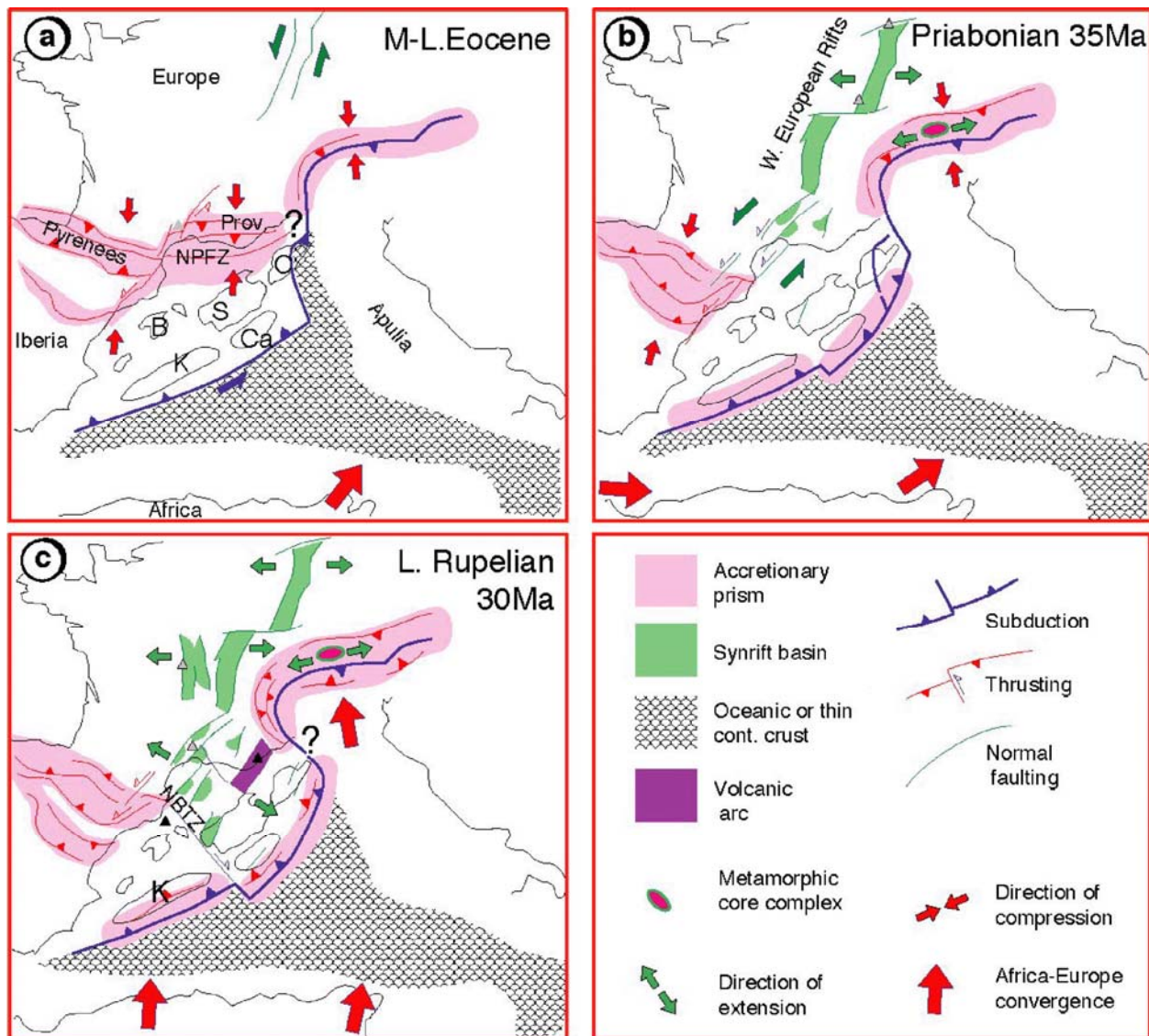


**Figure 4 : Geodynamic evolution of the north western Mediterranean from the middle Eocene to the early Oligocene (Séranne 1999).**

**Abbreviations :** Prov : Provence ; B: Baléares ; S : Sardaigne ; C : Corse ; K : Kabylies ; Ca : Calabre ; NPTZ : North Pyrenean Transform Zone ; NBTZ : North Baléares Transform Zone



## Lithostratigraphy

The Grès d'Annot *sensu lato* is a thick series of gravitational deposits (800m in the Sanguinière sector, 1200m in the Trois Evêchés sector) deposited from the mid Eocene (Bartonian) to the early Oligocene (Rupelian). It forms part of the classic 'Priabonian trilogy' defined in 1912 by Boussac, however it is now more aptly referred to as the 'Nummulitic trilogy' as its age is not confined to the Priabonian. The three constituent lithostratigraphic formations are (Figure 5) :

(1) The **Calcaires Nummulitiques** (Nummulitic Limestones) that unconformably overlie Mesozoic strata significantly deformed by the Pyrenean-Provençal orogen. The unconformity is locally marked by the presence of undated alluvial conglomerates, known as the 'infrannummulitiques' or the Poudingues d'Argens, that are preserved in local depressions bordering paleohighs. The Calcaires Nummulitiques comprise bioclastic limestones and resedimented polygenic breccias, interpreted as shallow marine deposits and slope deposits respectively, which were deposited during a marine transgression (Ravenne *et al.* 1987). The formation's thickness varies from 50 to 200m.

(2) The overlying **Marnes Bleues** (Blue Marls) consist of hemi-pelagic marls deposited in slope and distal ramp environments. The transition with the overlying Grès d'Annot is characterised by an enrichment in fine sandy turbidites known as the Marnes Brunes Inférieures (Lower Brown Marls). The average thickness of the Marnes Bleues is around 200m but with important local variations.

(3) The **Grès d'Annot** formation comprises gravitational deposits (siliciclastic turbidites, debris flows, slumps) which onlap paleoslopes of Marnes Bleues with onlap angles sometimes reaching 20°. Formation thickness is highly variable from some hundreds of metres over structural highs to more than a thousand metres in the centres of sub-basins. Three reference horizons are used to map the formation in the areas of NE Allos and Sanguinière (Jean 1985; Jean *et al.* 1985,1987; Elliott *et al.* 1985; and Figure 5); two mud-rich debris flows containing pebbles and metric to deca-metric blocks of sandstone, mudstone and limestone, and a shale-rich horizon of great lateral extent situated near the top of the formation. The formation again becomes enriched in fine grained turbidites toward its summit (Marnes Brunes Supérieures; Ravenne *et al.* 1987).

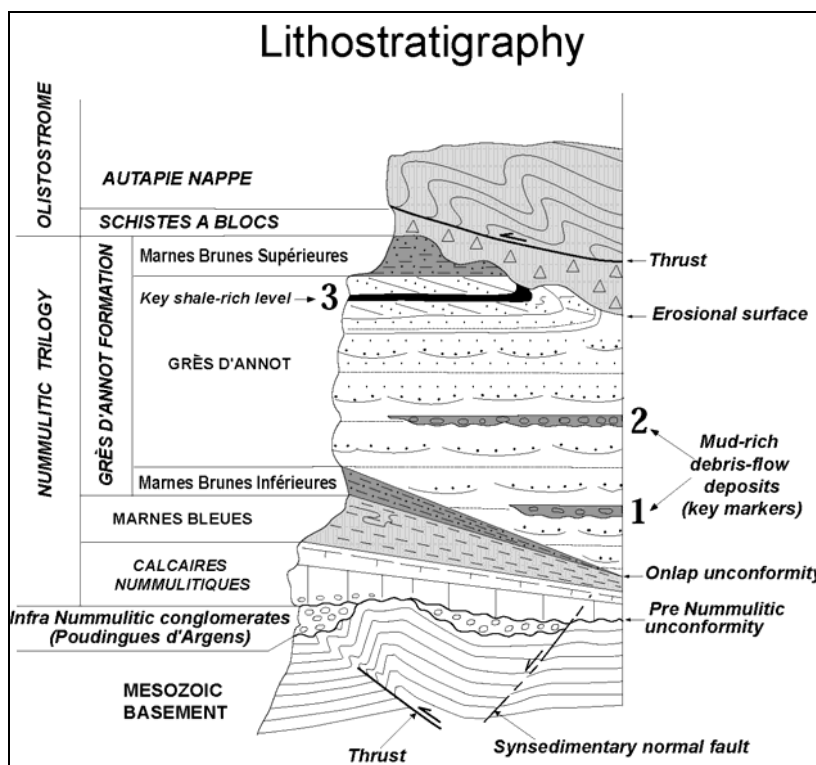


Figure 5 : Schematic lithostratigraphy of the Grès d'Annot Basin (Tertiary foreland basin) of SE France showing the Nummulitic trilogy (modified from Ravenne *et al.* 1987).

In the NE sector of the basin the Nummulitic trilogy is unconformably overlain by the heterogeneous 'Schistes à Blocs' formation, which infilled km-wide canyon-like incisions of depths up to a hundred metres (Ravenne *et al.* 1987). This formation is interpreted as a submarine olistostrome, emplaced on the sea floor ahead of the advancing Autapie Nappe, the lowest unit of the Embrunais-Ubaye nappes (Kerckhove 1969). The Autapie nappe then overthrust its olistostrome and the underlying Tertiary succession.

## Chronostratigraphy

The chronostratigraphic scale used in this guide (Figure 6) is based on the planktonic foraminifera zonation of Berggren *et al.* (1995) and the calcareous nannofossil zonation of Martini (1971). The numerical ages are updated from Hardenbol *et al.* (1998). More detailed information is available from Sztrakos and du Fornel (2003).

Systematic dating of the Marnes Bleues and of argillaceous levels within the Grès d'Annot (du Fornel 2003) has confirmed and more precisely constrained the strong diachronism of the Nummulitic trilogy as its deposition migrated from east to west (Campredon, 1977; Sztrakos and du Fornel, 2003 : Figure 7). In particular the beginning of deposition of the Grès d'Annot is dated as mid-Bartonian (Zone P14) in the Italian sector of Realdo, early Priabonian (Zone P15) in Peira Cava, Late Priabonian (P16) in Annot, mid-Rupelian (P20, Callec 2001) in the Grès de Ville, equivalent to the Grès d'Annot in the Barrême sub-basin. The Schistes à Blocs are not dated but they overlie Grès d'Annot of Priabonian age (NP19) at Peira Cava and of Rupelian age (NP21) in the north of the Sanguinière sector (Sztrakos and du Fornel 2003). Their lateral equivalent at Barrême are the Clumanc Conglomerates, which are dated as Upper Rupelian (P21/NP24, Callec 2001) and contain pebbles derived from internal Alpine units. Younger units in the Barrême sub-basin comprise the continental succession of the Molasses Rouges formation.

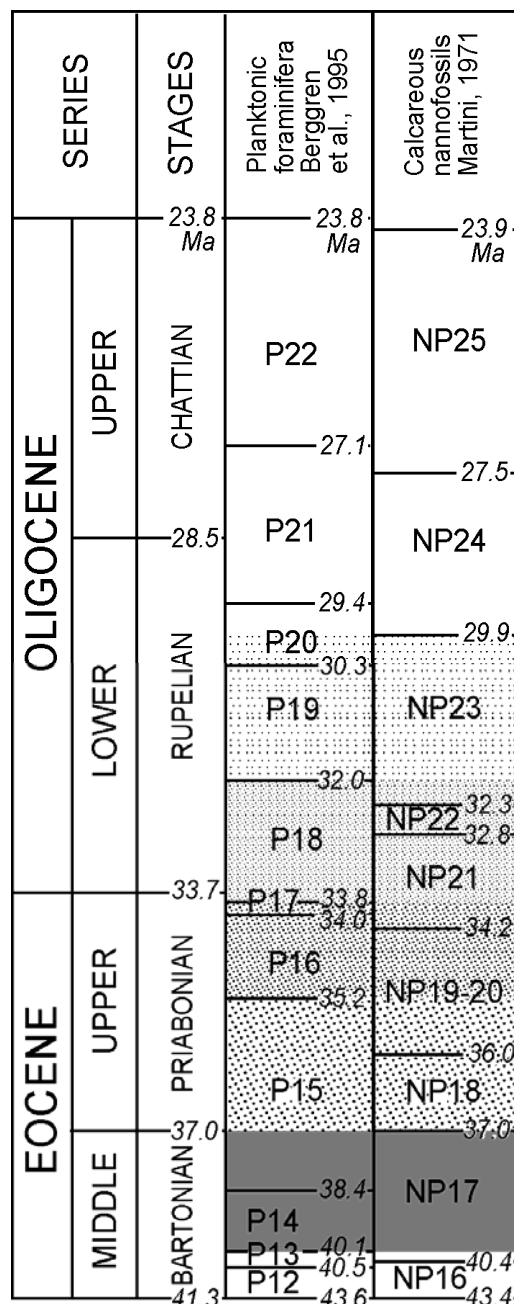


Figure 6 : Chronostratigraphic and biostratigraphic scales used in this guide (Joseph and Lomas 2004).

The stratigraphic units (1, 2, A, B, C, D, E, F et G) that have been correlated in the whole Grès d'Annot system, and which will be referred during this field trip, are indicated on Figure 7. They correspond to 4<sup>th</sup> order depositional sequences *sensu* Mitchum and Van Wagoner (1991) with an approximate duration of 200 – 400 ka.

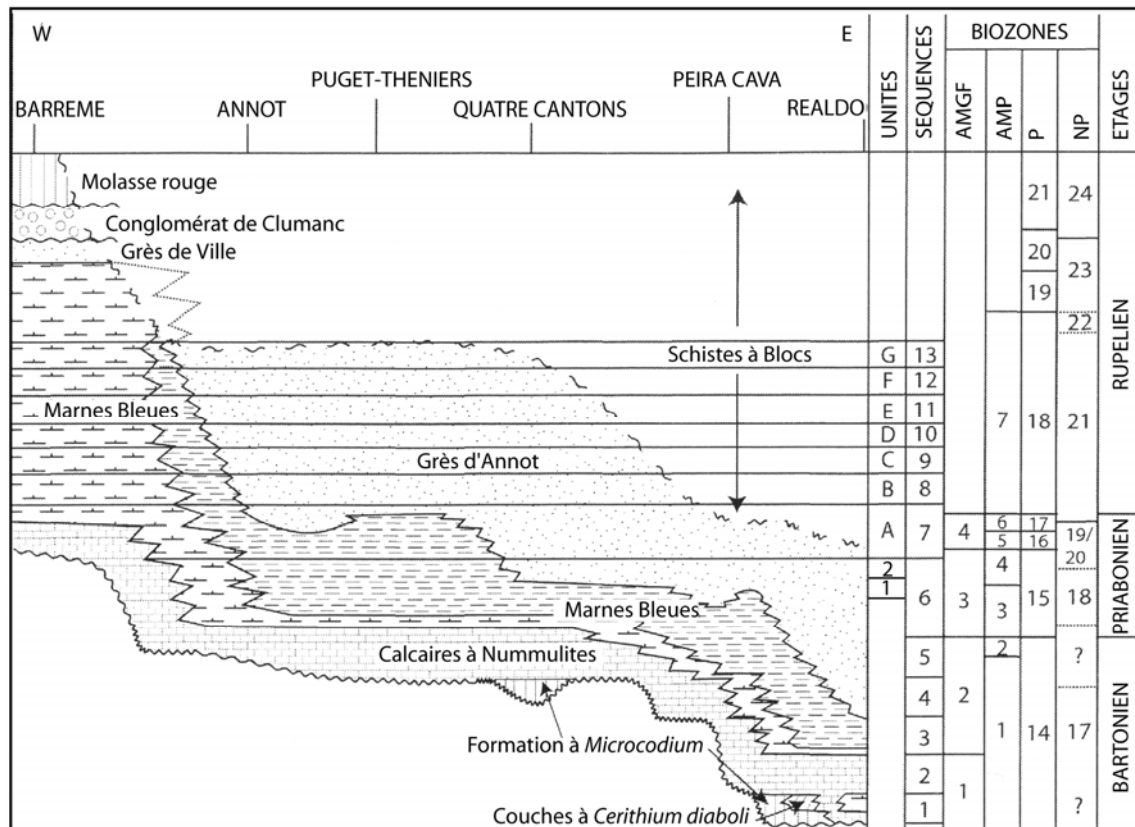


Figure 7 : Paleogene lithostratigraphy and biostratigraphy of the Alpes Maritimes and Provence (Sztrakos and du Fornel 2003).

### Structural evolution

The Grès d'Annot basin shows many of the characteristics of a peripheral foreland basin (Dickenson 1974), created as the European lower plate was flexurally loaded by the over-riding Alpine orogenic wedge. Mutti et al. (2003) present a conceptual model for the organisation of structural and depositional features across such an external orogenic zone where deformation and sedimentation are intricately interrelated (Figure 8) :

- The outer shallow water ramp
- The foredeep basin which is an asymmetrical trough parallel to the deformation front and which can be filled with turbidites. The outer foredeep can be affected by normal faults while piggy-back basins can develop above active thrust sheets in the inner foredeep.
- The external orogenic wedge is the actively shortening and thickening stack of thrust sheets on which piggy back basins (called wedge-top basins in Figure 8) can develop. The top of the wedge may be submarine or emergent. Therefore these basins may be infilled with marine, fluvio-deltaic or mixed facies sediments.

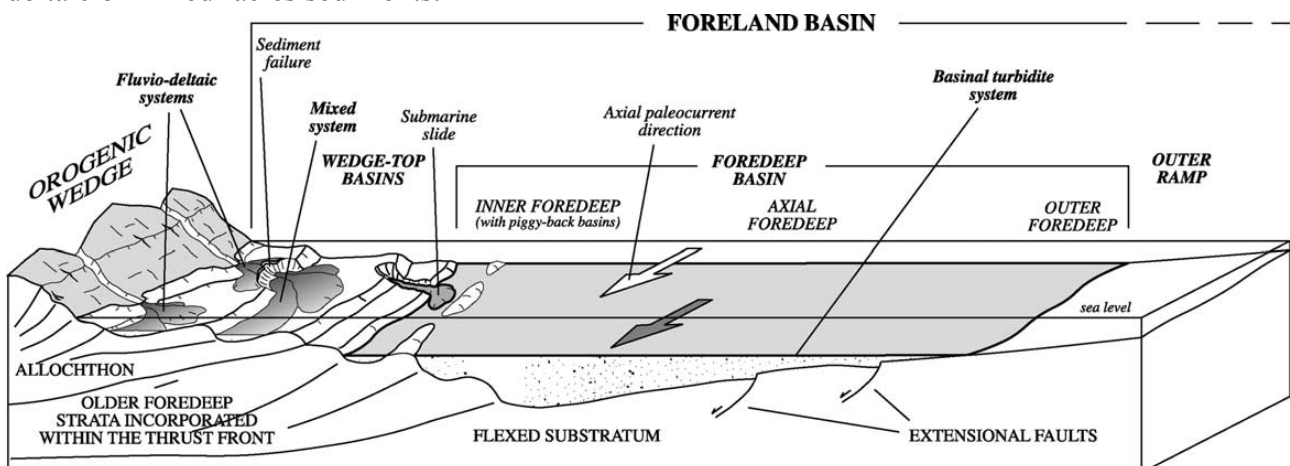


Figure 8 : Schematic model of the principal structural and depositional elements of a wedge-top type foreland basin which represents many of the characteristics of the Grès d'Annot basin of SE France (Mutti et al. 2003).

The three principal depositional zones will migrate outward with time as orogenesis progresses :

The evolution of the alpine basin can be described in three principal phases, which migrated westward with time:

- The first phase involved early flexural subsidence : the foredeep (*sensu* Figure 8) remained under-filled (sediment starved) and deepened toward the orogen. Calcaires Nummulitiques facies were deposited on the outer ramp while the Marnes Bleues facies were deposited in the deeper inner foredeep.
- During the second phase the foredeep basin was filled with siliciclastic turbidites, the Grès d'Annot. Basin infill was diachronous, becoming younger westward, due to migration of the flexural load and the deformation front.
- The last phase corresponds to the end of basin development. In the western-most depocentre of Barrême, sedimentation continued with shallow-water turbidites (Grès de Ville) being replaced by deltaic and alluvial sedimentation (Clumanc Conglomerates and Molasses Rouges units). At the same time more internal parts of the foredeep were overthrust by the Embrunais-Ubaye nappes, preceded by their olistostromic deposits (Schistes à Blocs).

This regional evolution is illustrated by a sequentially balanced cross section oriented approximately perpendicular to the shortening direction and cutting across the most external (westerly) Valensole basin, the Digne thrust sheet northeastward to the Frontal Penninic Fault (Lickorish & Ford, 1998; Figure 9). While some details are still under discussion, there is a broad consensus on the sequence of deformation presented in this model. The most notable uncertainty, due to lack of deep seismic profiles across the region, is the degree of involvement of crystalline basement in alpine shortening (Apps *et al.* 2004; Ford and Lickorish 2004).

From Jurassic to end Cretaceous (Figure 9e) the area subsided as part of the southern margin of the Vocontian Trough, a major fault-controlled basin within the Tethyan passive margin. From west to east there is a rapid increase in thickness from shallow water platform carbonates (Provençal facies) to deeper water marly deposits (Vocontian facies). Two major normal faults that separated the Provençal and Vocontian domains were reactivated as the frontal ramp of the Digne Thrust and as the Barrême thrust that defines the eastern border of the Barrême syncline. The Vocontian Mesozoic sequence reaches a thickness of just over 3 km and then thins gradually eastward onto what is today the Argentera massif.

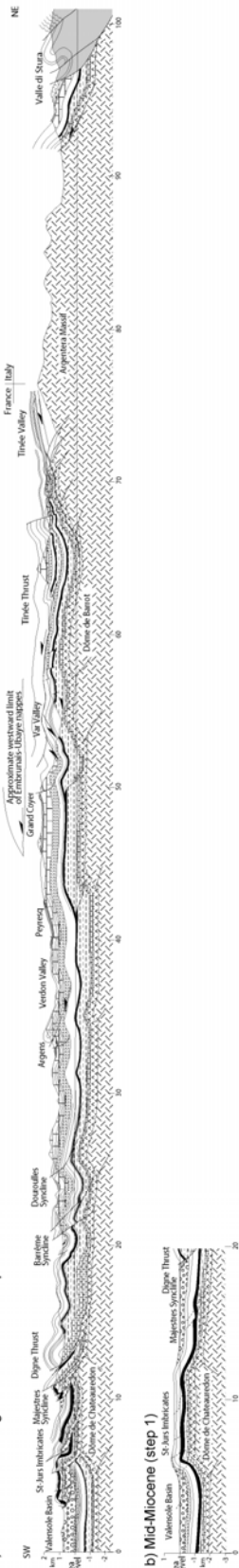
During the late Eocene regional flexure of the European plate created the early alpine foredeep, deepening from west to east and sediment starved. This flexural basin has been modelled using a effective elastic thickness for the European lithosphere of 20km (Ford *et al.* 1999). Gentle SW directed shortening within the Mesozoic succession exploited several décollement horizons : Triassic evaporates (the principal décollement), Middle and Upper Jurassic marls and Middle Cretaceous marls. Folds of relatively short wavelength (5-10km) created synclinal depocentres across the foredeep in which the Grès d'Annot was deposited (Figure 9d) during the latest Eocene and early Oligocene.

In the late Rupelian (Figure 9c) the Embrunais-Ubaye nappes were emplaced over the eastern sector of the basin, terminating the Grès d'Annot basin *sensu stricto*. Further west, activity on the Digne and Barrême thrusts created the Barrême piggy-back basin which records strong syn-sedimentary deformation.

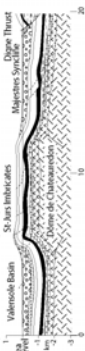
The Miocene and Pliocene saw the final emplacement of the Digne thrust sheet over the eastern margin of the Valensole basin and the uplift of the Argentera massif, the Dome de Barrot and the Dome de Chateaufort (Figure 9a and b).

**Figure 9 : A balanced and sequentially restored NE-SW cross section through the Valensole basin in the west, the Digne fold and thrust belt, the Argentera massif and the Frontal Pennine Fault (Lickorish and Ford 1998). The cross section is located on Figure 2 et la Figure 3.**

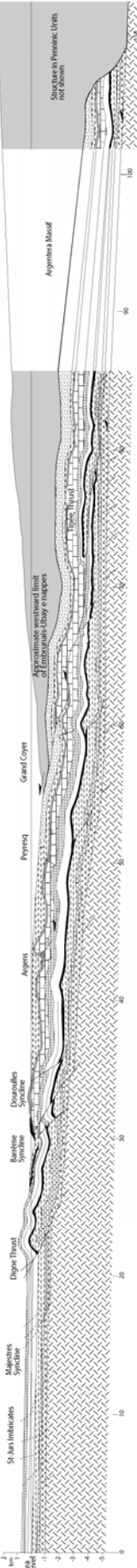
a) Cross Section through the Southern Subalpine Chains



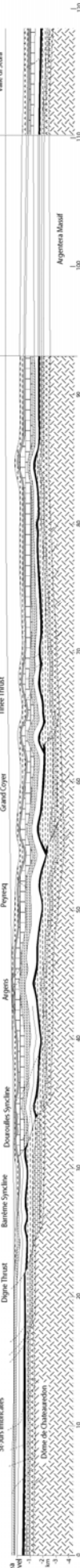
b) Mid-Miocene (step 1)



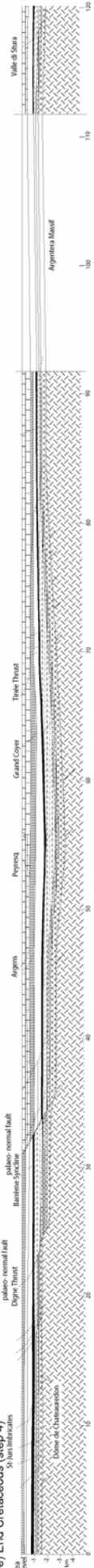
c) Early Oligocene (step 2)



d) Late Eocene (step 3)



e) End Cretaceous (step 4)





### ***Paleogeographic evolution of the Grès d'Annot sub-basins***

During the end Eocene and the early Oligocene the generation of NW-SE oriented folds within a Mesozoic succession already deformed by Pyrenean-Provençal folding (E-W oriented folds), created a complex topography on the floor of the alpine foredeep, in which several sub-basins were defined.

Thanks to a new dating campaign on the lower limit of the sand-dominated succession (i.e. of the Grès d'Annot : du Fornel 2003), the paleogeographic evolution of the foredeep can be more precisely reconstructed (Joseph and Lomas 2004; Figure 10).

(1) In the Priabonian ( Zones P15-P16-P17/NP18-NP19/20; a period of approximately 3 My; Figure 10a) the eastern sub-basin of Contes-Peira Cava was filled with coarse grained turbidites supplied from the Corsica-Sardinia block to the south. According to Amy *et al.* (2004) it corresponded to a closed basin confined to the east, north and west by high zones. Further west the conglomerate fan delta of Quatre Cantons was being deposited during this time and probably supplied sandy sediment to the Sanguinière sub-basin to the north. (However, there is a significant exposure gap between these two sectors and an as yet unidentified source area further east cannot be ruled out). The Sanguinière sub-basin was a narrow depocentre confined between the submarine highs of Argentera and Barrot-Allos as can be demonstrated by the respective onlaps to the east and west. It passed into the more distal sub-basin of Trois Evêchés to the NNW. During this period the Annot sub-basin was completely closed ('ponded basin'), being supplied either by the fan delta of Saint Antonin (First Detrital Formation), or by an unknown source area further south. On laterally equivalent high Marnes Bleues or Marnes Brunes facies were being deposited. In the Barrême sector, which corresponds to the most distal margin of the foredeep, Calcaires Nummulitiques facies were being deposited.

(2) During the early Rupelian (Zones P18/NP21-22, a period of approximately 2 My; Figure 10b) sedimentation rate was reduced in the subbasins of Quatre Cantons-Sanguinière-Trois Evêchés. The Annot sub-basin became completely filled at the very beginning of the Rupelian, overflowing into the Trois Evêchés-Chalufy sub-basins via a narrow channel situated at Grand Coyer. The end of sandy sedimentation is marked by a complete blanketing of the system by sandy deposits. During this period Marnes Bleues facies were being deposited at Barrême due to marine transgression.

(3) In the mid-Rupelian (Zones P19-P20/NP23; Figure 10c) the Schistes à Blocs and the Embrunais-Ubaye nappes were emplaced onto the eastern sector of the foredeep, however their southern and western limits are poorly known. Sedimentation in Saint Antonin continued to be conglomeratic (Second and Third Detrital Formations). At Barrême (Zone P20) shallow water turbidites of the Grès de Ville were deposited under storm influence, along the axis of the basin. An analysis of their heavy mineral populations shows that their source area was the Maures Esterels massif and no longer the Corsica-Sardinia block, which was separated by the Gulf of Lion rifting (Evans *et al.* 2004).

(4) In the late Rupelian (P21/NP24) the Clumanc conglomerates in Barrême were supplied from an eastern source area generated by emplacement of the alpine nappes. Their deposition marks the closure of the basin.

During the whole period, the relationship with the Pelvoux area (Grès du Champsaur) is poorly known because of the lack of precise dating and some problems of structural reconstruction.

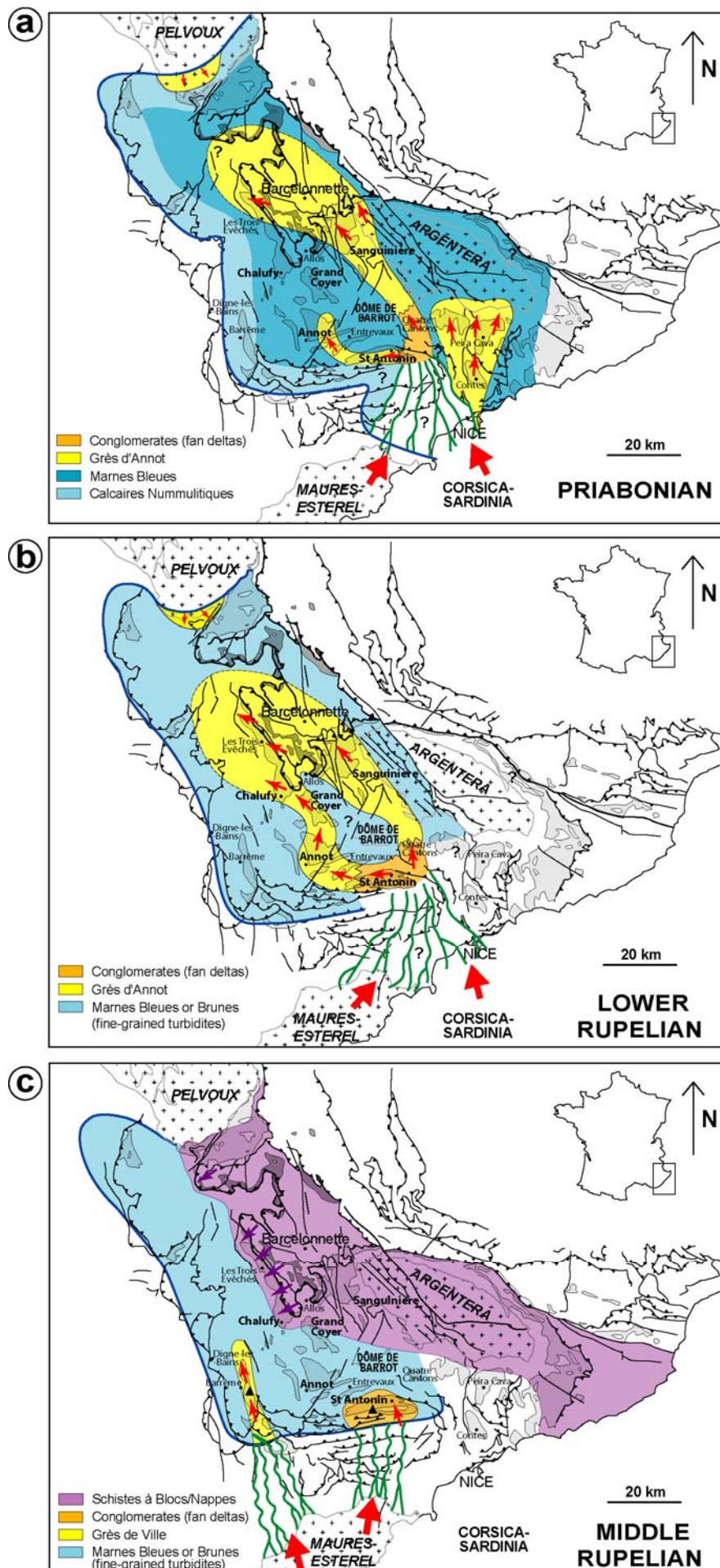


Figure 10 : Schematic models for the paleogeographic evolution of the Grès d'Annot basin during the Priabonian (units 1, 2 and A), early Rupelian (units B to G) and mid-Rupelian (Grès de Ville).

## **Regional correlations**

The functioning of the two principal sub-basins of Sanguinière-Trois Evêchés and Annot-Grand Coyer-Chalufy can be illustrated using two detailed stratigraphic correlation profiles (du Fornel 2003).

The first correlation profile is oriented SW-NE, perpendicular to sub-basin axes (Figure 11). Eight fourth order sequences (numbered 1, 2 then A to F), each representing 200 to 400 thousand years, can be recognised and correlated using reference horizons and key surfaces (du Fornel 2003). This correlation illustrates the principal infilling of the Sanguinière depocentre during the Priabonian (close to 600m for units 1, 2 and A, dated as upper P15-P16/NP19) while there were no sandy deposits of equivalent age in Grand Coyer (as yet inactive). The Sanguinière sub-basin was affected by syn-sedimentary deformation. Dips and thickness changes show that the depocentre was a syncline that was most active during deposition of the Marnes Bleues. On the stratigraphic profile, the NE border of the basin was also influenced by NW-SE to N-S normal faults (Trois Hommes fault zone), which affected the Calcaires Nummulitiques and were responsible for major thickening of the Marnes Bleues from around 50m at Bec de Marseille to the NE to more than 100m below Cime Dieu de Delfy in the Gialorgues Valley, 2 km to the SW (Jean 1985). The Grès d'Annot onlaps the Marnes Bleues paleoslopes on the flanks of the syncline, however, folding activity seems to have continued during deposition of Unit 2 : the thickness of the series between the two key debris flows (DF1 and DF2) doubles from the SE basin border (Cabane de l'Estrop) to the basin centre (Cime Dieu de Delfy).

During the early Rupelian sedimentation began in the Grand Coyer trough (Unit B, dated P18/NP21). An important erosive unconformity characterises the boundary between Unit C and the underlying Unit B that is tilted at Grand Coyer. The two sub basins (Sanguinière-Trois Evêchés and Annot-Grand Coyer-Chalufy) became connected during deposition of Unit D, due to overflow of sandy turbidites over the high zone of Sommet de Noncière northward of Grand Coyer, which is aligned with the Barrot-Allos high (Figure 10b). The depocentre for units E and F migrated toward Grand Coyer, while sedimentation in the Sanguinière sector decreased markedly.

The second correlation profile is oriented NW-SE and illustrates the proximal to distal evolution of the Grès d'Annot system of Saint Antonin – Annot - Grand Coyer – Chalufy - Trois Evêchés (Figure 12). During the Priabonian (Unit A, dated P16) and at the very beginning of the Rupelian (Unit B, dated P18), the Annot depocentre was a confined basin closed to the north by the Grand Coyer high. The Trois Evêchés was therefore supplied by turbidity currents from Sanguinière and low density fine grained turbidites were deposited in the Chalufy sector. It was only at the end of deposition of unit B that that fine grained sediments began to be deposited in the Grand Coyer trough.

Unit C is characterised by the abrupt appearance of pebble conglomerates at Saint Antonin, probably due to increased uplift of the source massifs ; this unit marks a major progradation of the whole system and is correlated with the reworked micro-conglomerate unit of Gastres at Annot and at Grand Coyer, with an erosive conglomerate that infills the base of a 2 km wide trough (du Fornel et al. 2004). A large volume of coarse material passed through the trough to supply the erosive channelised lobes of Chalufy-Trois Evêchés.

The aggradational unit D is also characterised by erosive coarse grained deposits but the two sub-basins appear to be no longer confined, the Grand Coyer trough having been infilled, and turbidite deposits were of wide lateral extent. Units E and F correspond to a reduction of sediment in the Saint Antonin fan delta and in the basin a return to fine grained turbidite deposition and a retrogradation of the whole system.

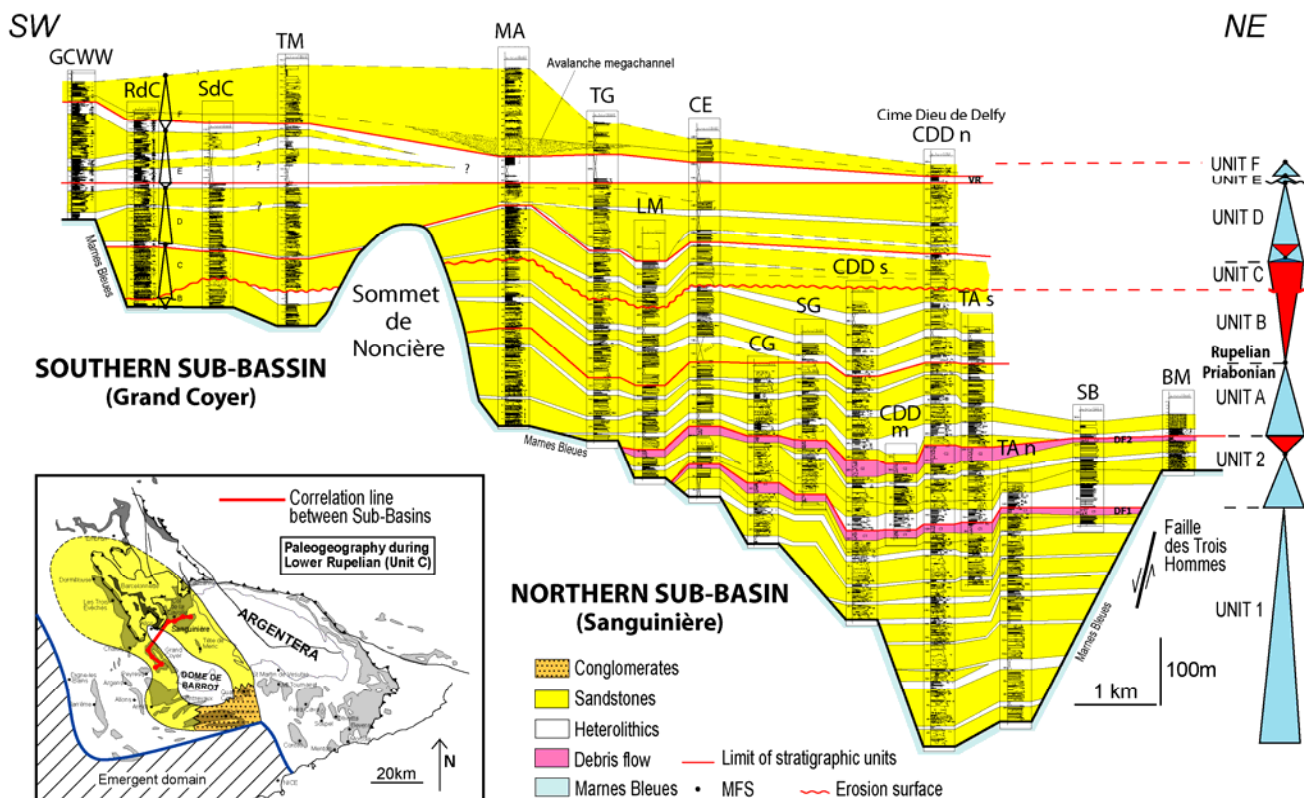


Figure 11 : SW-NE correlation profile across the sub-basins of Sanguinière and Annot-Grand Coyer (modified from du Fornel 2003).

Abbreviations : GCWW : Grand Coyer Ouest ; RdC : Rocher du Carton ; SdC : Sommet du Carton ; TM : Tête de Mouriès ; MA : Montagne de l'Avalanche ; TG : Tête de Gorgias ; LM : Lous Mourres ; CE : Cabane de l'Estrop ; CG : Col de Gialorgues ; SG : Sommet de Gialorgues ; CDD : Cime Dieu de Delfy ; TA : Trou de l'Anc ; SB : Serre de la Braïssa ; BM : Bec de Marseille ; VR : Key shale-rich level of Jean (1985)

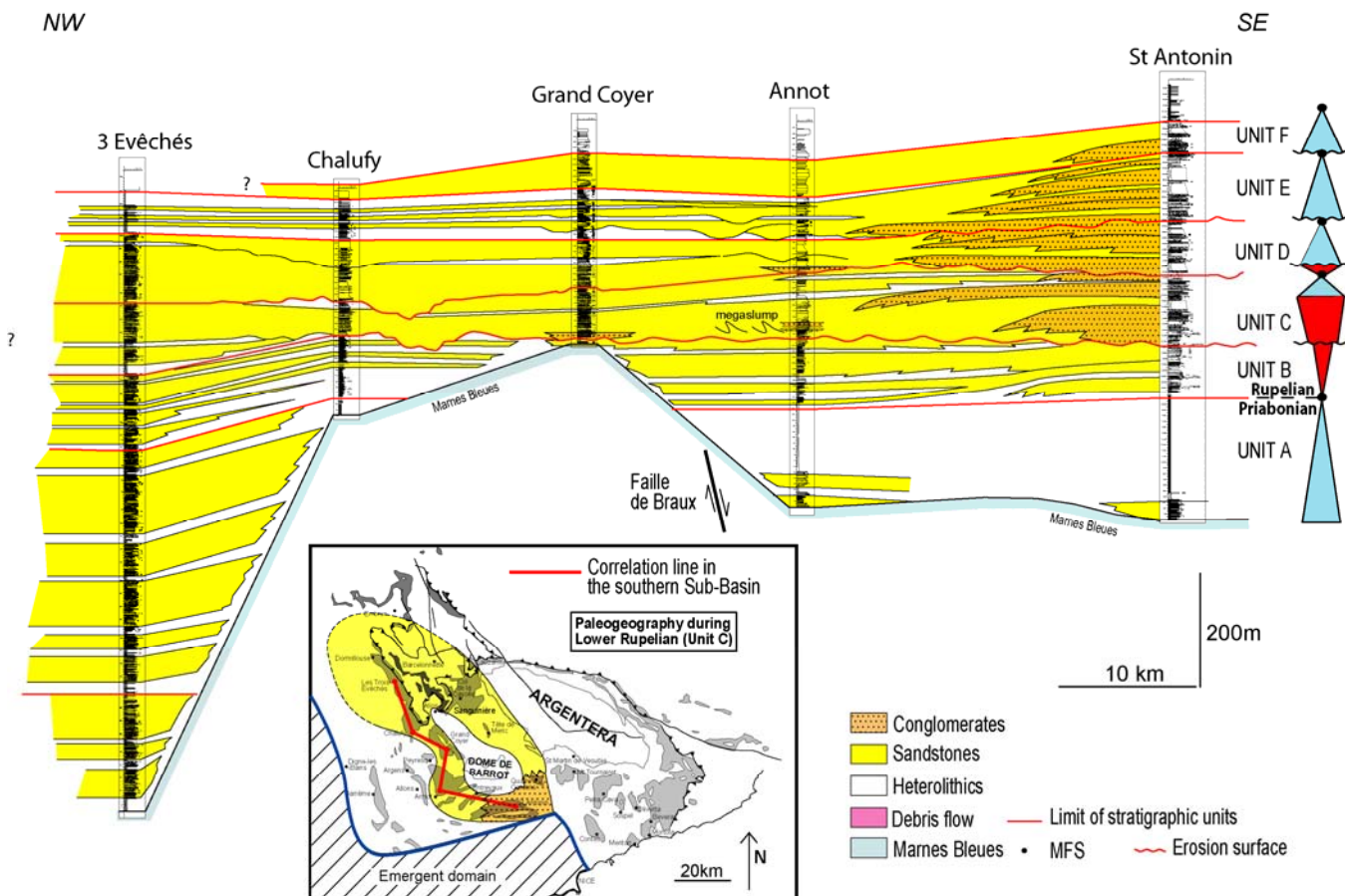


Figure 12 : NW-SE oriented correlation profile across the southern sub-basins of Saint Antonin – Annot - Grand Coyer – Chalufy - Trois Evêchés (modified from du Fornel 2003).



## Gravity flow facies models

Gravity flow deposits are highly variable and numerous facies models have been developed to describe them. Their interpretation in terms of processes is still a subject of considerable debate (cf. Mulder and Alexander 2001).

For practical purposes, we adopt the classification of Mutti (1992) which summarises the principal preceding models and is widely used in both academic and industrial applications.

This classification is based on the concept of the transformation of a gravity flow during its displacement (Mutti 1992; Figure 13).

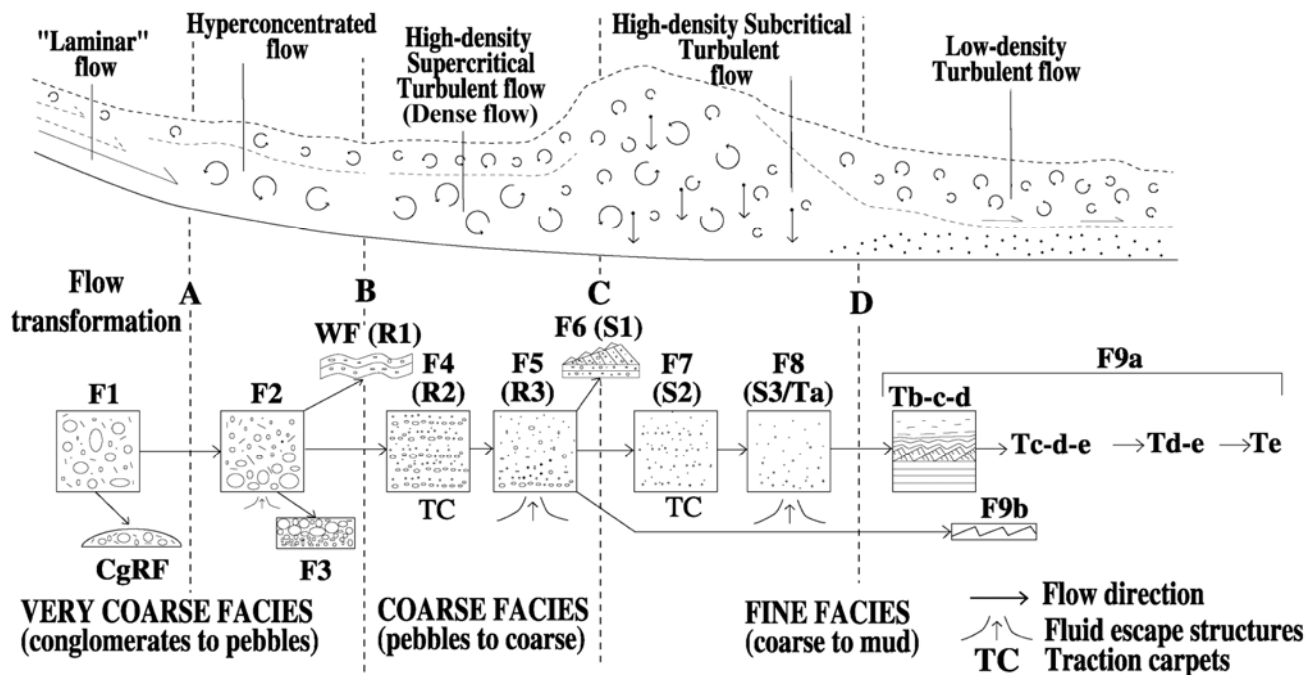


Figure 13 : Principal transformation phases of a gravity flow during its displacement (Mutti 1992) and associated facies (with their equivalents in the classification of Lowe 1982: Facies R and S, and Bouma 1962: facies T).

The initial flow is a cohesive laminar flow of debris flow type, in which the principal support mechanism is the cohesion of the silto-argillaceous matrix (a non-Newtonian flow of Bingham type fluid). The resulting deposit **F1** is a debrite with blocks of centimetre to decametre scale floating in the matrix, which is deposited en masse ('freezing').

Due to a loss of matrix cohesion, this debris flow evolves into a non-cohesive hyperconcentrated flow, which deposits conglomerates with a sandy-argillaceous matrix with floating pebbles (**F2** facies, sometimes graded) or clast-supported (residual facies **F3**). The principal support mechanism is the buoyancy of the dense matrix.

As the coarsest components are deposited the flow transforms itself into a dense sandy flow with gravel and small pebbles. Its upper interface is unstable (supercritical) and progressively becomes turbulent due to the incorporation of ambient water. This type of flow was first called a high density turbidity flow by Lowe (1982) : however, turbulence is not the principal support mechanism. Other mechanisms such as grain interaction (friction or collision) or overpressure of interstitial fluids are instead active, leading to other names being proposed : granular flow (Mutti et al. 1999), hyperconcentrated flow (Mulder and Alexander 2001), dense flow (Mutti et al. 2003). Resulting deposits are organised as follows, megaripples with pebbles at the base of the flow (**WF** facies, equivalent to **R1** facies of Lowe 1982), then a coarse sand facies with rough parallel lamination emphasised by grains (**F4** facies). The interpretation of this facies is highly controversial; the laminations sometimes show reverse grading and are therefore interpreted as due to traction carpets generated by shear of an abrupt deposit (frictional freezing) at the base of a dense



flow (**R2** facies of Lowe 1982). Other authors interpret these as simple laminar tractional deposits at the base of a suspension load (Mutti et al. 2003). The overlying coarse grained **F5** facies (**R3** facies of Lowe 1982) is massive or weakly graded and poorly sorted : it corresponds to a mass deposit from a dense flow and sometimes shows dewatering structures such as dish structures or vertical pipes.

The transformation, due for example to a change in slope, of the unstable supercritical flow to a completely turbulent sub-critical flow (i.e. with a stable upper surface) induces first, deposition of coarse **F6** sands organised in decimetric tractive mega-ripples (**S1** facies of Lowe 1982), then deposition of a sandy facies of medium to fine grain size, facies **F7**, which shows parallel lamination, interpreted as for the coarser grained **F4** facies, either as traction carpets induced by shearing of the overlying turbulent flow (facies **S2** of Lowe 1982), or as tractive laminations on the sea floor. Facies **F8** is graded and results from mass deposition from a turbulent suspension and also shows post depositional dewatering structures: it is equivalent to the **S3** facies of Lowe (1982) and **Ta** of Bouma (1962). It corresponds therefore to a high-density turbidite in the strict sense, that is a deposit deriving from a flow in which the dominant support mechanism is turbulence (Middleton and Hampton 1973).

The continued incorporation of water due to turbulence and the deposition of the coarser fraction leads to further dilution of turbidity flow, which becomes low in density. The classic fine grained facies of the Bouma sequence (low-density turbidite) are deposited by traction-suspension : **Tb**, **Tc**, **Td** and **Te** (facies 9a when the sequence is complete, facies 9b when it is limited to parallel lamination of **Tb** and ripples of **Tc**). Figure 14 illustrates the equivalence of sequences of coarse high density turbidites (Lowe, 1982), medium grained low density turbidites (Bouma 1962) and fine grained low density turbidites (Stow and Shanmugam 1980).

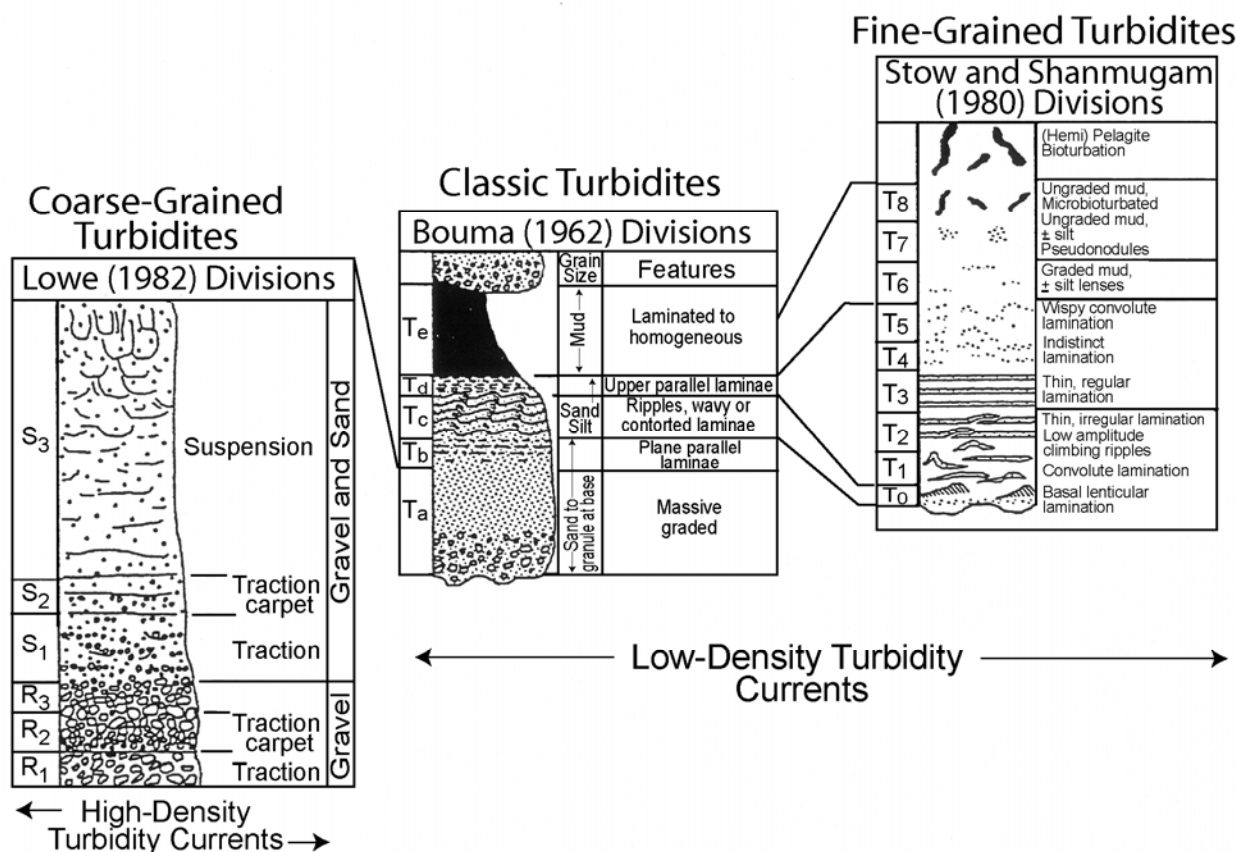


Figure 14 : Correlation between the facies schemes of Lowe (1982), Bouma (1962) and Stow and Shanmugam (2000) in Shanmugam (2000).

The debris flow therefore evolves (Figure 15) initially as a bipartite flow with a dense basal over-pressured layer overlain by a slower turbulent cloud. Then as the turbulent flow develops, it overtakes the dense current and becomes progressively diluted due to the incorporation of water.

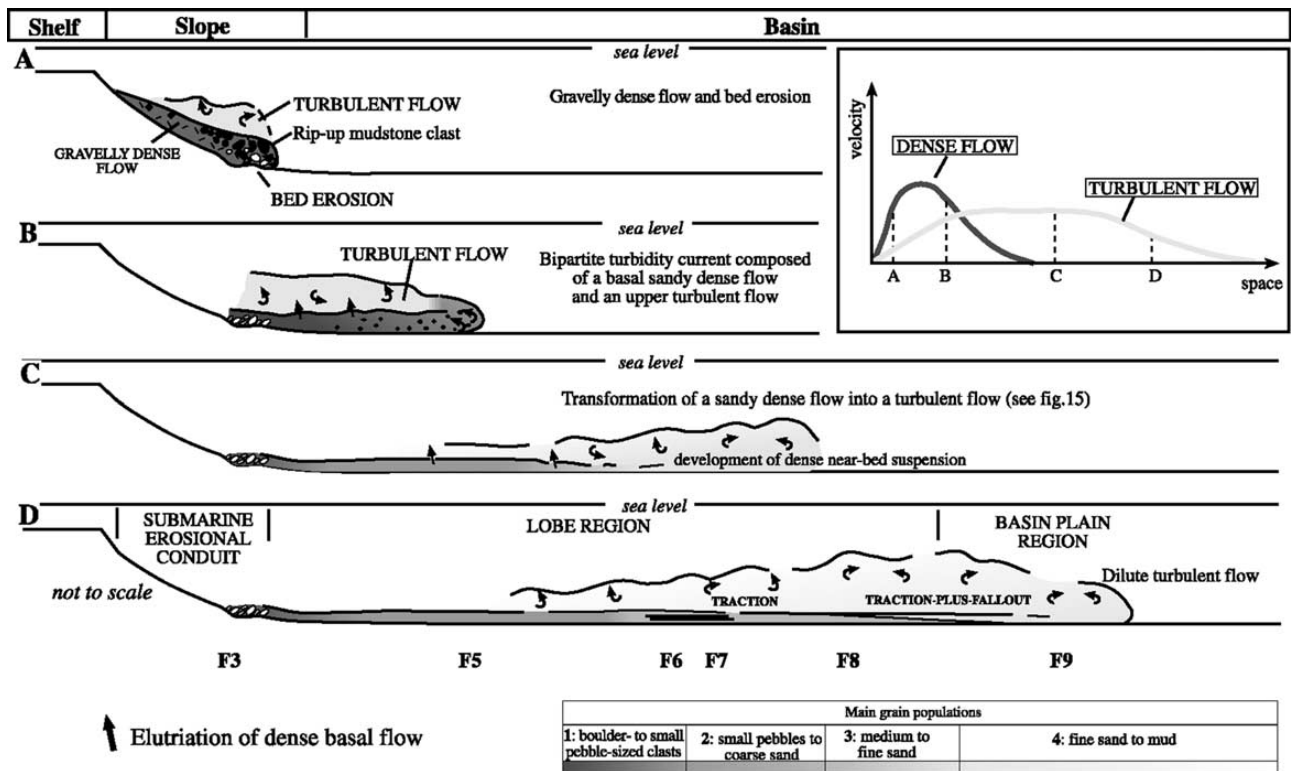


Figure 15 : Evolution from slope to basin of an idealised turbidity current (Mutti 2003).

### The turbiditic ramp model

The best-known model for deep-water turbidite systems is the classic model of the radial fan, fed by a canyon incised into the platform and continental slope (Reading & Richard 1994, Figure 16a). A less well known model, due perhaps to its more subtle morphology, is that of the turbiditic ramp, fed by multiple sources (Figure 16b).

This second model presents a characteristic organisation ((Figure 17) : during fluvial floods the mouths of braided deltas or fan deltas supply the slope with dense hyperpycnal flows (that is of a density higher than the ambient sea water due to its sediment load). These currents discharge along multiple ephemeral channels that can overflow but that do not construct stable levees. The infill of these channels is characterised by deposits of variable grain size from dense flows (F3-F5-F8 facies). Debris flows can be triggered on the slope (F1-F2-F3 facies). Hyperpycnal currents can supply elongated prograding lobes on the slope (sand tongues), but can also become turbulent flows by incorporation of water, which will construct lobes at the base of slope. These facies are therefore characteristic of turbidity flows (Facies F8-F9).

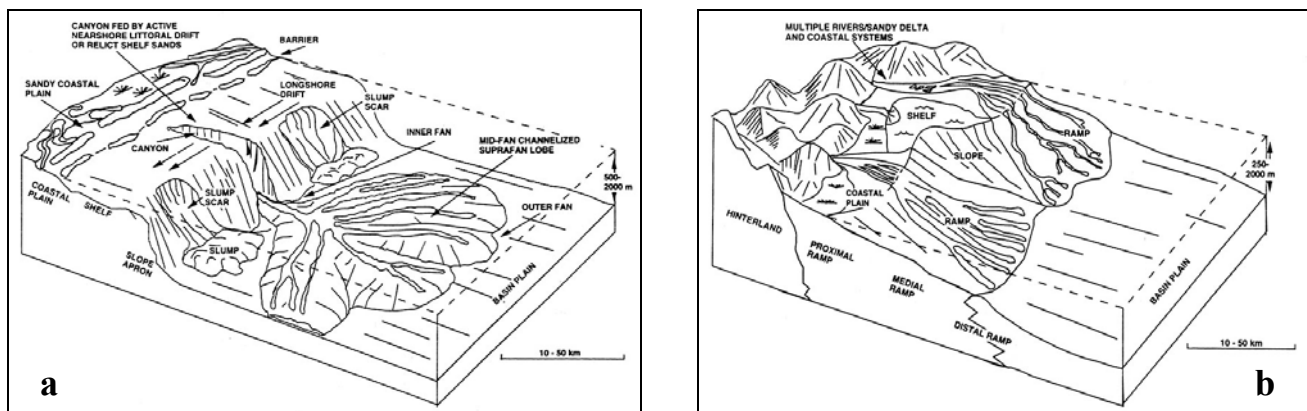
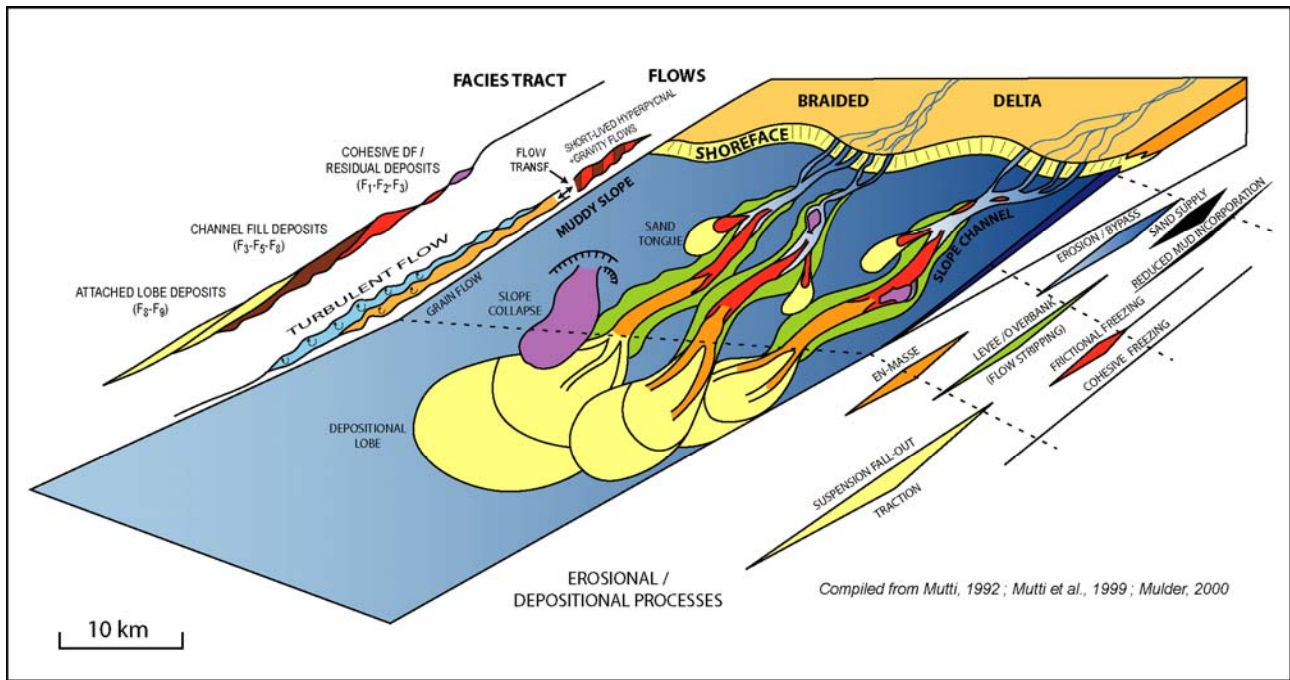
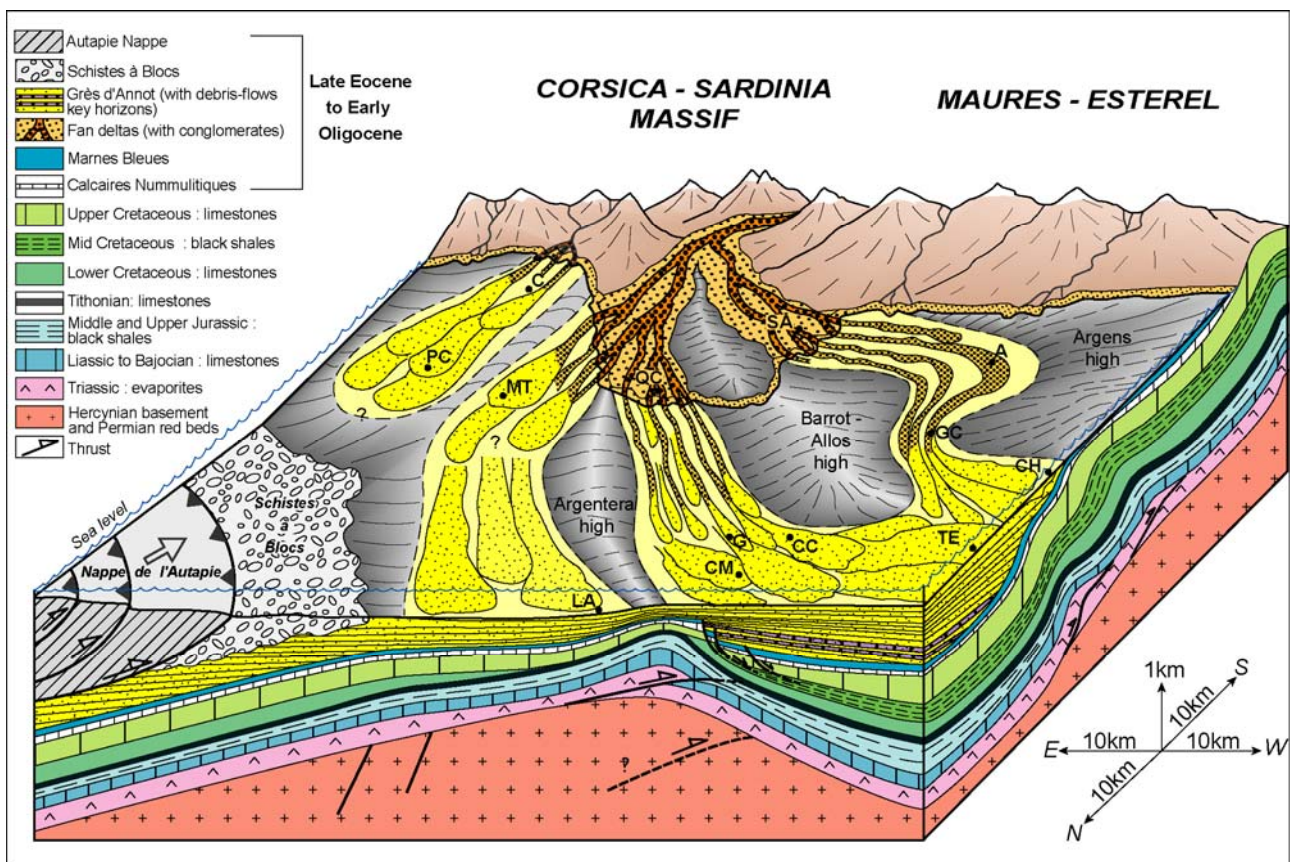


Figure 16 : Model of canyon-fed radial fan (a) and model of delta-fed turbiditic ramp (b) (Reading & Richards 1994).



**Figure 17 : Turbiditic ramp model and associated facies (compiled by F. Gaumet).**

In terms of facies and architectural elements the Grès d'Annot system represents a close analogue of the turbiditic ramp model (Figure 18) with the source fan deltas of Quatre Cantons and Saint Antonin, the channel systems feeding elongated lobes on the middle slope of Sanguinière, and the spreading out of turbiditic sands in the distal basin of Trois Evêchés. Its particular characteristic is the confinement of the system within several synclinal sub-basins, created by syn-sedimentary alpine compressional tectonics.



**Figure 18 : Schematic reconstruction of the Grès d'Annot depositional system at the beginning of the Oligocene (Joseph & Lomas 2004).**

**Abbreviations :** A: Annot; C: Contes; CC: Col de la Cayolle; CH: Chalufy; CM: Col de la Moutière; G: Gialorgues (Sanguinière); GC: Grand Coyer; LA: Lauzanier; MT: Mont Tournairêt; PC: Peira Cava; QC: Quatre Cantons; SA: Saint Antonin; TE: Trois Evêchés



This confinement generates specific depositional geometries, which vary in character from proximal to distal depocentres. Figure 19 illustrates these characteristic geometries for the early Oligocene sub-basins of Saint Antonin – Annot - Grand Coyer – Chalufy - Trois Evêchés.

- The fan delta of Saint Antonin (section 1) is characterised by plurimetric prograding conglomeratic bars that pass laterally and distally within several kilometres into deposits of hyperconcentrated sandy flows ;
- After the ponded basin was infilled in the Priabonian, the Annot sector (section 2) functioned as a transit zone, with the progressive migration from east to west of channels due to syn-sedimentary deformation (folding), recorded in particular by the Gastres megaslump (microconglomeratic Unit C). In units D and E kilometric scale channels strongly eroded tabular bedded deposits of sandy high density turbidites. These channels are infilled by coarse grained hyperconcentrated flows. The overall sand:mud ratio is 80%.
- The Grand Coyer trough (section 3) initially functioned as a by-pass zone, and then it became infilled with hyperconcentrated conglomerate facies (Unit C) and coarse grained channelised sandy facies from high-density turbidite currents (Unit D). The top most unit E is non-confined and is characterised by an organisation of interfingering sandy bodies with lateral compensation effects. It is interpreted as the transition between channels and turbidite lobes. The overall sand:mud ratio is 90%.
- The Chalufy sector (section 4) is characterised by an alternation of decametre scale sandy bars and heterolithic argillaceous horizons (sand/mud ratio around 55%). The sandy bars correspond to tabular lobes, sometimes strongly erosive at the base, which onlap a lateral paleoslope in the Marnes Bleues ; they comprise deposits from hyperconcentrated flows, slumps and high-density turbidity currents. Heterolithic levels comprise an alternation of fine low-density turbidites and marls that can drape the paleoslope.

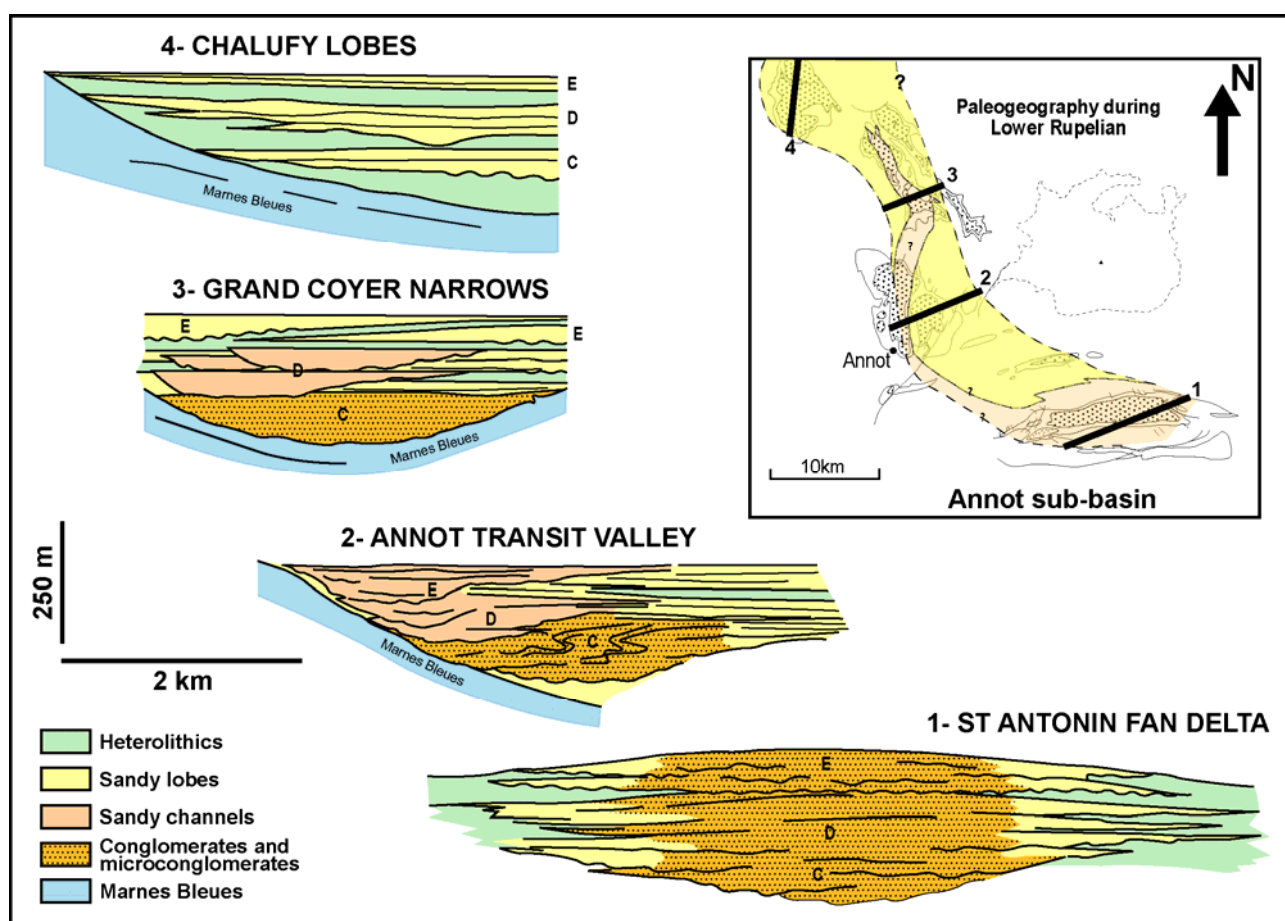


Figure 19 : Schematic representation of characteristic depositional geometries within the sub-basins of Saint Antonin – Annot - Grand Coyer - Chalufy within early Rupelian deposits (Units C, D and E).  
Vertical exaggeration of 4.

## **Saint Antonin**

**Philippe JOSEPH, Yannick CALLEC and Elodie du FORNEL**

*The first day of this field trip is devoted to the study of the infill of the Saint Antonin basin during Late Priabonian and Early Rupelian.*

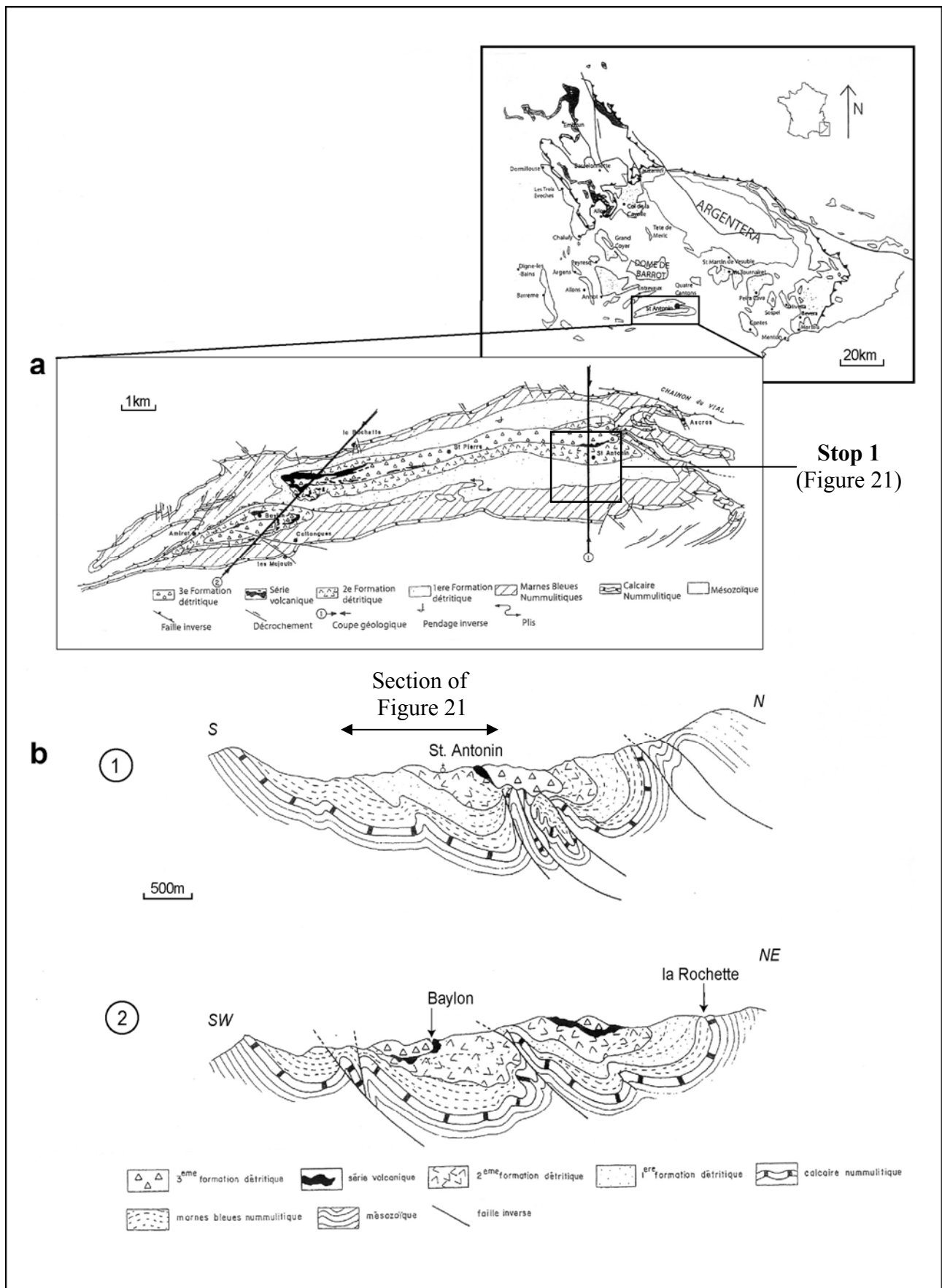
*During this day, we will examine the conglomerate facies of the Saint Antonin fan delta, which was the feeder system of the Annot sub-basin. The two synclines of Annot and Saint Antonin are located in the southern part of the Nummulitic Basin, between the dôme de Barrot and the Castellane arc (cf. location in Figure 3 p. 11).*

### **General geological framework of the Saint Antonin syncline**

The Saint Antonin syncline is oriented ENE – WSW and is about 20 km long and 4 km wide. Its hinge zone comprises two synforms separated by a faulted anticline (Figure 20a). Its northern flank is nearly vertical and overthrust at northeast corner. According to Campredon & Giannerini (1982), during Upper Eocene the basin underwent a synsedimentary compressive deformation that induced N140 oriented folds : the Oligocene detrital formations display important thickness variations and internal unconformities (Figure 20b). During the Miocene, alpine deformation reoriented the folds with an E-W axis and created southward verging thrusts.

The Nummulitic Series includes the classic units of Calcaires Nummulitiques and Marnes Bleues, topped by a coarse-grained detrital series equivalent to the Grès d'Annot. Bodelle (1971) has distinguished and mapped three detrital formations (Figure 20a) : the first one is made of sandstone beds and conglomerates including pebbles of sedimentary and metamorphic rocks, this formation locally erodes the Marnes Bleues or passes transitionally into them through an alternance with fine-grained turbidites. The second detrital formation is characterised by the arrival of andesitic pebbles in the conglomerates and the deposition of several volcanic breccias toward the top. The third formation rests unconformably on the two first: it is made of sandstones and andesite conglomerates interstratified with shaly levels.

Petrographic studies show that the sediment source was located to the south, with a direct supply from the Maures – Esterel and Corsica – Sardinia massifs and that andesitic volcanism could be local (cf. Callec 2001 and du Fornel 2003 for more details).





### Stop n° 1 : Saint Antonin section. Fan delta facies.

The most continuous sedimentological section outcrops close to the Saint Antonin village, along the D 427 road that goes to Pont des Miolans (Figure 21). The First Detrital Formation may be observed in the bottom part of the road at Bau de l'Ours, the second one below the Saint Antonin village and at the cemetery, and the third one near Pra Roustand.

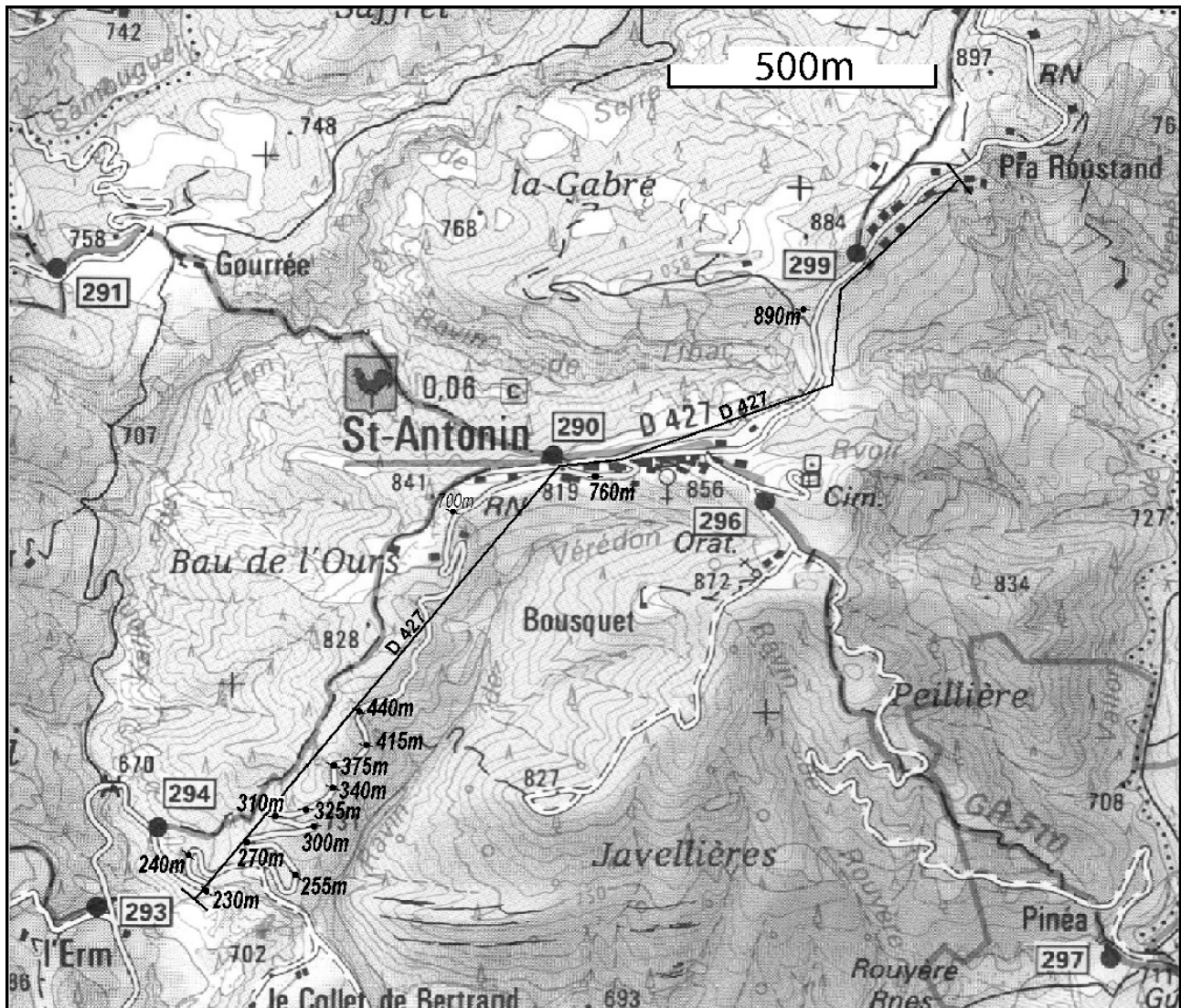


Figure 21 : Location of the geological section of Saint Antonin on IGN 1/25000 map, with the elevations of the sedimentological section of Figure 22.

The thickness of the whole series is around 1000 m : its schematic log is provided on Figure 22 (du Fornel *et al.* 2004), with the identification of the three detrital formations of Bodelle (1971).

Stanley (1980) has interpreted these three formations as three coarsening-upward megasequences (A, B et C), separated by shaly levels with fine-grained turbidites : he related each sequence to a progradation phase of the fan delta system, on the northern border of a massif submitted to active uplift.

During this field trip, we will look in detail at the A and B megasequences *sensu* Stanley (1980), which correspond to 3<sup>rd</sup> order depositional sequences. The facies analysis allows us to subdivide them into smaller scale units (**units A to G**) that are interpreted as 4<sup>th</sup> order depositional sequences (du Fornel 2003 : Figure 22 and detailed log in Figure 23 of **units B and C**). Each of these prograding –retrograding units is limited by deeper facies (fine-grained turbidites) or lower energy deposits.

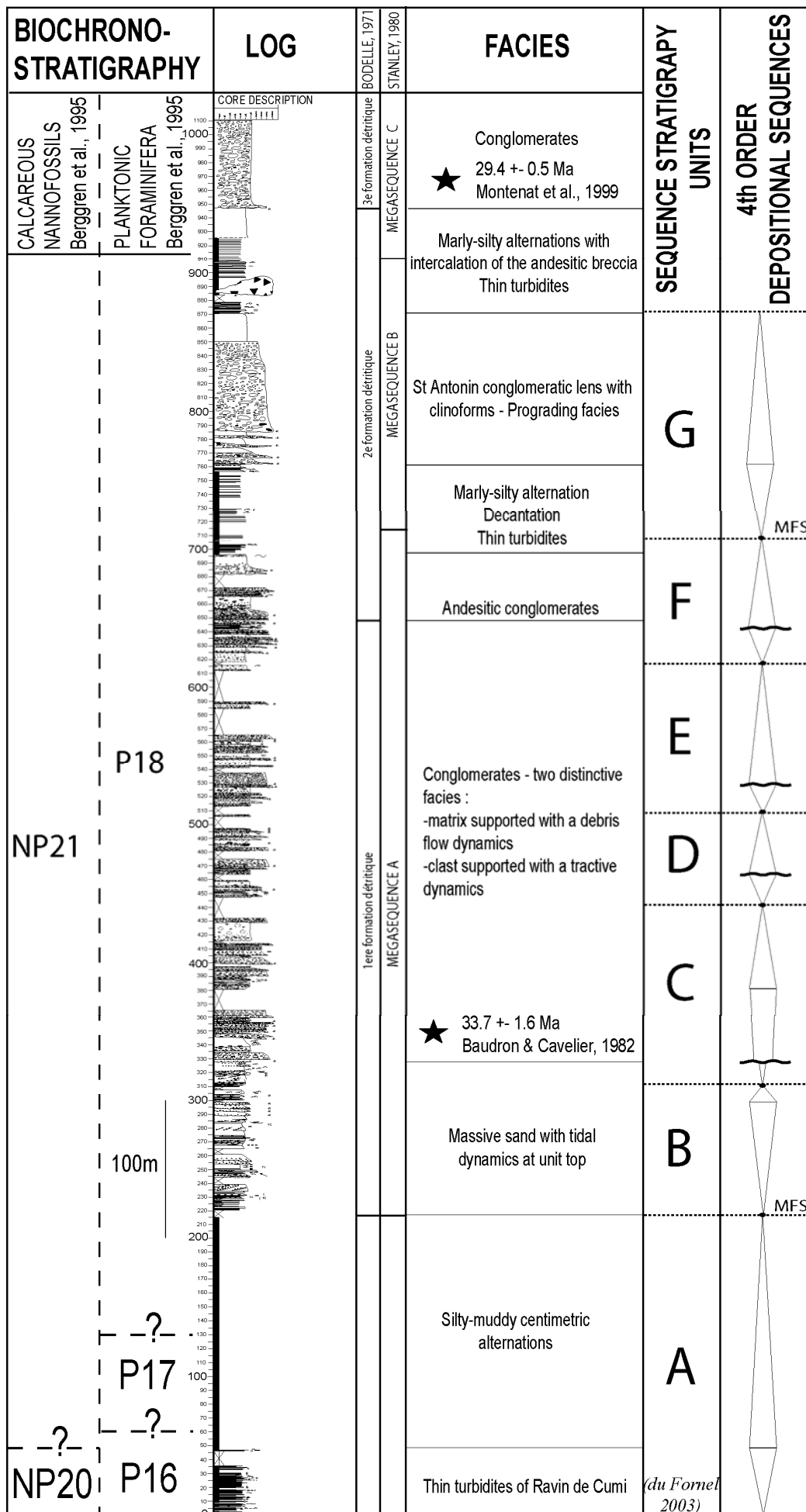


Figure 22 : Schematic sedimentological log of the Saint Antonin section (modified from du Fornel *et al.* 2004).

Saint Antonin (1) 1/500e

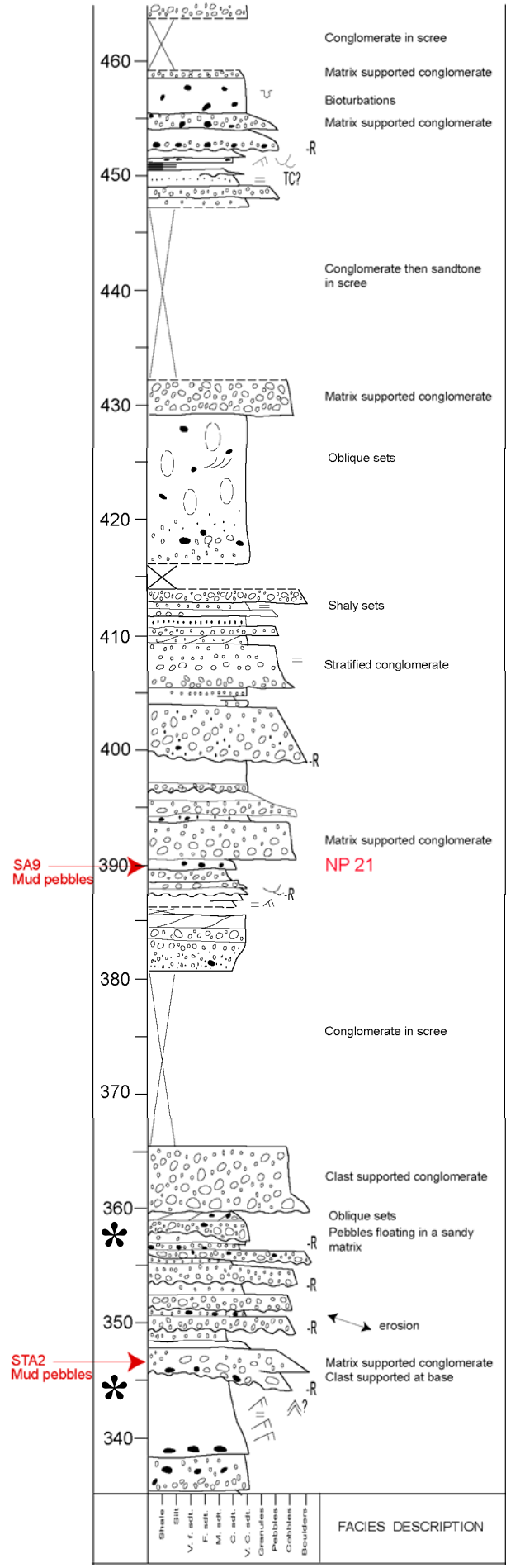
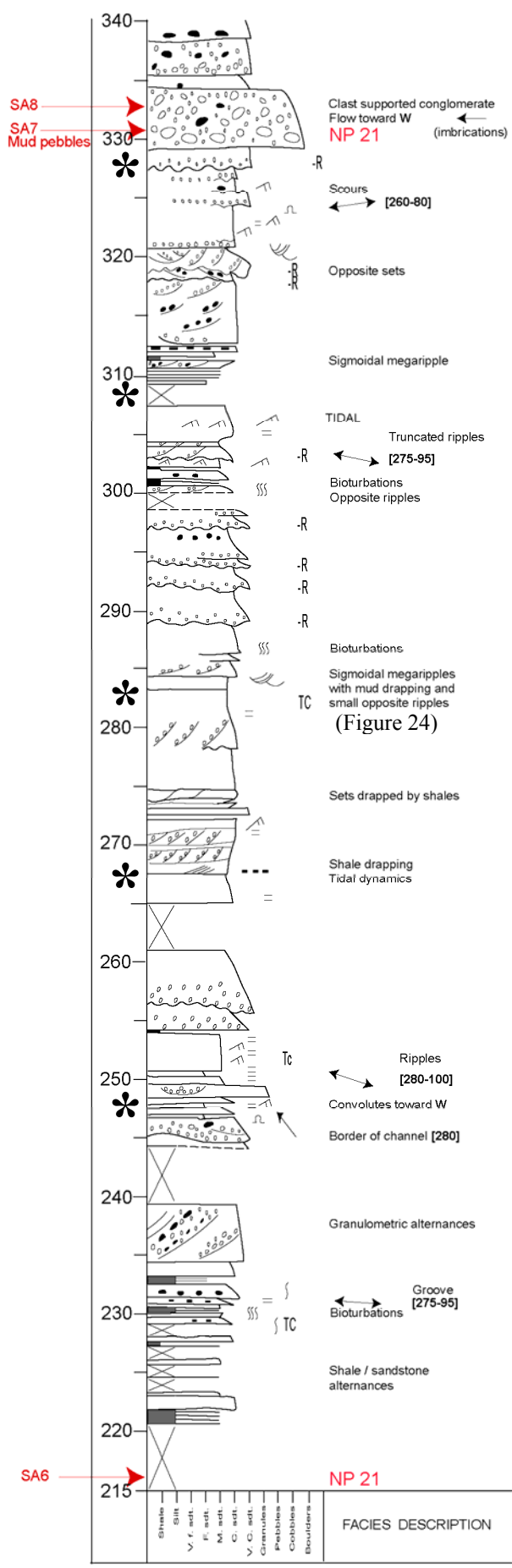


Figure 23 : Detailed sedimentological log of the lower part of the Saint Antonin section (description by E. du Fornel and S. Lesur) : stars indicate particularly interesting observations.

580

Conglomerate / sandstone in scree

570

Conglomerate - debris flow

560

Clast supported conglomerate

-R

Conglomerate - abundant clasts at base

Debris flow

550

TC?

Pebbly tractive laminations

Debris flow

540

Clast supported conglomerate

Matrix supported conglomerate

Debris flow clast supported at base

530

Imbrications : [220] (2), [210] (2) & [230] (2)

Clast supported conglomerate

520

NP 21 Conglomerate

510

Conglomerate / sandstone in scree

500

Conglomerate / sandstone / conglomerate / sandstone in scree

490

Tractive dynamics

480

Clinoforms ?

Matrix supported conglomerate

Debris flow

Crude megapipples

Indurated bed

470

Conglomerate in scree

460

Shale

Silt

F. sdt.

M. sdt.

C. sdt.

V. C. sdt.

Gravel

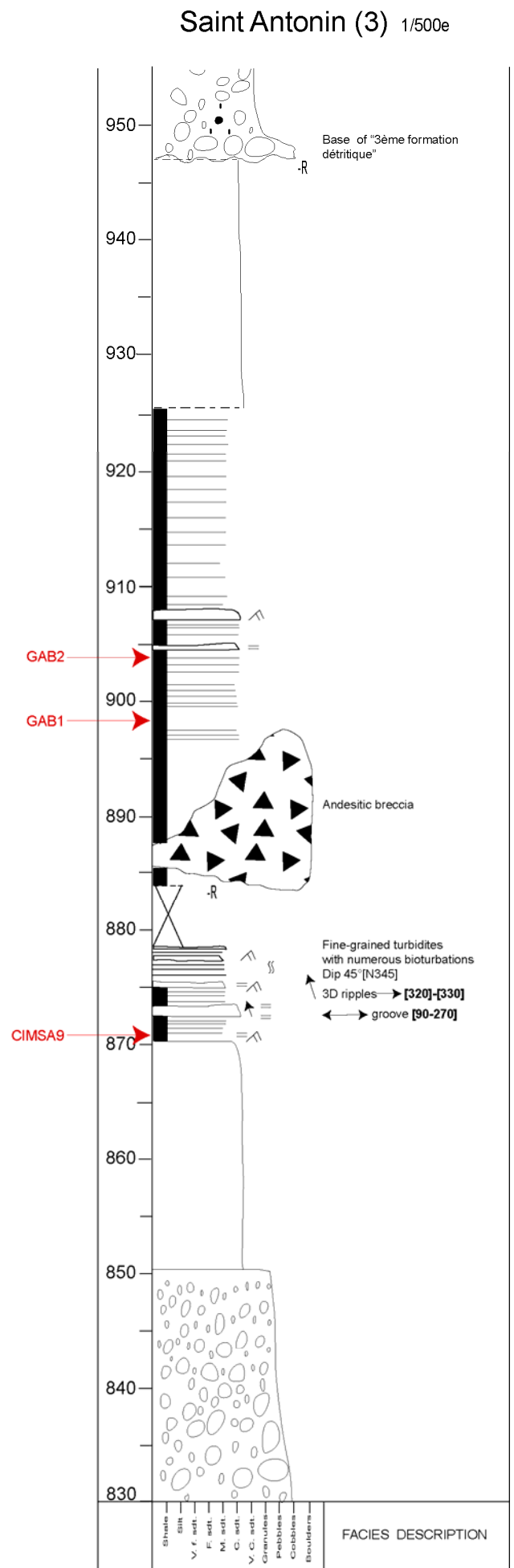
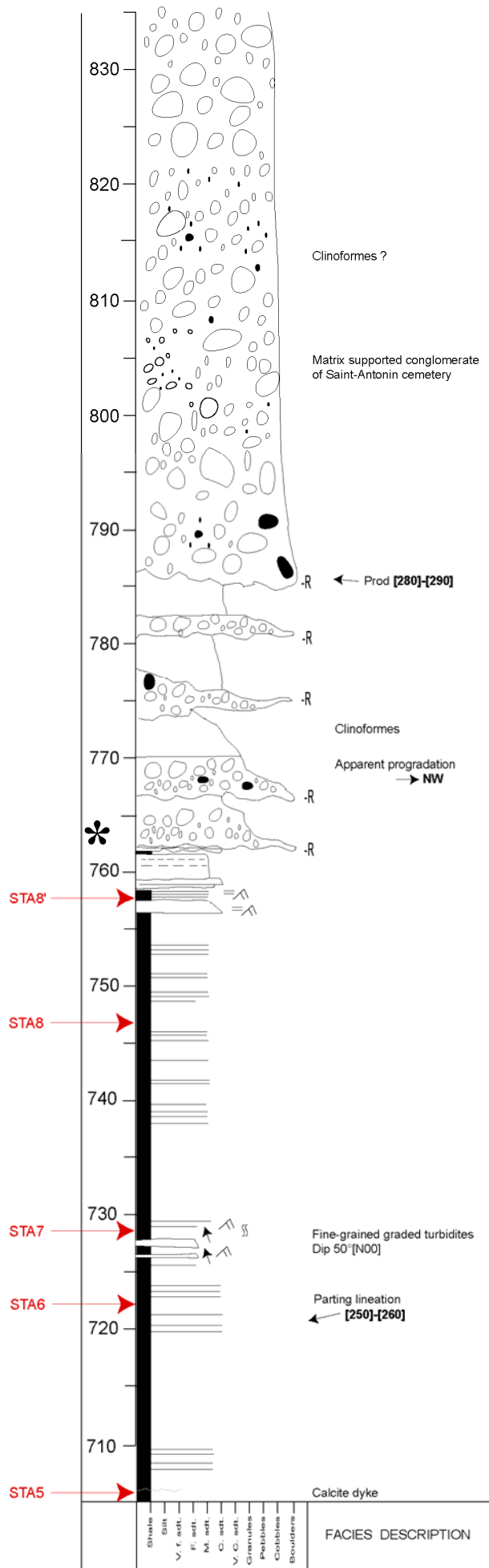
Pebbles

Cobbles

Boulders

FACIES DESCRIPTION







The basal **unit A** (0 – 215 m), which crops out in Ravin de Cumi below the road , is composed of alternations of muddy-sandy couplets that du Fornel (2003) interprets as thin-bedded low-density turbidites. The foraminifera associations would indicate a water depth between 200 et 500 m. However Callec (2001) considers that a part of the unit might have been deposited under storm influence (presence of Hummocky Cross Stratifications).

**Unit B** (215-310 m) starts with muddy – sandy alternations, which are overlaid with thickening and coarsening-upward massive sandstone beds. Grain size in these massive beds varies from coarse to very coarse. Sedimentary features like sigmoidal megaripples or clay draping are found at the top of Unit B, which may indicate a tidal influence suggesting therefore a shallow paleobathymetry (elevations 283 m : Figure 24).



**Figure 24 : Sigmoidal megaripples with shaly layers (Unit B : elevation 283 m).**  
These sigmoidal megaripples with small opposite ripples on the left hand side of the photo are interpreted as tidal.

There is an abrupt change in facies at 330 m, with the arrival of thick bedded, massive conglomerates and thick coarse sandstones. These coarser facies characterise the overlying succession up to its top, with a few preserved finer levels, which are used to differentiate units : **Unit C** (310-450 m); **Unit D** (450-510 m); **Unit E** (510-620 m); **Unit F** (620-710 m) and **Unit G** (720-875 m).

Two types of conglomeratic facies can be recognised :

- conglomerates with pebbles to cobbles floating in a sandy matrix (mass-flow deposits, Figure 25),
- conglomerates with joined pebbles, sometimes with large oblique stratification with imbricated pebbles (deposits under unidirectional tractive flow, Figure 26).

These conglomerates present a strong analogy with facies of sigmoidal bars induced by floods arriving in a shallow water area (Mutti *et al.* 1996) : the transformation of the hyperconcentrated flow into a more turbulent and diluted flow induces specific facies associations (Figure 27). The coarser-grained facies 1 can fill large erosive scours (Figure 28).



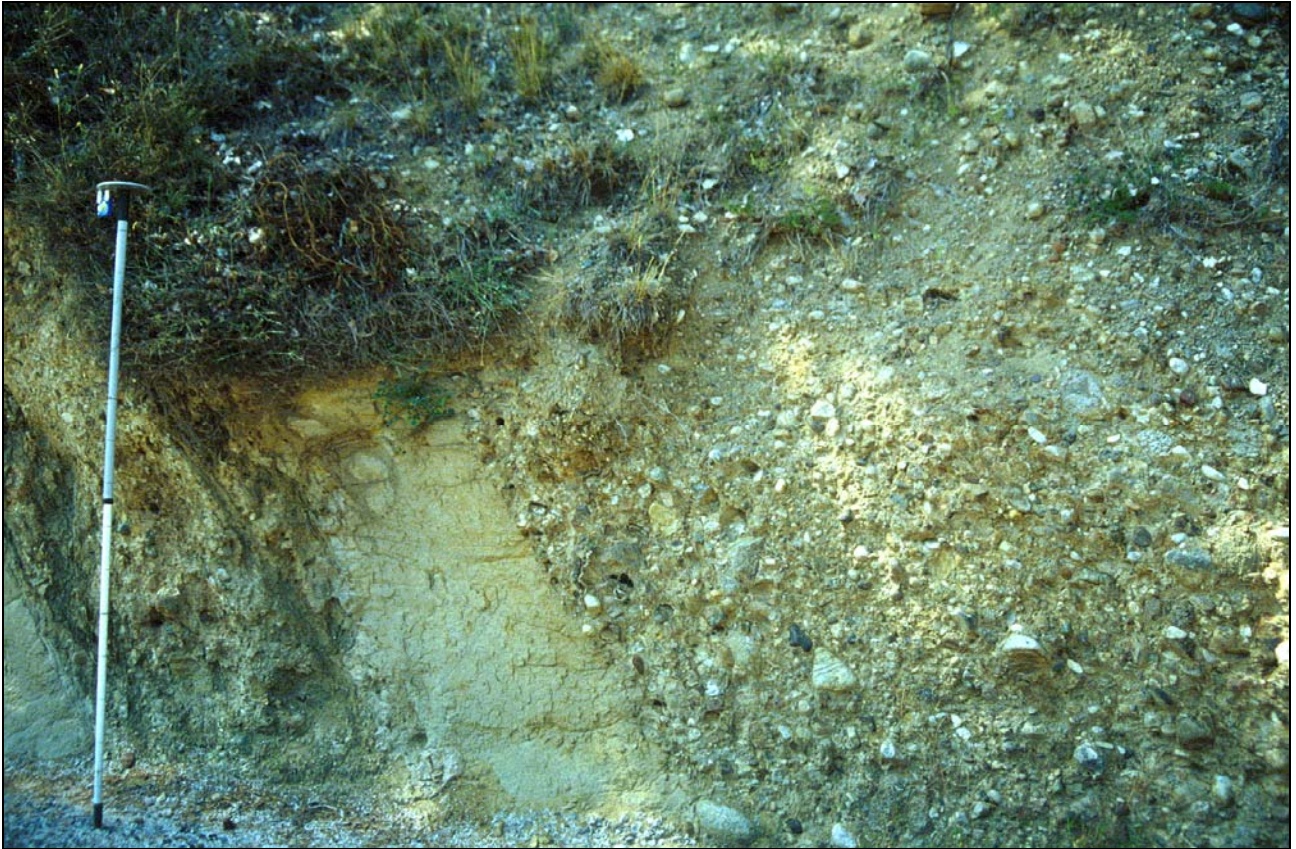


**Figure 25 : Sandy matrix supported conglomerates (Unit F : elevation 650 m).**



**Figure 26 : Clast supported conglomerate eroding a pebbly sandstone with pebbles organized in oblique stratifications (Unit C : elevation 360 m).**



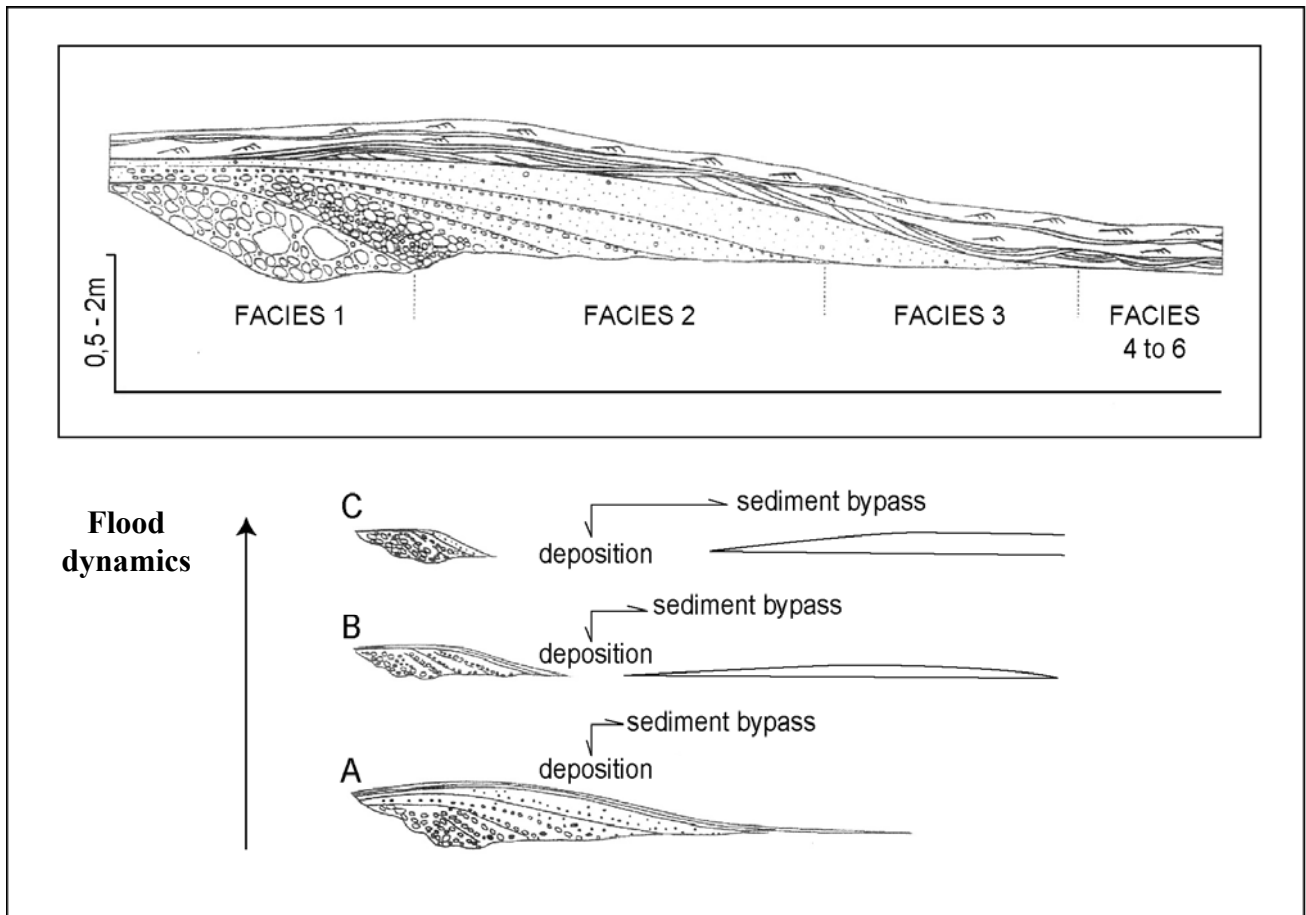


Figure 27 : Geometry and facies of sigmoidal bars generated by floods (Mutti *et al.* 1996, in du Fornel 2003).



Figure 28 : Conglomerates filling large erosive structures at Chamengearde.



**Stop n° 2 : Saint Antonin cemetery. Channelized conglomeratic system.**

Below the Saint Antonin cemetery, we can observe the geometry of the conglomeratic body outcropping below the Saint Antonin village (Unit G : elevation 760 m).

On dip view below the Saint Antonin village, the conglomeratic beds are organized in clinoforms with an apparent progradation to the NW (Figure 29).



**Figure 29: Large-scale clinoforms in Unit G (elevation 760 m) below the Saint Antonin village.**

On strike view below the Saint Antonin cemetery, the geometry is lens-shaped and the conglomeratic beds are clearly strongly erosive onto medium-grained sandstones and fine-grained graded turbidites alternating with marls (Figure 30).



**Figure 30 : Erosive conglomeratic lens in Unit G below the Saint Antonin cemetery.**





## **Annot**

**Philippe JOSEPH, Yannick CALLEC and Elodie du FORNEL**

*During this second day, we will study the filling during Late Priabonian of the Annot ponded basin and we will discuss the influence of synsedimentary tectonics on turbidite flows and facies (section of the Braux road eastward of Annot : cf. location in Figure 3 p. 11 ).*

*Then, we will observe large-scale synsedimentary deformation (megaslump of Gastres outcrops).*

*Finally, we will examine the facies organisation and the 3D architecture of channels that controlled the transit of coarse-grained material to the distal area during the overspill of the ponded sub-basin during Early Rupelian (outcrops of Scaffarels - La Chambre du Roi).*



**Scaffarels outcrops**

### General geological framework of the Annot syncline

The Annot syncline is located on the Digne thrust sheet, 30 km east of the thrust front, between the Dome de Barrot and the Castellane Arc (cf. Figure 2 p. 10). It is oriented NNW – SSE and is about 16 km long and 11 km wide (Figure 31a). It is limited to the north by the E-W Aurent Anticline, to the west by the NW-SE Puy de Rent Anticline, and to the east by the senestral strike-slip faults of Rouaine and Var, trending NE –SW.

As indicated by the strong contrasts in thickness of the Tertiary series (Figure 31b), these faults had an important synsedimentary activity that will be discussed. The classic units of the Nummulitic Series can be identified : Infrannummulitiques Conglomerates (so-called Poudingues d'Argens), Calcaires Nummulitiques, Marnes Bleues, Grès d'Annot, with different members (Crête de la Barre, Gastres, Scaffarels et Garambes), which young toward the west.

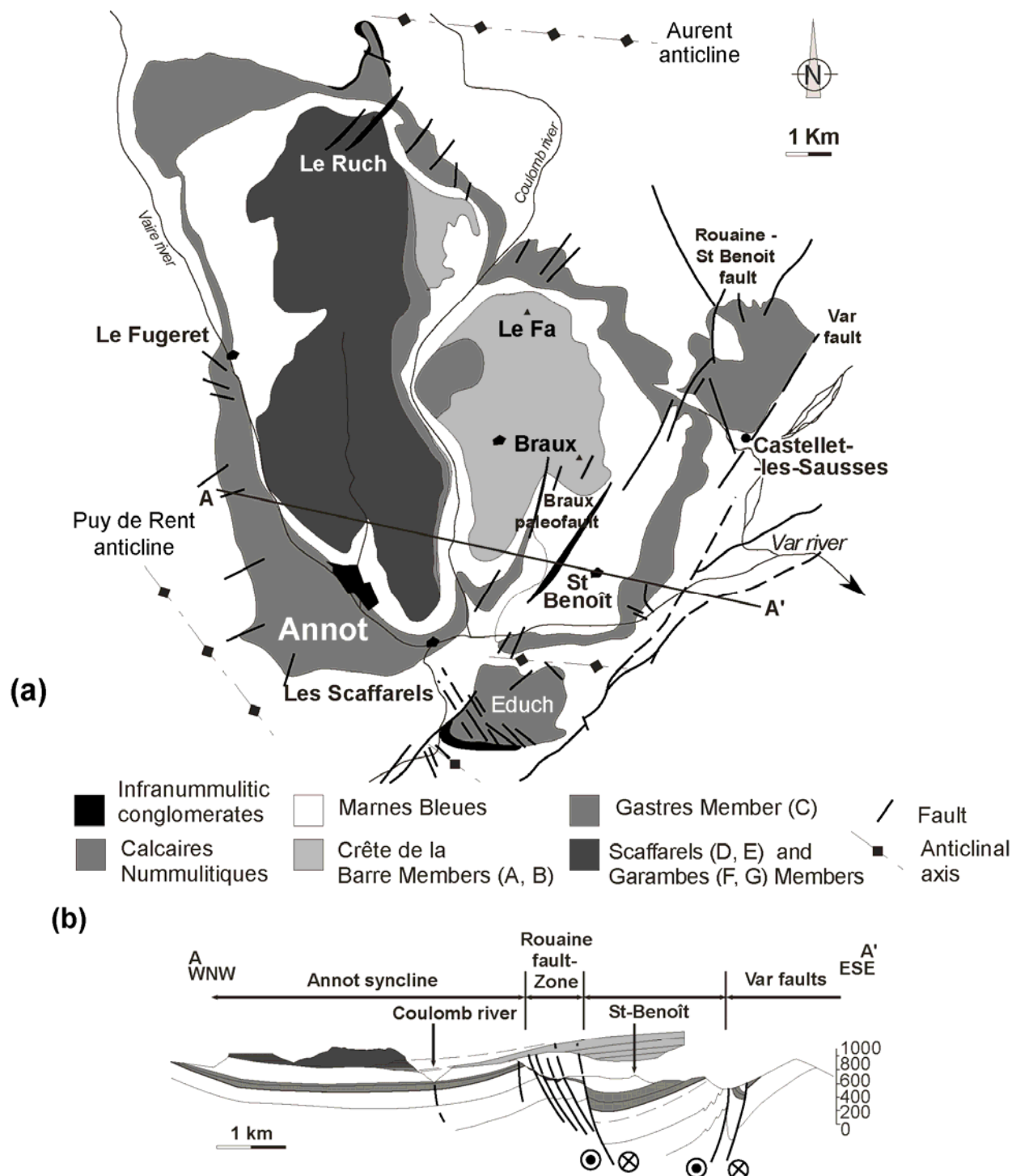


Figure 31 : (a) Simplified geological map of the Annot syncline ; (b) Simplified structural section across the Annot syncline (modified from Callec 2004).



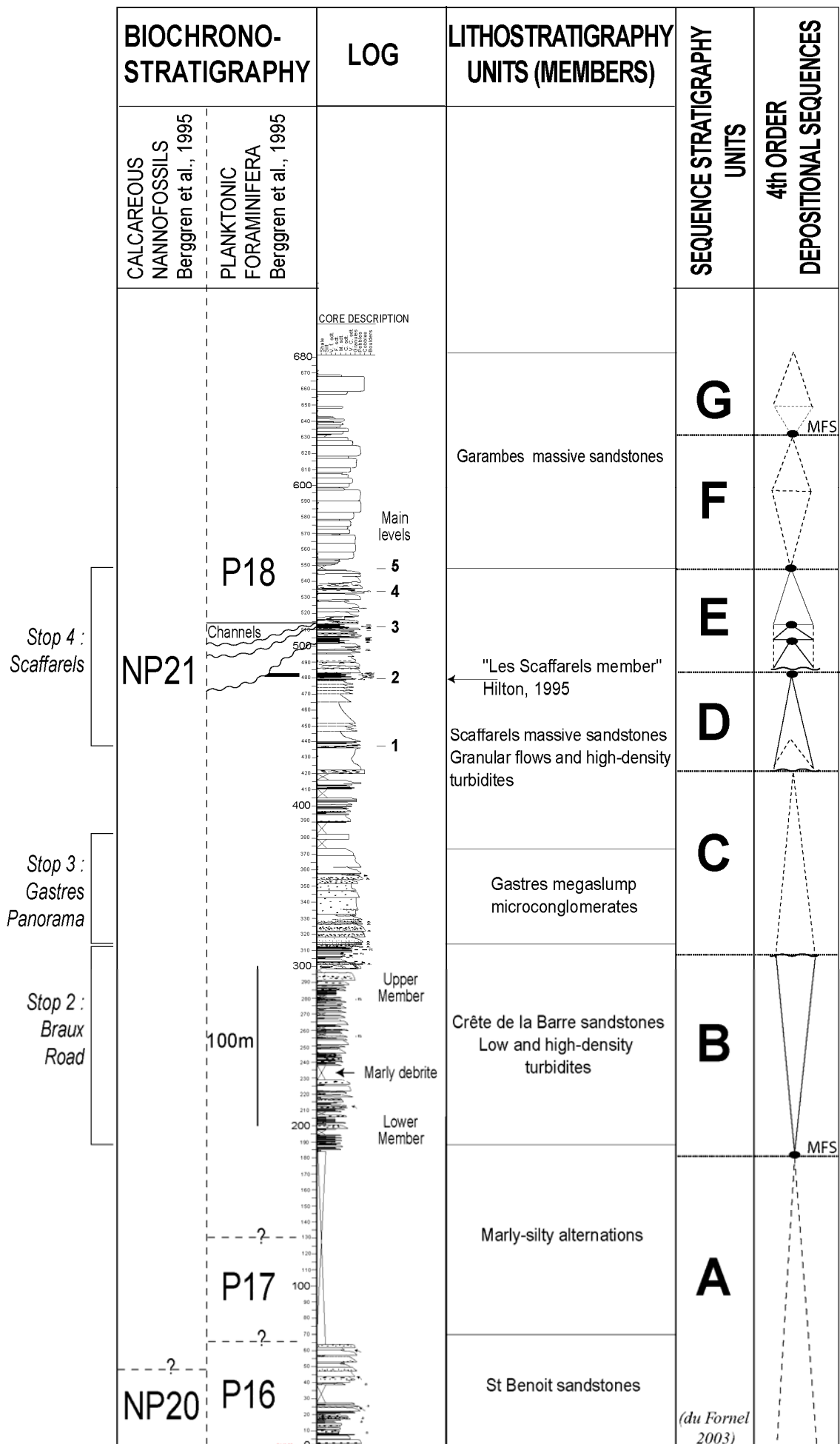


Figure 32 : Composite log of the Grès d'Annot in the Annot syncline (modified from du Fornel *et al.* 2004).

## Stop n° 1 : Panorama from Plateau d'Educh

The panorama from Plateau d'Educh (cf. point 1 on Figure 33) provides a global view of the syncline and illustrates its geometric configuration (Figure 34). The Calcaires Nummulitiques rest unconformably on the Upper Cretaceous (Conacian - Santonian) and outcrop along the Vaire valley : this formation is covered by the Marnes Bleues Formation, which constitutes the floor of the Coulomp and Saint Benoît valleys.

The thickness of the two formations changes markedly from one side of the Braux paleofault to the other, which can be easily identified by the shift in the position of the Calcaires Nummulitiques : this fault (also called the Gros Vallon fault (Pairis 1971), Saint Benoît fault (Beaudoin *et al.* 1975, Elliott *et al.* 1985 ; Tomasso & Sinclair 2004) or the Savelet fault (Puigdefabregas *et al.* 2004)) is a N-S branch of the Rouaine fault system. The Calcaires Nummulitiques thickness changes from 100 m to the east to 20 m to the west (Ravenne *et al.* 1987 : Figure 35) and the Marnes Bleues thickness varies from 400 m to 200 m with a minimum of 70m immediately west of the paleofault. The fault plane is draped by a calcareous synsedimentary breccia (Beaudoin *et al.* 1975), which includes nummulites : indicating that this paleocliff was active during the Late Eocene. The Marnes Bleues also drape the paleofault. The first Grès d'Annot unit (unit **A**, so-called the Saint Benoît Member) is present only on the east side and onlaps onto the Marnes Bleues toward the fault. The thickness of unit **B** (the so-called Crête de la Barre member) diminishes rapidly, but the upper part of the unit passes above the paleofault without displacement, which indicates that activity on the Braux fault died out during the Late Eocene. This unit onlaps onto the Marnes Bleues in the Coulomp valley. The upper units **C**, **D**, **E** also disappear westward by successive onlap : we are thus observing the western margin of a confined basin.

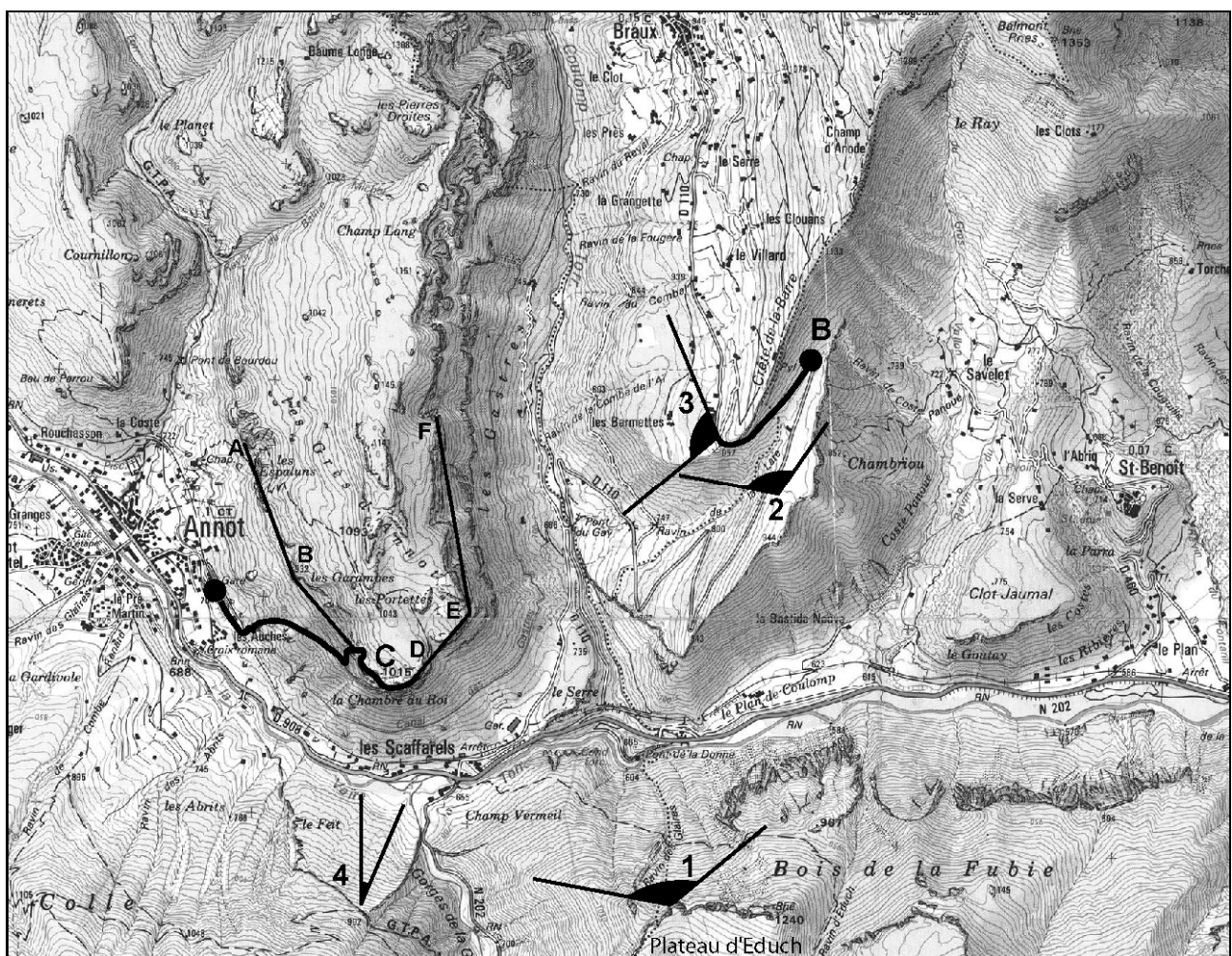


Figure 33 : Location of view points (1 : Plateau d'Educh ; 2 : Braux road ; 3 : Les Gastres ; 4 : Les Scaffarels), stops (C : Scaffarels - Chambre du Roi ; B : Route de Braux) and panorama of Annot – Les Scaffarels – La Chambre du Roi outcrops of Figure 51 (A-B-C-D-E-F).

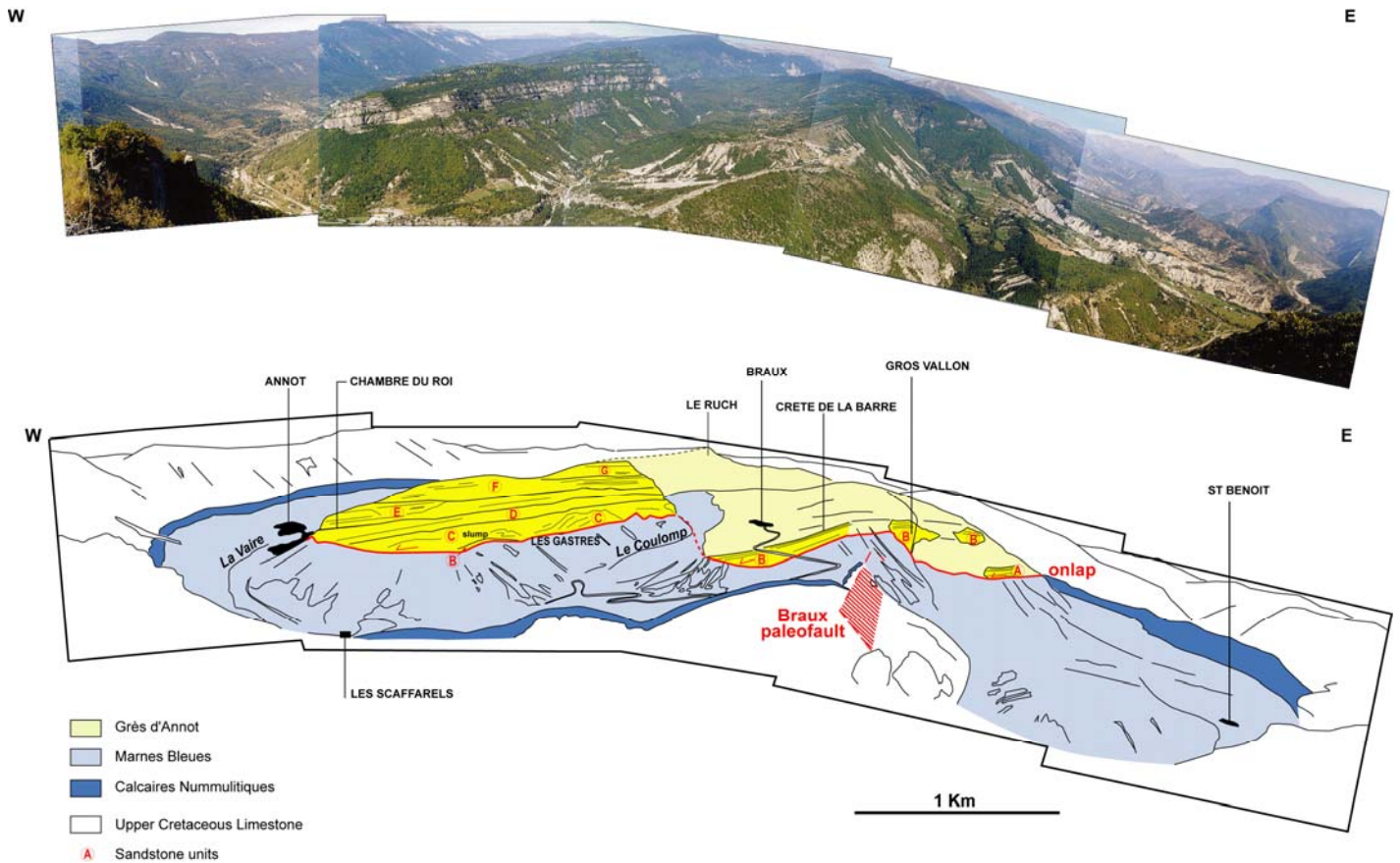
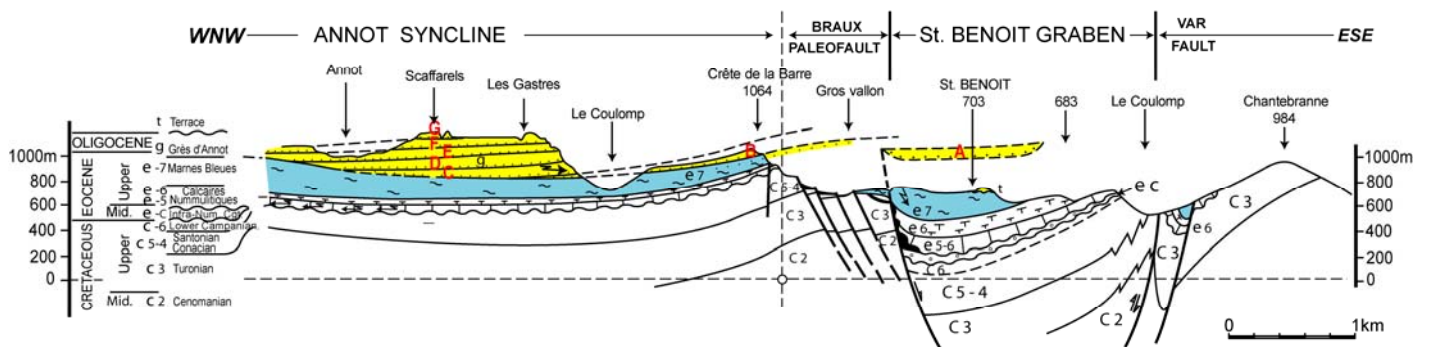


Figure 34 : Panorama of the Annot Syncline viewed from Plateau d'Educh (view point 1 of Figure 33).

### Cross-section across the Annot cliffs



### Reconstruction of Braux paleofault at the end of Grès d'Annot sedimentation

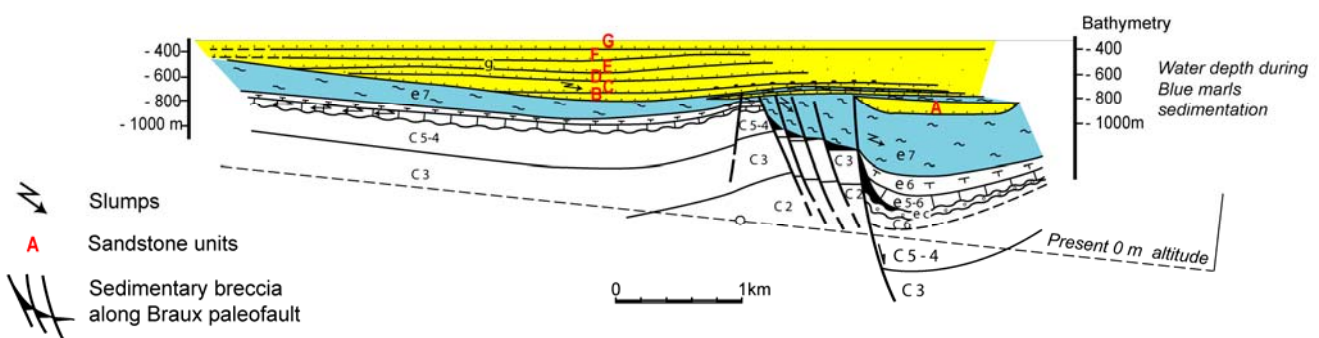


Figure 35 : Structural section across the Annot Syncline and restoration of the section to the end of Grès d'Annot sedimentation (modified from Ravenne *et al.* 1987).

The location of this section is indicated as A – A' on Figure 31.



Figure 32 provides a schematic log of the formation, with the equivalence between the names given to members by Callec (2001) and sandstone units defined by du Fornel (2003), which are interpreted as 4<sup>th</sup> order depositional sequences. These units mapped on Figure 36 are approximately equivalent to the stratigraphic units defined by Albussaïdi & Laval (1984). This is a composite log because the vertical superposition of all these units is never observed : this is due to a westward shift of the depocenter of approximately 2.3 km, induced by the tilting of the eastern border of the basin during Oligocene (Figure 37).

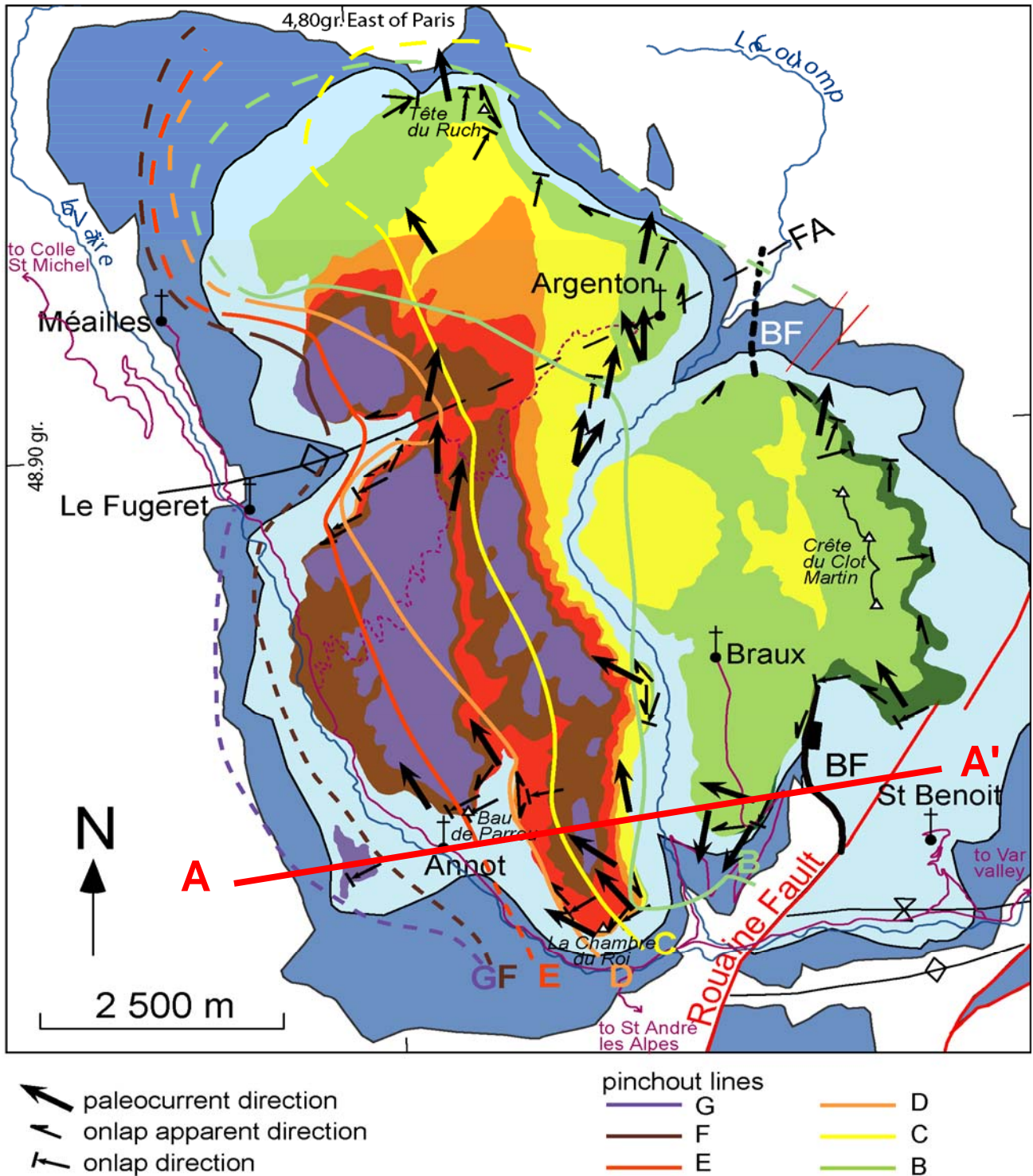
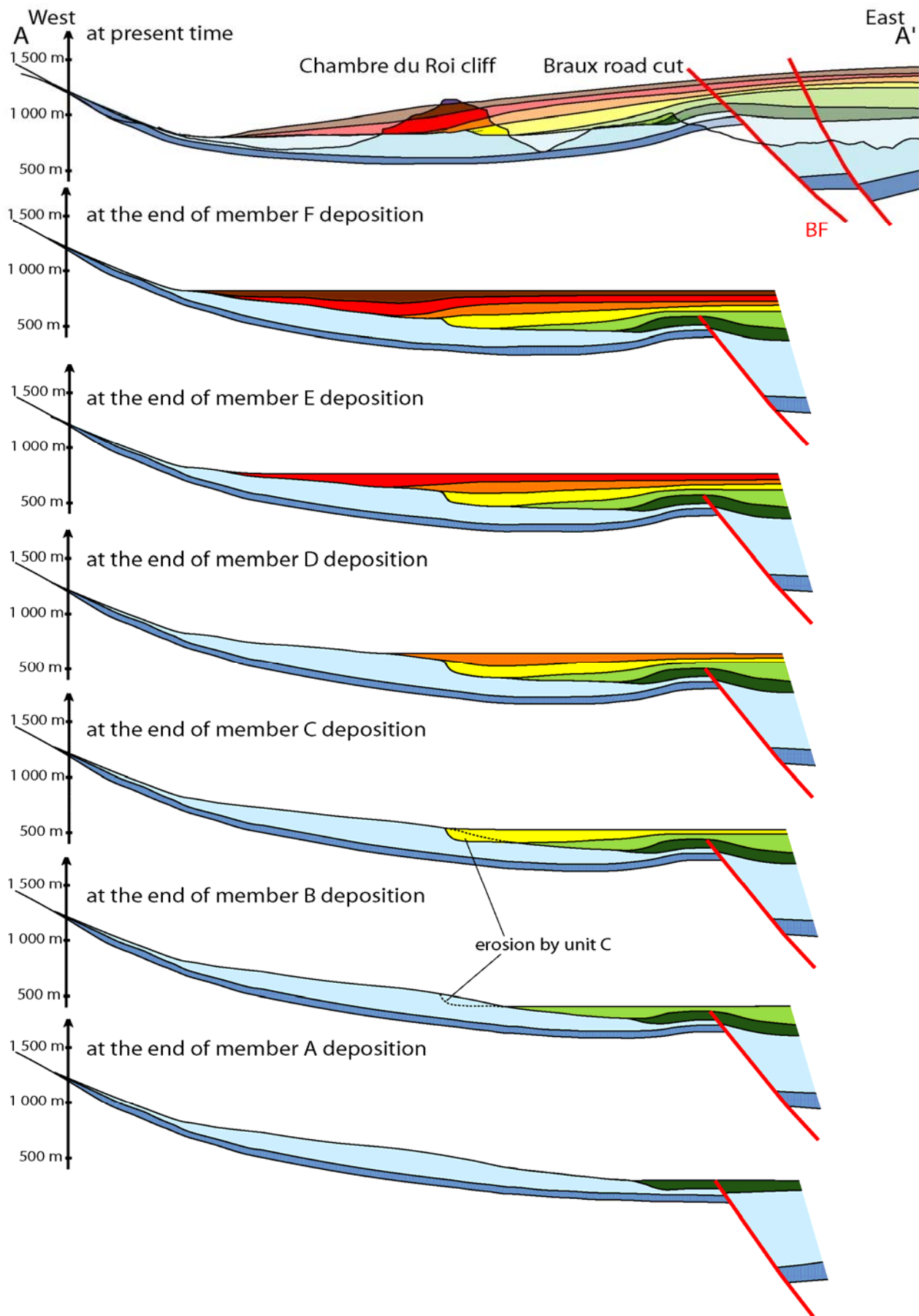


Figure 36 : Geological map of the Annot Syncline (modified from Salles et al., in revision). Members of the Grès d'Annot Formation were mapped by Albussaïdi and Laval (1984), Callec (2001) and Puigdefàbregas et al. (2004). Paleocurrents directions and true and apparent onlaps have been compiled from Albussaïdi and Laval (1984), Callec (2001), Du Fornel (2004), Puigdefàbregas et al. (2004) and Joseph (2001, 2005 & 2007). The red line gives the location of the section AA' of Figure 37.



**Figure 37 : Sequential restoration of the AA' cross-section of Figure 36 (modified from Salles et al., in revision). Note the progressive rotation of the Calcaires Nummulitiques immediately to the west of the Braux fault (BF). Sandstone deposition is strongly influenced by the active syncline. To the west of the Braux normal fault, cumulative displacement of the depocentre is around 2.3 km. Deposition of the older members A and B is also influenced by the Braux normal fault.**

## **Stop n° 2 : Braux road. Confined lobes and interaction of turbiditic flows with topography.**

The purpose of this stop is to examine the topography that is induced by the synsedimentary tectonics and their impact on gravity flows and facies.

### **Panorama of Crête de la Barre**

The panorama of the Braux road (D110) enables us to observe the onlap configuration between the Marnes Bleues and the Crête de la Barre member (unit **B**), close to the Braux paleofault (Figure 38). The location is indicated on Figure 33 p. 42 (view point 2).

Synsedimentary activity on the paleofault induced a topography, which was only partly filled by the Marnes Bleues deposits. From east to west, we can observe a strong thinning of the Crête de la Barre Lower Member, which, west of the fault, appears as a very limited unit, presenting both eastward and westward onlaps (Figure 38).

A 20m-thick muddy debrite including slumped blocks overlies this Lower Member and the Upper Member passes continuously above the paleofault and onlaps toward the west. Its sandstone beds have a broad lateral extent and can be easily correlated across 3 km : they are interpreted as a system of turbidite lobes that were confined by the depression induced by the paleofault.

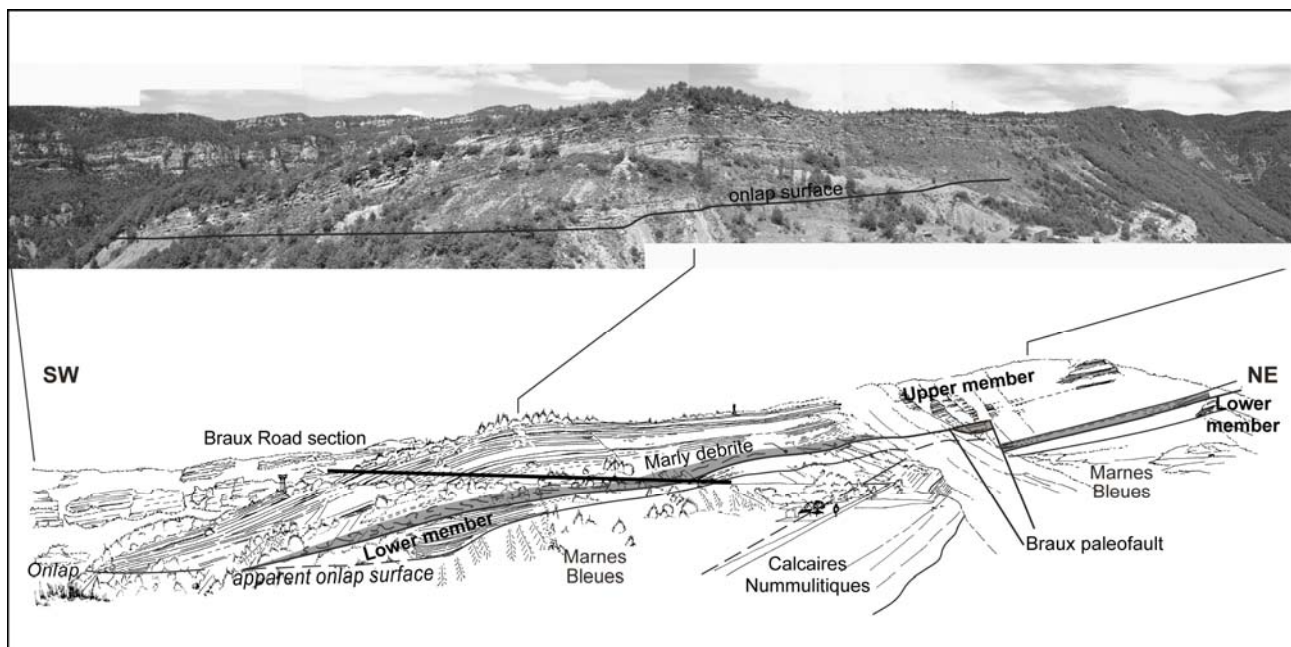


**Figure 38 : Panorama of Crête de la Barre (Unit B) along the Braux road (modified from Callec 2004).**

Tomasso & Sinclair (2004) relate this configuration to three phases of activity on the Braux fault :

- During the Bartonian (Figure 39A), extension induced a normal play on the fault and initiation of a half-graben filled by the Calcaires Nummulitiques, and by the lower part of the Marnes Bleues, that draped the paleofault (Figure 39B).
- During the Priabonian (Figure 39C), strike-slip movement on the fault induced a small monoclinical fold parallel to the fault : the remaining topography to the east was filled with coarse-grained turbidites of the Lower Member, whereas flow stripping induced deposition of fine-grained sediments in small topographic lows west of the fault.
- At the beginning of the Rupelian (Figure 39D), fault activity stopped and coarse-grained turbidites of the Upper Member were deposited above the fault and pinched out westward by onlap onto the slope.



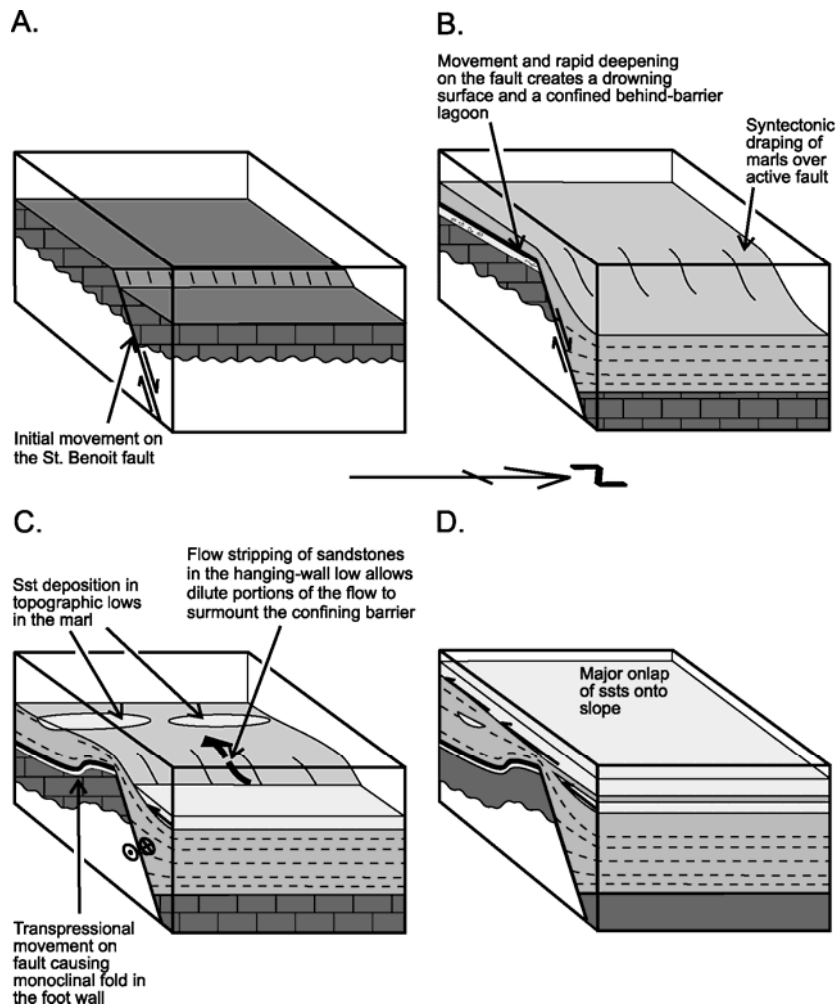


Figure 39 : Evolutionary model of the Braux Paleofault (Tomasso & Sinclair 2004).

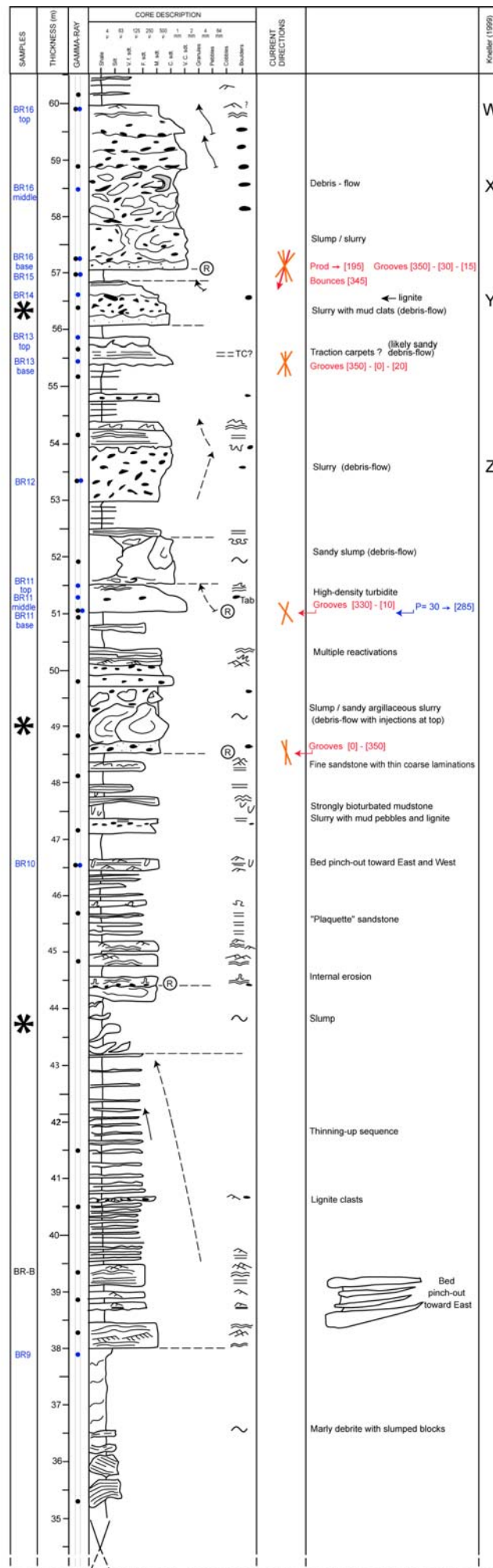
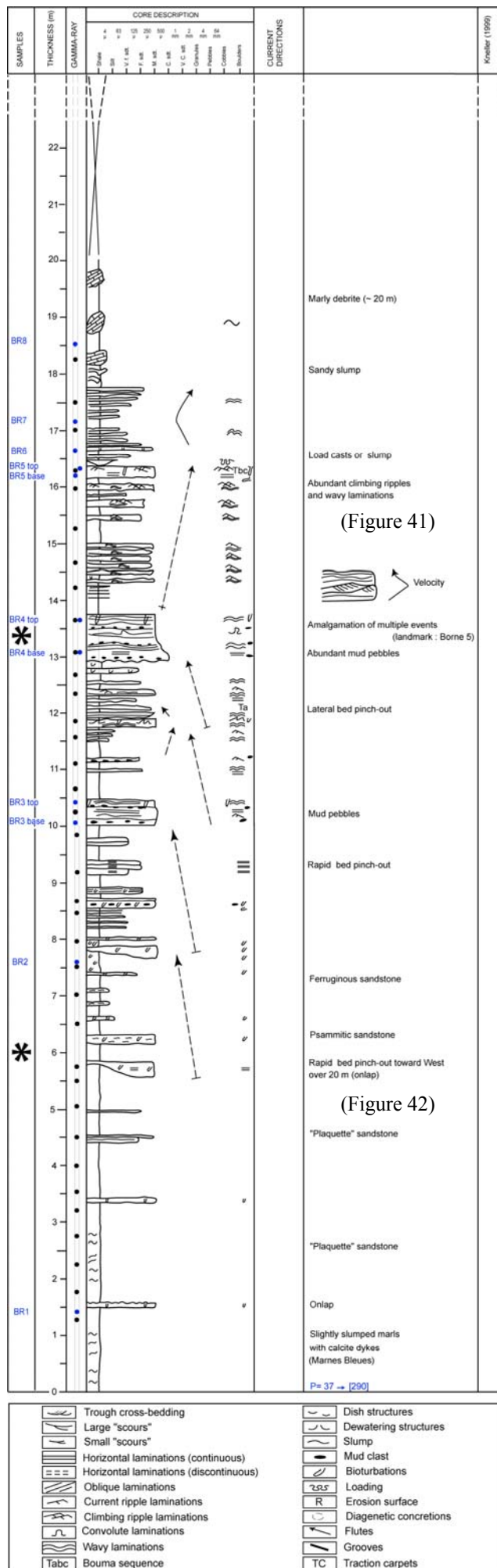
This change in fault activity might be related to the evolution from a flexural regime inducing local normal faults, to a compressive regime related to thrust migration, which induced a strike-slip displacement on the faults.

### Section of Crête de la Barre

This section is located along the Braux road (D110) and enables us to study in detail the turbidite facies close to the onlap onto the Marnes Bleues. The detailed log is provided on Figure 40.

Following the description of gravity deposits in page 22, we have used the term "**debris-flow**" for non-graded facies, with structures revealing laminar transport of centimetre to decimetre-scale elements floating in a sandy-silty matrix (parallel stratification, aligned mud pebbles) ; "**slump**" for facies showing contorted beds and "**turbidite**" for facies indicating transport by a turbulent suspension (obvious grading, Bouma sequence).

"**Slurry**" is a descriptive term used only when the facies includes a dominant component of mud pebbles mixed with a sandy-silty matrix.



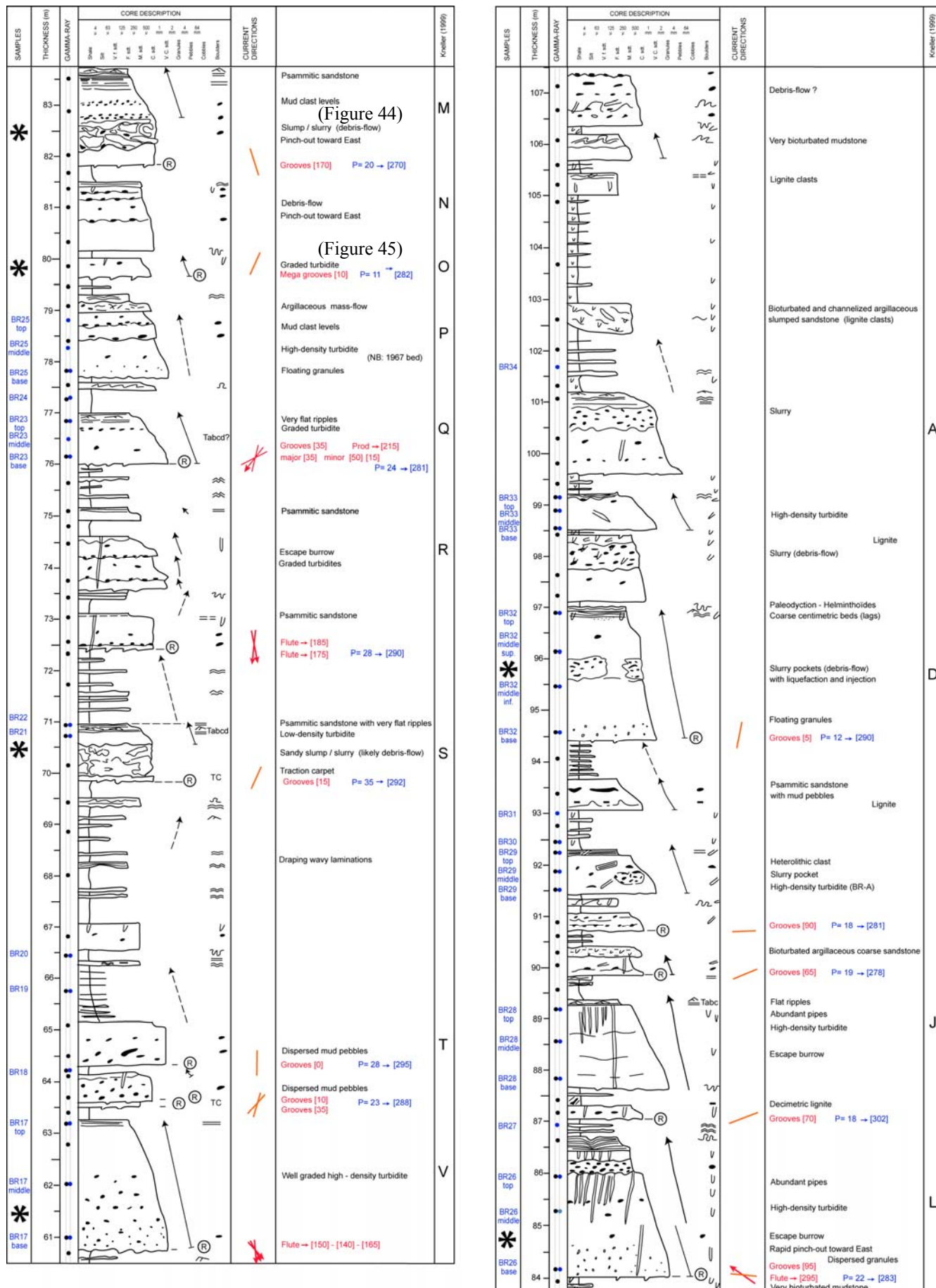


Figure 40 : Sedimentological log of Grès d'Annot at Crête de la Barre along the Braux road (data from IFP Energies nouvelles « Turbidites » consortium). Stars indicate particularly interesting observations.



Three sets can be recognised :

(1) The lower set from 0 to 48 m is made of thin sandstone beds, fine to medium grained, very rich in parallel and wavy laminations, convolutes, current ripples that are sometimes climbing (Figure 41). These beds are interpreted as low-density turbidites (Bouma sequences Tb et Tc). A muddy debris that includes slumped limestone blocs is interstratified between levels 18 et 38 m : it separates the Lower Member and the Upper Member of the Crête de la Barre.



**Figure 41 : Low-density turbidites Tbc along the Braux road (elevation 15.5 m).**

At the base of the section, the onlap contact (Figure 42) shows an abrupt thinning of the sandstone beds, with a clear change of their dip : this corresponds to a draping of the paleoslope by the fine-grained part of the turbidite flow; The real angle of the paleoslope is much lower than the apparent onlap angle, that correspond to the climbing angle of the bed pinchouts as the slope aggrades (Figure 43 : Smith & Joseph 2004).

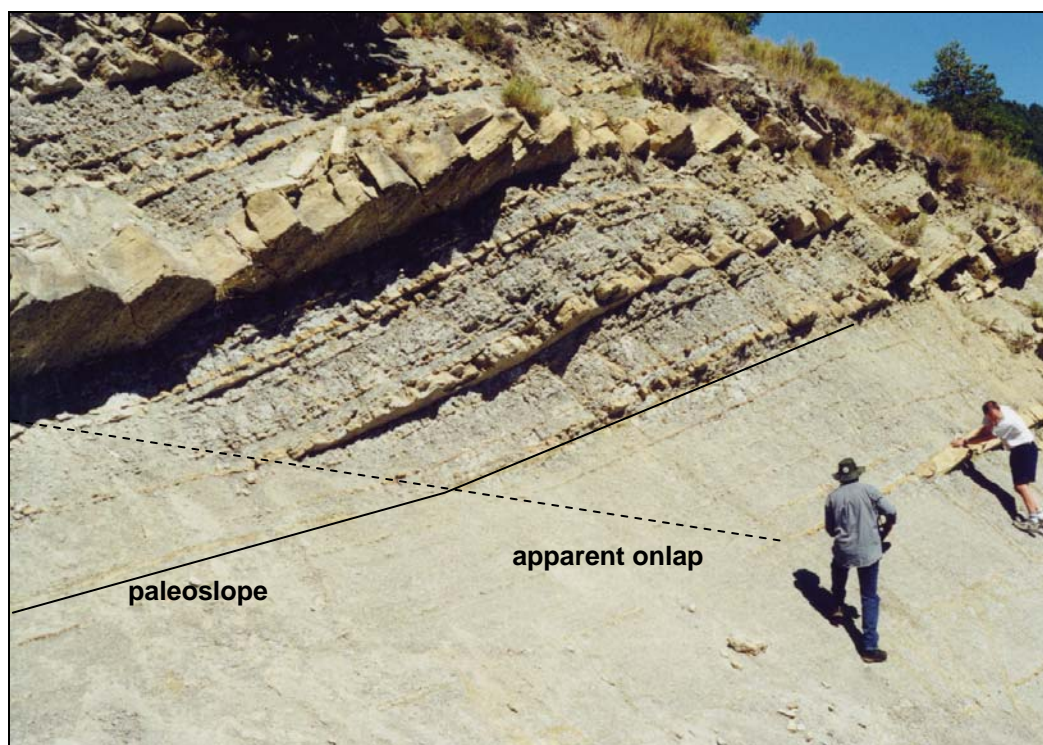


**Figure 42 : Apparent onlap with pinchout of fine-grained turbidites into Marnes Bleues along the Braux road (elevation 6 m).**

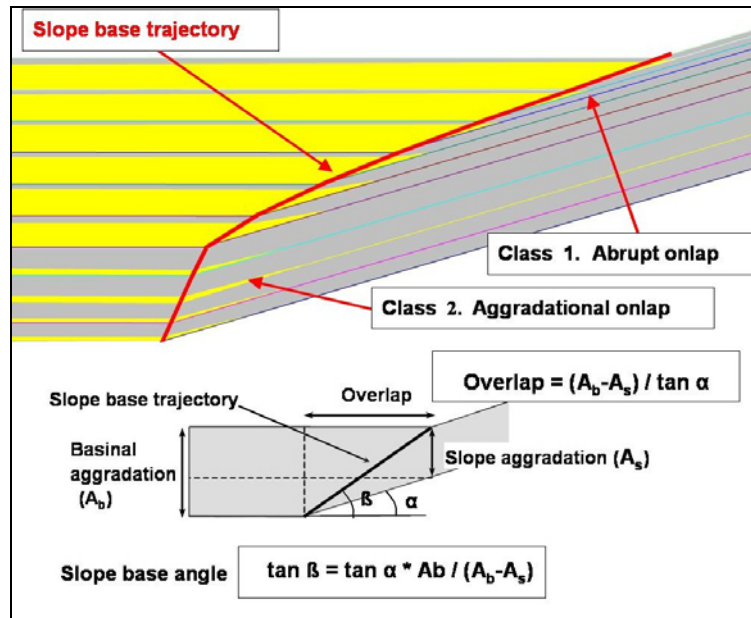


Figure 43 : Evolution of the apparent onlap angle  $\beta$  (slope base trajectory) as a function of the paleoslope angle  $\alpha$  and the respective basin aggradation rate  $A_b$  and slope aggradation rate  $A_s$  (in Smith & Joseph 2004).

(2) The middle set from 48 to 84 m is characterised by thicker (meter-scale) and coarser (medium to coarse-grained) beds. Numerous beds include shaly mud pebbles and are characterised by a tripartite organisation (Figure 44) : massive sandstone at base, chaotic unit in the middle (sometimes with sand injections from the basal unit), graded bed at top. These three parts are genetically linked and this « sandwich bed » is interpreted as resulting from the interstratification of a debrite inside a turbidite, because of the erosion of the lateral marly slope by the high-density turbidity current (Kneller & McCaffrey 1999). The increase of the debrite thickness toward the onlap is in agreement with this hypothesis (Figure 44).

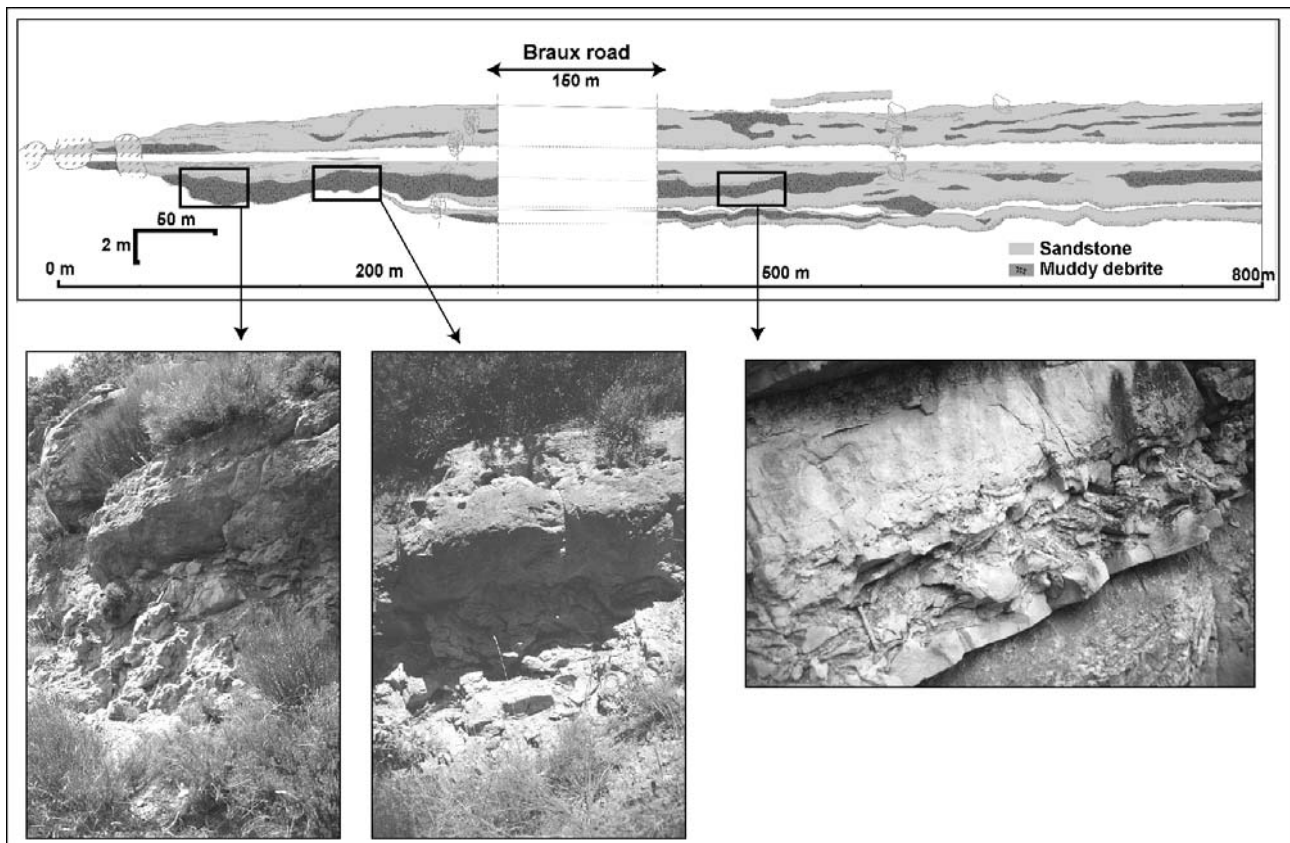


Figure 44 : Lateral evolution of a débrite interstratified in a turbidite along the Braux road, modified from Callec (2001) (M bed : elevation 83 m).



In this set, current casts (flutes et grooves : Figure 45) are numerous at the base of the beds and in several places they indicate southward oriented paleoflow directions (with an important dispersion) : these directions are very different from the mean flow direction in the syncline (toward NW) and they are in fact parallel to the direction of the paleoslope induced by synsedimentary activity of the Braux fault (oriented N-S).



**Figure 45 : Megagrooves at the base of sandstone bed O (elevation 80 m).**

(3) The upper set from 84 to 107 m is made of more homogeneous massive beds, with fewer mud pebbles. Some beds show a clear grading (from very coarse to fine-grained), water escape structures (« pipes ») and escape burrows traversing the beds (beds J et L). They correspond to real high-density turbidites. Paleocurrent directions are now toward West, and perpendicular to the paleoslope.

This evolution is interpreted by Kneller & McCaffrey (1999) in terms of spatial variations of the flows. The upper set would correspond to depletive divergent flows coming from the east, which settle high-density graded beds (step 1 of Figure 46).

The flows are reoriented toward the south by the slope : current lines turn and converge southward (step 2 of Figure 46) : the erosion of the slope by these currents induces the interstratification of mud pebbles and previously deposited beds as a debrite inside the dense flow. This step corresponds to the « sandwich beds » of the middle set.

Then the dense basal part of the turbidity current flows parallel to the slope (step 3 of Figure 46), whereas the diluted upper part may drape the slope or be reflected. This corresponds to the fine-grained low-density turbidites of the lower set.

Because of the aggradation of the turbidites, that induces a retreat of the slope toward the west, sedimentation areas progressively migrate westward (3, 2 then 1) : this migration creates the vertical sequence of the three sets as previously described : the lower set with fine-grained low-density turbidites, the middle set with debrites, the upper set with coarse-grained high-density turbidites.

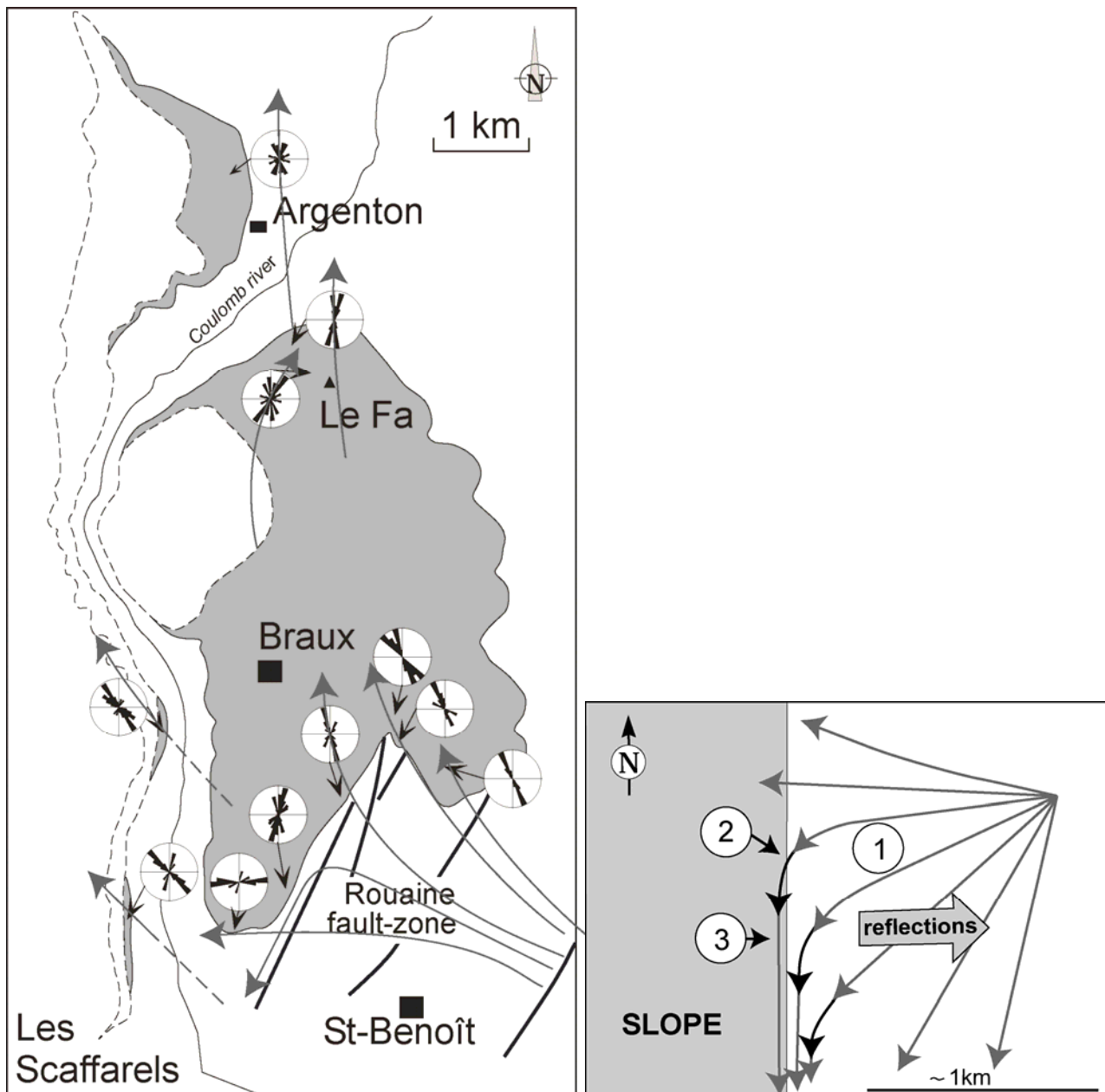


Figure 46 : Current directions in the upper member of Crête de la Barre (modified from Callec 2004) and evolution scheme of current lines and deposition regime of a turbidite flow approaching a slope (modified from Kneller & McCaffrey 1999).

Spectral gamma-ray measurements (potassium, thorium and uranium) were performed on the Braux road section using a portable gamma-ray apparatus. The log signature (Figure 47) is in good agreement with the facies interpretation and the vertical sequence described above.

The lower set of the section corresponds to low-density turbidites with tractional structures (horizontal laminations, ripples and convolute beds), which are interpreted as onlap facies close to the slope and deposited under uniform conditions (Kneller and McCaffrey, 1999). This lower part is characterised by a fairly constant low amount of potassium and thorium, which may be explained by the high amount of carbonate mud in these low-energy deposits draping the paleoslope.

The middle set of the section contains a high proportion of “sandwich beds” – sandstone-debrite-sandstone triplets – interpreted above as turbidites with intercalated coeval, locally-triggered debrites. This subsection is characterised by a higher amounts of potassium and thorium with weak variations due to the poor grading of the deposits.

The upper part corresponds to poorly sorted massive sandstones with grading at the top and dewatering structures: They are due to rapid deposition from a turbulent suspension under depletive conditions in the basin far away from the paleoslope. Each sandstone bed displays a clear vertical trend, with either a progressive increase of the radioactivity from the coarse-grained (sandy) bottom to the fine-grained (shaly) top, or a slight decrease followed by an increase: that on careful observation can be explained by a higher proportion of radioactive K-feldspars grains (coarser than quartz grains) at the bottom of the bed. Both observations can be related to the grading of the turbidite bed, with segregation of coarser grains at the bottom.

Geochemical measurements follow this trend, with progressive increases of Al, Fe, Mg, Ca, Ti, Cr toward the top of each bed (related to enrichment in shale). This trend is also in good agreement with deposition from a turbulent suspension. As shown by the increase in Zr in the laminated top of the sandstone beds, heavy minerals are concentrated by sorting into the parallel laminations (tractional part) at the top of the turbidite. By way of contrast, as we will see later, the geochemical composition of the coarse-grained deposits in channel-fills at Annot is very homogeneous with no evidence of sorting (implying either deposition via progressive aggradation beneath steady, turbulent flows, or en-massive freezing of homogenous, cohesive flows).

The whole sequence is therefore characterised by a global increase in potassium and thorium (with a higher variability at top); this reflects the vertical evolution from fine-grained onlap facies (rich in carbonate mud and close to the paleoslope) to basinal deposits, made of turbidites rich in K-feldspars and covered by shaly mudstone drapes.



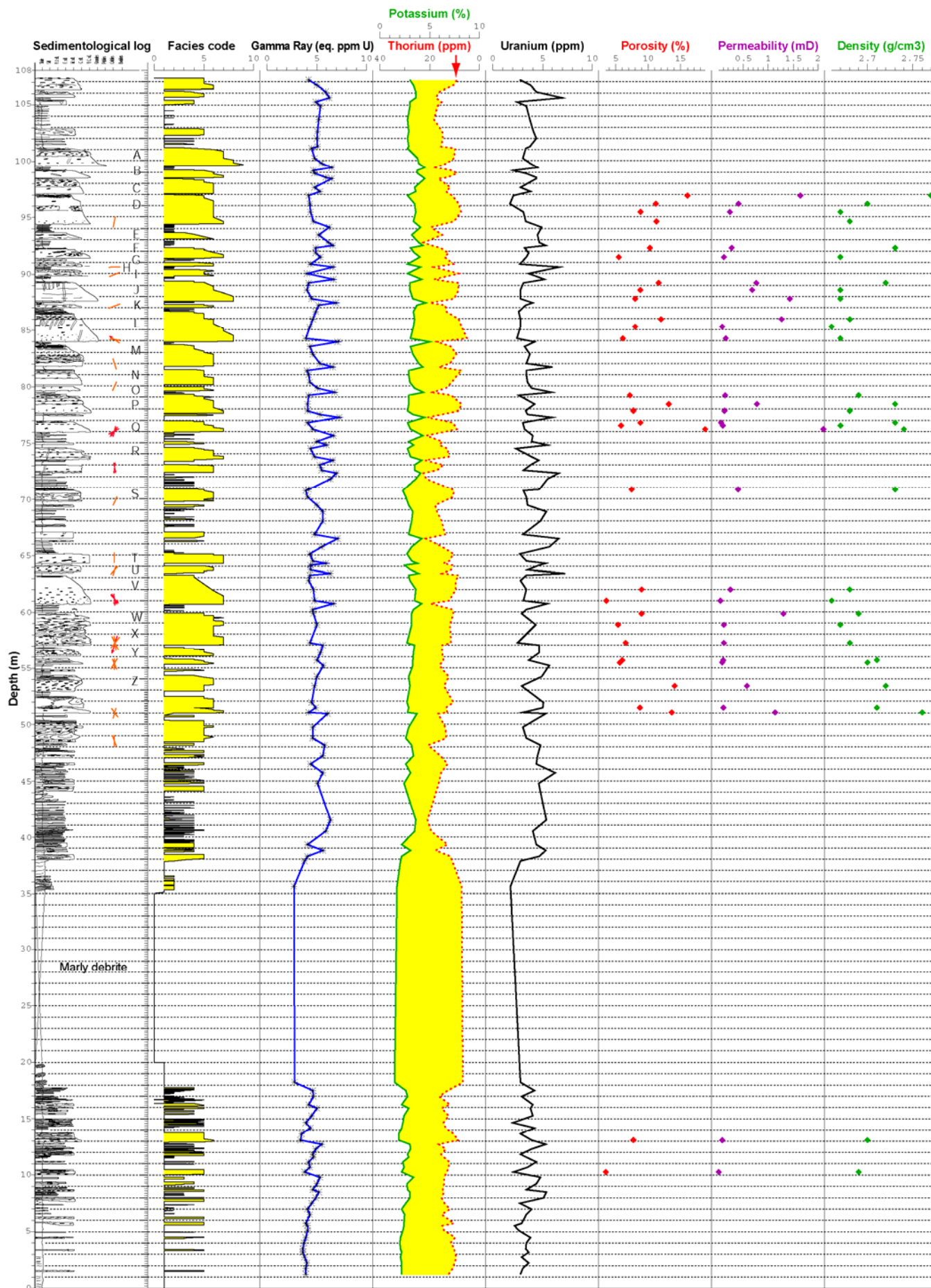


Figure 47 : Log signature of the section of Crête de la Barre (Braux road).

### Stop n° 3 : Panorama of the Gastres megaslump

The turn in the road at the extremity of the Crête de la Barre section enables us to observe the internal organisation of unit **C**, called the Gastres Megaslump, which outcrops along the right bank of the Coulomp (location on Figure 33 p. 42 : view point 3). This lenticular massive unit has a maximum thickness of 100 m (Callec 2004 : Figure 48). Its base may erode the totality of the Upper member of Crête de la Barre (unit **B**) : the Gastres Unit then lies on the Marnes Bleues, but disappears rapidly in a few hundred meters by onlap toward the WSW. The unit is made of microconglomeratic massive sandstone beds, which include granules and centimetre-scale pebbles in a sandy matrix. To the north near Argenton, the size of the elements can reach 15 cm (Callec 2004).

The internal organisation is very chaotic. Callec (2004) distinguishes four zones :

- zones a and c are characterised by large scale folds, interpreted as synsedimentary folds (Stanley *et al.* 1978),
- zone b is marked by a set of oblique faults with an apparent movement toward the north,
- zone d is made of a set of massive sandstone beds.

In a classical way, this unit is interpreted as a gravity megaslump, sliding from south to north. It was probably induced by tectonic activity : in several places we can observe small synsedimentary faults sealed by the conglomeratic body (Figure 49). Puigdefabregas *et al.* (2004) also considers that this unit registered a tectonic event, which suddenly increased the supply of coarse-grained sands and pebbles, and was probably contemporaneous with the arrival of conglomerates at Saint Antonin in the Early Rupelian. However these authors reject the idea of a single gravity slide and consider that the synsedimentary folds were induced by the sudden arrival of very coarse-grained, hyperconcentrated flows, that were able to delaminate and deform the underlying sediments.

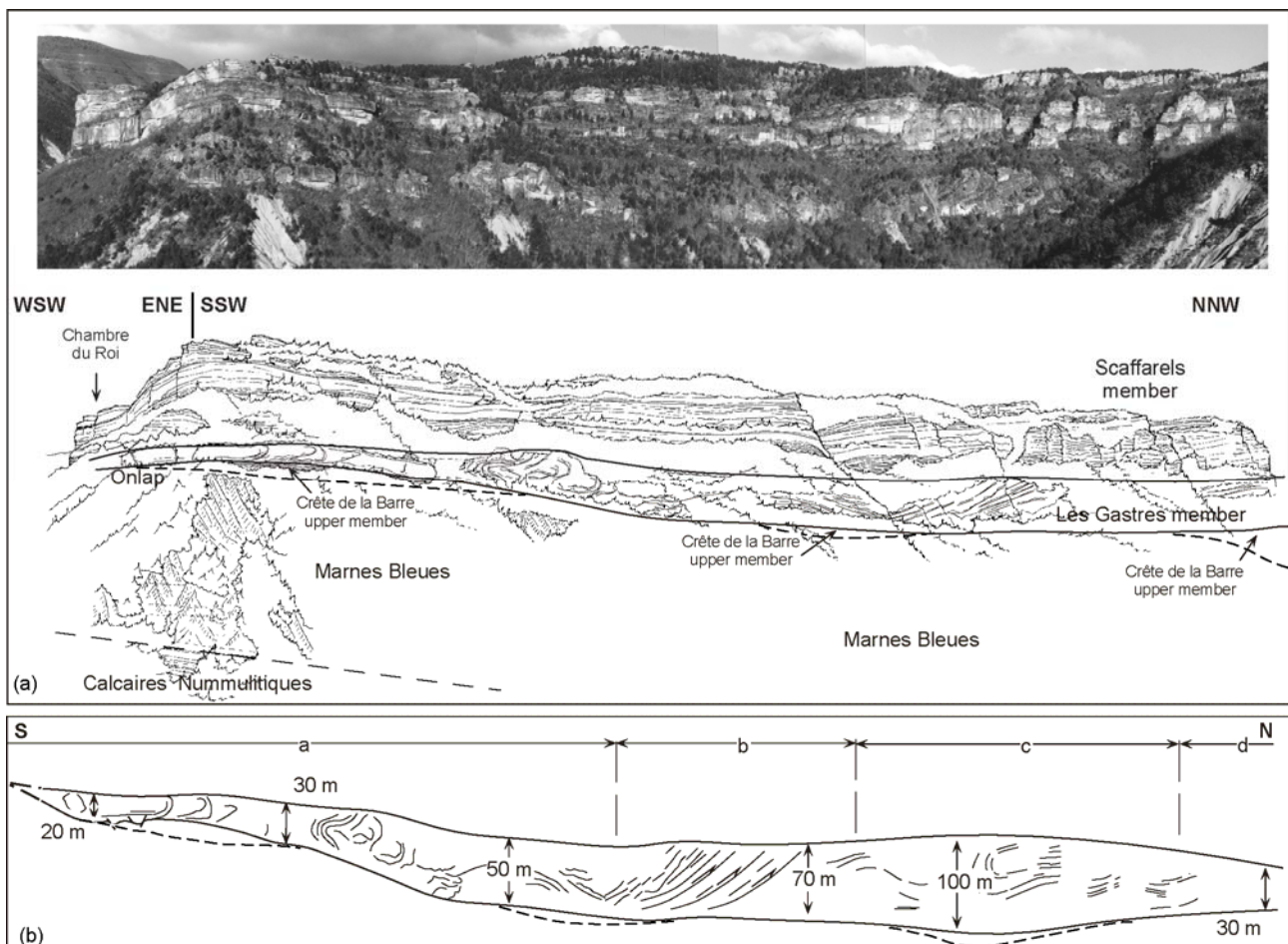


Figure 48 : Panorama of the Gastres megaslump viewed from the Braux road (modified from Callec 2004).



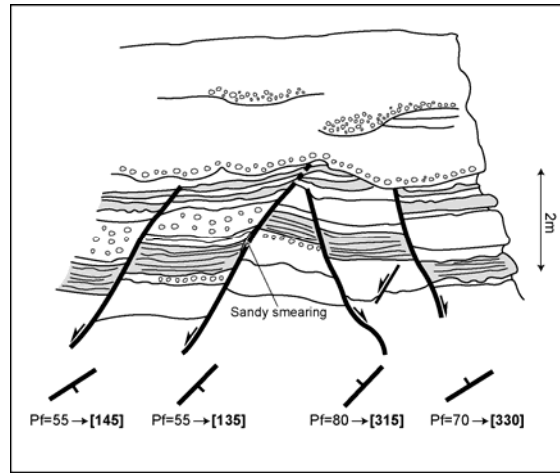


Figure 49 : Synsedimentary faults sealed by the conglomerate body of the Gastres megaslump.

#### **Stop n° 4 : Annot. Transit channels of Scaffarels - la Chambre du Roi.**

The purpose of this field stop is to analyse the 3D large-scale and small-scale architecture of high net-to-gross (97 %) sandstone deposits, which correspond to a proximal channelized transit system, and to discuss the facies in terms of sedimentary processes.

##### **Panorama of the Scaffarels cliff**

The outcrops that are described during this stop correspond to the very well exposed cliffs located east of the town of Annot, above the village of Scaffarels : they are limited to the west and south by the Vaire River, and to the east by the Coulomp River (location on Figure 33 p. 42 : stop C). They are located west of the Braux road section, and lie in a stratigraphically higher position than the Crête de la Barre and Gastres Members (units **B** et **C**) : they correspond to units **D** et **E** of the Scaffarels Members (cf. panorama of Figure 34 p.43).

These cliffs are known as the Scaffarels or Chambre du Roi outcrops. They offer a very good view from three sides and are particularly well adapted for 3D reconstruction of the sedimentary system. The outcrops can be subdivided into five sub-vertical cliffs (Les Espaluns, Les Garambes, La Chambre du Roi, Les Scaffarels and Les Gastres) and in order to avoid image distortion, five photo-panels have been taken in front of each of these cliffs in the dip axis, at a distance of between 1 and 2 km (location on Figure 33). In order to get a global view of outcrop and to facilitate the correlation work, these five photo-panels have been gathered into a general photo-mosaic of the outcrops (Figure 51) : this photo-mosaic shows that the successive sandstone units pinch out by onlap toward the west onto the Marnes Bleues paleoslope. This onlap surface (light blue surface on the figure) is often marked by flute casts that indicate a flow toward NNW (Figure 50).



Figure 50 : Flute casts at the contact between Marnes Bleues and Grès d'Annot (Garambes section).

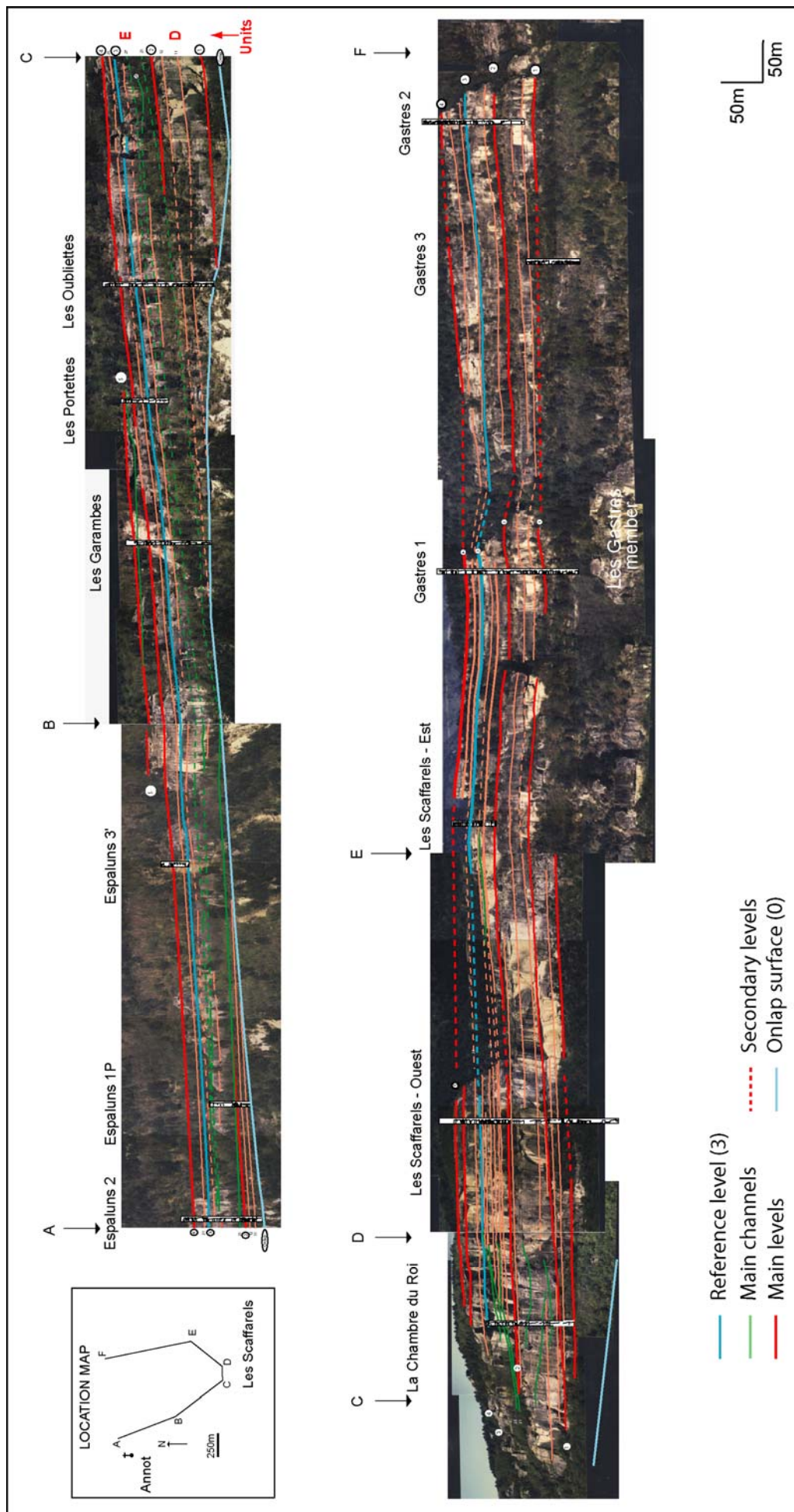


Figure 51 : General panorama of the Annot – La Chambre du Roi outcrops (Joseph *et al.* 2000).

On this photo-mosaic, major correlatable stratigraphic surfaces (in red) and erosion features (in green) have been drawn and the sedimentological sections have been superimposed in order to calibrate the faciological characteristics of each unit.

Continuous surfaces (in red on Figure 51 and Figure 52) may be followed all along the outcrop : they correspond to fine-grained heterolithic levels, which limit the tabular sandstone units (unit **D** between surfaces 1 and 2, unit **E** between 2 and 5). The analysis of enlarged photo-panels (for example La Chambre du Roi - Les Scaffarels taken from view point 4 on Figure 34 p.43) shows inside these tabular sand units the existence of large incisions (several meters deep) which truncate previous deposits. For example, in unit **E** (between level 2 and level 3), the three erosional surfaces 21, 25 and 27 (in green on Figure 52) erode laterally more than 30 m of tabular sandstone beds alternating with heterolithic layers (Les Scaffarels Ouest section) : they are filled with massive coarse-grained sandstone without fine-grained levels.

These incisions have been interpreted by Hilton (1995) et McCaffrey & Kneller (2004) as large scours, locally developed and filled nearly immediately. As they can be followed on several hundreds of meters, we rather consider that they correspond to deep channels that were used for the downstream transit of coarse-grained sediments (Joseph *et al.* 2000, Callec 2004).

The identification and correlation of the main surfaces on the detailed photo-panels enables a schematic general correlation panel of all the sedimentological sections to be drawn (Figure 53). This panel is a 2D developed representation of the correlation along the 3D outcrops, from northwest (Espaluns: A and Garambes: B) to south (La Chambre du Roi: C and Les Scaffarels: D and E) and northeast (Gastres: F). It displays the closure of unit **D** westwards (Espaluns 3 section) and in unit **E** the imbricated channels incising the lateral tabular deposits. The top of this unit is more tabular, with limited channels (Les Portettes section).



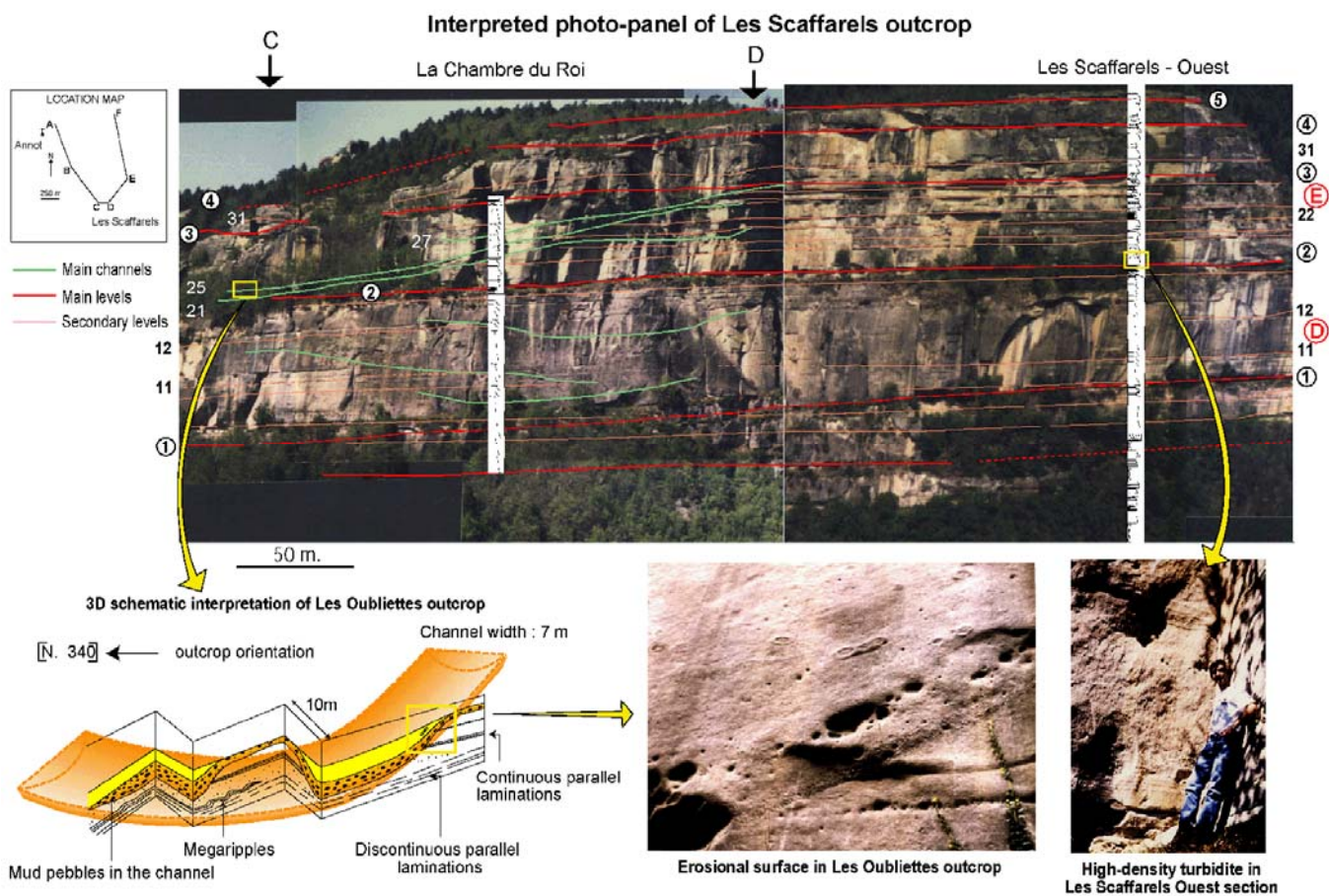


**Figure 52 : Detailed panorama of Les Scaffarels outcrops from view point 4 of Figure 33 (Joseph *et al.* 2000).**

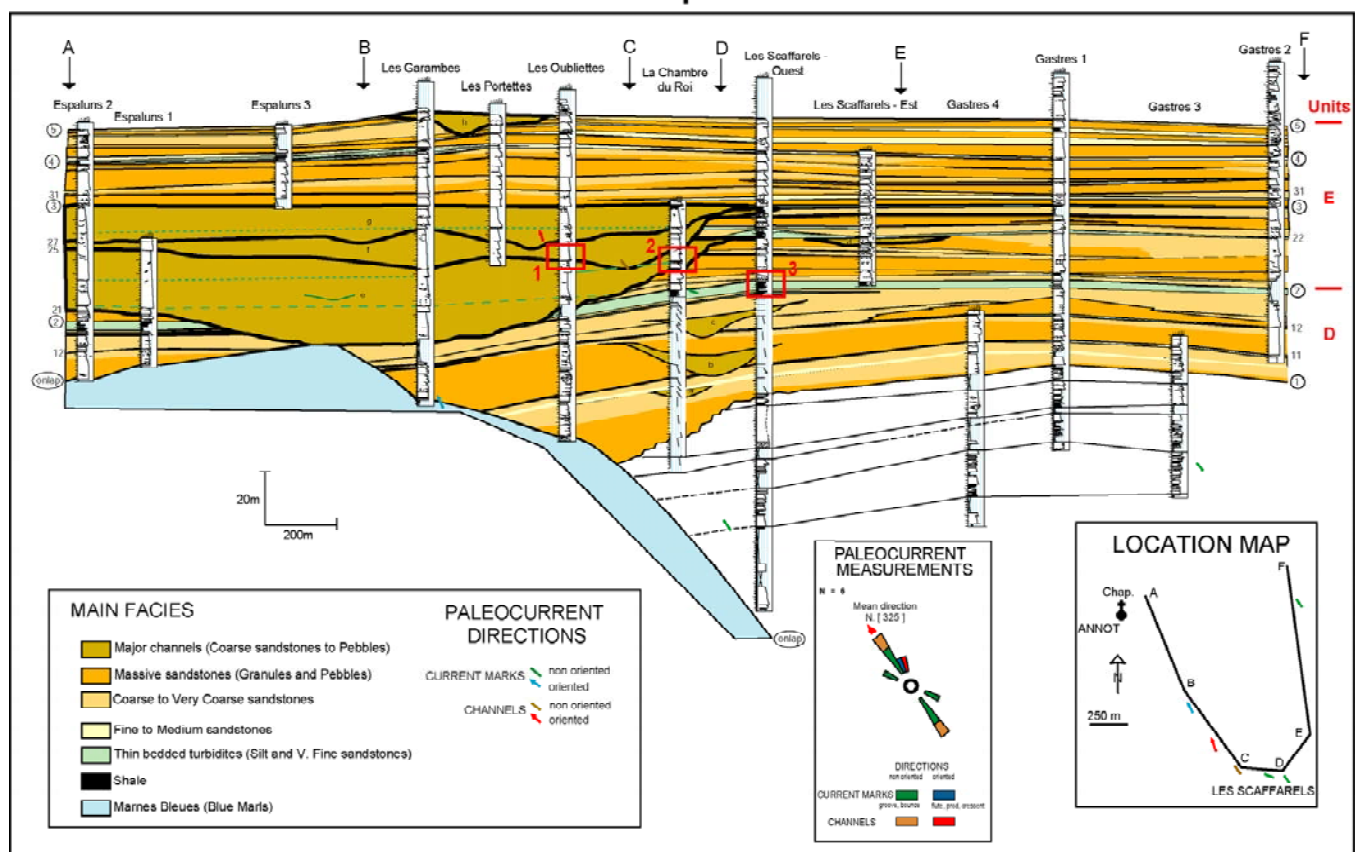


**Figure 53 : General correlation of Annot – La Chambre du Roi outcrops (Joseph *et al.* 2000).**



In order to appreciate the 3D geometry of the sedimentary units, the correlation panel has been reconstructed in 3D space, by putting each cliff at its exact location using the topographic map (Figure 54). This spatial reconstruction allows a better understanding of the geometrical difference between the different panels : the western panel A-C (Espaluns - Garambes) is oriented N330 and parallel to the average current direction N325: this panel is thus parallel to the axis of the erosional channel system and this is the reason why the channels appear very extended in this direction. In contrast, the southern panel C-E (Les Scaffarels) is oriented N 50 and perpendicular to the average current orientation. In this direction, the channels appear very erosive and their borders pinch out very rapidly eastward.

The evolution of the current directions from N290 in La Chambre du Roi in the south to N335 in Les Garambes in the north indicate that the channel was slightly sinuous. It has been mapped up to Le Fugeret, 4 km to the north (Callec 2004). The base of this low-sinuosity channel directly erodes the Marnes Bleues near the Espaluns 3 section and its thickness reaches 45 m. The gravelly material that fills the channels was trapped along the paleoslope, probably because of the deflection of high-density turbidity currents by the onlap surface that was curved (Puigdefabregas *et al.* 2004). This topographic control seems to be reinforced by a progressive gentle deformation from east to west of the substratum during the deposition of the Grès d'Annot, that might induce a westward shift of the depocenter.

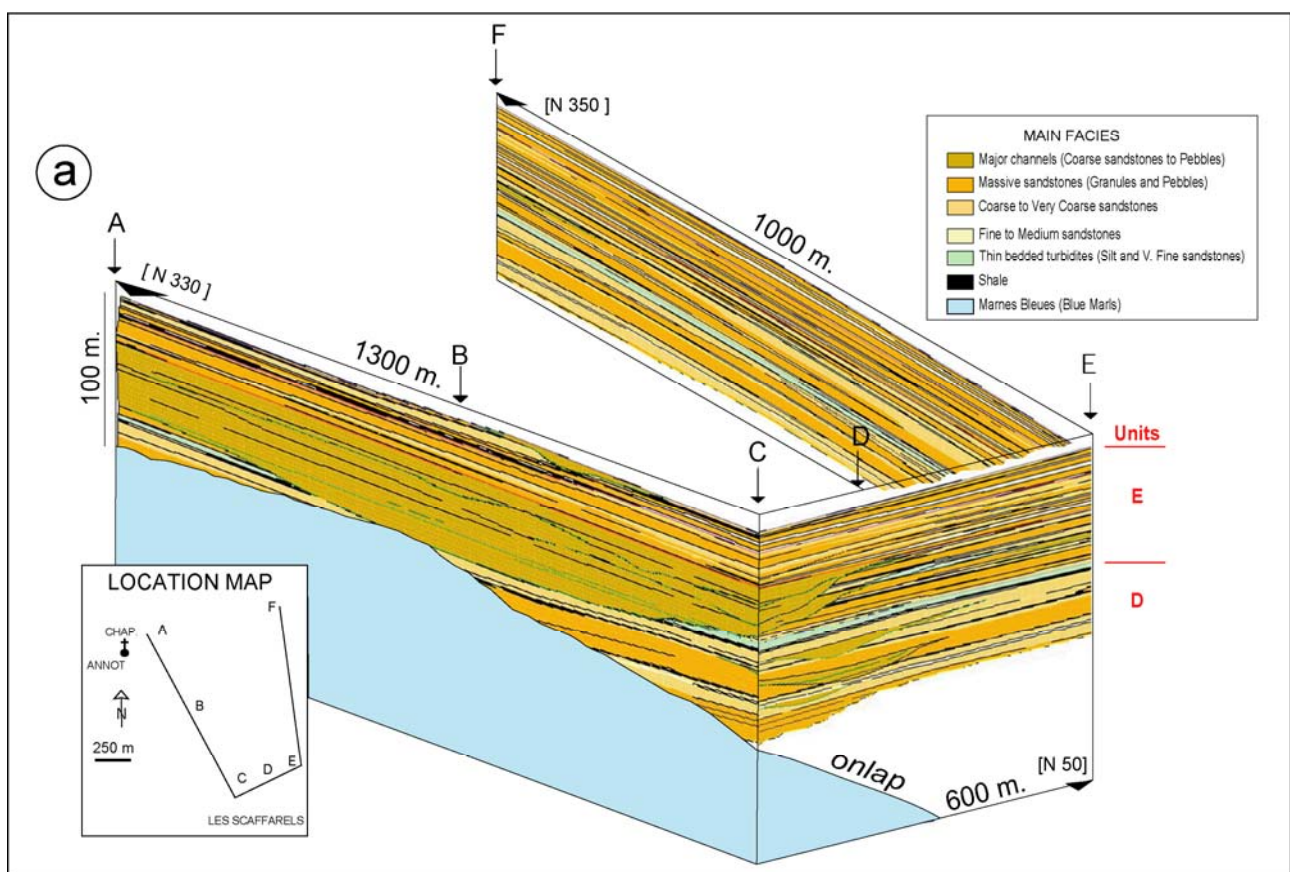


**Figure 54 : 3D reconstruction of the Annot channelized transit system (Joseph *et al.* 2000).**

The outcrops are reached along the path going from the railway station to the climbing area (cf. Figure 33 p. 42). We can observe the whole series, with the onlap contact (base of Les Oubliettes section) that shows a very rapid pinchout of the first sandstone beds onto the Marnes Bleues.

After a poorly exposed set of coarse-grained turbidites corresponding to unit **D**, the outcrops of Les Oubliettes, La Chambre du Roi and Les Scaffarels Ouest reveal the small-scale architecture and the facies filling the transit channels of unit **E** and the lateral tabular units (cf. location on Figure 53).

## Les Oubliettes outcrop – Transit channels

The Les Oubliettes outcrop (located 1 on Figure 53 p. 60) enables us to go inside the massive sandy unit E thanks to a fracture between two blocks : the zigzag trajectory of this fracture allows us to precisely reconstruct the 3D geometry of a channel (Figure 52 : Joseph *et al.* 2000 et Figure 55) : this small channel appears very erosive and narrow (10 m wide by 3 m deep) and weakly sinuous (sinuosity around 1.10). Its average orientation is N340. It truncates a set of very coarse-grained and amalgamated massive beds without shaly interbeds. The bottom of these beds is often erosive and marked by granules and small pebbles. The beds are made of rough planar or wavy laminations, with local development of traction carpets with inverse grading (F4 facies of Mutti 1992). The bottom of the channel is marked by a decimetre-thick level with pebbles and granules, and in the depressions, by the accumulation of shaly mud pebbles that are found in different places of the rock face. It is filled by very coarse-grained massive sandstones, with some dish structures and a weak grading at the top with some parallel lamination Tb. Diagenetic concretions are locally developed (cf. detailed photo of Les Oubliettes in Figure 52). These facies are interpreted as resulting from very concentrated flows (granular flows), partly turbulent at their top (F5 facies of de Mutti 1992).

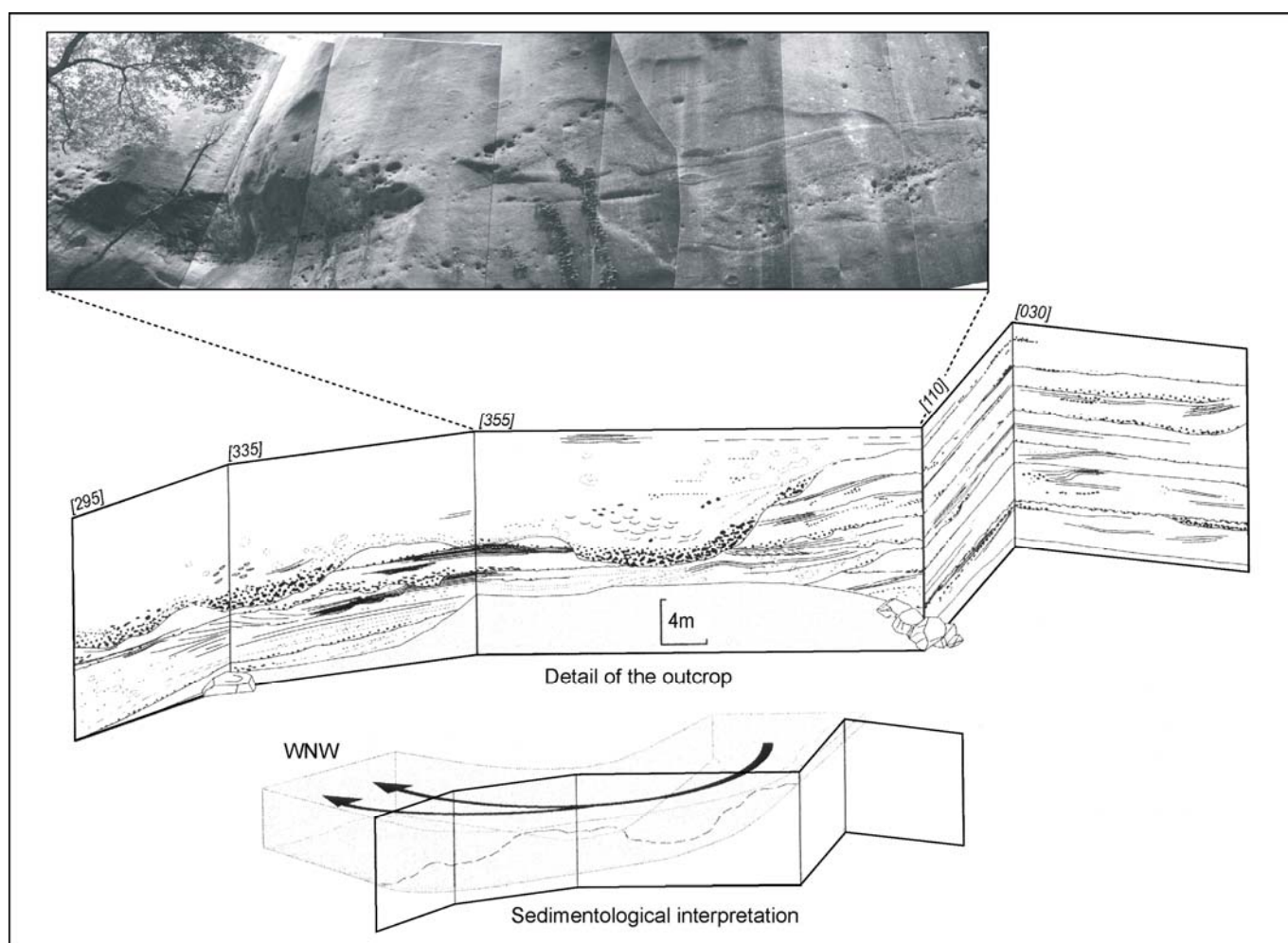


Figure 55 : Geometry of a channel in unit E (photo from McCaffrey & Kneller 2004 ; drawing from Callec 2001).

### Outcrop of La Chambre du Roi – Border of the transit channels

This outcrop (located 2 on Figure 53 p. 60) enables us to observe the facies at the border of a channel (Figure 56). Plurimeter-scale beds show a clear vertical organisation from centimetre-scale pebbles and shaly mud clasts (F5 facies) to medium-grained sandstones (F7 – F8 facies) then fine-grained sandstones with parallel laminations (F9 facies) : these beds are strongly convoluted and truncated by a sharp erosion surface, which preserve some pebbly “pockets” of a former deposit, which was strongly deformed. The upper deposits correspond to sandstones with millimetre-scale gravels.

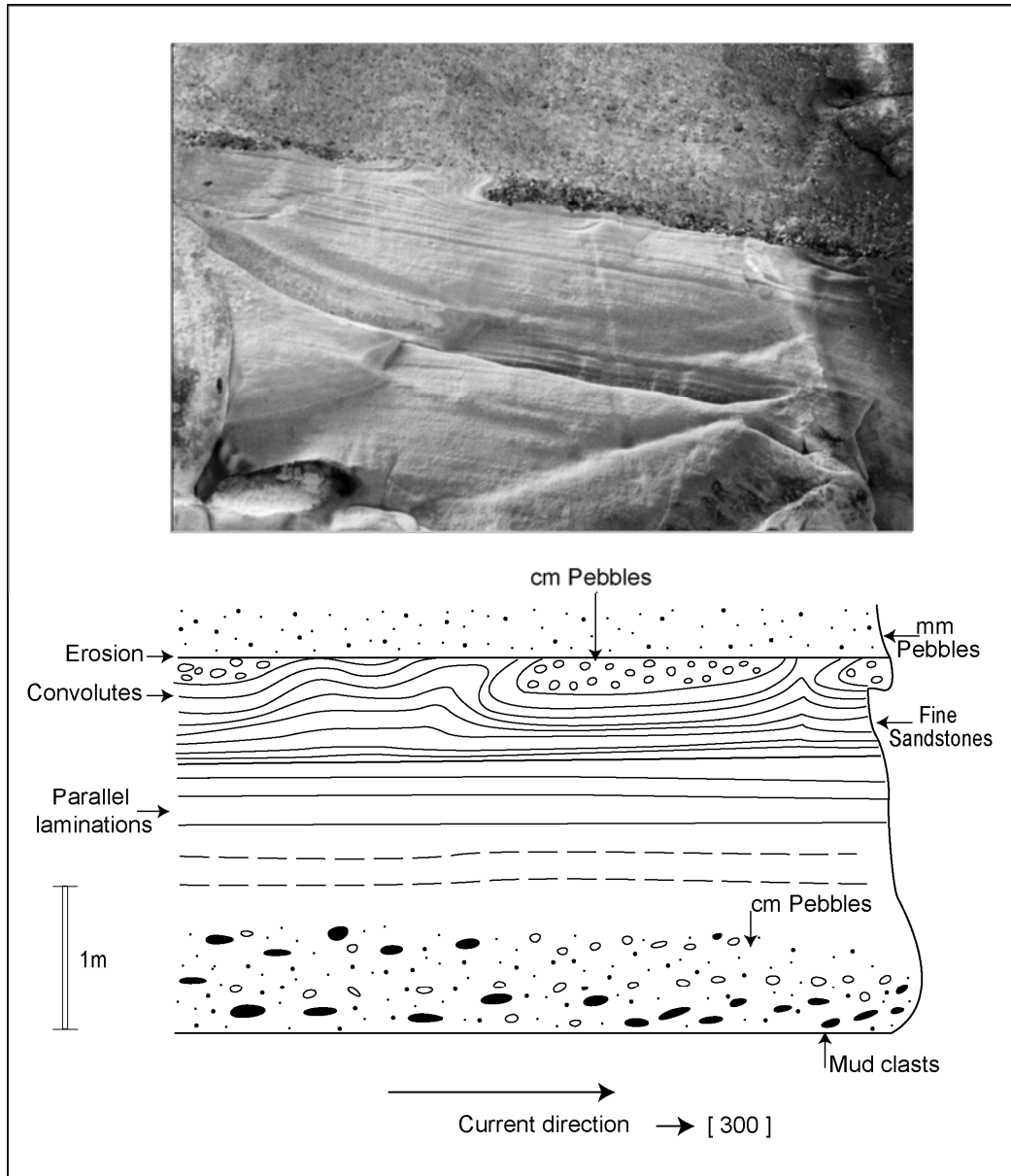


Figure 56 : Internal deformation inside the coarse-grained infill of the channels of La Chambre du Roi.

## Outcrop of Les Scaffarels Ouest – Lateral tabular deposits

This outcrop (indicated 3 on Figure 53 p. 60) is located along the ledge in the middle of the cliff and enables us to observe heterolithic layers interstratified inside the tabular deposits that are lateral to the channelized system (this level is so-called « Les Scaffarels member » by Hilton 1995 : cf. Figure 32 p. 41).

These heterolithic levels are made of decimetre-scale alternances of thin sandstone beds (5 to 40 cm thick) and silty interbeds. The grain size of the sandstones beds varies from medium to fine. These beds are strongly bioturbated and their top surface is rippled. (Figure 57). They display strong thickness variations in a few meters. They are interpreted as low-density turbidites with Tabc or Tbc sequences (F9 facies of Mutti 1992) : they correspond either to overbank deposits from a lateral channel, or to a decrease in the clastic supply linked to the system abandonment.

The sandstone beds are one to several meters thick, with a grain size from small pebbles to fine sand. Their thickness does not vary much and they are often separated by flat joints or shaly interbeds. Some beds are graded (cf. detailed photo of Les Scaffarels Ouest in Figure 52). These beds are interpreted as high-density turbidites (F5 et F8 facies of Mutti 1992).

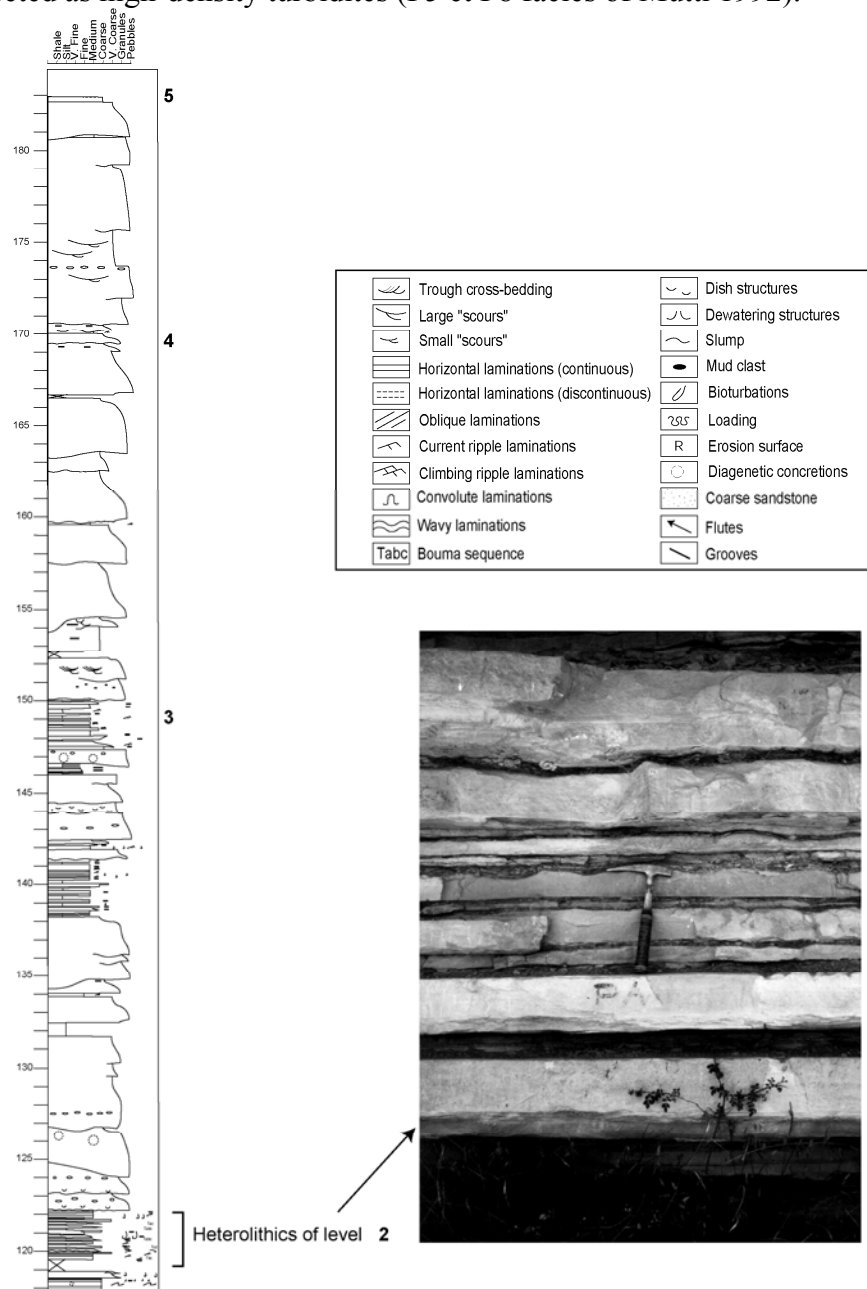


Figure 57 : Heterolithic layers in Les Scaffarels Ouest section (level 2).



## Interpretation in terms of processes

The interpretation of these different facies in terms of processes is very debated. The importance of tractive structures and the weak grading in the fill of channelized systems would indicate a dominance of by-pass and deposition of very concentrated and poorly turbulent flows, which control the transit of coarse-grained material to the downstream area of Grand Coyer and Chalufy, through ephemeral braided channels.

In contrast, the development of high-density turbidites in the tabular sandstone beds would indicate the dominance of depletive turbulent flows that are not channelized and spread as a lobe in the basin. Low-density turbidites correspond to the overbank deposits of a lateral channelized system, or an interruption in sediment supply that stopped system activity.

In the Annot Syncline, the vertical organisation of the whole Grès d'Annot formation records first the filling of the basin by turbidite lobes (these lobes are laterally confined by the paleoslope controlled by the synsedimentary activity of the Braux Fault : units **A** et **B** of St Benoît –Crête de la Barre). After the deposition of the Gastres Megaslump (unit **C**), very concentrated facies infilled erosive transit channels (units **D** and **E** of Scaffarels) : this second phase corresponds to the complete filling of the Annot ponded basin, and the overspill of gravity deposits into the downstream area (Chalufy) through the Grand Coyer trough.

### 3D reservoir and seismic modelling

A 3D model of the geometry of the main sedimentary units (limiting surfaces) have been reconstructed using a geomodeller (GOCAD software). Inside this framework, the facies distribution has been reproduced by using geostatistical techniques (HERESIM software) and enables us to get a complete 3D geocellular model (Figure 58).

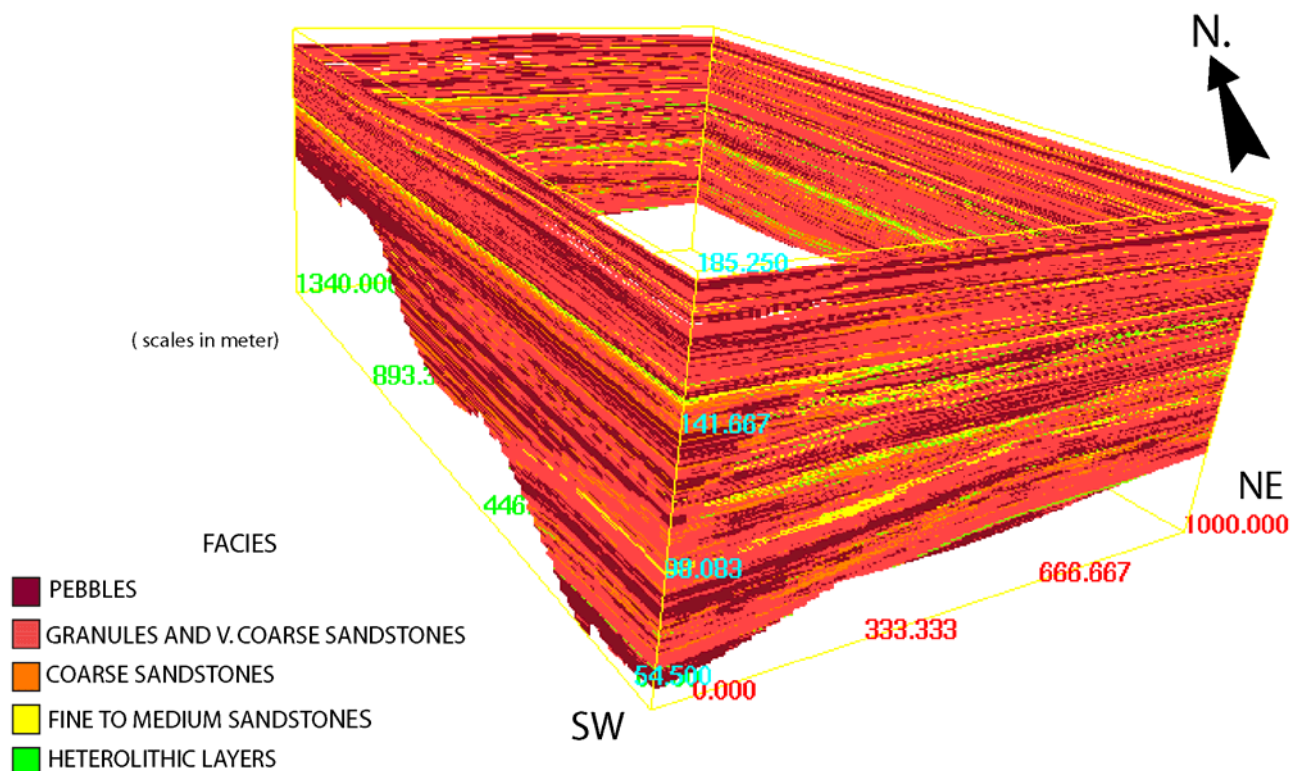


Figure 58: Fence diagram view from the South of the 3D facies geocellular model.

A seismic modelling of this 3D synthetic model has been performed using a 1D convolution of each vertical column of the facies model. Acoustic parameters (velocity and density) have been associated to each facies, by using mean values characteristic of the facies of the PETROBRAS Namorado field (Albian-Cenomanian turbiditic deposits in the Campos Basin, offshore Brazil).

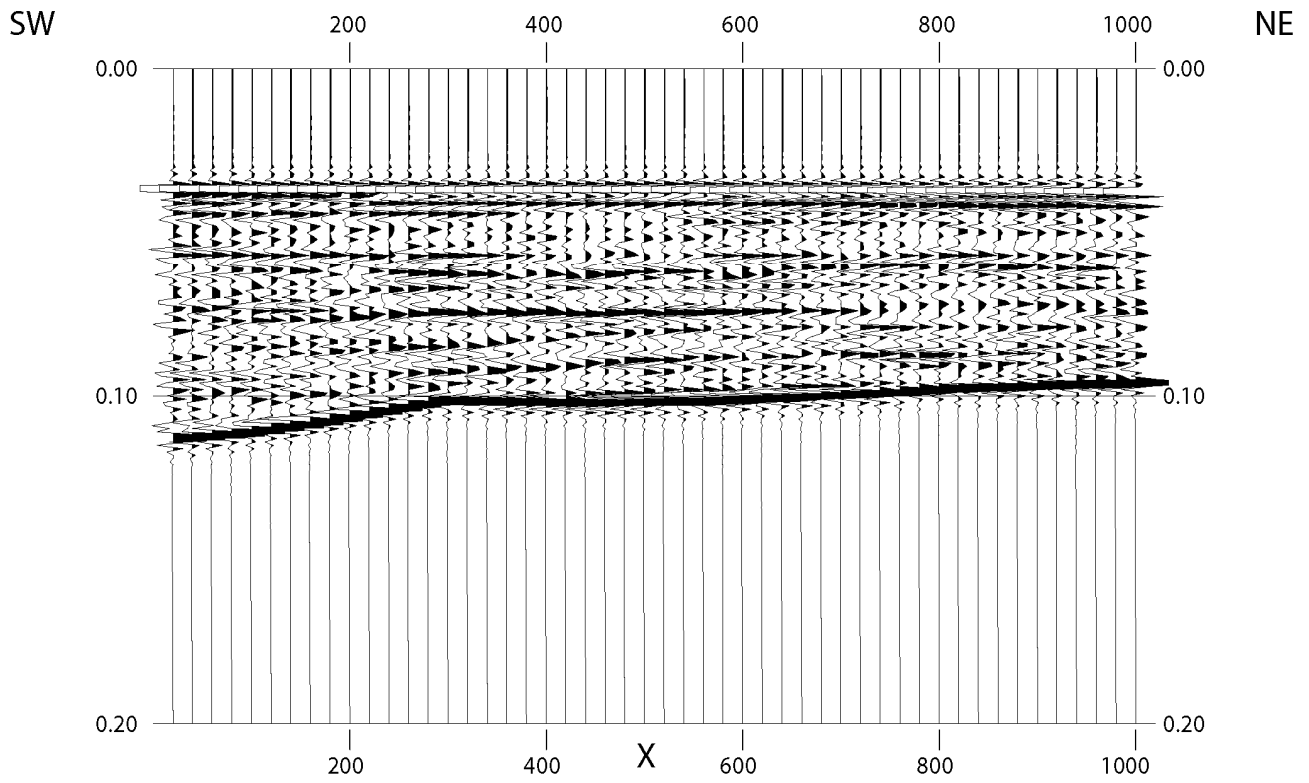
**Table of facies acoustic parameters**

Facies	Vp (m/s)	Vs (m/s)	Density (g/cm3)
shale	3400	1700	2.40
heterolithics	3300	1650	2.25
fine - medium	3250	1625	2.20
coarse	3200	1600	2.15
very coarse - granules	3200	1600	2.15
pebbles	3150	1575	2.10
boulders	3300	1650	2.25
muddy debris-flows	3400	1700	2.30
Blue Marls	3600	1800	2.50

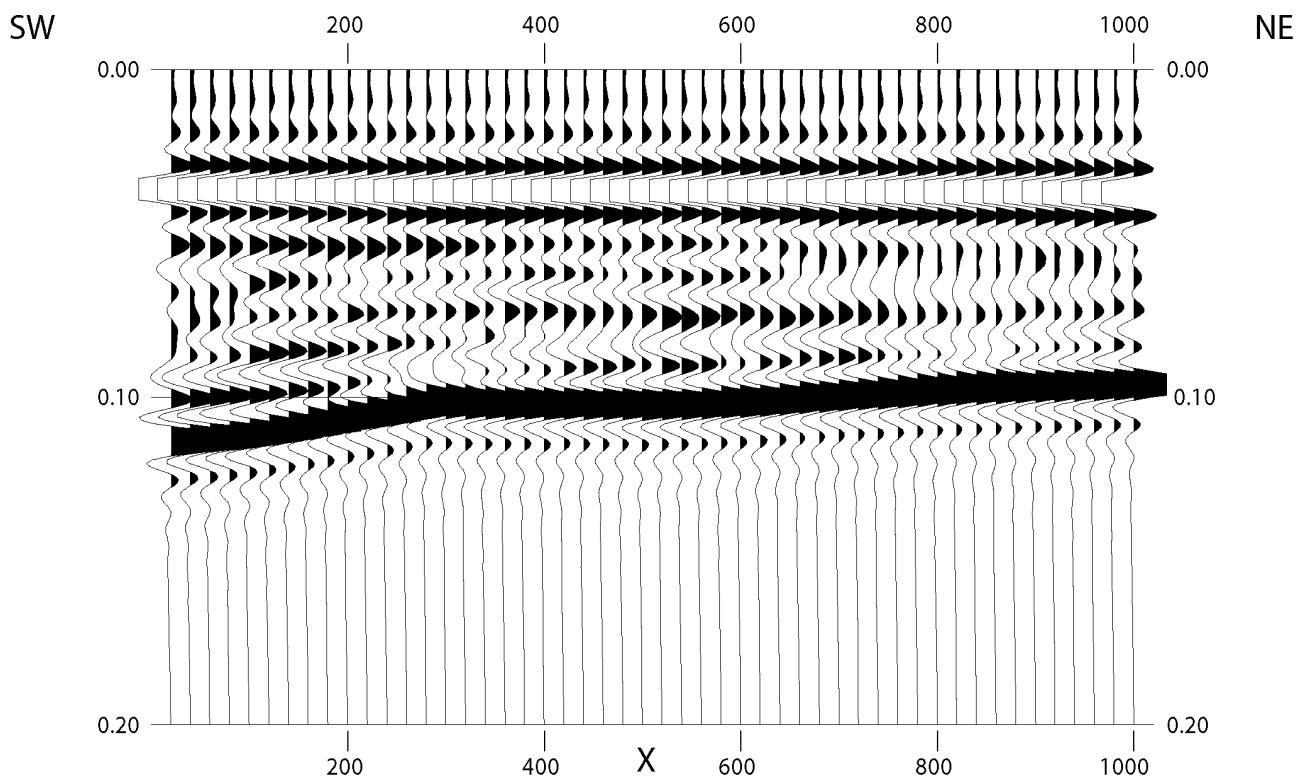
These acoustic parameters enable us to transfer the 3D block in facies into a 3D block of acoustic impedance. Then a 1D convolution of each vertical column has been performed with different frequencies in order to test the resolution which may be obtained : sampling at 1 ms (512 Hz), 2 ms (250 Hz), 3 ms (166 Hz), 4 ms (125 Hz), 6 ms (83.3 Hz), 8 ms (62.5 Hz), 10 ms (50 Hz), 12 ms (41.6 Hz) and 16 ms (31.25 Hz).

Figure 59 and Figure 60 provides the outputs corresponding to the 1 ms (512 Hz) and 4 ms (125 Hz) sampling for the southern border of the 3D facies model (SW-NE section). We can therefore see that if some internal channel fills may be identified on the high-resolution simulation, it is much more difficult on the lower resolution simulation. In both cases, the onlap configuration can be easily identified because of the strong contrast between the Marnes Bleues and the Grès d'Annot.

This complete 3D seismic block can be used to test seismic interpretation (the initial model is perfectly known), or to apply techniques of seismic attributes analysis or seismic inversion methods.



**Figure 59 : Seismic modelling of the 3D facies model (512 Hz).  
SW-NE section.**



**Figure 60 : Seismic modelling of the 3D facies model (125 Hz).  
SW-NE section.**





## **Chalufy**

### **Philippe JOSEPH**

*The third day of this field trip is devoted to the study of the distal part of the Annot and Sanguinière sub-basins which were connected during Rupelian times. the Chalufy outcrops are located on the southern margin of the Trois Evêchés Massif , at equal distance between Allos et Digne-les-Bains (location on Figure 3 p. 11).*

*During this day, we will study different depositional architectures (tabular lobe and large incision features) and we will study different modalities of onlap of the sandy lobes on the Marnes Bleues paleoslope : in particular we will discuss the impact of the different types of gravity flows on the internal architecture of turbidite wedges at the slope border and the related facies.*

### **General geological framework**

The Chalufy outcrops are located 6 km north of Thorame Haute village and 23 km Northwest of Annot. They can be accessed from La Valetta village by climbing the steep Ravin des Raichas (Figure 61) path. The duration of the climb is around 1h30.

From Sommet de Denjuan to Défens des Barres, the southern flank of Montagne de Chalufy enables us to observe, along 3 km, the spectacular onlap of the Grès d'Annot onto the Marnes Bleues paleoslope. This paleoslope can be continuously traced to the north over 30 km along the Trois Evêchés massif, up to Dormillouse : the lower levels of the Grès d'Annot Formation progressively appear, with a cumulative thickness of up to 1200 m (Ravenne *et al.* 1987).

During the Priabonian and Rupelian, the Chalufy area corresponded to the southern border of the Trois Evêchés sub-basin, which constituted the downstream successor depocentre (and merging) to both the northern Sanguinière sub-basin and the southern Annot sub-basin (Figure 18 p. 25). These basins were connected during the Rupelian (unit C), after the overspill of the Grand Coyer trough (Figure 12 p. 21).

The outcrops are NW-SE oriented and oblique to the paleocurrents (average orientation N280). A path from Cabane de Chalufy to Colle Meyère allows us to observe the onlap evolution.

### **Stop n° 1 : Panorama of Peymian. General architecture of the series.**

The panorama from Sommet de Peymian (2156 m : view point 1 of Figure 61) enables us to have a general overview of the exposures (Figure 62) : at their base, the onlap of the Grès d'Annot onto the Marnes Bleues can be continuously traced over 3 km south-eastward. The Grès d'Annot Formation is characterised by the alternance of sandy units (up to 100 m thick) and pluridecameter-scale levels made of shales and heterolithic sandstone beds. The overall net-to-gross is around 55 %, much less than the equivalent deposits in Annot (97 %) and Grand Coyer (81 %). The Marnes Bleues and the bottom of the sandy formation are dated as Upper Priabonian (zone P16), and the rest of the sandstones is dated Lower Rupelian (zone P18-NP21 : du Fornel 2003). They are contemporaneous with the upper deposits in Annot.

Four sandy units (C, C', D et E) may be correlated along the outcrop (Figure 63), despite a network of faults that can cause a strong shift of the series. These sandy units correspond to the 4<sup>th</sup> order depositional sequences that have been identified at Saint Antonin and Annot.



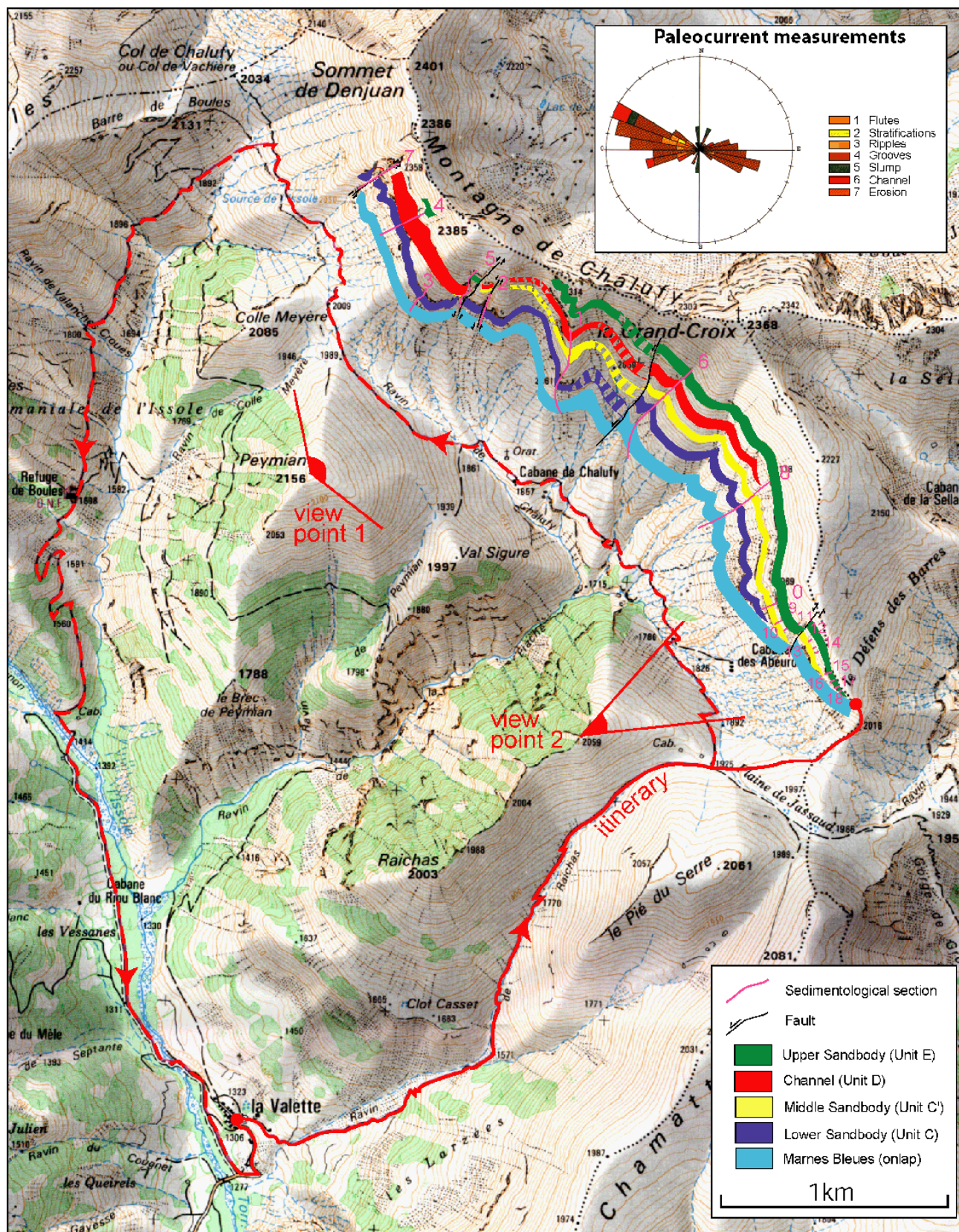


Figure 61 : Itinerary and simplified geological map of the Chalufy outcrops (modified from Joseph *et al.* 2000). View point 1 corresponds to the general panorama from the Sommet de Peymian (Figure 62) and view point 2 to the detailed panorama of Defines des Barres (Figure 66).



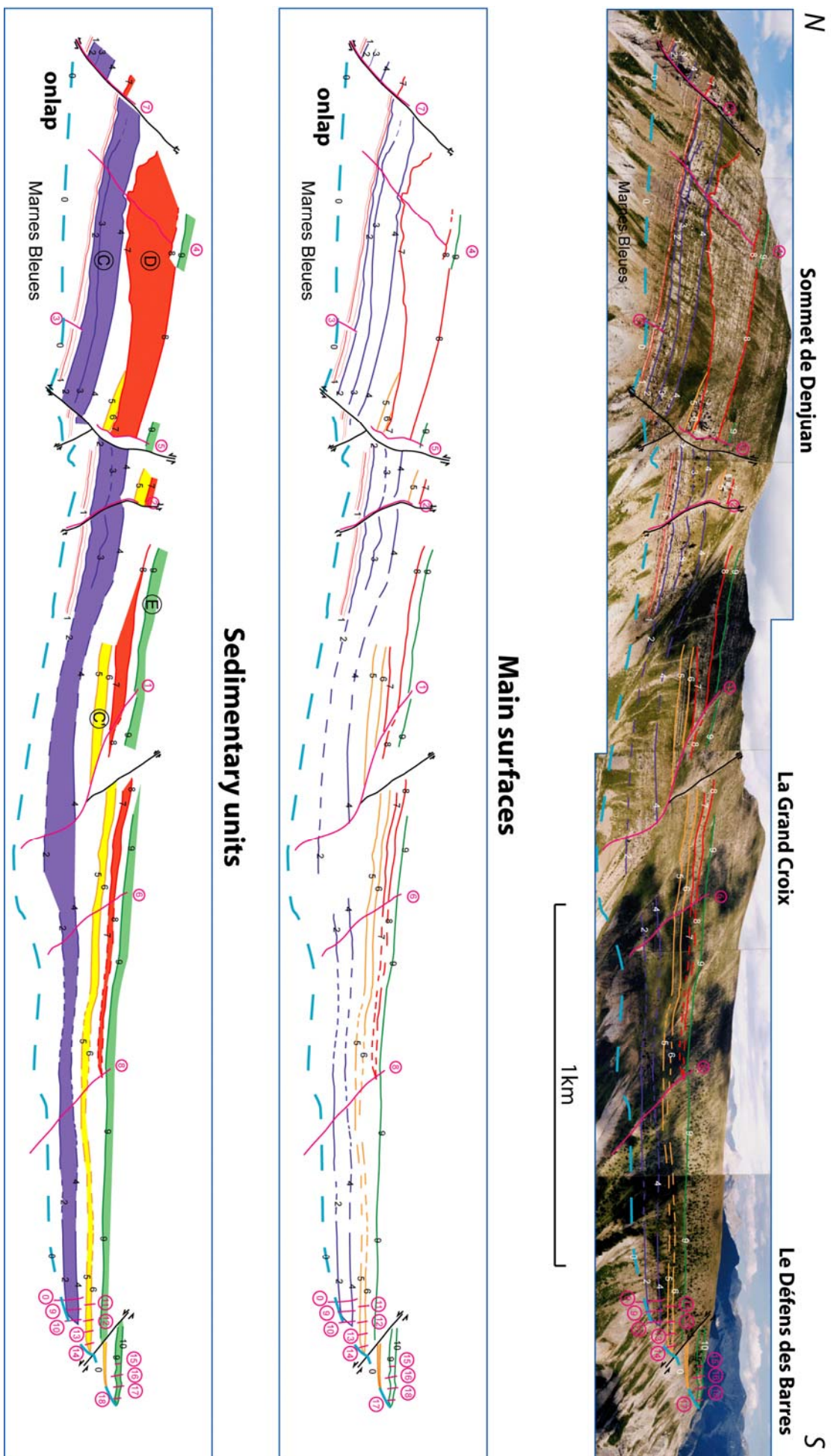


Figure 62 : General overview of the Chalufy outcrops from Sommet de Peymian (Joseph *et al.* 2000).

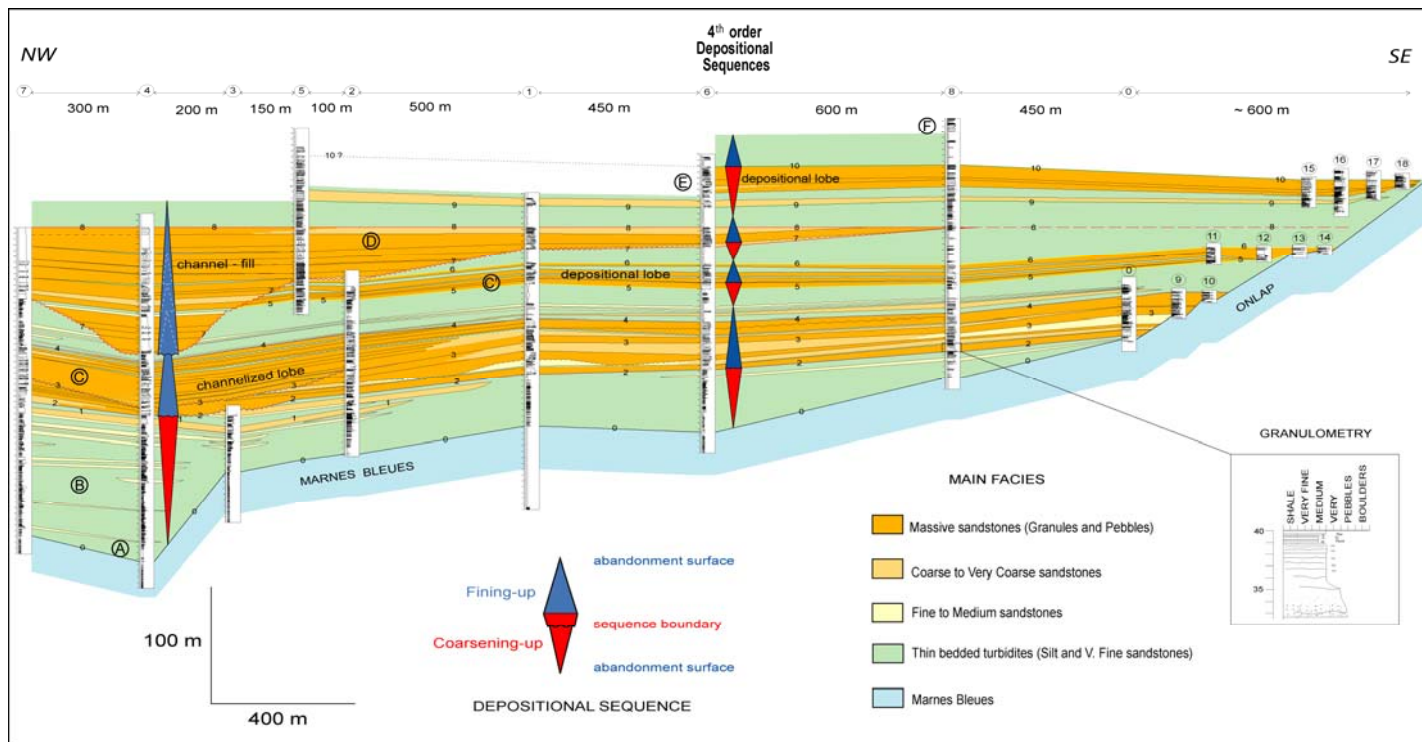


Figure 63 : General correlation of the Chalufy outcrops (Joseph *et al.* 2000).

As shown on the correlation panel, the most spectacular feature of the outcrop is the development at its north-western border, below Sommet de Denjuan, of a very big incision infilled with onlap by very coarse-grained tabular gravity flows (red unit **D** on Figure 62 and detail on Figure 64). This incision is 500 m wide and fully truncates the underlying heterolithic levels, and another sandy tabular unit (orange unit **C'** on Figure 62). This incision reaches a depth of one hundred meters, but the sandstone units which filled it pinch out completely over 2 km (see red unit **D** on Figure 62).



Figure 64 : Megachannel below Sommet de Denjuan (unit D).



Because of the abrupt border of the incision and the lack of overbank deposits, this "megachannel"-like feature is tentatively interpreted either as the result of a sudden cut-off (large scour), or an erosive scar induced by gravity sliding on the slope. The base of the fill of the incision is made of a gravel-rich matrix-supported debris-flow, with numerous pebbles and mud clasts (Figure 65), then by graded and very coarse-grained sandstones with granules. The Chalufy "megachannel" is characterised by a progressive filling (without major erosion) of the depression by very well developed (10 to 20 m thick) tabular deposits, which aggraded vertically. Dominant facies are hyperconcentrated flows (F4 and F5 facies of Mutti 1992). The filling of this incision differs notably from the multiple scour-and-fills of the channel system at Annot (which induced bed amalgamation).



**Figure 65 : Detail of the basal filling of the Chalufy megachannel (debris flow).**

The three other sandy units are more tabular and pinch out onto the onlap surface (Figure 63). Because of its grain size (very coarse sand to granules) and of the multiple internal erosion features, the first unit **C** is interpreted as a channelized lobe. The two other units **C'** et **E** are made of thinner beds (10 to 50 cm), less erosive and finer-grained : dominant facies are F6 (tractive megaripples) and F7 – F8 (high-density turbidites). These units are interpreted as more distal depositional lobes.

Thick shaly levels correspond to abandonment periods of the lobe activity. Four depositional sequences (55 to 100 m thick) can be identified (Figure 63) : they are limited by the thick shale-rich levels and each of them show a coarsening-up than a fining-up trend. They are correlated with the 4<sup>th</sup> order depositional sequences ((**A** to **E**) that have been identified at Saint Antonin and Annot (du Fornel *et al.* 2004).

Channel-fills and channelised lobes contain a larger amount of high-density gravity flows (hyperconcentrated flows and turbidites) compared to depositional lobes which are richer in low-density turbidites. In particular, channel-fills and channelized lobes seem to be characterised by well-developed fining-upward genetic sequences with a complete evolution of facies, whereas depositional lobes display a coarsening upward trend, with a more blocky pattern, symmetric genetic sequences, and a clear bimodality of the facies (very coarse to pebbly sandstones dominant on one hand, heterolithics on the other hand, the fine to coarse sandstones being very little developed). This may be due to density stratification in the flow, inducing a flow decoupling between the high-density and the low-density fractions (Sinclair, 1994; Kneller and McCaffrey, 1999).

## Stop n° 2 : Panorama of Défens des Barres. Geometry of the onlap.

The panorama taken from Crête du Raichas, in front of Cabane des Abeurons and Défens des Barres (view point 2 of Figure 61 p. 70) enables us to study the onlap configuration of the different sandy lobes on the Marnes Bleues paleoslope (Figure 66). Detailed views and correlation panels allows us to develop an interpretation in terms of processes and facies.

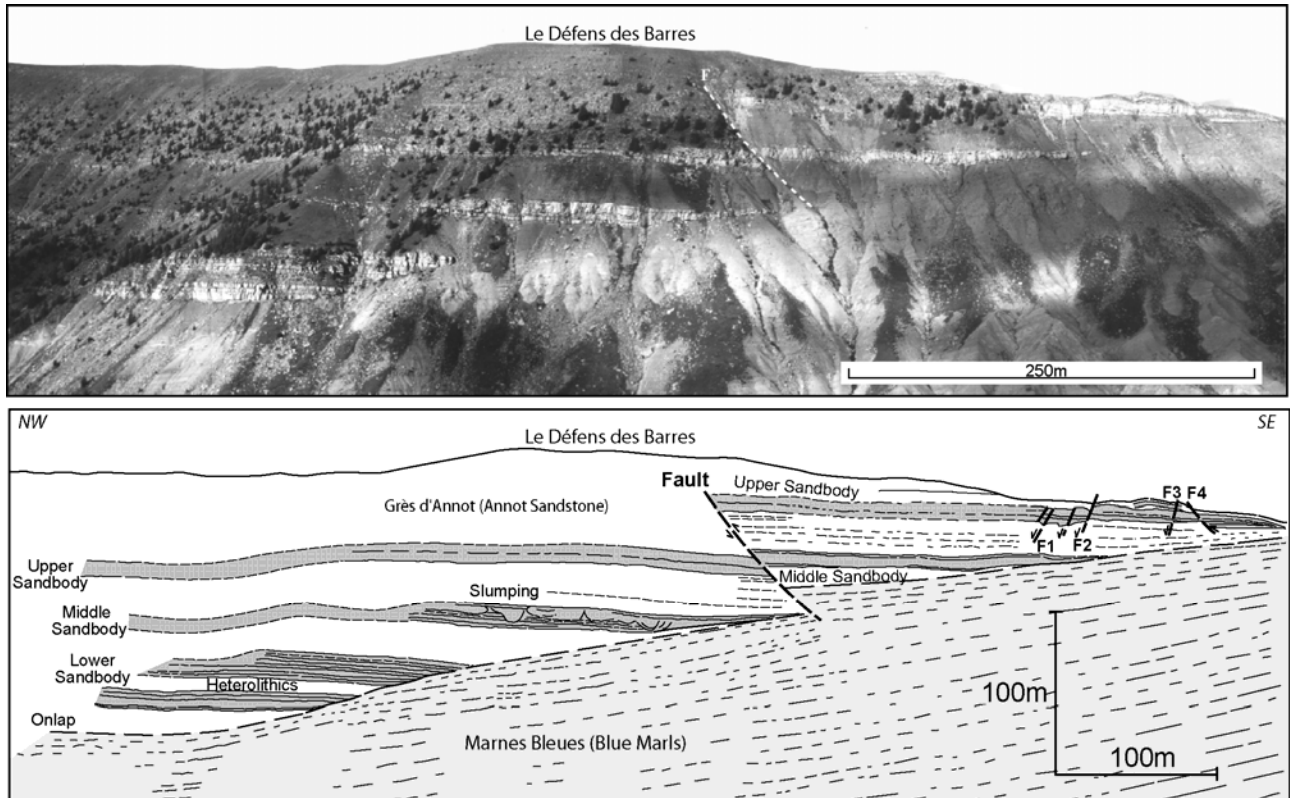


Figure 66 : Panorama of Défens des Barres.

The three sandstone units are displaced by an important fault : this fault appears to be inverse, but is, in fact, a near vertical normal fault, very oblique to the outcrop plane (Figure 67 : Puigdefabregas *et al.* 2004). On the right hand side (south) of this fault, the upper unit is affected by numerous small faults (F1 to F4 on Figure 66). The three units show very different onlap geometries.

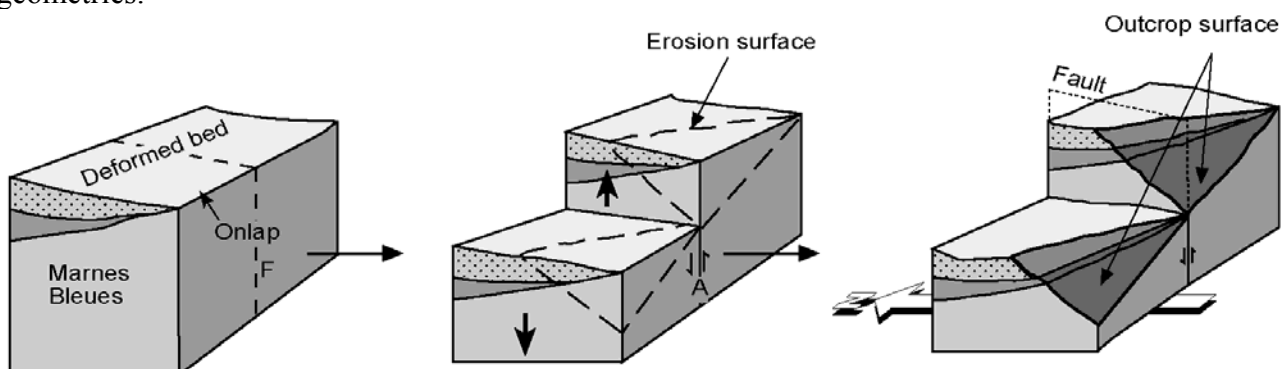


Figure 67 : Reconstruction of the Défens des Barres fault, in Puigdefabregas *et al.* (2004).

The Lower Sandbody of Figure 66 corresponds to the lateral evolution of the first channelized lobe (unit C). This sandbody is made of a set of regular sandstone beds alternating with siltstones, which may be easily correlated from one section to another (except for the beds at the top which seem to be eroded). These sandstone beds of great lateral continuity thin abruptly (within a

few meters) onto the onlap surface and rest directly on the Marnes Bleues which has an important dip ( $20^\circ$ ).

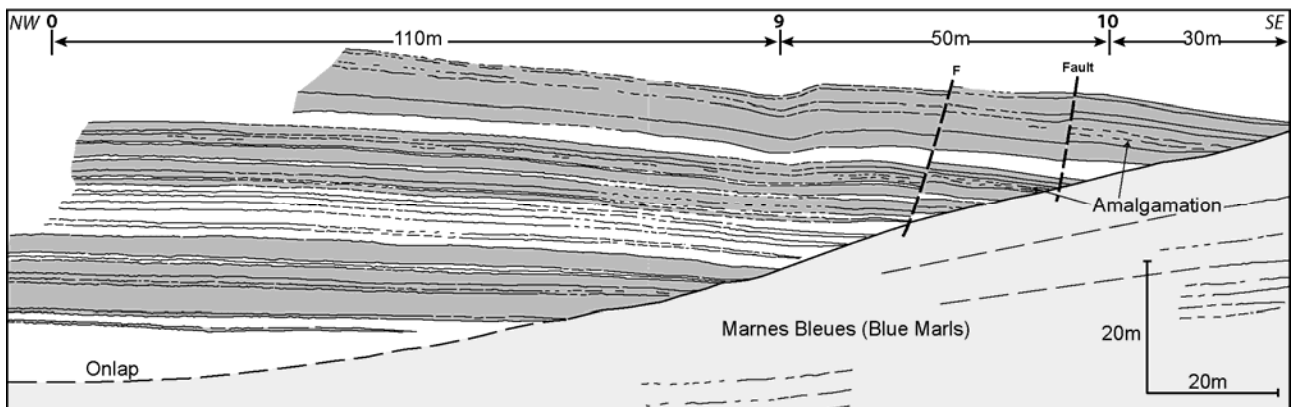


Figure 68 : Onlap of the Lower Sandstone body of Chalufy (unit C).

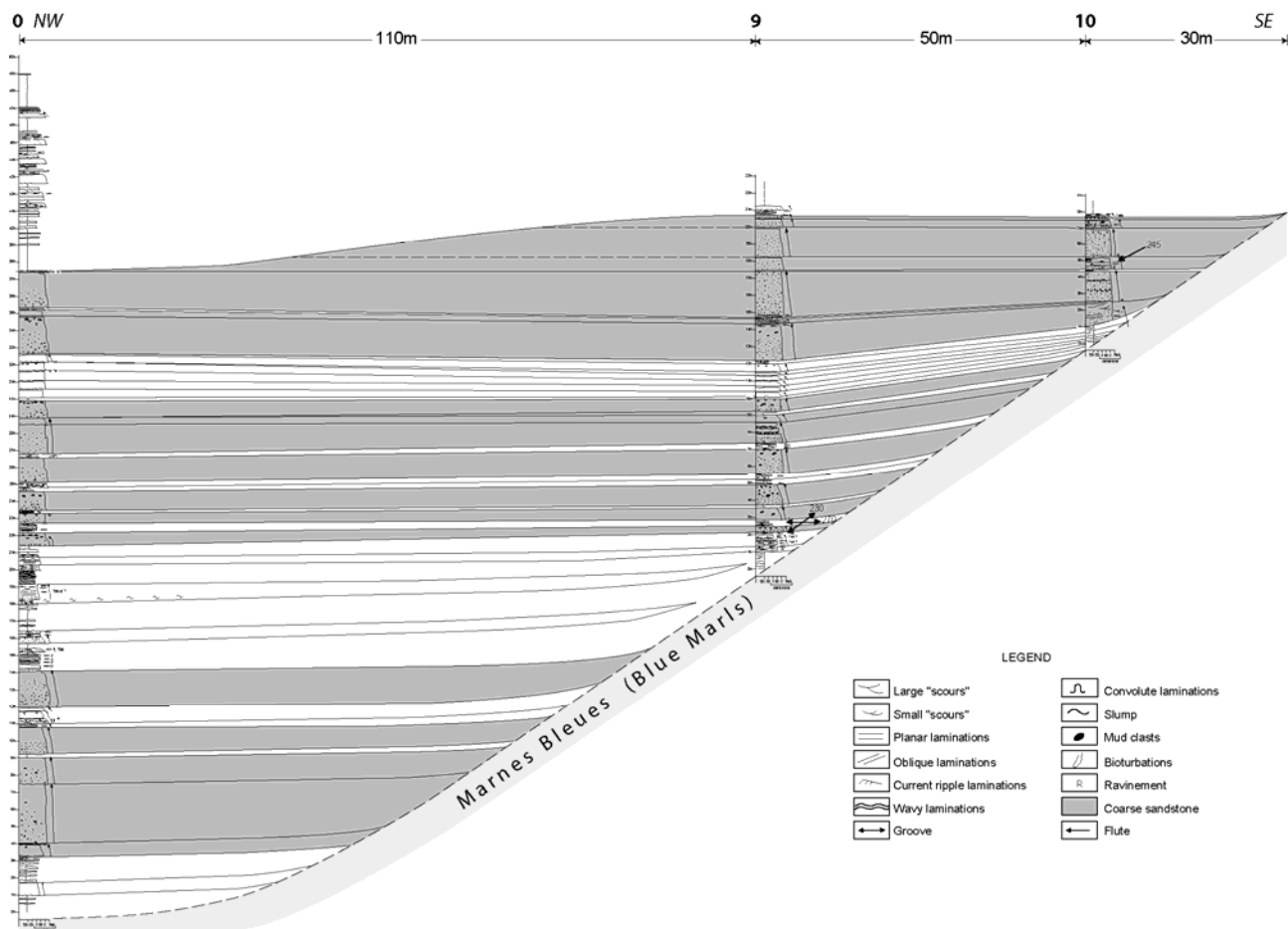


Figure 69 : Detailed correlation of the Lower Sandstone body of Chalufy (unit C).



Facies comprise mainly coarse-grained thick layers with granules and interstratified horizontal mud clasts. Thick beds are generally ungraded, except at the top, and they display internal dish structures (Figure 70). Very few erosional sole structures (grooves) can be found on their bases. These beds were probably deposited under very dense laminar flows, with little turbulence (except at the top). Thinner beds in the middle of the sand package correspond to fine-grained low-density turbidites with Bouma sequences. This Lower Sandbody displays no strong evolution of bed thickness and facies except in the immediate vicinity of the onlap slope. The weak turbulence and the limited thickness of the dense flow may explain the impossibility for the flow to drape the slope and the abrupt pinchout of beds. The lack of erosion (as scours) and the presence of continuous mudstones at the top of each sandstone bed induce a poor vertical connectivity between the thick sandstone beds.



**Figure 70 : Hyperconcentrated deposit with dish structures in the Lower Sandbody of Chalufy (unit C).**

The Middle Sandbody corresponds to the lateral evolution of the first depositional lobe (unit C'). This sandbody is made of two parts (Figure 71) :

- the lower part is made of a tripartite bed including a muddy debrite with abundant mud pebbles (« slurry »), which is interstratified in a high-density turbidite. This basal unit pinches out toward the onlap and is eroded by the upper slump,
- the upper part is very coarse-grained and entirely made of a 10 m thick slump, with spectacular symsedimentary folding (Figure 72) ; this slump evolves laterally into a massive sand unit (high-density turbidite), which onlaps directly onto the Marnes Bleues and drapes the paleoslope. The slump corresponds to wet-sediment deformation. It was probably induced by local sliding of unstable turbidite deposits at the border of the paleoslope. Internal erosion and sliding cause an increase in thickness of the reservoir body near the slope and a connection between the two sand layers.



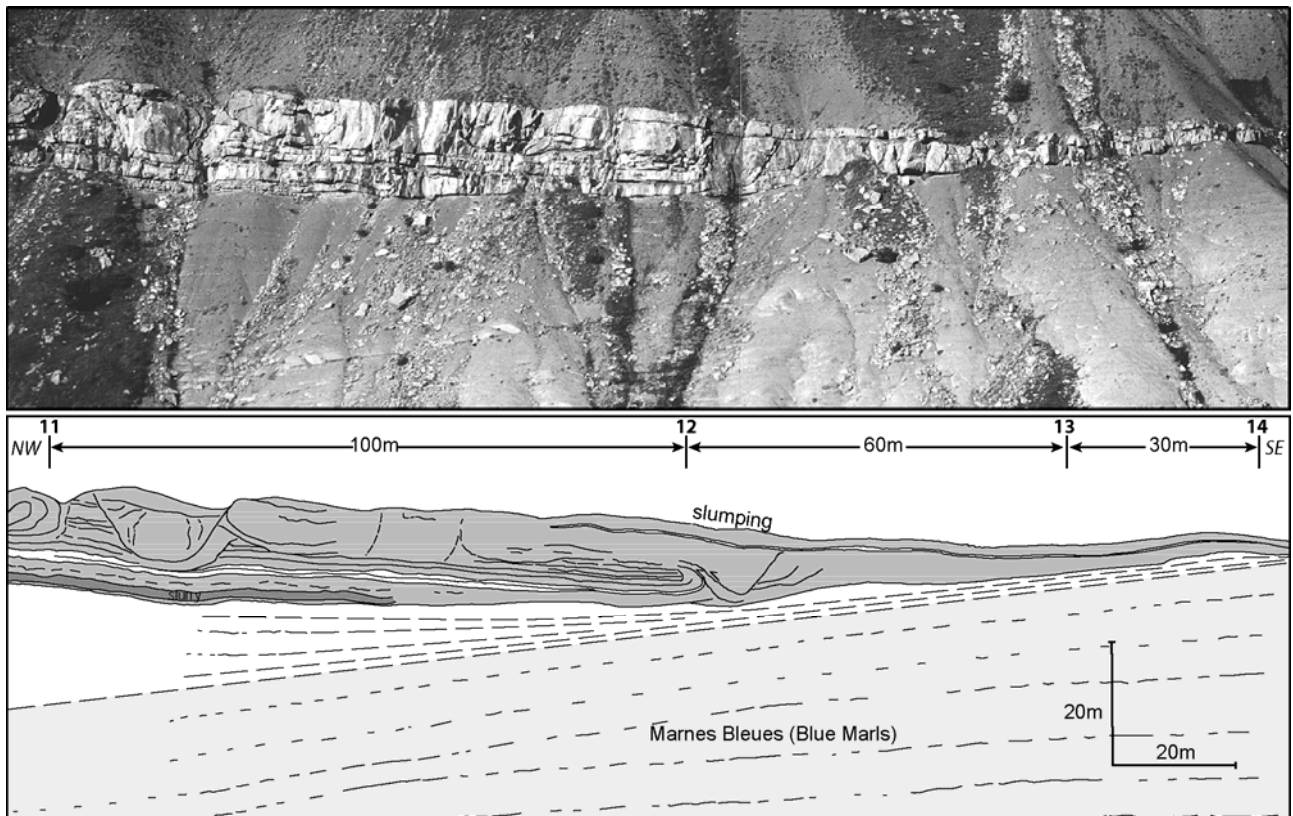


**Figure 71 : Onlap of the Middle Sandbody of Chalufy (unit C').**



**Figure 72 : Detail of synsedimentary folds (slump) at the onlap border of the Middle Sandbody (unit C').**

**Stop n° 3 : Detailed organisation of the Upper Sandbody – Interaction of gravity flows with the topography.**

The Upper Sandbody corresponds to the lateral evolution of the second depositional lobe (unit **E**) and is much more heterogeneous than the previous ones (Figure 73).

The lower part is shaly and made of thin-bedded Bouma sequences, alternating with siltstones and small argillaceous slumps (Figure 74). The thin-bedded low-density turbidites (Tb, Tbc, Tc : Figure 75a) pinch out very progressively toward the onlap and they drape the paleoslope. The thickness of the slumps also diminishes rapidly toward the onlap surface.

The upper part is sandy and made of massive sandstone beds, which are amalgamated and mud-clast rich (evolution up into a "slurry"). The thickness of these sandstone beds shows very rapid variations due to internal erosion and internal amalgamation, which makes it difficult to correlate from bed to bed. The medium-scale sandstone beds are characterised by a better developed grading from coarse to medium or fine sandstone (Ta, Tab sequences : Figure 75b) and the development of erosional sole structures such as flutes indicates that the flows were fully turbulent. The thickness of the sandstone beds progressively diminishes toward the onlap surface and some beds pinch out before reaching the Marnes Bleues paleoslope (that has a dip of 10°). The thickness of the whole sandbody decreases strongly several tens of meters before the contact with the Marnes Bleues. These facies are characteristic of relatively thick turbulent flows that are able to drape the slope and to settle their finer-grained fraction.

The first massive sandstone bed (Figure 74 et Figure 75c) displays a lateral evolution from a « slurry » very rich in mud clasts to a massive bed with a graded top, then to a thin bed with tractive structures (planar or low-angle oblique laminations) close to the onlap surface : this evolution indicates a transition from a turbulent dense flow (with an intercalated debrite) to a laminar flow, probably in relation to a decrease in the flow thickness and/or increase in the velocity near the border (Sinclair 1994). The lateral vanishing of the argillaceous slumps and slurries toward the onlap and the multiple erosion surfaces and amalgamations between sand beds improve the vertical connectivity of the sandbody close to the onlap border (Figure 75d), even if the net thickness of the reservoir is smaller (reduction of individual bed thickness).

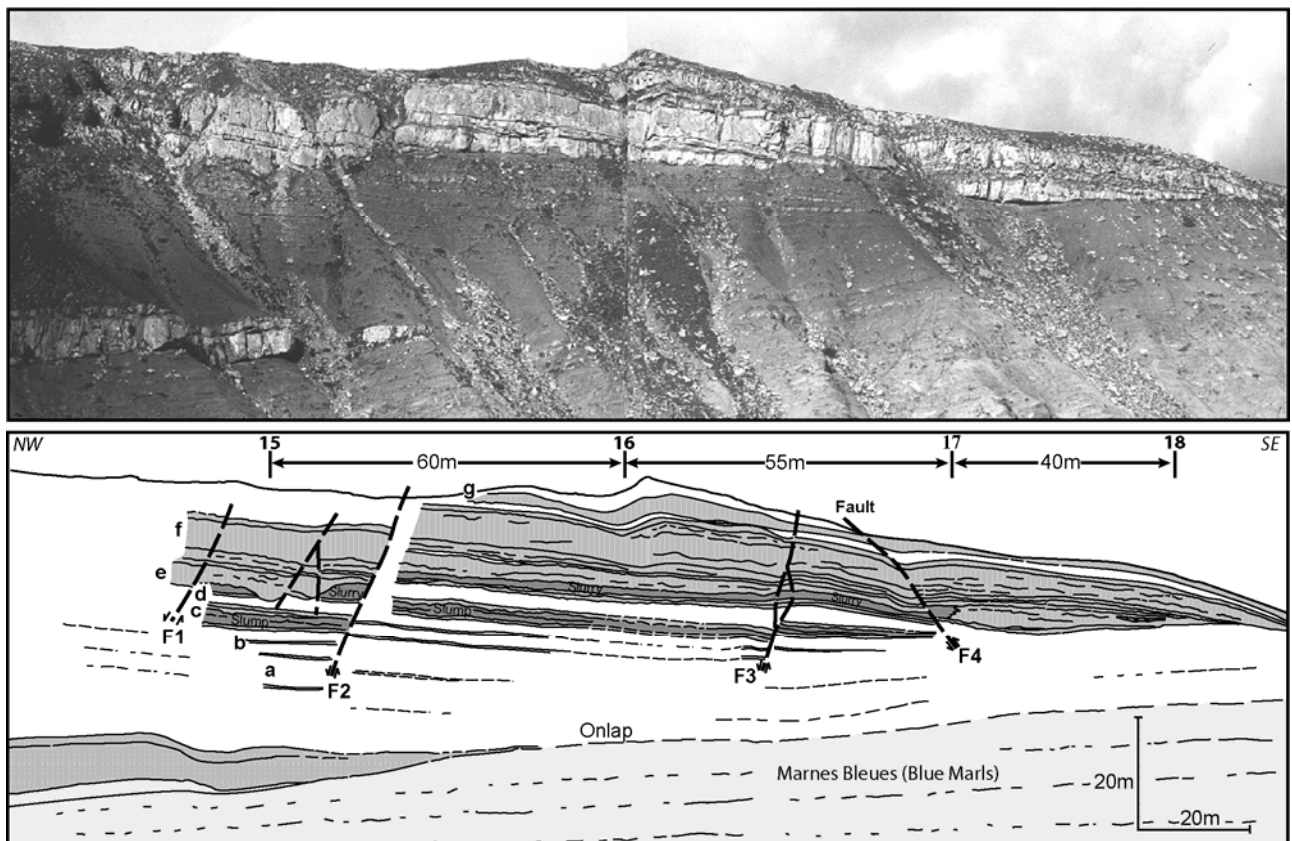


**Figure 73 : Onlap of the Upper Sandbody of Chalufy (unit D).**



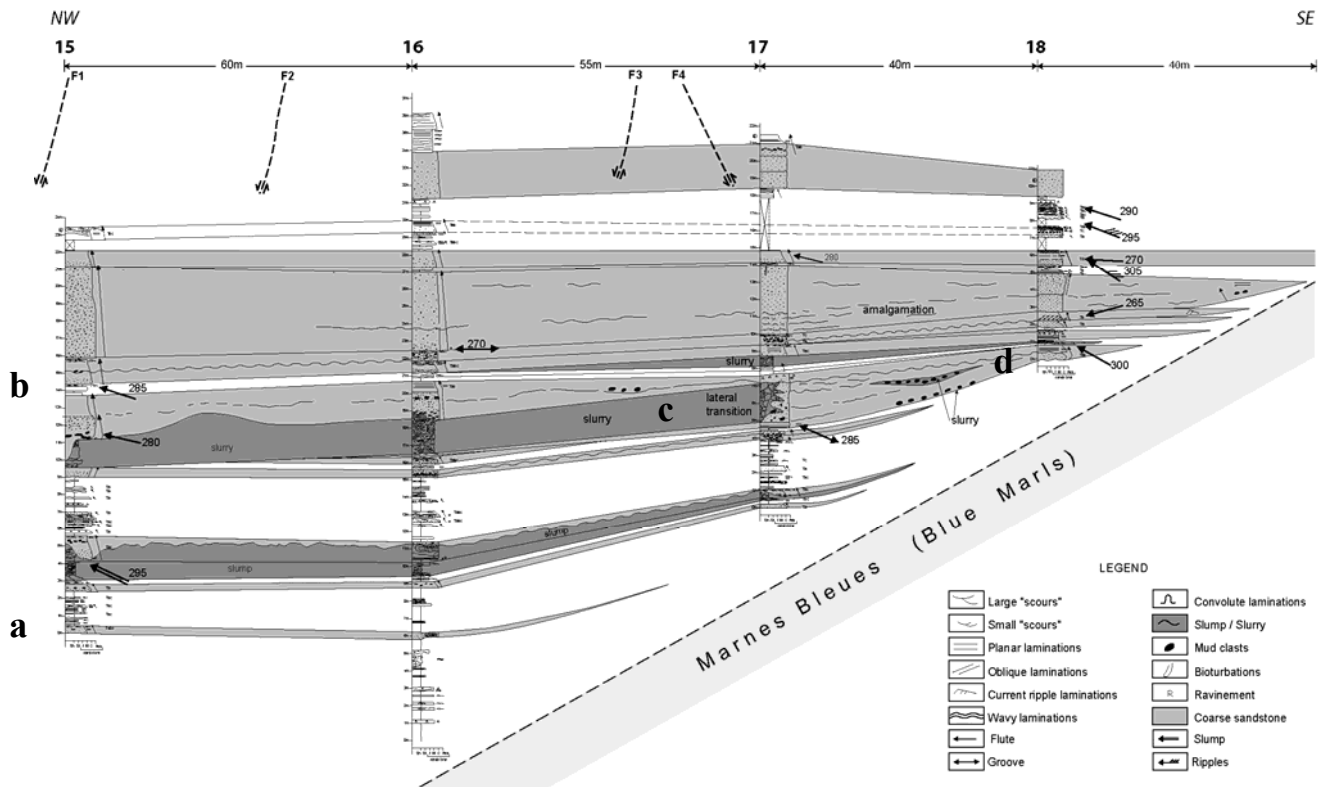


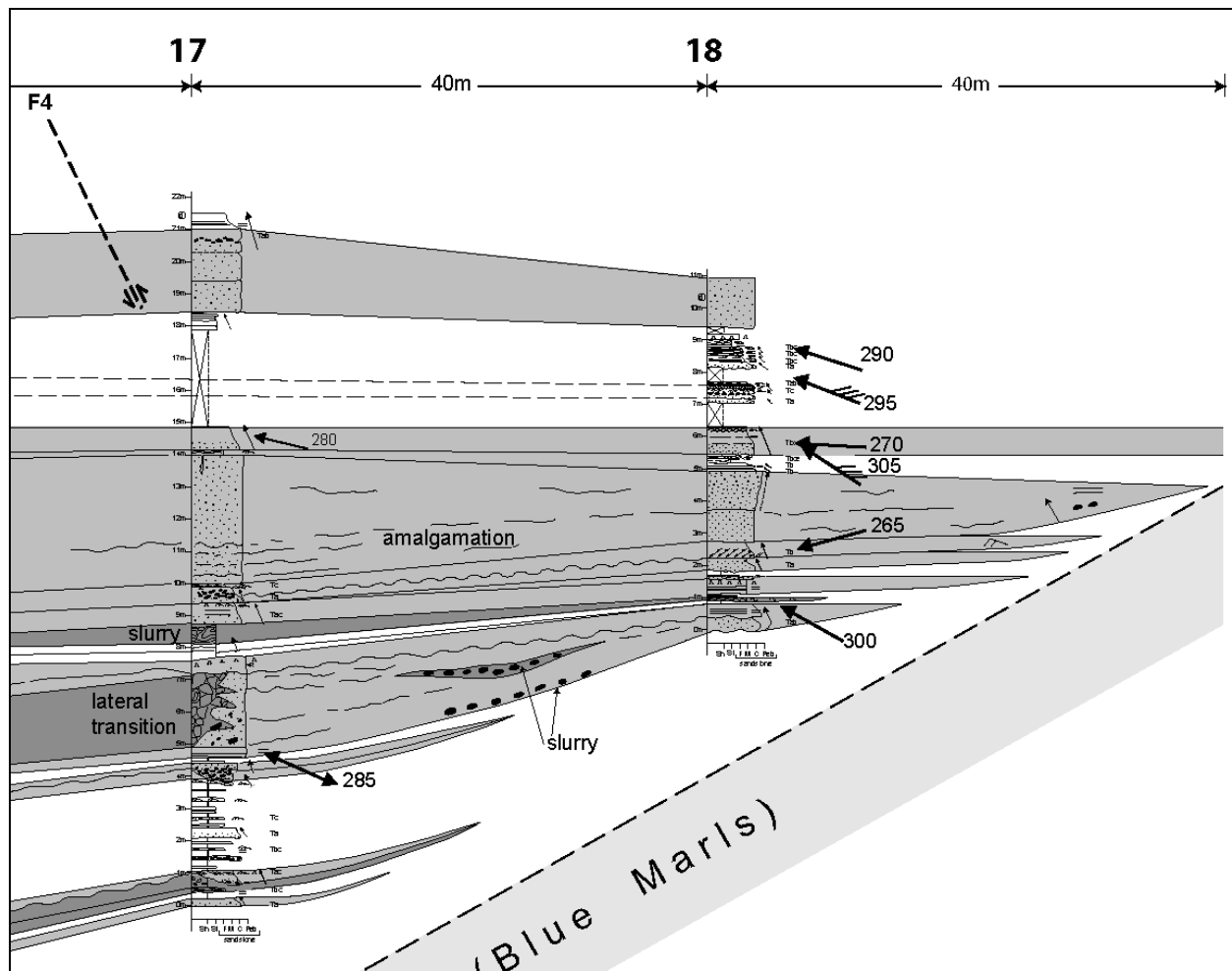
Figure 74 : Detailed correlation of the Upper Sandbody of Chalufy (unit D).



Figure 75 : Facies of the Upper Sandbody of Chalufy (unit D).

a : fine-grained low-density turbidite Tbc ; b : coarse-grained high-density turbidite Tab ; c : abrupt lateral transition from a "slurry" to a massive sandstone bed ; d : pinchout of a "slurry" pocket toward the paleoslope.





Detail of Figure 74 : Evolution of facies at the onlap border in the Upper Sandbody of Chalufy.

The Chalufy outcrop displays two types of onlap of gravity deposits onto a pre-existing paleoslope, which can be related to the topography and the flow dynamics (Figure 76) :

- **abrupt onlap** of sandstone beds, which pinch out sharply onto the paleoslope. This may be due to two factors : the high angle of the slope that prevents a draping, or the nature of the flow (stratified cohesive flow). The weak development of the dilute turbulent cloud will reduce the draping of the slope, and the hyperconcentrated flows will pinch out abruptly onto the lateral slope,
- **aggradational onlap** : sandstone deposition in the depression is contemporaneous with the aggradation of the slope, which is due to the draping of the slope by fine-grained sediments. This may be due to a lower angle of the paleoslope, or to the nature of the flow : thick diluted turbulent flows are able to climb onto the slope and to drape it (Smith & Joseph 2004).

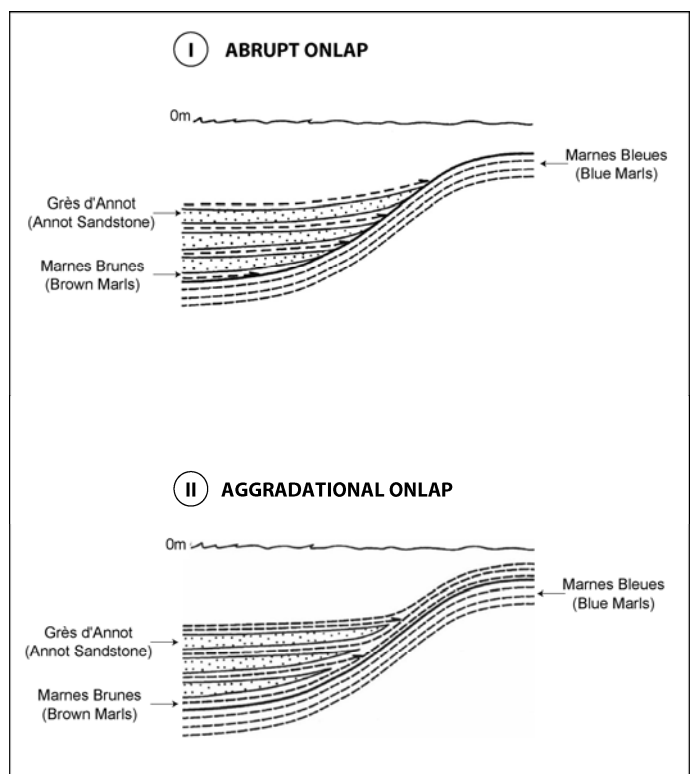


Figure 76 : Two types of onlap configuration of gravity deposits onto a pre-existing paleoslope.

# The Barrême Syncline - a Piggy-back Basin

Yannick CALLEC

The fourth day of this excursion is focused on the last marine deposits of the whole Paleogene foreland basin located in the Barrême Syncline. The Barrême Syncline is the most western area of the Digne thrust belt affected by the Nummulitic transgression during latest Priabonian to Rupelian time (Figure 77). The syncline represents a unique structural and stratigraphic setting where the closure of the Alpine foredeep is recorded by the last Paleogene sediments deposited upon the Digne Thrust sheet and the development of synsedimentary folds during deposition of the Clumanc Conglomerates and their lateral equivalents.

The first part of the excursion (Figure 78) considers the early period of basin deepening recorded by the transition from a carbonate platform sequence to hemipelagic marls (Stop 1). The Grès de Ville, that overlies the silty marls with a gradational contact, is the lithostratigraphic equivalent of the Grès d'Annot, although not of the same age. The Grès de Ville was deposited under offshore to shoreface paleobathymetric conditions (Stop 2). We then analyse the alluvial dynamics of the overlying Clumanc Conglomerates (Stop 3) and the associated synsedimentary fold on the eastern limb of the syncline that records tectono-eustatic interactions (Stop 4).

The second part of the excursion focuses on the Saint-Lions area (Stop 5), where we will study in detail the geometry and depositional processes of the Saint-Lions Conglomerates with a well-developed Gilbert delta at the top of the marine sequence, below continental deposits of the Red Molasse.

The last part of the excursion concerns the southern Senez area of the Barrême syncline where the Grès de Senez Formation comprises shoreface calcareous sandstones that prograded to the north (Stop 6). The Grès de Senez was affected, like the Clumanc Conglomerates, by a synsedimentary fold on the eastern flank of the syncline (Stop 7).

The early deformation of the Paleogene series in the Barrême Syncline has the characteristics of a thrust-sheet-top basin evolution that corresponds to the closure of the whole Paleogene foredeep before and during final emplacement of the Digne thrust.

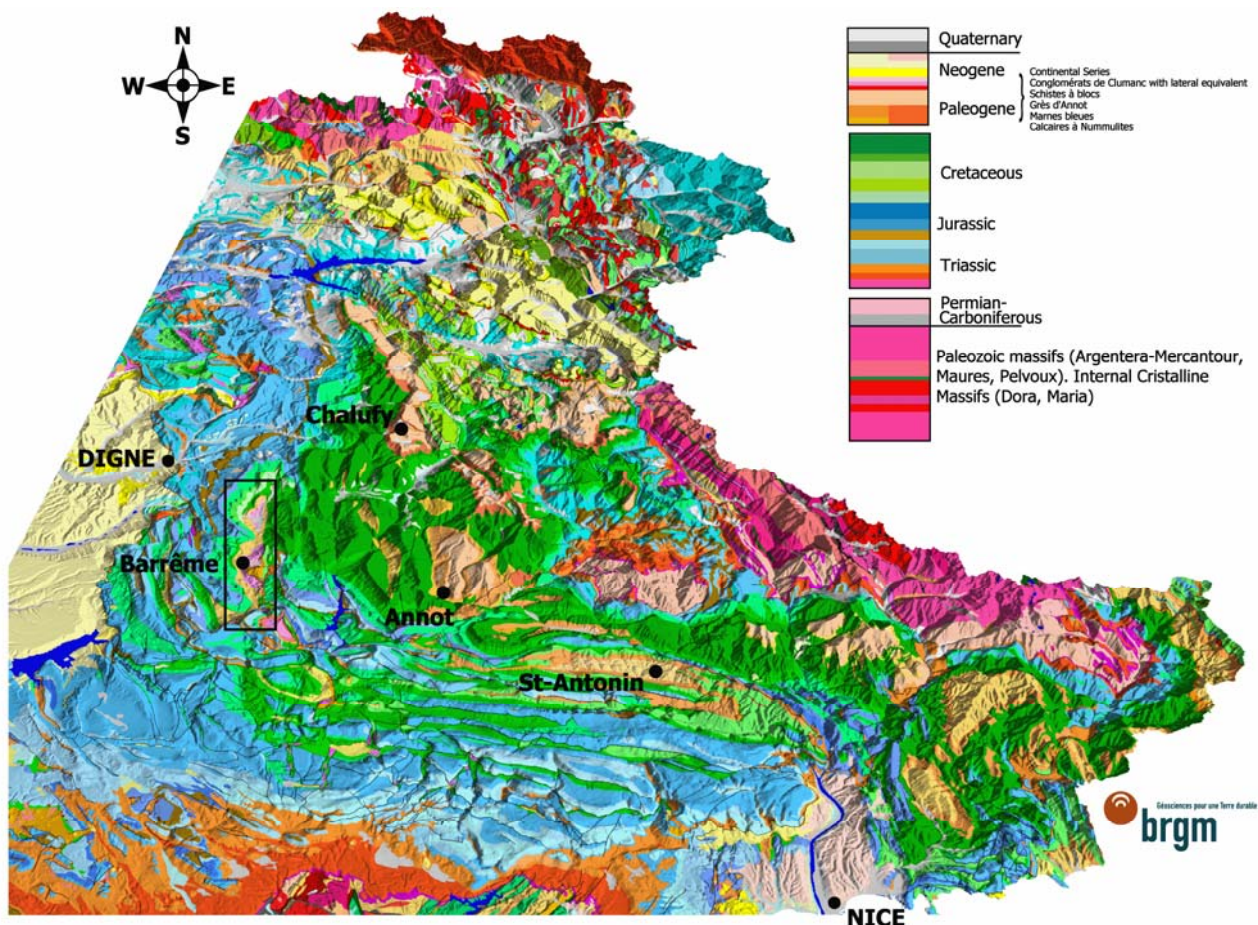


Figure 77 : Geological map of the Southern Subalpine Domain in SE France superimposed on a DEM image (IGN database). The Barrême syncline is located few kilometres east of the Digne Thrust Front.

## ***Geological setting of the Barrême Syncline***

### **- Structural setting (Figure 77 & Figure 78)**

The Barrême syncline is located in the southern external Alps (Southern Subalpine chains), 10-15 km east of the Digne thrust front. This syncline preserves Paleogene stratigraphy that represents the most northwestern extent of the Nummulitic Basin of the Castellane Arc. It has a N-S axis with an axial length of 20 km, parallel of the Digne thrust front. It is bordered on its eastern limb by N-S transpressive faults associated with the Gevaudan Triassic diapir, and on its western limb by the imbricate stack immediately beneath the Digne Thrust

Structural analysis shows the superposition of E-W Pyrenean folds with N100° to N120° axes in the Mesozoic substratum, and later N-S (around N175°) Alpine folds. These younger folds developed synchronously with Paleogene marine sedimentation (Goguel, 1936 ; de Lapparent, 1938 ; Chauveau & Lemoine, 1961). Folds oriented NW-SE (N140°) are developed in the youngest continental series (de Graciansky, 1972).

All these structures were modified by dextral strike-slip faults with a minor thrust component located essentially on the eastern limb of the syncline

### **- Geometry of the Barrême Syncline (Figure 79)**

The basin is preserved as an asymmetrical syncline with a gently dipping western limb and a steeper and more complex eastern limb that is locally overturned. Paleogene deposits are folded and locally cut by dextral strike-slip faults (Lickorish & Ford, 1998). The youngest sediments are systematically located on the eastern limb of the syncline where unconformities are often observed. This geometry and the asymmetrical infill are typical of a thrust-top-sheet basin.



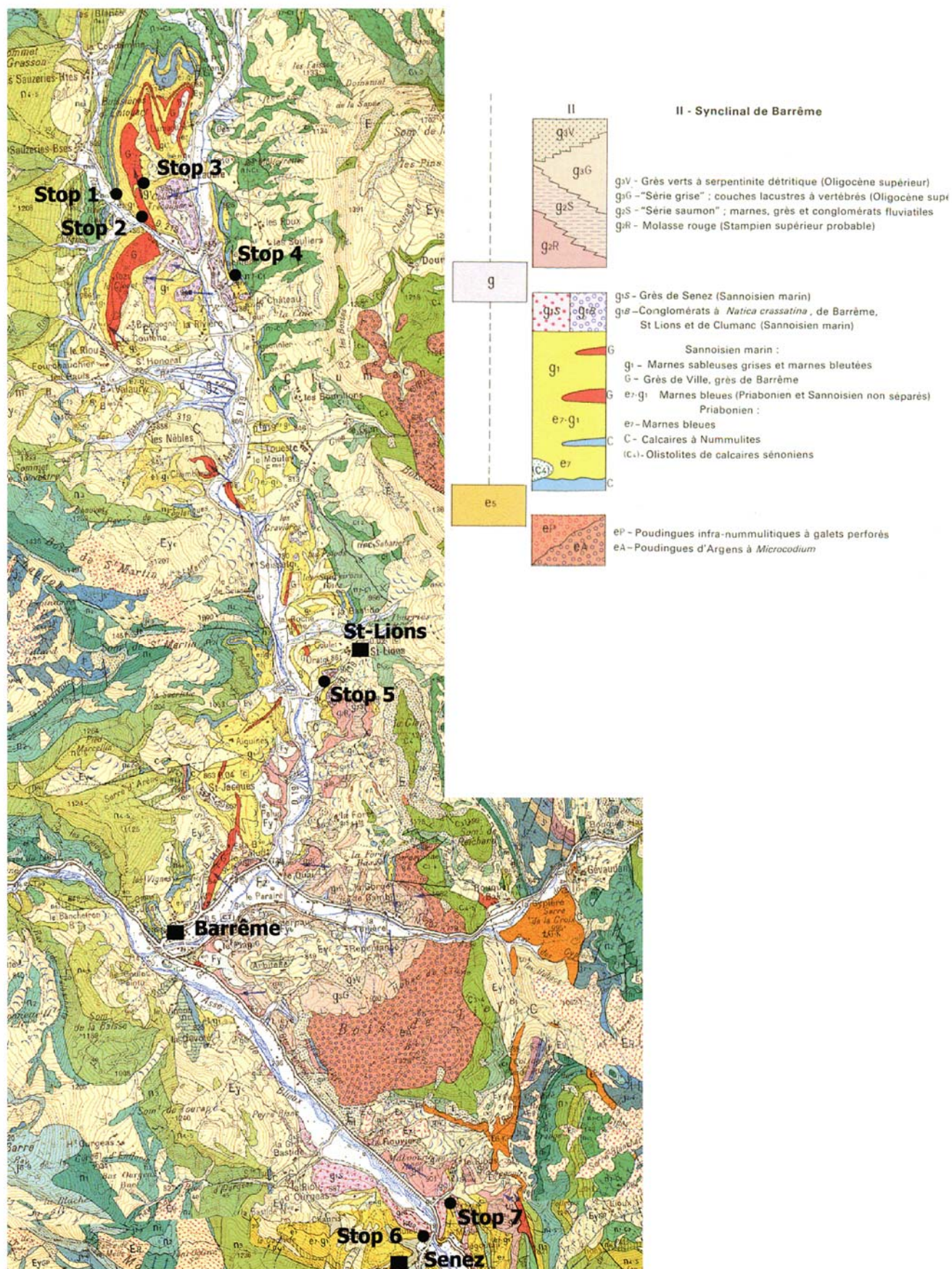
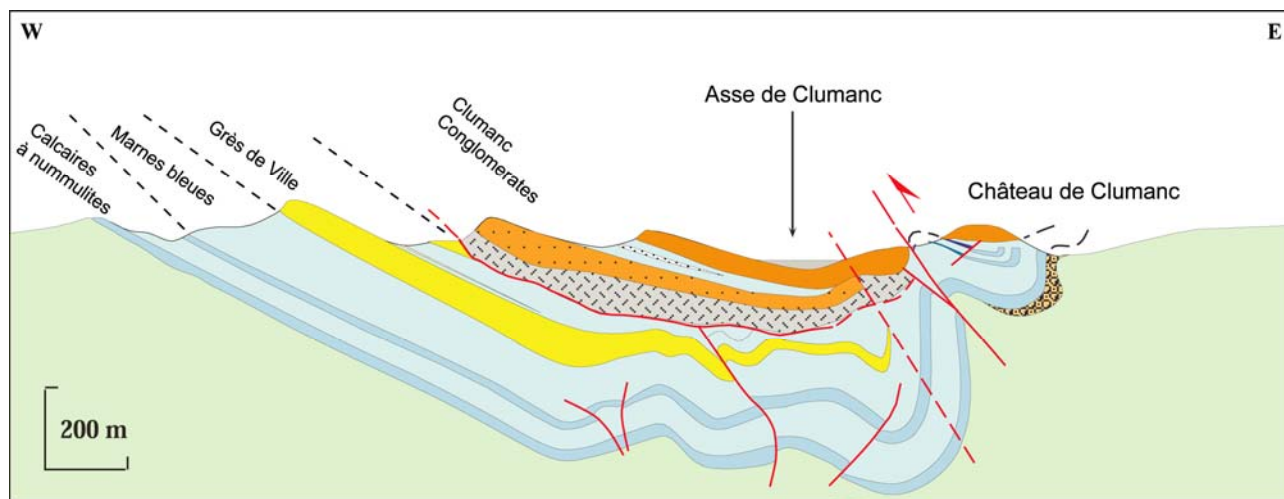


Figure 78 : Geological map of the Barrême Syncline. Taken from the French Geological Survey maps at a scale of 1 : 50 000-Digne n°944 and Moustiers-Ste-Marie n° 970 (BRGM Editions).





**Figure 79 : Schematic E-W section across Tertiary deposits of Barrême syncline in the northern Clumanc area (Callec, 2001).**

The asymmetry of the Barrême basin is associated with several unconformities: these have been known since Boussac (1912) and confirmed by Goguel (1936), Lapparent (1938) and Chauveau & Lemoine (1961) in the Clumanc and Senez areas and in the overlying continental series by Chauveau & Lemoine, (1961). However, different geometrical models have been proposed (Elliot et al., 1985 ; Artoni & Meckel, 1998 ; Evans & Elliot, 1999).

### **- Paleogene litho-biostratigraphy of the Barrême Syncline (Figure 80)**

The Tertiary succession unconformably overlies the Cretaceous substratum (dated from Hauterivian to Turono-Santonian) and is 900m thick.

- The early succession is represented locally by calcareous breccias and overlain by infranummulitic conglomerates with an Argens-type facies corresponding to alluvial deposits several hundred meters thick (Gubler, 1958 ; Bodelle, 1971).

- The early marine deposits known as the **Calcaires à Nummulites** are characterised by calcarenites, frequently with bored conglomerate clasts, or boundstone facies. Near the towns of Barrême and Blieux, large Senonian (latest Cretaceous) olistoliths are intercalated with the carbonates (Chauveau & Lemoine, 1961). The **Calcaires à Nummulites** are dated as **late Priabonian**, with a *Nummulites* association of **Zone SBZ 19** (Serra-Kiel et al., 1998).

- This unit is overlain by thick succession of marls with planktonic fauna corresponding to the **Marnes Bleues** or Marnes à Méletta (Espitalié & Sigal, 1960 ; Pairis, 1988), dated as Upper Eocene to Lower Oligocene. The first marly interval intercalated between the two carbonate levels is dated by planktonic Foraminifera of the P16 to P17 Zones. The Eocene/Oligocene boundary is located at the top surface of the **Calcaires à Nummulites** where the transition with the hemipelagic marls is abrupt. Calcareous nannoplankton data define the NP21 Zone and the planktonic foraminifera data define the P18-P19 Zone for the lower part of the Marnes Bleues.

- The **Grès de Ville**, (also called the Grès de St-Jacques or Flysch de Barrême) has a gradational contact with the underlying Marnes Bleues (Boussac, 1912 ; Lapparent, 1938). Paleocurrent measurements, derived from sole marks and current ripples, give NNE-NNW orientations (Stanley, 1961) similar to the Grès d'Annot in subbasins to the east. Heavy mineral analysis of the Grès de Ville confirms a southern provenance in the Permian to Triassic cover of the Maures-Esterels Massif (Evans & Mange-Rajetsky, 1991 ; Evans et al., 2004). The first Grès de Ville intercalations in the Marnes Bleues appear in the P20 planktonic foraminifera Zone on the western limb of the syncline. On the eastern limb, near the Château de Clumanc, the Grès de Ville

was not deposited and its P20 Zone equivalent is represented by a marly sequence, similar to the Marnes Bleues facies.

The overlying succession is highly variable from north to south and includes the Clumanc Conglomerates, the Saint-Lions Conglomerates and the Grès de Senez. Again, several correlation schemes have been proposed.

- In the Clumanc area, very coarse conglomeratic deposits, known as the **Conglomérats de Clumanc** (Boussac, 1912), are intercalated with silty micaceous marls. Total thickness exceeds 150m. The Clumanc Conglomerates record paleoflows from east to west. Petrographic analyses show a progressive upward increase in elements derived from the internal alpine in these conglomerates (Termier, 1895 p. 884 ; Gubler, 1958) and some andesitic material that could be correlated with the Saint-Antonin andesitic volcanism, dated between 31 Ma. (Féraud et al., 1995) and 29,4 Ma. (Montenat et al., 1999). Biostratigraphic data give a upper Rupelian age for the Clumanc Conglomerates. The silty marls intervals have given planktonic foraminifera of P20 to P21 Zone and Nannoplankton of NP24 Zone.

- In the middle sector of the Barrême syncline, we observe a 50m thick conglomeratic series, called the **Conglomérats de St-Lions**. These are overlain by a small biostrome just below the Red Molasse (Gubler, 1958 ; Chauveau & Lemoine, 1961 ; Bodelle, 1971). Paleoflow was from north to south (Graciansky et al., 1982 ; Elliot et al., 1985 ; Evans & Elliot, 1999). The Saint-Lions Conglomerates also contain pebbles coming from internal alpine units (Bodelle, 1971 ; Evans & Mange-Rajetzky, 1991). These conglomerates evolve progressively to the south into silty marls with abundant *Natica crassatina* gastropods (Tournouër, 1872).

- In the southern area, around Senez town, we observe a sandy succession, called the **Grès de Senez** (Zürcher, 1895). This is interpreted as comprising shoreface deposits prograding to the north. Stratigraphic relationships with the other northern formations are unclear and controversial (Chauveau & Lemoine, 1961 ; Ravenne et al., 1987 ; Evans & Mange-Rajetzky, 1991). These sandy deposits are overlain by conglomeratic deposits with E-W imbrication (Bodelle, 1971) that are followed by lacustrine and fluvial deposits of the Red Molasse.

Everywhere in the Barrême Syncline, the continental series unconformably overlies the marine succession (Gubler, 1958). We distinguish in stratigraphic order : the **Molasse Rouge** (Red Molasse), with a total thickness of 100m to 150m, composed of conglomeratic intercalations in red flood plain sediments, the 60m thick **Série Saumon** (Salmon Serie) dominated by fluvial and alluvial facies, the **Série Grise** (Grey Serie) with 10m to 150m of lacustrine deposits giving an age of late Chattian (MP28 Zone), based on vertebrate microfauna and palynofacies (Carbonnel et al., 1972). The last unit, called the **Série des Grès Verts**, is characterised by serpentine green sandstones dominated by fluvial deposits (Graciansky et al., 1971 ; Graciansky et al., 1982) that unconformably overlie all older formations and constitute the last Tertiary deposits of the Barrême syncline (Chauveau & Lemoine, 1961).



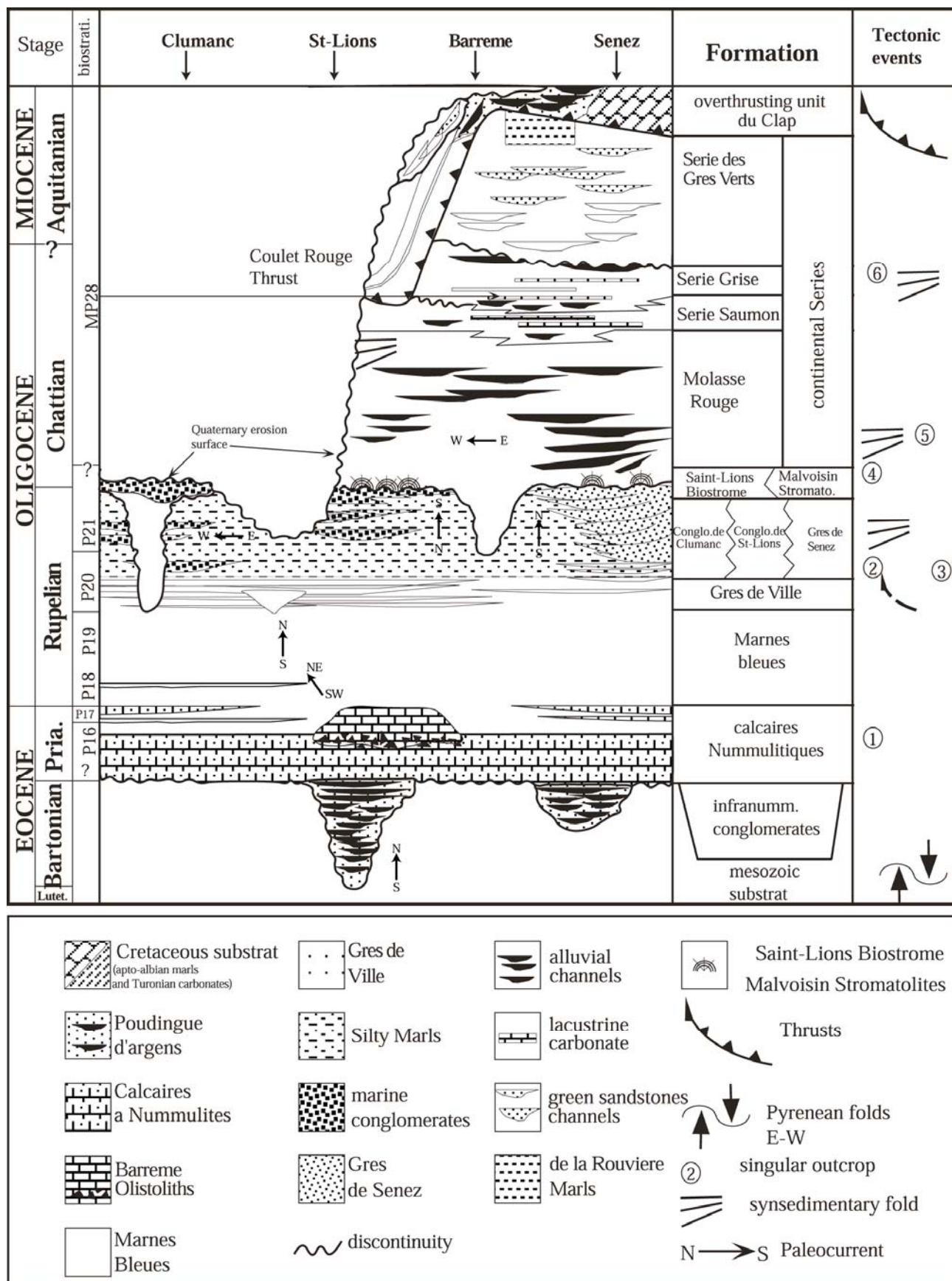


**Figure 80 : Chronostratigraphic diagram of the whole Tertiary series of the Barrême Syncline.**

We observe a high variability in depositional environments associated with a continuous modification of paleoflow orientations. Several distinct geometries record the Paleogene synsedimentary deformation events : 1- Barrême and Blieux Olistoliths ; 2 & 3- synsedimentary fan geometries in the Clumanc Conglomerates and Grès de Senez ; 4- unconformity at the base of the Red Molasse ; 5- synsedimentary fan geometry in the Red Molasse of the Malvoisin Anticline; 6- synsedimentary folds of the Série Grise and the unconformity at the base of the Grès Verts à Serpentine.

## Stop n°1 : The Nummulitic Trilogy of the Sauzeries section

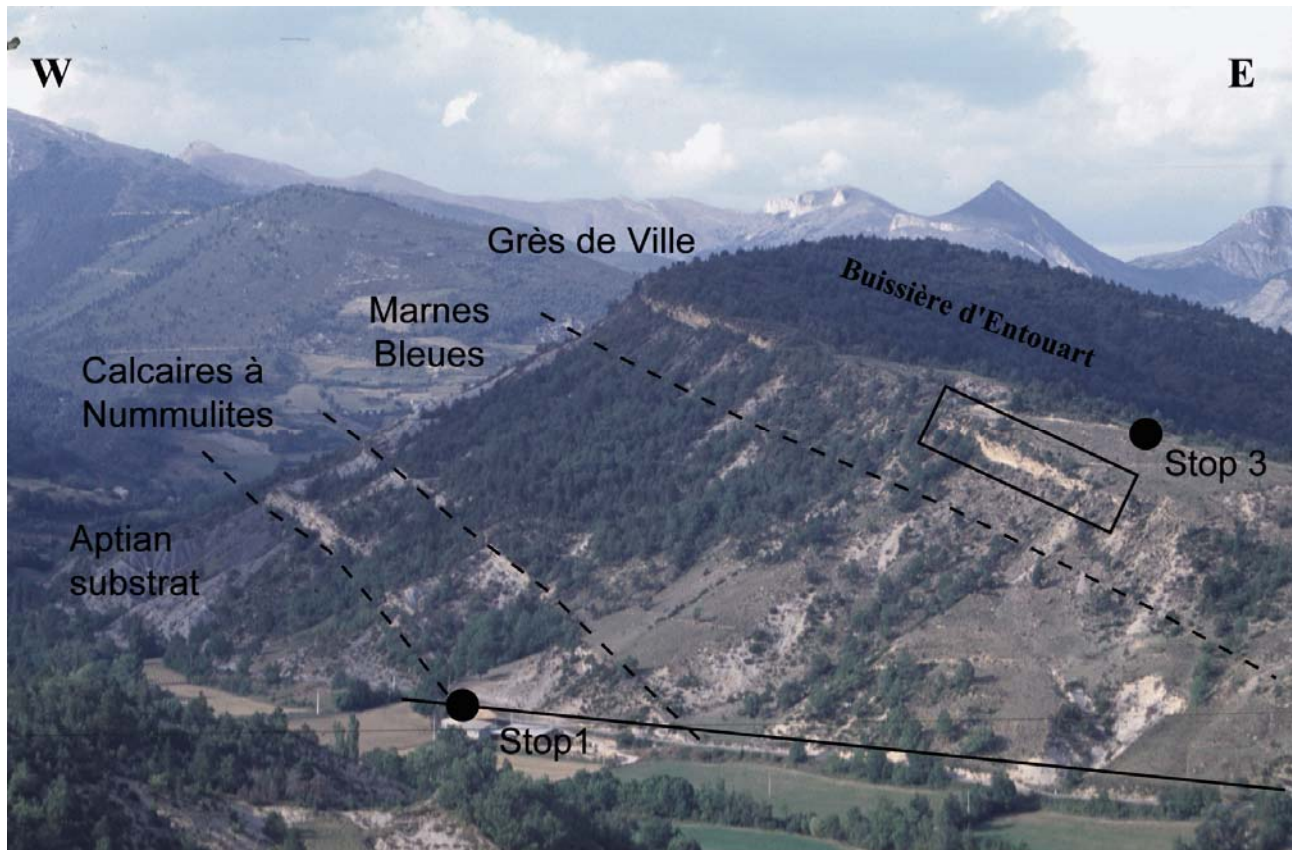


Figure 81 : General view of the western limb of the Barrême Syncline near les Sauzeries. Outcrop Boundaries for each formation of the Nummulitic Trilogy are distinguish along the hill flank of Buisière d'Entouart.

### - Access

The Sauzeries section is located along the D219 road on the left-hand bank of the Sauzeries River (Figure 81). On the western limb of the syncline, Paleogene deposits lie in a monoclinical structure with a gentle dip of 30° East so that it is possible to cross the whole Nummulitic Trilogy succession (Figure 82). The first marine Paleogene deposits, characterised by the Calcaires à Nummulites, unconformably overlie the Cretaceous marls (Aptian to Albian).

### - Vertical facies evolution (Figure 82)

The Calcaires à Nummulites starts with a first massive bar 10m thick of bioturbated bioclastic calcarenites (0 to +11m) with abundant fauna (nummulites, bivalves et gastropods) and that is very bioturbated at its summit. The sequence gradually becomes marl dominated with several decimetric parasequences with shelly transgressive sands. 15m of calcareous marls lie above with an intercalation of biodetritic coarse sandstone (+27m). The top of this transgressive lobe deposit is intensively bioturbated. The contact with the overlying marls is sharp. The second massive bar is characterised by a 3m thick calcareous sandstone (+33m to +36m). Bioturbation is well-developed and very abundant with plant debris, large bivalves and gastropods. The top of the Calcaires à Nummulites presents a condensation surface with very abundant fauna of *Ostrea*, Gastropods, and Polyps in glauconitic sands.

The succession passes upward abruptly ,without a transitional facies, into 70m of hemipelagic marls. A decimetric intercalation of erosive calcarenite appears at + 52m displaying a

classic turbidite facies (Tabc) with sole marks. The top of the bed is also intensively bioturbated. The overlying hemipelagic marls are the classic Marnes Bleues with a very homogeneous facies and abundant planktonic fauna. Above +97m, the marls become more silty and micaceous presaging the beginning of the Grès de Ville sedimentation. The Grès de Ville itself forms a 50m thick succession along the Sauzeres road characterised by an alternance of silty marls and fine to medium sandy intervals with abundant current ripples and HCS structures. Across the Sauzeres road, the Grès de Ville also outcrops along the Buissières d'Entouart on the left bank of the Sauzeres River and on the other side of the Le Clouet high.

### **- Tectonic and eustatic interpretations**

The Sauzeres succession records an evolution from internal platform conditions to an external platform environment that implies a continued deepening of the basin. This evolution is contemporaneous with **the global transgressive interval of the TA4 second order sequence (Haq et al., 1987)**. The maximum flooding surface (mfs) in the Sauzeres succession is located in the Marnes Bleues and is dated within the P19 Zone that is compatible with the mfs of the TA4 second order sequence (Hardenbol *et al.*, 1998). This second order deepening trend shows higher frequency variations of accommodation space with third and fourth order depositional sequences. These variations with biostratigraphic controls form the basis for a sequence stratigraphic interpretation and correlations with the standard eustatic scheme. Thus it is proposed that the Calcaires à Nummulites corresponds to the three third order depositional sequences of the Priabonian (Pr1, Pr2, Pr3 from Hardenbol *et al.*, 1998), and the Marnes Bleues and the Grès de Ville correspond to the first two third order sequences of the Rupelian (TA4.1, TA4.2 from Haq *et al.*, 1987 ; Ru1, Ru2 from Hardenbol *et al.*, 1998).



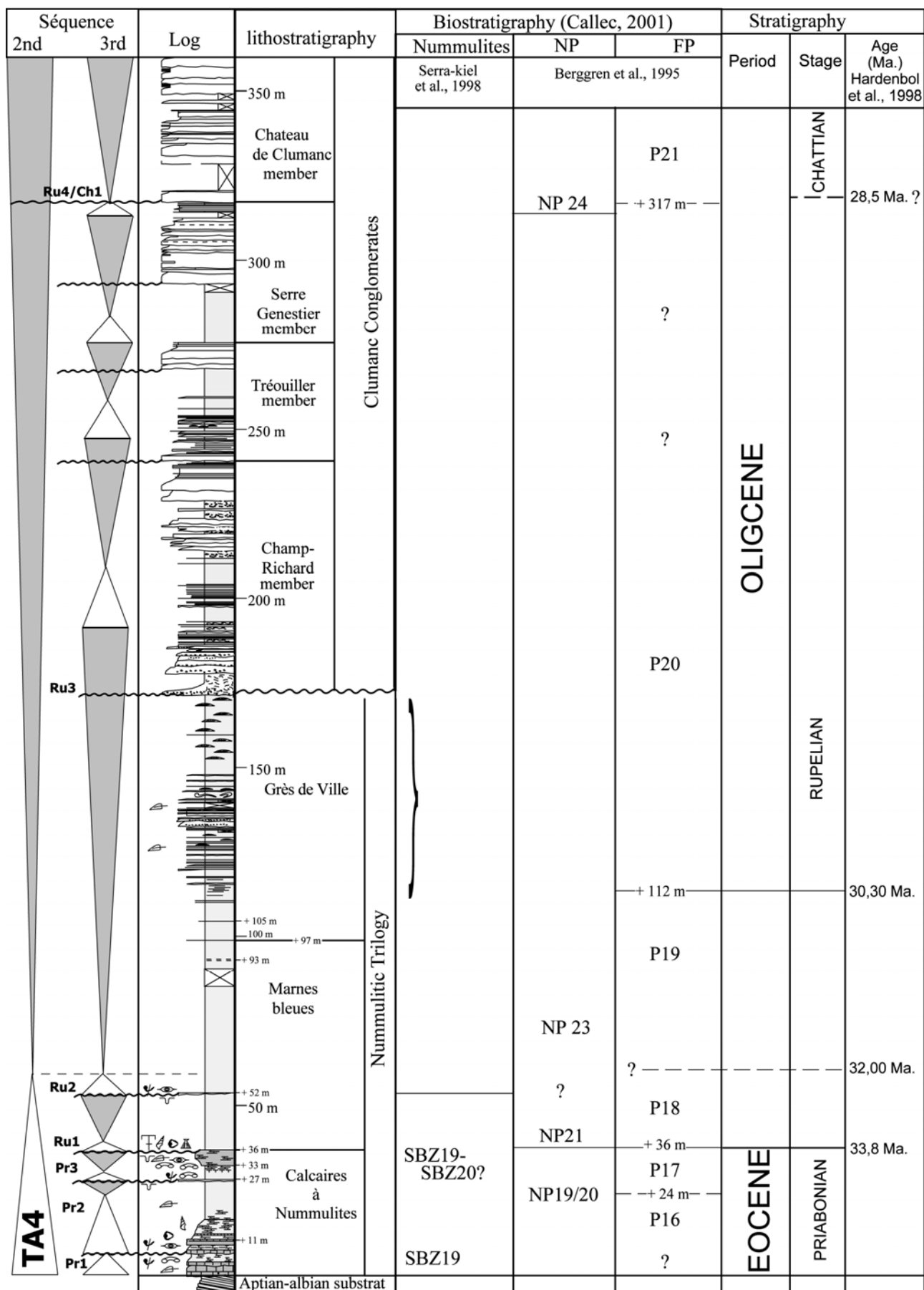


Figure 82: Sedimentary log of the Sauzeres ravine from the Calcaires à Nummulites to the top of the Clumanc Conglomerates, showing lithostratigraphic divisions, biostratigraphic data and second and third order depositional sequences.

## **Stop n°2 : The Grès de Ville Formation**

Along the road D219 to the Poste de Clumanc locality, we cross the Buissière d'Entouart high where the Grès de Ville is well-developed with 50m of thickness.

### **- Map pattern of the Grès de Ville (Figure 83a & b)**

A detailed geological map was constructed (Figure 83a) of the northern closure of the Barrême Syncline revealing second order folds within the principal fold hinge zone. These folds do not affect the Clumanc Conglomerates in which deformation is instead concentrated on the eastern synclinal limb (Figure 83b). The Grès de Ville however, shows a train of N-S oriented faulted fold pairs that are disharmonic with respect to folds in the two underlying Nummulitic limestone bars.

### **- Vertical facies evolution of the Grès de Ville along the road D219 (Figure 84 & Figure 85)**

The Grès de Ville section along the D219 road shows a 50m thick succession with four distinct sandy intervals interbedded with decametric silty marls. Each sandy interval shows a fining and thinning-up organisation. Each interval starts with lenticular bedding of very fine to fine sandstone with discrete current ripples. HCS structures. Gutter-casts appear progressively with rare lower turbidity deposits (Bouma sequences like Tab, Tac). In the upper part of each interval, HCS and gutter-casts become common with frequent current influences recorded on the top of each bed. Wavy bedding and wave ripples are frequent on the upper part of the Grès de Ville.

The second sandy interval evolves to a channelised coarse sandstone body with well-developed flute-casts on the erosive base (spot height 1013m cf. Figure 86).

The last coarse interval of the Grès de Ville is thicker with a 10m vertical extent. It starts with a large, 6m thick, slide characterised by contorted marls and frequent Grès de Ville boulders. Overlying sandstones are thicker and more erosive with abundant sole-marks and mud-clasts. HCS structures and wave ripples become very abundant and fine intervals become more silty and micaceous.

Paleocurrents measured from sedimentary structures highlight homogeneous flows with a mean northward directed flow, between N330-150°/N020°-200°. Perpendicular crestlines of current ripples give similar orientations.

The Grès de Ville Formation, considered as the western equivalent of the Grès d'Annot, shows a facies uncommon in the Grès d'Annot, with abundant HCS structures and wave-ripples. This facies association emphasises platform paleobathymetry from lower offshore to upper offshore conditions, and perhaps upper offshore/lower shoreface for the top of the Grès de Ville deposits because of the abundance of wave ripples.

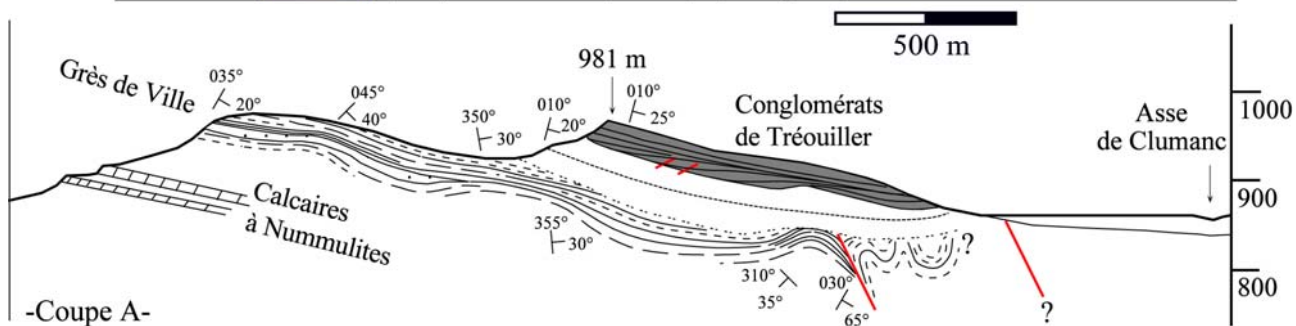
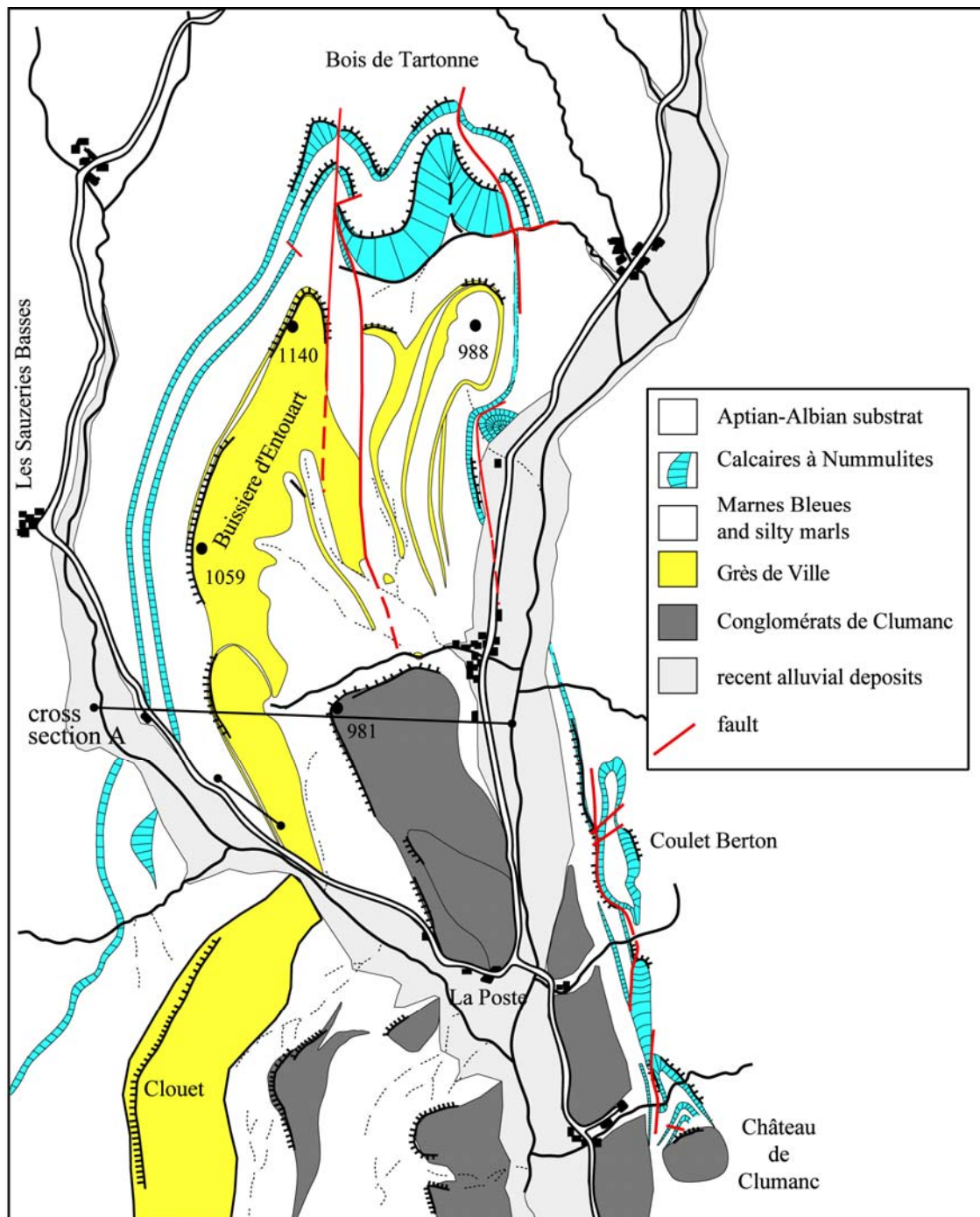


Figure 83 : a – a – Geological map of the northern closure of the Barrême syncline in the Nummulitic Trilogy and the Clumanc Conglomerates.

b- East-West cross-section showing the stratigraphic organisation of the western limb of the asymmetrical Barrême syncline near its northern closure. Note the vertical exaggeration.



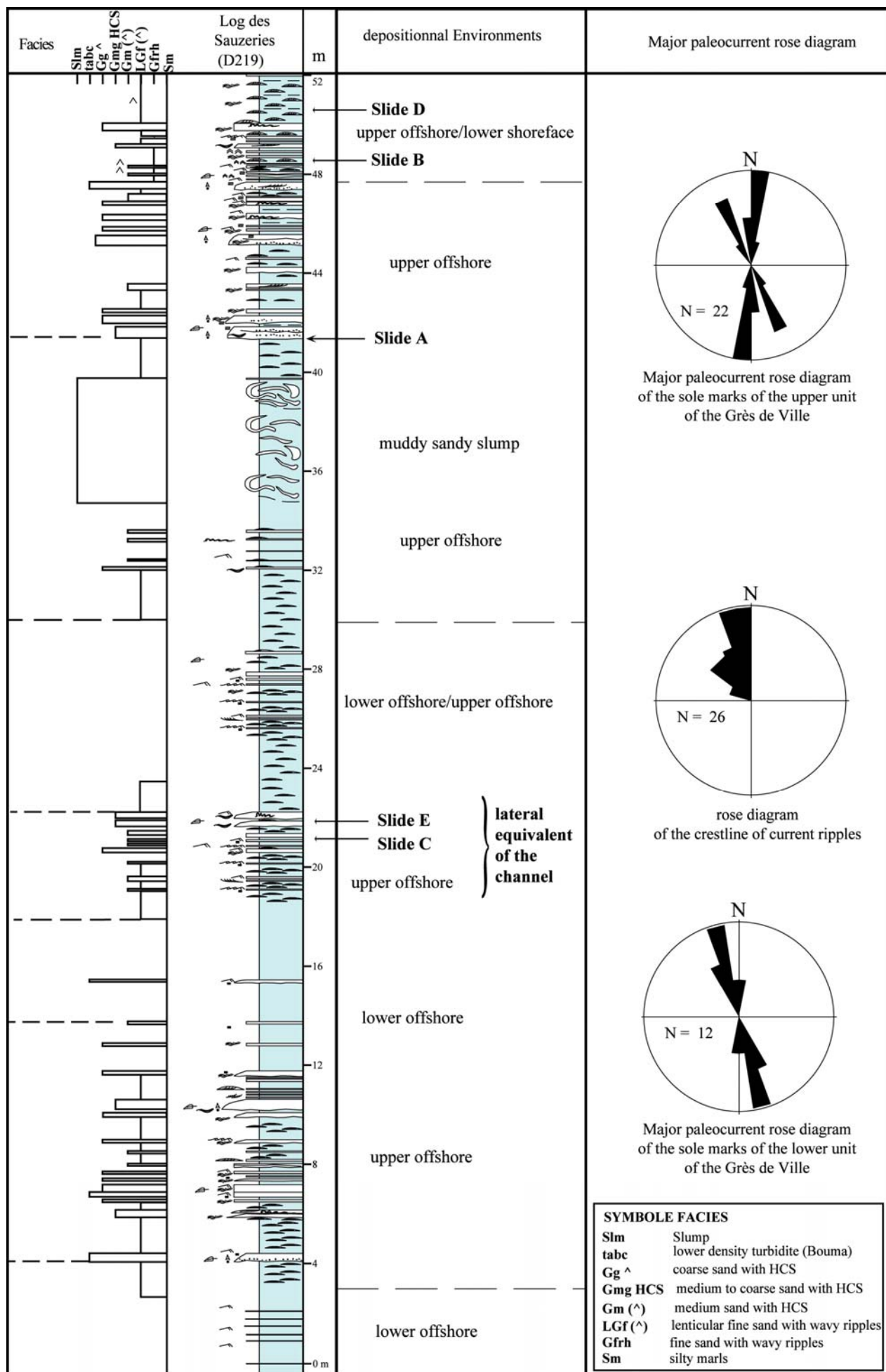


Figure 84 : Vertical facies evolution of the Grès de Ville on the D219 Sauzeries log.



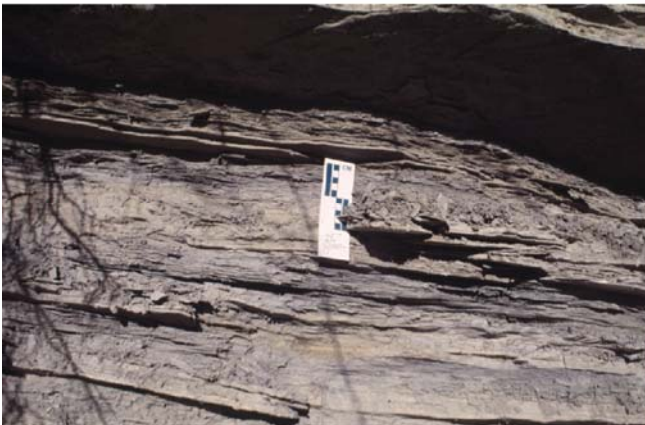
**Slide D** -fine lenticular bedding with aggrading and graded ripples. frequent HCS structures (Facies LGf(^))



**Slide E** - fine to medium laminated sandstone with aggrading HCS. (Facies Gm^)



**Slide C** -medium to coarse sandstone with HCS structure. convoluted laminations on the top (Facies Gg^).



**Slide B** - silty to very fine sandstone with wavy ripples intercalated into silty marls. (Facies Gfth)



**Slide A** -medium to coarse erosive sandstone with HCS structure (Faciès noté GmHCS)

**Figure 85** : The most important facies of the Grès de Ville characterised by wavy and storm influences. Each photograph is located on Figure 84.



**- Detail of the lenticular body of Grès de Ville at 1013m of la Buissière d'Entouart (Figure 86)**

On the western flank of the Buissière d'Entouart hill (location on Figure 81) several pluridecametre-scale lenticular bodies occur. The tabular aspect of each body with a length/depth ratio of  $< 8$ , indicates a shallow incision of the sea floor. Frequent flute-casts and intraformational truncations with low-density turbidites (F7 to F9a (Ta) facies from Mutti, 1992) show a close similarity to a channelised body in the axis of the basin with south to north paleoflows (Evans et al., 2004)

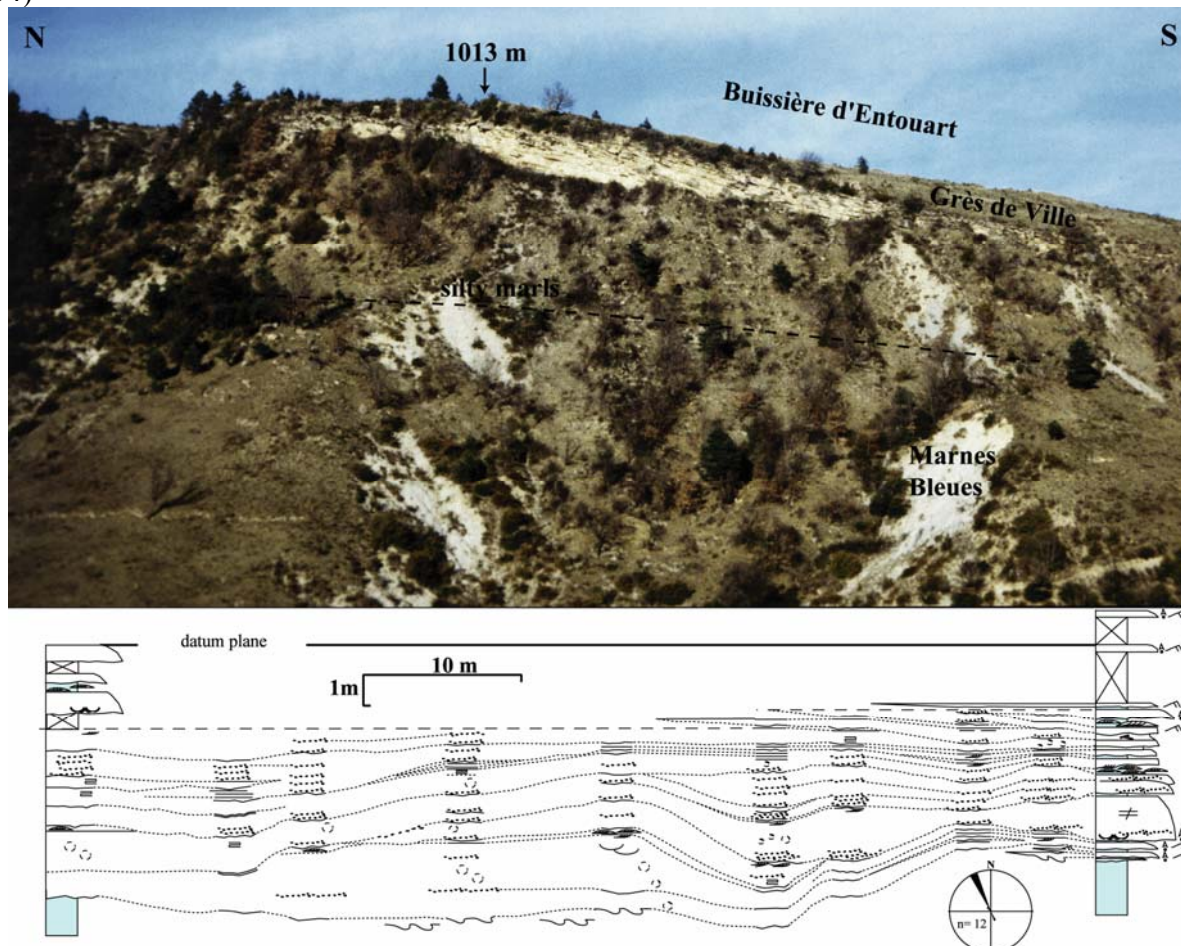


**Figure 86 : Detail of the Grès de Ville lenticular body near spot height 1013m of the Buissière d'Entouart.**

This remarkable outcrop shows that during deposition of the Grès de Ville, under wave and storm conditions, several events were characterised by gravity processes with turbidite deposits and channelised geometries. Measurement of paleocurrent directions from sole-marks, cross-laminations and ripple crestlines gives a homogeneous south to north paleoflow parallel to the actual syncline axis. This confirms the early development of the fold that formed a N-S depression with axial drainage of the detrital fluxes (Callec, 2001; Evans et al., 2004).

**- Interpretation**

The vertical evolution of paleobathymetric conditions from lower offshore to upper offshore/lower shoreface environments emphasises a detrital progradation into a confined N-S basin with a progressive decrease in accommodation space. Gravity flows and turbidites flowed along the axis of the basin and did not occur on the deforming and uplifting eastern limb. So **the maximum deepening period was during deposition of the Marnes Bleues and corresponded to the second order maximum flooding surface of the TA4 supersequence of Vail et al. (1987)**. The overlying sequence records first more proximal environments, from external platform to internal platform (Grès de Ville with storm to wave influences), then an alluvial fan environment during deposition of the Clumanc Conglomerates. **This prograding regime characterises a regressive interval dated as Lower Rupelian to Late Rupelian, similar to the regressive interval of the TA4 supersequence.**



### Stop n°3 : The Clumanc Conglomerates. The Champ-Richard-Tréouiller Section

#### - Access

The best panoramic view from which to observe the geometry of the Clumanc Conglomerates is located on the Buisnière d'Entouart hill, near the spot height 1013m. The Clumanc Conglomerates form 3 successive cuestas in the landscape on the western limb of the syncline while on the steep and complex eastern limb they occur only on and around the Château de Clumanc high. Each cuesta characterises a conglomeratic member intercalated with silty marls (Figure 87).

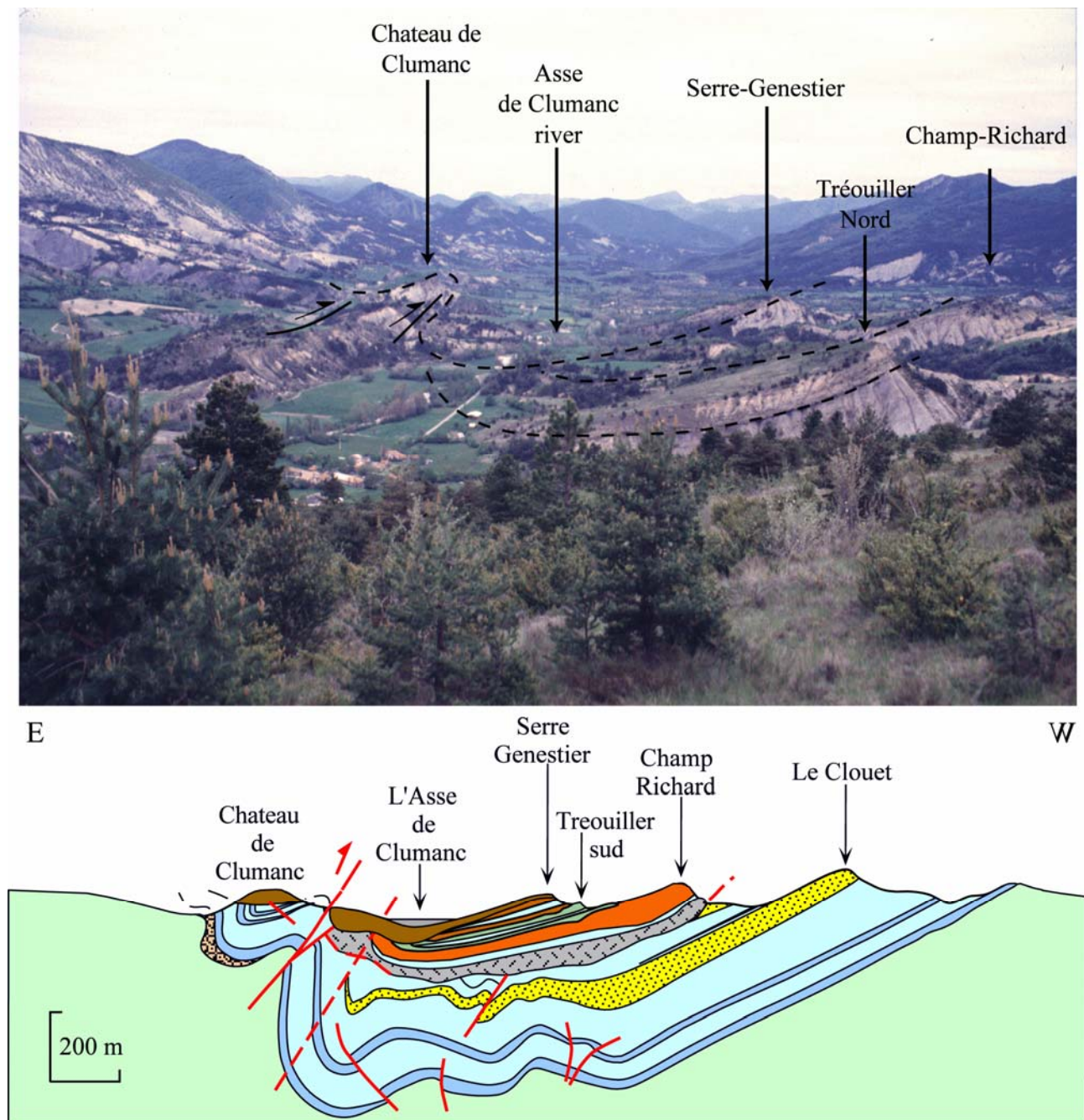


Figure 87 : General view toward the south of the successive cuestas of the Clumanc Conglomerates . E-W cross-section highlighting the asymmetrical geometry of the syncline and the synsedimentary deformation with complex internal unconformities on the eastern limb of the syncline.

The Clumanc Conglomerates can be divided into four different members (Figure 88). These are :

- the Champ-Richard Member (high 972 m),
- the Tréouiller Member (high 981 m-908 m). It can be further divided into two levels (lower and upper) because of the intercalation of a silty interval.
- the Serre-Genestier Member (high 932-941m),
- the Château de Clumanc Member (high 943 m). This last member is poorly developed on the right (west) bank of the Asse de Clumanc River where it is never more than 10m thick. It is principally developed on the left (east) bank of the river where it is strongly tilted and folded and forms the top of the Chateau de Clumanc hill.

### **- Strong modification of depositional environments and paleoflows (Figure 88).**

The underlying Grès de Ville is dominated by storm deposits (Elliot *et al.*, 1985) where the mean paleocurrent direction is N330° and N010° highlighting a N-S basin floor topography and a southern provenance for the sediment.. Heavy mineral analysis confirm the southern provenance FO the Grès de Ville with a major contribution of the Permian and Triassic cover of the Maures Esterel Massif (Evans & Mange-Rajetzky, 1991 ; Evans et al., 2004).

The **Conglomérats de Clumanc** represent a rapid progradation of an alluvial-deltaic system (Bodelle, 1971 ; Elliot *et al.*, 1985). Paleoflow was from East to West and assemblages of internal alpine elements increase progressively with the occurrence of andesitic material in the Treouiller member (Gubler, 1958 ; Graciansky *et al.*, 1971 ; Bodelle, 1971). The unconformity located at the top of the Grès de Ville separates two distinct sedimentary environments corresponding to two different feeder systems and associated drainage areas, one oriented N-S for the Grès de Ville, the second E-W for the Conglomérats de Clumanc. The unconformity also corresponds to an abrupt modification of basin floor topography ; -

### **- Facies Model for the Conglomérats de Clumanc (Figure 89).**

**The Conglomérats de Clumanc have several characteristics of an alluvial fan delta** (sensu Mc Pherson *et al.* , 1988 ; Nemec & Steel, 1988). We remark :

- **A small lateral extent (few kilometres).**
- **A complex internal organisation of each conglomeratic member with amalgamated channels of fluvial affinity** (Coleman & Wright, 1975 ; Galloway, 1975).
- **The very coarse grain size with abundant boulders and frequent plant debris indicate a low transfer of material and the proximity of relief.**
- **The less frequent occurrence of wave structures and the abundance of hyperconcentrated and flood deposits.**
- **The lack of bioturbation in the prodelta facies characterises a poor marine environment and/or an intense sedimentary flux.**
- **The high frequency of gravity deposits and reworked deposits in the prodelta and delta front record delta front gravitational instability and deformation of the basin floor.**

Facies associations allow the definition of a facies zonation that can be related to the different sedimentary processes that were active during deposition of the Conglomérats de Clumanc Formation (Figure 89).

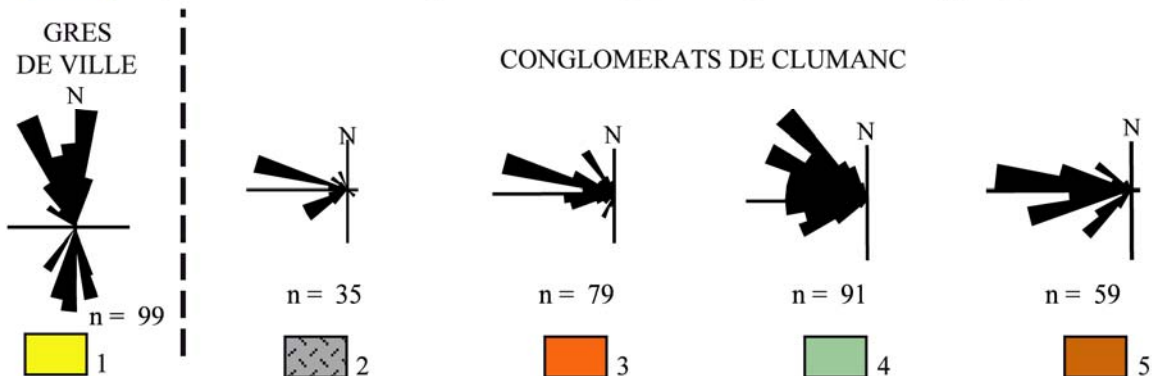
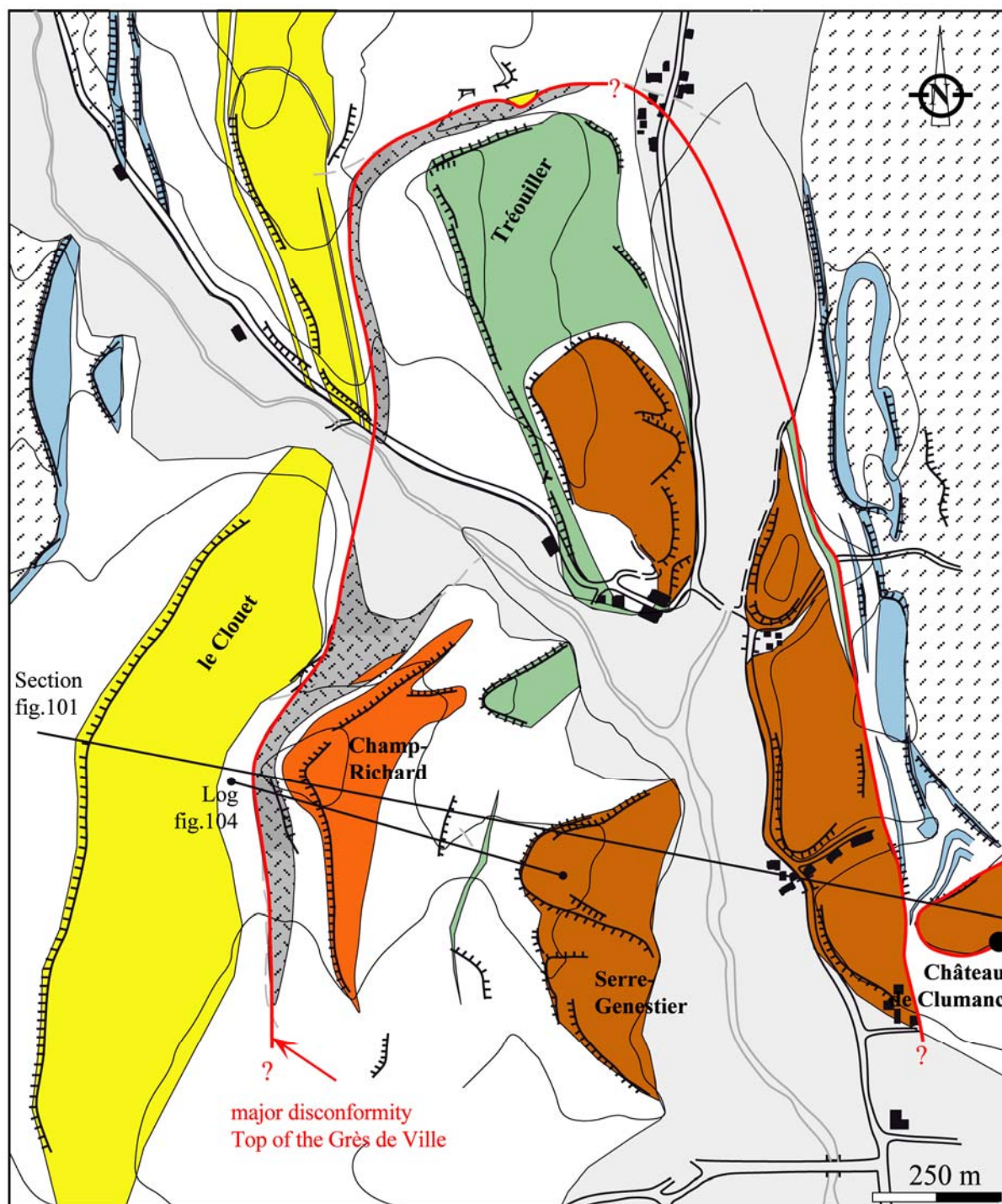


Figure 88 : Map of the members of the Conglomérats de Clumanc Formation. Paleoflow rose diagrams for the Grès de Ville and the superposed Clumanc Conglomerate members. 1/ Grès de Ville ; 2/ gravity deposits ; 3/ Champ-Richard Member; 4/ Treouiller Member; 5/ Serre-Genestier and Château de Clumanc Members.



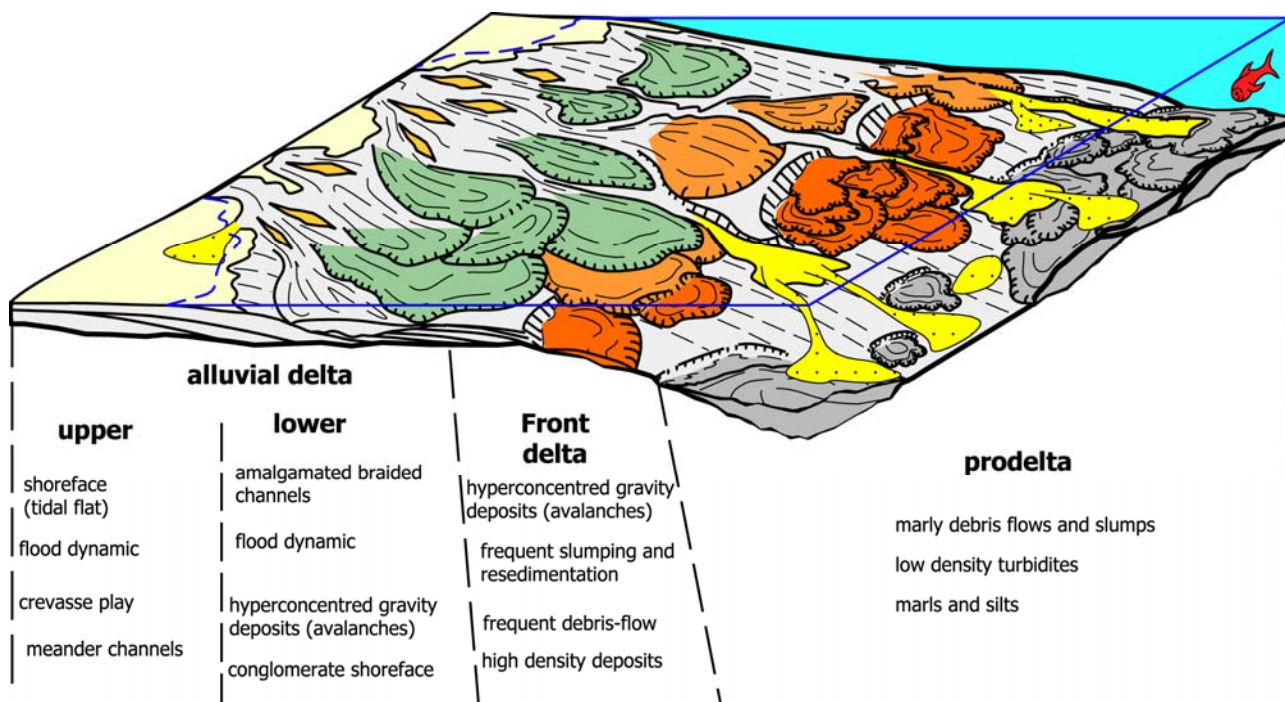


Figure 89 : Facies model of the alluvial system of the Conglomérats de Clumanc Series. Spatial repartition of the major sedimentary processes.

### - Vertical Facies Evolution (Figure 90 & Figure 91a, b).

The synthetic section is located on the right bank of the Sauzeries River. It starts at the top of the Grès de Ville near the Champ-Richard mound and extends to the 908 m spot height (location on Figure 88) and then to the Serre-Genestier mound.

The Conglomérats de Clumanc Formation starts with gravity deposits (reworked muddy debris-flows, slumps, sandstone turbidites) and evolves up into prodeltaic facies with silty marls. Delta Front facies appear progressively with amalgamated coarse debris-flows and coarse sandstones with plant debris and bioclasts (Champ-Richard Member).

The lower part of the Tréouiller Member comprises deltaic facies with well-developed flooding sequences and channels. The channels show a braided organisation with composite channels indicating a weak aggradation. The upper part of the Treouiller Member consists of a tidal flat succession with current ripples. The Serre-Genestier Member is characterised by conglomeratic shoreface deposits in which **several intervals prograde to the west on the underlying marls**. Finally the Château de Clumanc Member comprises a clear alluvial sequence dominated by erosive gravitational flows (avalanches) with abundant and very large mud clasts.

### - Interpretation

The vertical facies succession reveals a **general progradation of delta environments from prodelta to alluvial fan**. This corresponds to a generalised regression, which could be correlated with the regressive second order interval of the Early Oligocene (TA4 Supersequence of Haq *et al.*, 1987 ; Hardenbol *et al.*, 1998). However the effects of the tectonic closing and uplift of the synclinal basin are superimposed here on the global eustatic signature. We can therefore simply speak of a forced regression in the sense of Posamentier *et al.* (1992). Each conglomeratic interval corresponds to a fourth order progradation associated with third order lowstand system tracts.

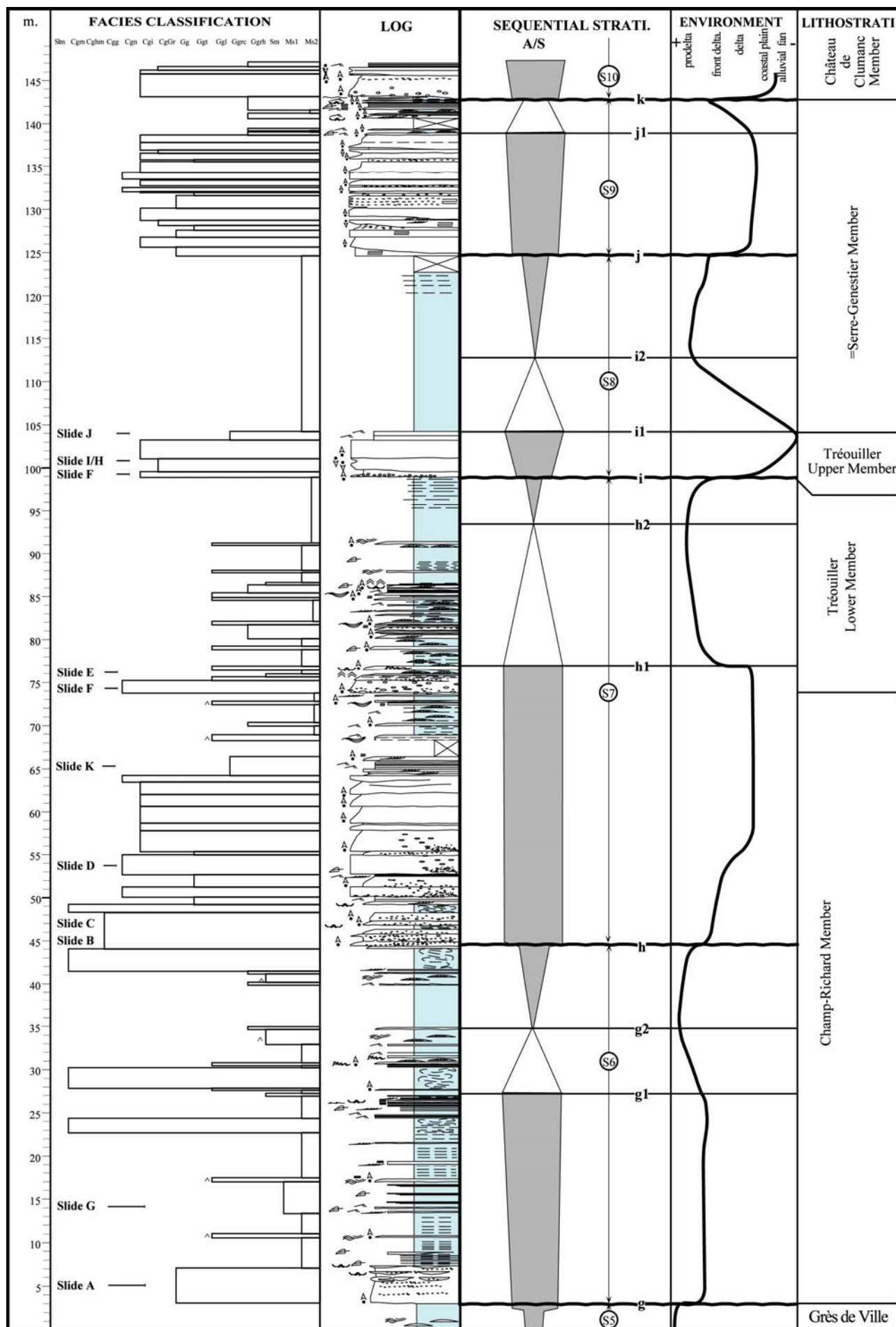


Figure 90 : Synthetic log of the Clumanc Conglomerates from Champ-Richard to Serre-Genestier hills. Depositional environments and sequential interpretations are given. Log 1 located in Figure 88.





**Slide A-** sandy slump remobilized from the Grès de Ville Formation.



**Slide A-** Marly debris flow with mud clasts supported (from D. Mercier, ENSMP).



**Slide D-** Hyperconcentrated debris flow with polygenic clasts in a coarse matrix supported (from D. Mercier, ENSMP)



**Slide C-** Marly debris flow



**Slide E-** Symmetric wavy ripples at the top of the Treouiller Lower member

**Slide F-** Flood sequence from the bottom of the Treouiller upper Member







**Slide G-** Flame structure in silty clays deposits (prodelta deposits)



**Slide I-** Ungrading clast supported conglomerate corresponding to the F1 facies from Mutti et al., 1996



**Slide H-** Successive inverse grading in conglomerates and boulders deposits in the Treouiller upper Member (F2 facies from Mutti et al., 1996)



**Slide K-** Coarse sandstone with well-preserved plants debris of genus *Cinnamomum* (Lauracea) which translate tropical to subtropical conditions



**Slide J-** Current ripples interpreted as tidal flats deposits at the top of the Treouiller upper Member

**Figure 91a et b : Major facies of the Conglomérats de Clumanc.**



**Stop n°4 : General view of the Château de Clumanc hill. Geometry of the synsedimentary fold in the Clumanc conglomerates.**

- Access

The panoramic view of the Château de Clumanc hill is located to the east of the town La Lèche on the road D19 on the left bank of l'Asse de Clumanc River. Follow the path indicated by the Alpes de Haute-Provence Geological Reserve

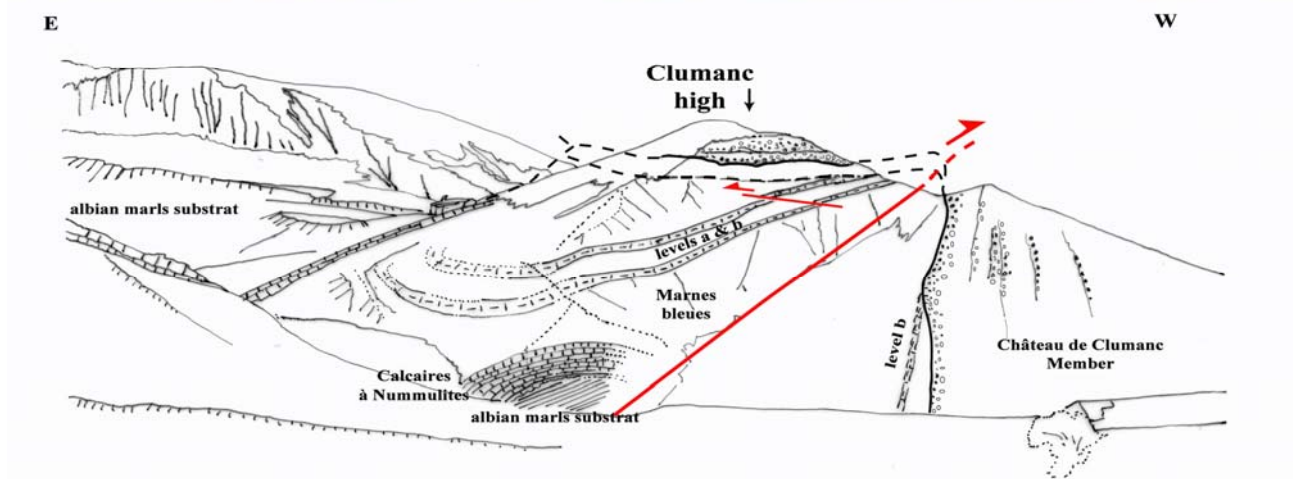


**Figure 92 : General view toward the south of the Château de Clumanc hill.**

a : Albian marls ; n : Calcaires à Nummulites ; m : Marnes Bleues ; c : Conglomérats de Clumanc

On the eastern limb of the syncline, the Calcaires à Nummulites are folded and show steep dips, locally overturned and affected by dextral strike-slip faults and minor thrusts.

Early synsedimentary deformation is recorded by the lateral variations in thickness of the levels a & b within the Marnes Bleues (Figure 92). These levels show a thickening toward the syncline and a thinning toward and above the anticline indicating that folding occurred during deposition of the Marnes Bleues Formation.

The Château de Clumanc unconformity is well known since 1912 from the work of Boussac (1912), Lapparent (1938), Chauveau & Lemoine (1961) who introduced the idea of synsedimentary deformation (Figure 93). This unconformity is placed between the thinned and folded Sauzeres Series (absence of Grès de Ville, thinning of Calcaires à Nummulites and Marnes Bleues) and the

silty marl equivalents of Serre-Genestier (S8); which are themselves eroded by the conglomerates of the Château de Clumanc Member.

**- Geometry of the synsedimentary fold: relationships between deformation and sedimentation (Figure 93a, b)**

Several models for the synsedimentary fold geometry have been proposed since Elliot et al. (1985). Our sequence stratigraphic interpretation and the tracing of major stratigraphic surfaces (mfs, SB) across the whole Clumanc area have led to a new detailed geometrical model (Figure 93a).

Detailed geological mapping of the depositional sequences reveals the asymmetric nature of the sedimentation (Figure 94). On the western limb, sequences were well-developed and recorded a significant subsidence rate. On the eastern limb, the Clumanc Conglomerates are thinner and show frequent gaps. On the Château de Clumanc hill, located in the thrust unit, we only observe a reduced silty marl unit, the lateral equivalent of the thick transgressive marls of Serre-Genestier (S8 sequence), which are themselves truncated by the conglomerates of the Château de Clumanc Member (S10 sequence).

The spatial and temporal organisation of the successive discontinuities and the associated system tracts results from the deltaic response to eustatic variations (global processes) and local folding of the eastern limb (local processes). The superposition of both parameters generated a synsedimentary fan geometry.



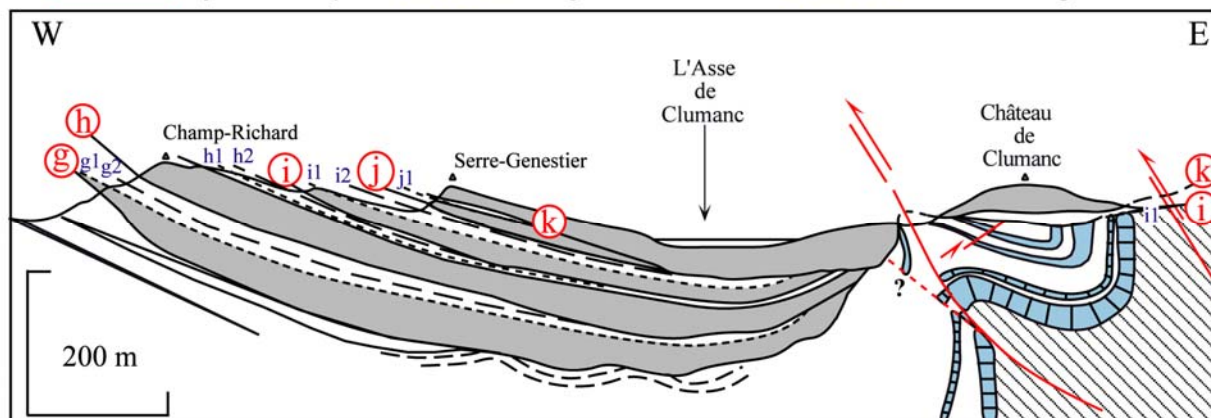
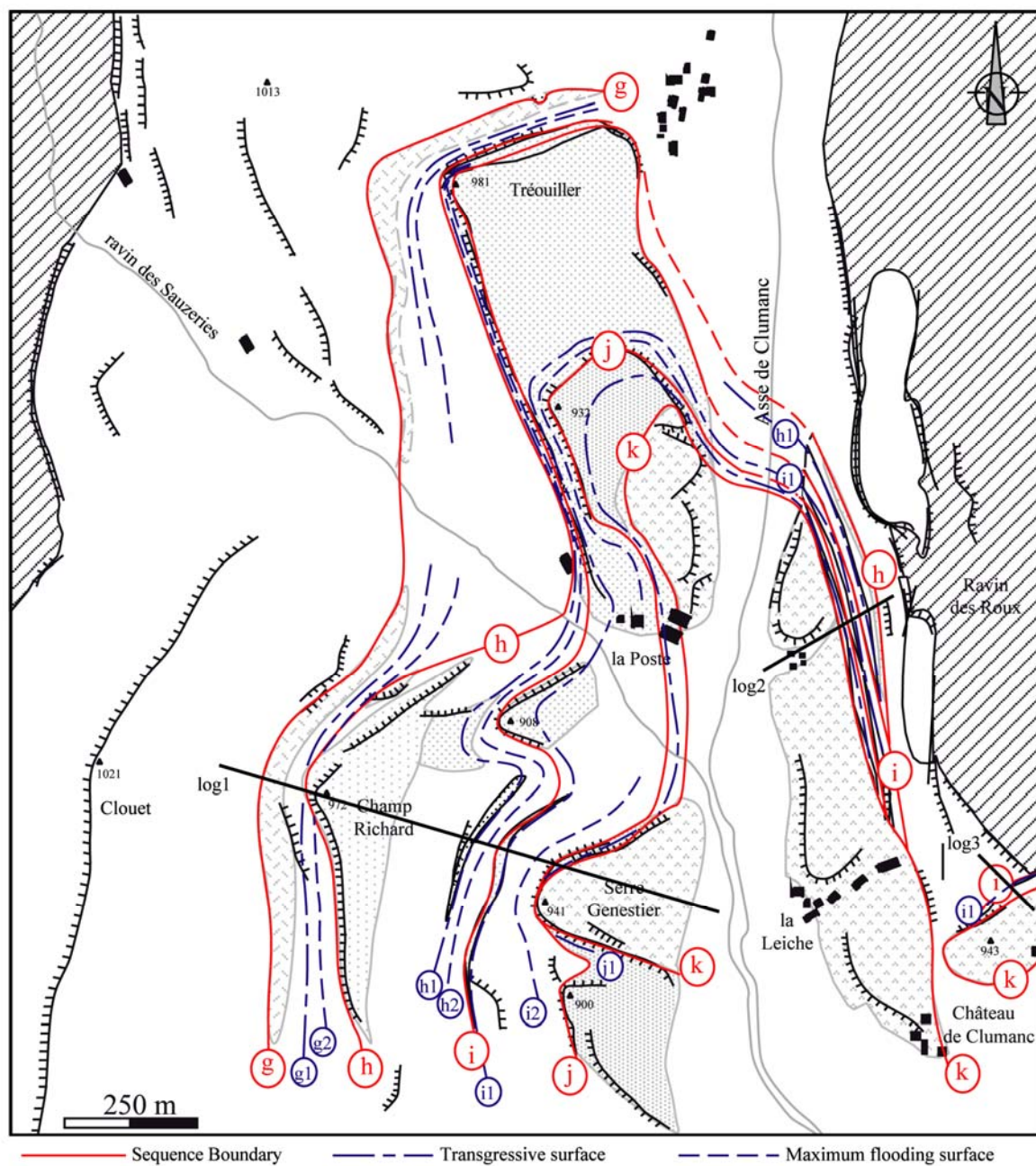


Figure 93a, b : A- Map of the major surfaces in the Conglomerats de Clumanc. Surfaces are located on the synthetic log on figure 104. B- Geometry of the synsedimentary fold of Clumanc illustrating the superposition of folding and sea-level fluctuations.

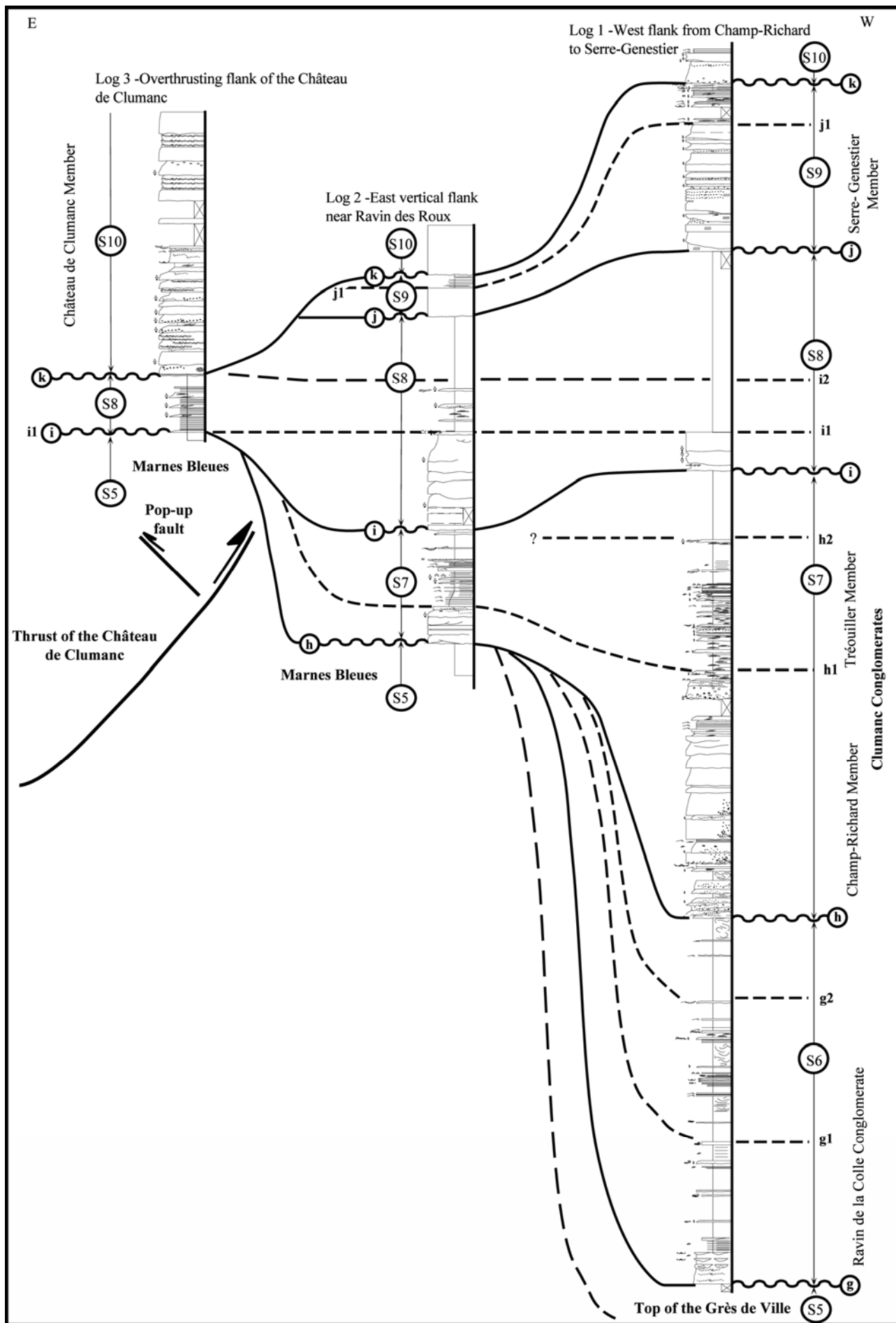


Figure 94 : Sequential correlation between the eastern and western limbs of the syncline. Relationships with the synsedimentary fold, see Figure 93.

## Stop n°5 : Saint-Lions Gilbert Delta. Evolution and Geometry of the Conglomérats de St-Lions

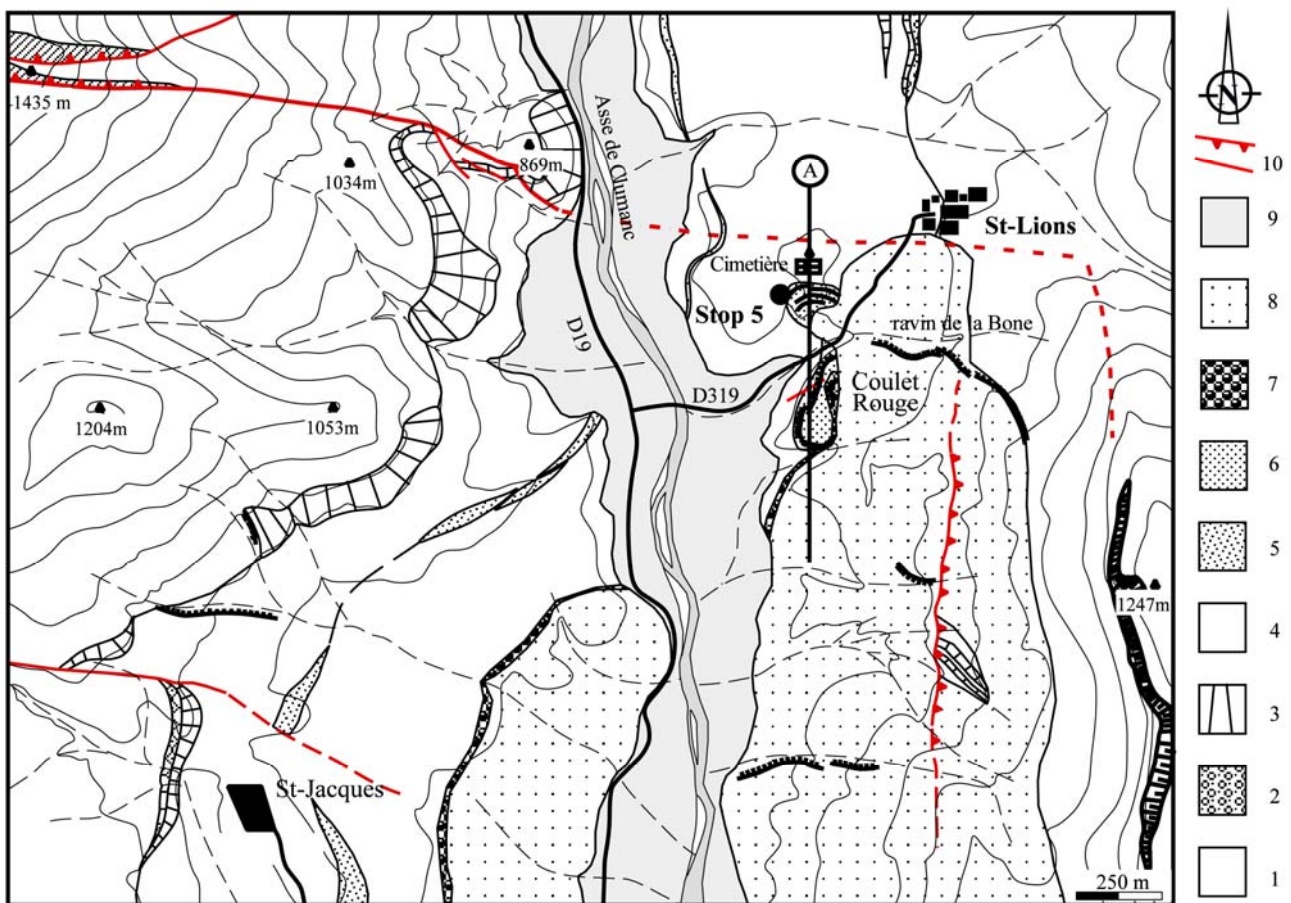
### - Access

Follow the road D319 toward Saint-Lions between Clumanc and Barrême. Then in Saint-Lions town take the road to Saint-Lions cemetery on the left.

### - Tectonic structures (Figure 95)

The Conglomérats de St-Lions are located on the left bank of l'Asse de Clumanc River, between the D19 road and St-Lions town. This formation outcrops in the both sides of the Ravin de la Bone and can be divided into two units : the St-Lions Cemetery Member to the north and the Coulet Rouge Member to the south.

A N-S cross section, from the St-Lions cemetery to the Coulet Rouge shows a pronounced deformation of the cemetery area due to the presence of a steeply dipping limb of an E-W oriented fold (Figure 96). This zone of complex deformation may be due to the superposition of two stress regimes: the alpine E-W compression, as seen in the Clumanc area and a local N-S compression related to the presence of lateral tip folds to the Digne thrust (Dourness units) (Cf. Figure 77 & Figure 78).



1-Cretaceous substrat ; 2-bored conglomerates; 3-Calcaires à Nummulites ; 4-Marnes bleues ; 5-Grès de Ville ; 6-Saint-Lions Conglomerates  
7-Saint-Lions Biostrom ; 8-continental series (Molasse rouge, Série grise, Série saumon) ; 9-Quaternary ; 10-Major Faults

Figure 95 : Detailed geological map of the Saint-Lions area.



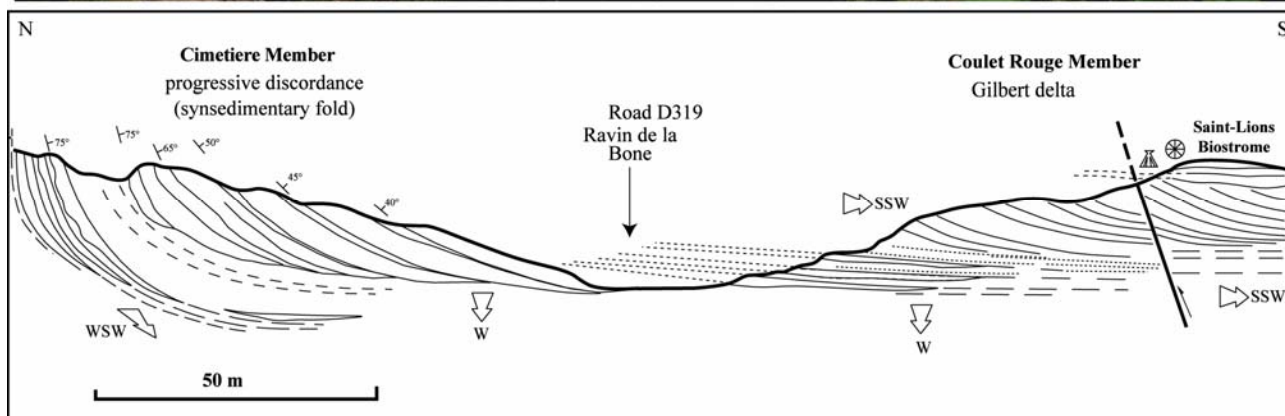


**Figure 96 : North South profile through the St-Lions Tertiary exposures (view to the east) from the Cemetery to the Coulet Rouge. Major paleocurrent orientations shown by open arrows.**

The first deposits of the Conglomérats de St-Lions (Cemetery Member) are folded to a vertical dip. The bedding dip decreases progressively southward. In the Coulet Rouge area, two conglomeratic units, characterised by 10m high forests prograde over silty marls. They are cut by a small thrust fault dipping 65°S. The foresets are overlain by tabular conglomeratic beds interpreted as topsets. On the top of the Coulet Rouge Member, we observe a small unconformable biostrome of polyp and *Ostrea* below the first conformable continental deposits of the Molasse Rouge (Figure 98).

### **- Vertical facies evolution of the Conglomérats de Saint-Lions (Figure 97)**

The synthetic log of the Conglomérats de St-Lions is a composite section because of the migration of depocentre to the south (Figure 98). The Grès de Ville is thin and its contact with the Conglomérats de St-Lions is poorly exposed in this area.

The Conglomérats de St-Lions are similar to the Conglomérats de Clumanc in that they contain the same assemblage of exotic elements. Facies associations are equivalent but not so diverse.

At its base, the Cemetery Member shows coarse debris-flows. Deposits rapidly pass upward into clast supported conglomerates with frequent imbrication indicating westward directed paleocurrents. The first conglomerates of the Coulet Rouge Member have the same paleoflow direction, recorded by large oblique stratification with dips from 15° to 25° to the south (Figure 98b et Figure 99). These are interpreted as foresets of a small Gilbert Delta. The top of the Conglomérats de Saint-Lions is characterised by tabular conglomeratic beds interpreted as the *topsets* of the Gilbert Delta (Figure 113) Then occur glauconitic sands with planar cobble beds (Figure 98c), characteristic of gravelly *shoreface* environments, overlain by the small Biostrome de Saint-Lions. This last marine deposit is directly overlain by red mudstones of the Molasse Rouge.

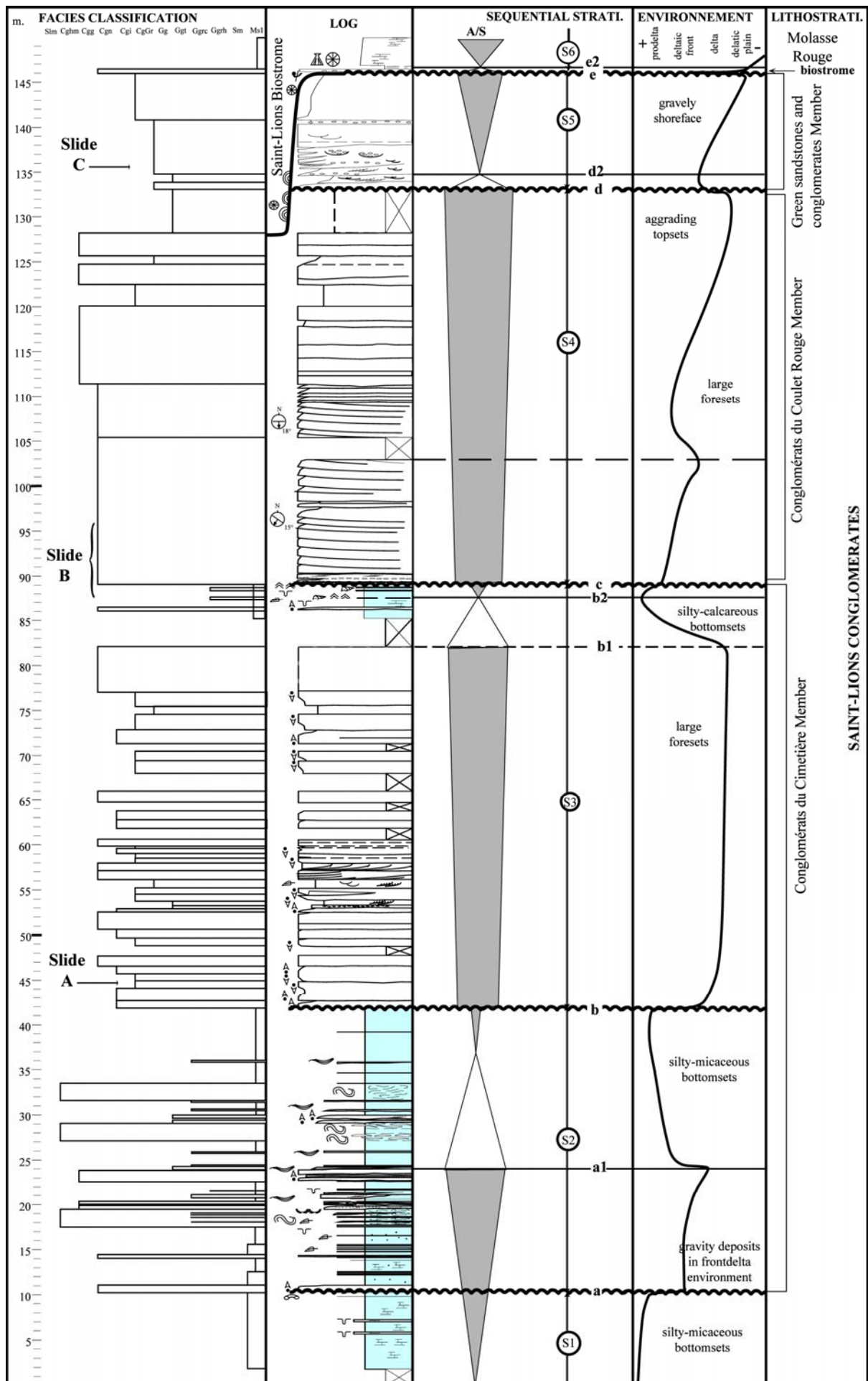


Figure 97 : Synthetic and composite log of the Saint-Lions Conglomerates.

Several characteristics define the Saint-Lions system as a fluvial deltaic regime (Postma, 1990) :

- The very coarse grain size of the material and the height and dip of large oblique foresets
- The near absence of wave influences in the bottomsets facies, the high frequency of the reworking in the prodelta, bottomset and even in the foreset facies.

In the Coulet Rouge area, the spatial organisation and the stratigraphic architecture of the conglomeratic deposits are characteristic of a Gilbert delta (Gilbert, 1885 ; Fayol, 1888) with a progradation to the south (Elliot *et al.*, 1985 ; Evans & Elliot, 1999). Pinch-out of the foresets into the bottomsets is abrupt due to the very coarse grain size of the material. The transition from topset to foreset may be truncated or define a sigmoidal-oblique geometry (Figure 99).

### **- Interpretation**

The geometry of the Saint-Lions Gilbert delta defines a complex sigmoid-oblique delta (Colonna, 1988). This architecture emphasises a high progradation rate and relatively low subsidence rate. These observations confirm the fluvial characteristics of the deltaic system. Paleoflow started in an east to west orientation and rapidly became southward directed implying rapid and significant modifications of the basin floor topography during sedimentation.

Sedimentological analysis highlights the regressive trend of the Conglomérats de St-Lions, similar to the regressive trend observed in the Clumanc area and this could be time equivalent to the regressive interval of TA4 supersequence from Haq *et al.* (1988). Like in the Clumanc deltaic setting, spatial organisation is characteristic of a forced regression (Posamentier *et al.*, 1992), with progressive migration to the south of depocenters associated with a prograding trend. The Saint-Lions Biostrome records a short but intense transgression, which could be correlated with the first transgression of the Chattian time. The lack of better stratigraphic data prevents a precise age attribution for this transgressive interval.

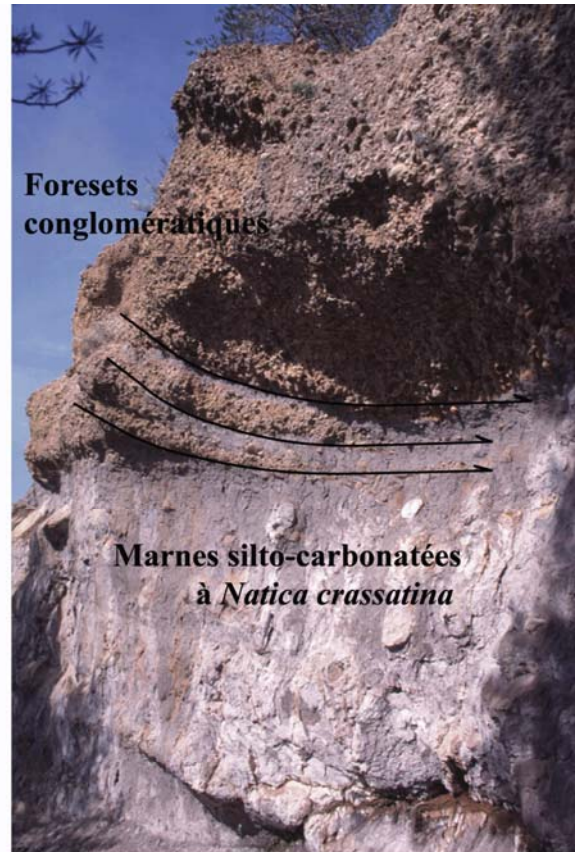




**Slide A-** Imbricated conglomerates observed in the foresets of the Saint-Lions conglomerates Member



**Slide C-** Gravely shoreface of the green sandstones and conglomerates Member below the Saint-Lions Biostrome



**Slide B-** Pinch-out of the conglomeratic foresets of the Saint-Lions Gilbert-delta.



**Slide D-** general view of the Saint-Lions Gilbert-delta. View from the road D19. Pinch out toward the South of the foresets to silty calcareous bottomsets.

**Figure 98A :** clast imbrication developed in foresets of the Saint Lions Gilbert Delta. **B-** Large conglomeratic foresets and rapid pinch-out to bottomsets. **C-** Shoreface deposits in the Sables Verts Member and the Conglomerates of Coulet Rouge. **D-** General view of the Gilbert delta.



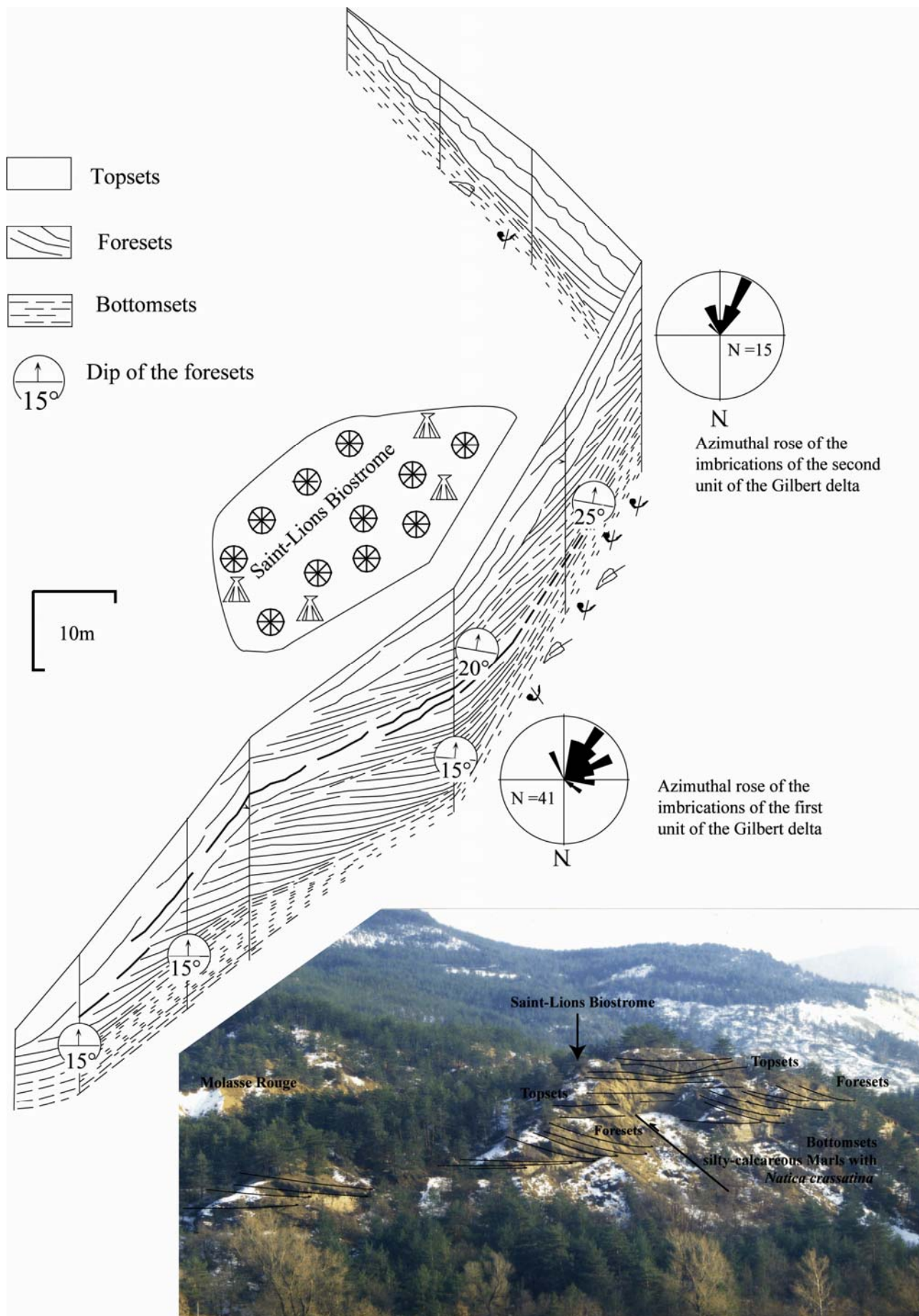


Figure 99 : General view of the Gilbert delta (View to the SE) and geometric diagram of the Gilbert delta of Saint-Lions (Coulet Rouge member) with the overlying Biostrome.

## **Stop n°6 : General view of the Senez town. The Grès de Senez**

### **- Access**

Follow the national road N85 from Barrême to Castellane along the Asse de Blieux River. Take the Senez Bridge toward Senez town.

The Grès de Senez is exposed in the southern sector of the Barrême Syncline (Figure 100). These deposits outcrop on both banks of l'Asse de Blieux River and form well-exposed bars and cliffs. On the eastern limb of the syncline, the Grès de Senez only outcrops near Senez town and around the Malvoisin locality. The Nummulitic Series is cut by dextral strike-slip faults that displace the Grès de Senez.

### **- Sedimentological data (Figure 101 et Figure 102)**

The Grès de Senez contrasts considerably with its northern equivalent formations. Grain size is medium to coarse sand, often bioturbated, with abundant plant debris and bivalves or gastropods. Conglomeratic facies appear at the top of the succession (Conglomérats de Malvoisin Member). The whole of the Grès de Senez sequence is dominated by sand with a coarsening-up trend from silty calcareous marls to coarse sandstone at the top (Figure 102). Near Senez Bridge, well-developed large stratification is observed with a progradation to the north (Figure 102). **Several erosional surfaces are observed and can be followed in different areas.**

The overlying Conglomérats de Malvoisin are characterised by well-sorted and often bored cobbles. These are the last marine deposits below the Molasse Rouge and are more developed on the eastern limb of the syncline.

### **Three distinctive sedimentary environments are defined:**

- **Upper offshore to lower shoreface:** developed at the base of the Grès de Senez with bioturbated silty marls with abundant plant debris and frequent HCS structures. These facies occur again in the Grès Verts member.

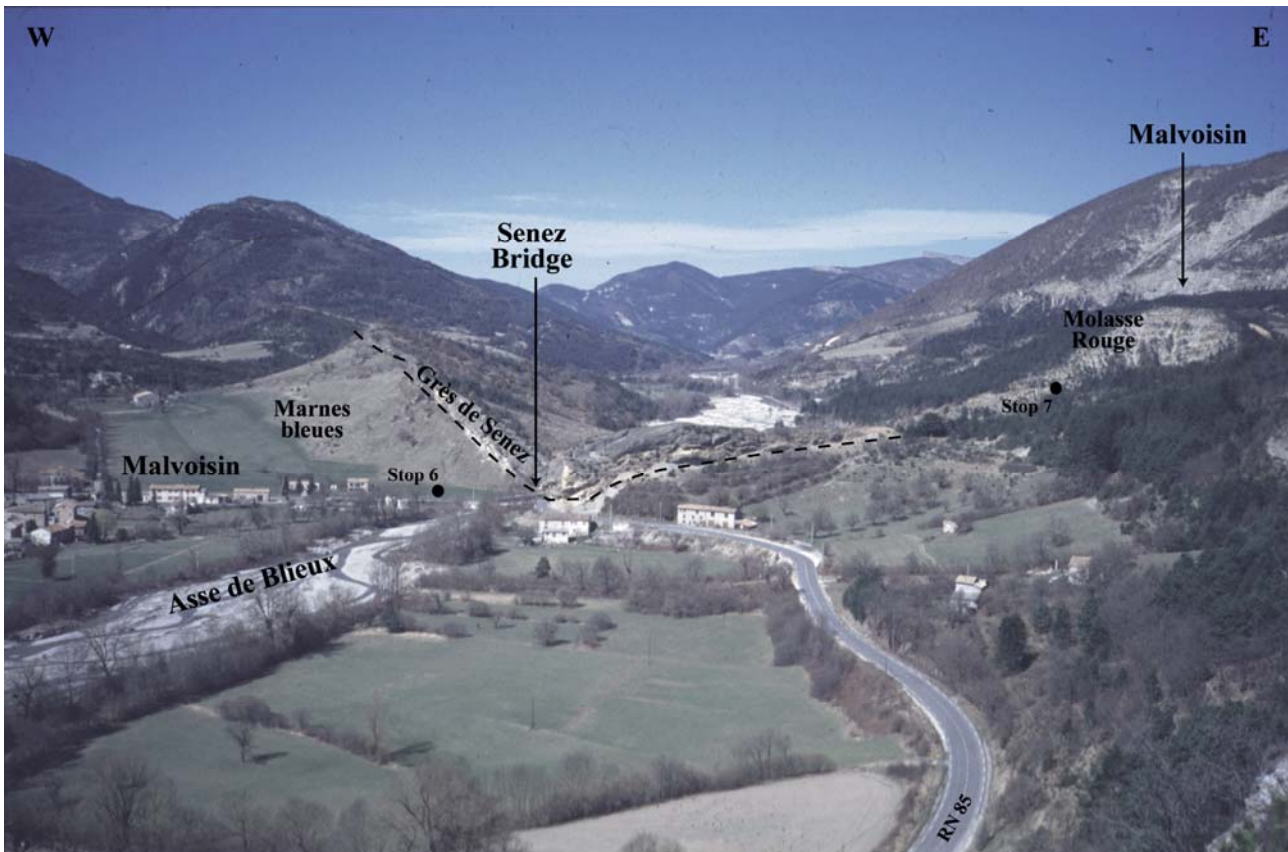
- **Sandy shoreface :** corresponds to the massive bar of the Grès de Senez (lower member of the Grès de Senez *s.s*) and shows large oblique stratification prograding to the north with cross lamination, current ripples, abundant fauna and bioturbation.

- **a confined environment :** subaquatic to lagoonal environment. These deposits occur only in the Dégoutail Member and are particularly well-exposed on the eastern limb of the syncline. Oxidation surfaces, and brackish facies with associated ostracods are often present.

As in other areas, we observe the same general scheme of confinement and progradation that record a regressive trend of the upper part of the marine series in the Barrême Syncline.



- Structures and Geometries of the Grès de Senez



General view to the North of the Grès de Senez Cuesta at the Senez Bridge

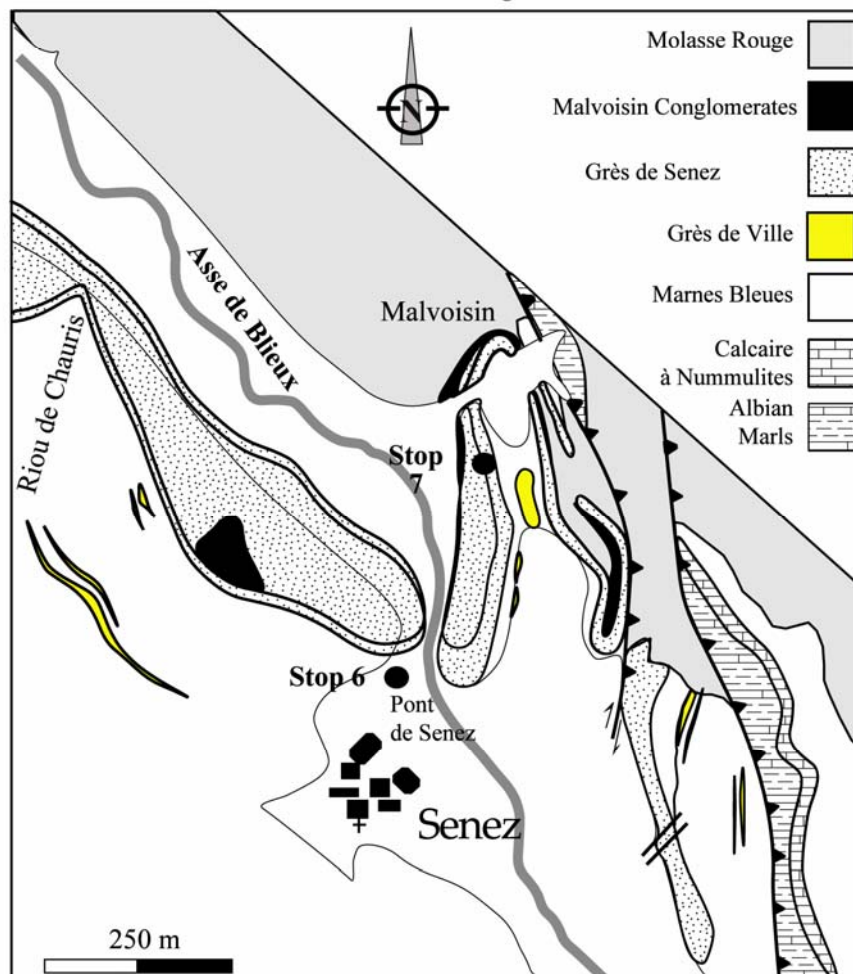
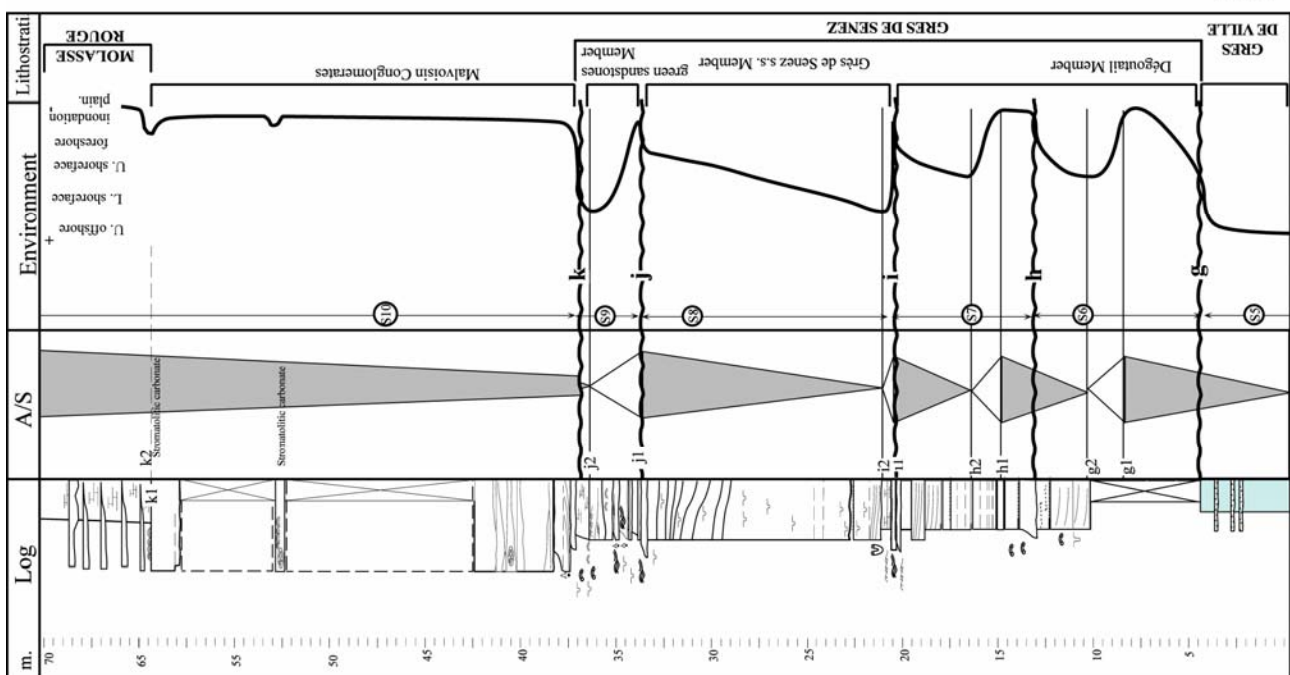


Figure 100 : (a) General view to the north of the Senez cliffs. (b) Simplified geological map of the Senez area.



**Figure 101 : General view of the left bank of l'Asse de Blieux River near the Senez Bridge. The Grès de Senez programmes to the north and is characterised by large oblique stratifications with a general regressive trend.**

**Figure 102 : Synthetic log of the Grès de Senez (Malvoisin section).**



## **Stop n°7 : General View of the Roche Blanche. The Malvoisin anticline**

### **- Access**

The way to the Malvoisin anticline is near the mill on the right hand side of the Asse de Blieux River. Take the path to the Rote Blanche and follow the crystalline of the Grès de Senez above the national road 85.



**Figure 103 : Panoramic view of the Malvoisin anticline (view to the north). The synsedimentary fold was developed during deposition of the Grès de Senez and seems to die out during deposition of the Molasse Rouge.**

### **- The Malvoisin synsedimentary fold**

The most spectacular record of synsedimentary deformation in the Senez area is the Malvoisin Anticline (Figure 103), a growth anticline that developed during deposition of the Grès de Senez and the Conglomérats de Malvoisin and seems to have died out during deposition of the Molasse Rouge (Chauveau & Lemoine, 1961).

We observe a progressive thickening of deposits across the western limb of the anticline away from its hinge, while deposits are thin on the eastern limb of the anticline. Different characteristic surfaces (mfs, Ts) can be followed and constrain the dynamic growth of this anticline from the lower Grès de Senez member to the top of the Conglomérats de Malvoisin (Figure 104). The superposition of the growth of this fold and variations of the sedimentary flux controlled the amplitude of internal unconformities and the thickness of the transgressive deposits. The eastern limb of the basin was affected by continuous deformation recorded by the Malvoisin Anticline, which generated progressive unconformities.

Large slides are well-developed in the Grès de Senez near the Senez bridge (Figure 105). These are not present on the other bank of the river. These may have been caused by the progressive destabilisation of proximal deposits during growth of the Malvoisin anticline.



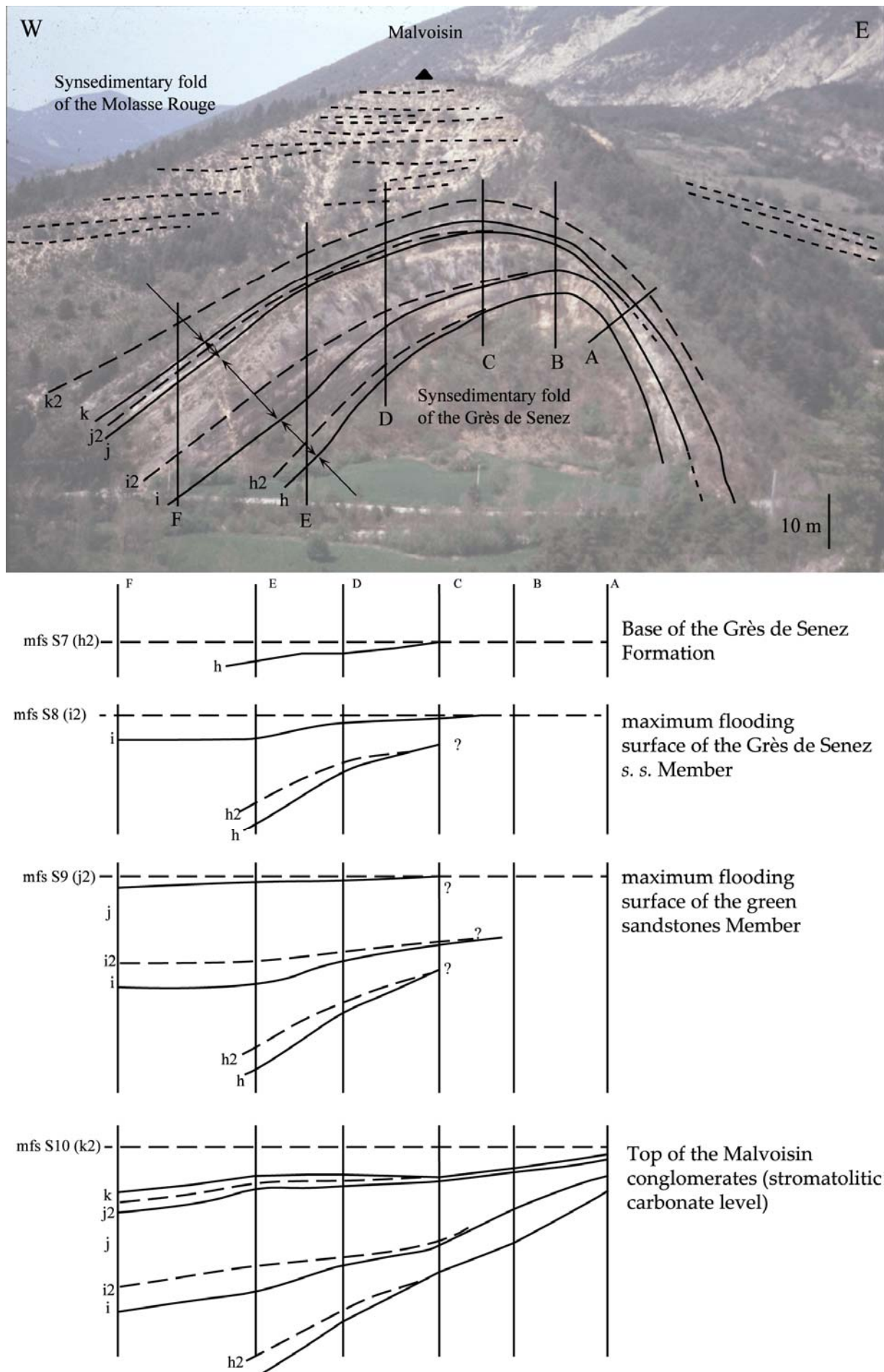


**Figure 104 : Progressive evolution of the depositional geometry of Grès de Senez and the Malvoisin Conglomerates in relationship with the genesis of the Malvoisin anticline.**



General view of the Grès de Senez on the right border of the Asse de Blieux River



Large slide into the Grès de Senez Formation



folded slide into the Grès de Senez. way to the Roche Blanche.



Detail of the slide into the Grès de Senez Formation

discordance and pinch-out into the silty calcareous marls  
below the Grès de Senez Formation



**Figure 105 : Folded slides in the Grès de Senez Formation along the N85 road.**

## Synthesis

The evolution of the sedimentary infill of the Barrême Basin was strongly controlled by tectonic forcing. We identify two successive episodes (Figure 106) :

- **The first interval records the general deepening of the whole Barrême Basin characterised by a high rate of tectonic subsidence** as recorded by the transition from the Calcaires à Nummulites to the Marnes Bleues. This phase corresponds to the transition from the A Zone to the B Zone in the model of Posamentier & Allen (1993) (Figure 107). Progressively, subsidence rate becomes higher than the eustatic variations. Barrême Basin is located in the B Zone and sea level falls have minor effect in the Barrême basin (type II sequence boundaries). It's synchronous with the TA4 transgressive interval. During this period, tilting of the eastern limb of the basin begins with moderate folds (Château de Clumanc outcrop). The Grès de Ville deposits are drained in the N-S axis of the Basin and subsidence rate seems to be similar to the sedimentary flux because of the persistence of same paleobathymetric conditions during the Grès de Ville deposition.

- **The second interval records the rapid infilling of the Barrême basin that corresponds too with the final closure of the whole marine Paleogene foreland basin of the southern subalpine domain.** The infilling is associated with a folding deformation on the eastern limb of the Barrême basin, from Clumanc area to Senez area. Sedimentation is also dominated by a rapid detrital progradation from the internal alpine zones for the Clumanc alluvial delta and Saint-Lions delta and from the south with the denudation of the Maures-Esterel massif for the Grès de Senez.. During this period, the basin is characterised by a lowering of accommodation space. It corresponds to the regressive interval of TA4 second order sequence (Haq et al., 1987). Locally Tectonic uplift develops force regression, well-known in synorogenic basin (Gawthorpe *et al.*, 2000). The Barrême basin is located in the C Zone of Posamentier & Allen Model C (Figure 107). For this period, we observe a rotation of 180° of paleoflow orientations that indicates drastic modifications of basin floor topography and significant modification in the alpine paleogeography with the genesis of a new Digne thrust front. Growth folding was associated with dextral strike-slip faulting and minor thrusting that generated uplift of the eastern limb of the syncline with the systematic development of second order synsedimentary folds. These observations emphasise the thrust-sheet-top character of the Barrême Basin.



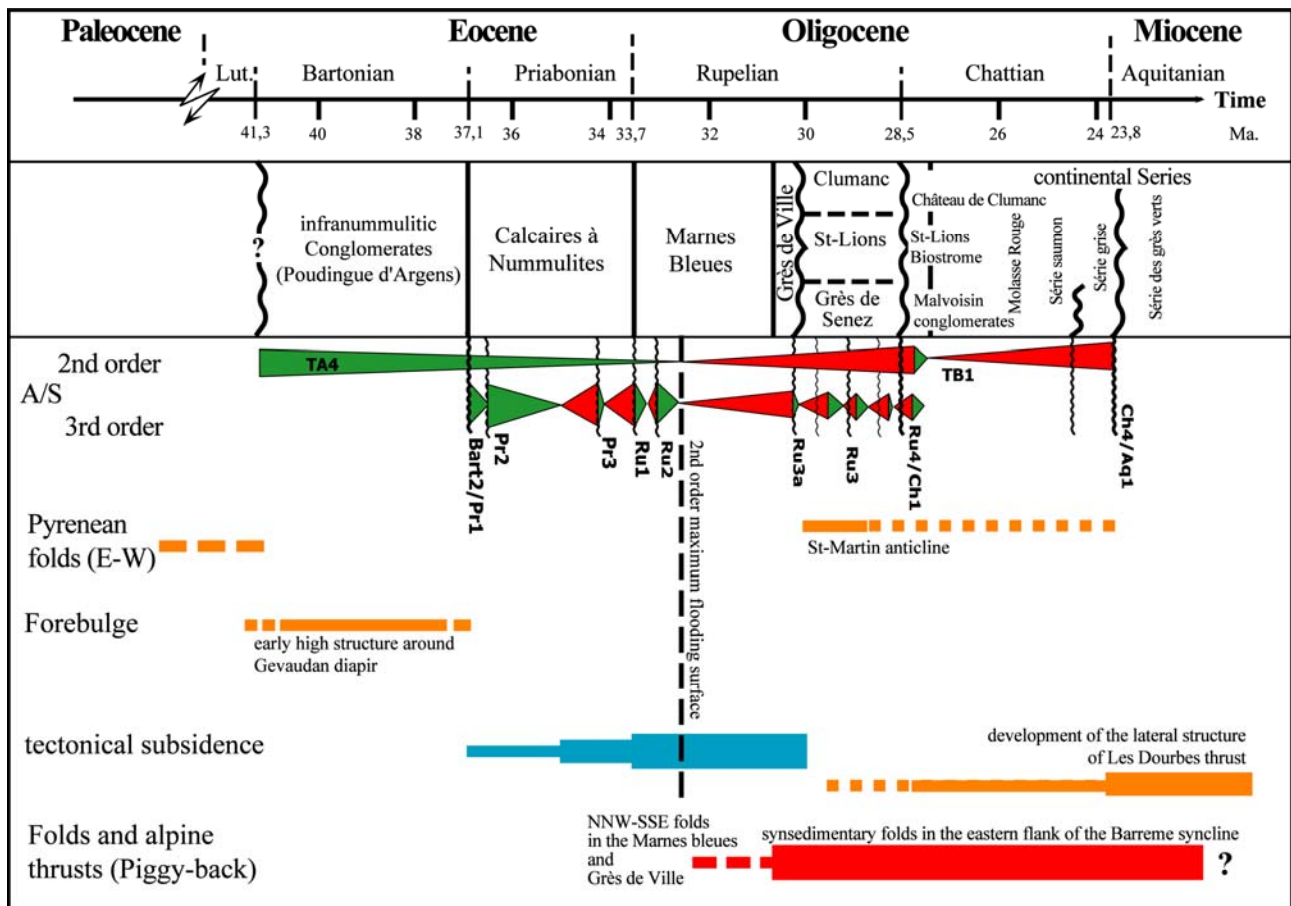


Figure 106 : Chronology of tectonic events and depositional sequences during the Paleogene history of the Barrême Basin.

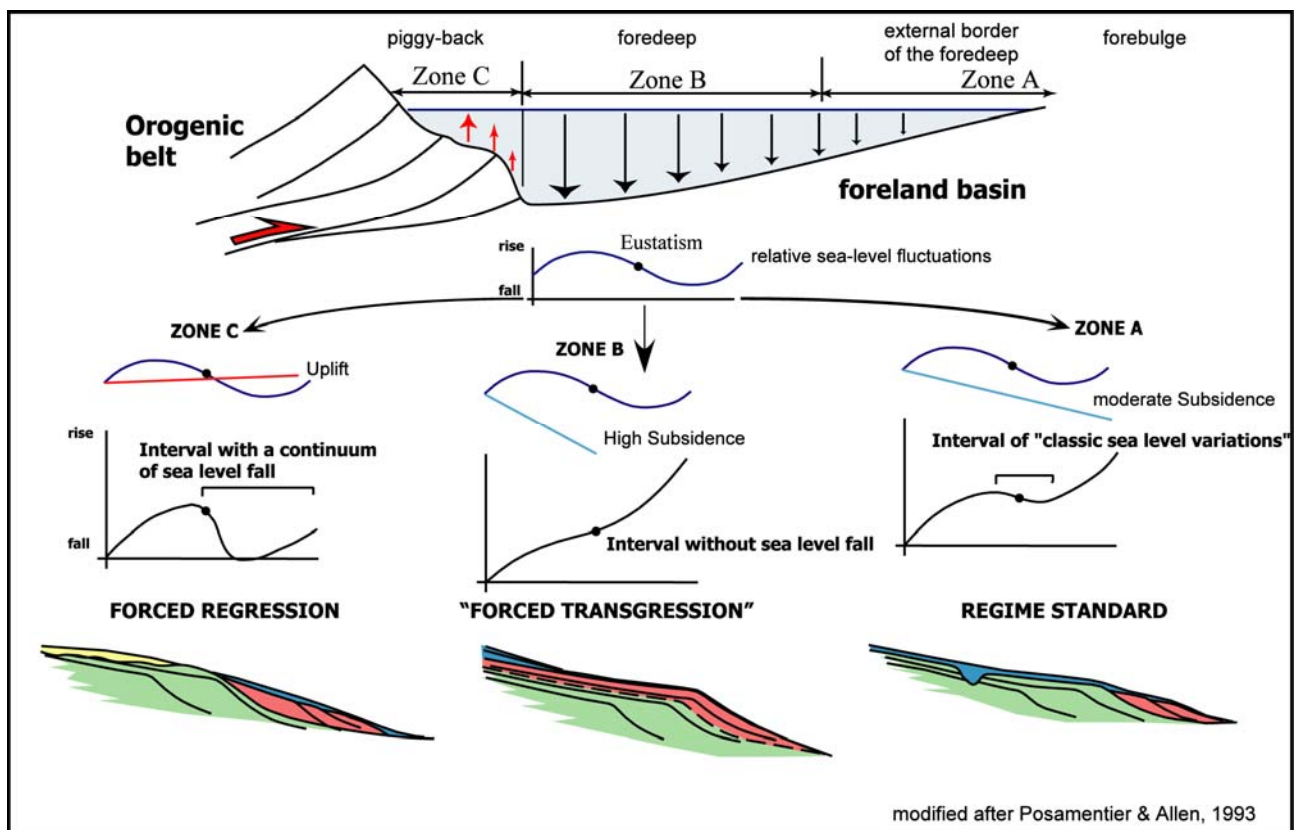


Figure 107 : Tectono-eustatic model for infill of a foreland basin (modified after Posamentier & Allen, 1993).



## Bibliography

- ALBUSSAIDI, S. & LAVAL, A. 1984. Nouvelles observations de la série Priabonienne. Evolution latérale en relation avec la tectonique. *Diplôme ENSPM ref 32677*.
- ALLEN, A. & BASS, J. P. 1993. Sedimentology of the Upper Marine Molasse of the Rhône Alps Region, Eastern France : Implications for Basin Evolution. *Eclogae geol. Helv.*, 86/1. p.121-172.
- ALLEN, J.R.L. 1973. A classification of climbing-ripple cross-lamination. *Journal of the geological Society, London*, 129, 537-541.
- AMY, L.A., MCCAFFREY, W.D. & KNELLER, B.C. 2004. The influence of lateral basin-slope on the depositional patterns of natural and experimental turbidity currents. In : Joseph P. & Lomas S.A. (eds). *Deep-Water Sedimentation in the Alpine Basin of SE France: New Perspectives on the Grès d'Annot and Related Systems*, Geological Society, London, Special Publications, 221, p. 311-330.
- APPS, G.M. 1985. The Grès d'Annot foreland basin, Haute Provence: the control of turbidite deposition by structurally induced basin floor topography. *6th European Regional Meeting of Sedimentology IAS Lleida*: 18-21.
- APPS, G.M. 1987. Evolution of the Grès d'Annot Basin, South West Alps. *PhD thesis: Liverpool UK, University of Liverpool*: 352 p.
- APPS, G., PEEL, F. & ELLIOTT, T. 2004. The structural setting and palaeogeographic evolution of the Grès d'Annot basin. In : Joseph P. & Lomas S.A. (eds). *Deep-Water Sedimentation in the Alpine Basin of SE France: New perspectives on the Grès d'Annot and related systems*, Geological Society, London, Special Publications, 221, p. 65-96.
- ARTONI, A. & MECKEL, L. D. III 1998. History and deformation of a thrust sheet top basin : the Barrême basin, western Alps, SE France. Cenozoic Foreland Basins of Western Europe. Ed. A. Mascle, C. Puigdefabregas, H. P. Luterbacher & M. Fernandez. *Geol. Soc. Spec. Publ.* 134. p. 213-237.
- B.R.G.M. 1996. Carte géologique de la France au 1:1000000, *Bureau de Recherches Géologiques et Minières*, Service Géologique National, Orléans.
- BEAUDOIN, B., CAMPREDON, R., COTILLON, P. & GIGOT, P. 1975. Alpes méridionales françaises – reconstitution du bassin de sédimentation. *IXe Congrès International de Sédimentologie*.
- BERGER, A. 1988. Milankovitch theory and climate. *Reviews of Geophysics*, 26, 624-657.
- BERGGREN, W.A., KENT D.V., SWISHER, C.C. & AUBRY, M.P. 1995. A revised Cenozoic geochronology and chronostratigraphy. *SEPM Special Publications*, Tulsa, 54: 129-212.
- BERTRAND, L. 1896. Etude géologique du Nord des Alpes-Maritimes. *Bull. Serv. Carte Géol. Fr.*, t. XI., n°56.
- BODELLE, J. 1971. Les Formations Nummulitiques de l'Arc de Castellane. Thèse de Doct. ès Sc., Univ. Nice, 540 p.
- BOUMA, A.H. & COLEMAN, J.M. 1985. Peïra-Cava Turbidite System, France, in: Bouma A. H., Normark W. R. & Barnes N. E. (eds) *Submarine fans and related turbidite systems*. Springer-Verlag, New York, 217-222.
- BOUMA, A.H. 1962. Sedimentology of some flysch deposits: a graphic approach to facies interpretation, *Elsevier Publ.* 6, 159 pp.
- BOURGEOIS, A., JOSEPH, P. & LECOMTE, J.C. 2004. Three-dimensional full wave seismic modelling versus one-dimensional convolution: the seismic appearance of the Grès d'Annot turbidite system. In : Joseph P. & Lomas S.A. (eds). *Deep-Water Sedimentation in the Alpine Basin of SE France: New perspectives on the Grès d'Annot and related systems*, Geological Society, London, Special Publications, 221, p. 401-417.
- BOUROULLEC R., CARTWRIGHT J.A., JOHNSON H.D., LANSIGU, C., QUÉMENER J.M. & SAVANIER D. 2004. Syn-depositional Faulting in the Grès d'Annot Formation, SE France: High-Resolution Kinematic Analysis and Stratigraphic Response to Growth Faulting. In : Joseph P. & Lomas S.A.(eds). *Deep-Water Sedimentation in the Alpine Basin of SE France: New perspectives on the Grès d'Annot and related systems*, Geological Society, London, Special Publications, 221, p. 241-265.
- BOUSSAC, J. 1912. Etudes stratigraphiques sur le Nummulitique alpin, *Mém. Carte Géol. France*, 662 p.
- BROUCKE, O., GUILLOCHEAU, F., ROBIN, C., JOSEPH, P. & CALASSOU S. 2004. The influence of syndepositional basin floor deformation on the geometry of turbiditic sandstones: a reinterpretation of the Côte de l'Âne area (Sanguinière-Restefonds sub-basin, Grès d'Annot, Late Eocene, France). In : Joseph P. & Lomas S.A. (eds). *Deep-Water Sedimentation in the Alpine Basin of SE France: New perspectives on the Grès d'Annot and related systems*, Geological Society, London, Special Publications, 221, p. 203-222.
- CALLEC, Y. 2001. La déformation synsédimentaire des bassins paléogènes de l'arc de Castellane (Annot, Barrême, Saint-Antonin). Thèse de doctorat. ENSMP. Vol. I&II. 674 p.
- CALLEC, Y. 2004. The turbidite fill of the Annot sub-basin (SE France): a sequence stratigraphy approach. In : Joseph P. & Lomas S.A. (eds). *Deep-Water Sedimentation in the Alpine Basin of SE France: New perspectives on the Grès d'Annot and related systems*, Geological Society, London, Special Publications, 221, p. 111-135.
- CALLEC, Y., MERCIER, D. & WERNLI, R. 1998. Two types of synsedimentary deformation in contemporaneous paleogene foreland basins. Barreme and Annot synclines. SE France.-15ème Congrès International de l'IAS. Alicante, Espagne, 13-17/04/98.
- CAMPREDON, R. 1977. Les formations paléogènes des Alpes maritimes franco-italiennes. *Mémoire hors série de la Société Géologique de France*, 9.
- CAMPREDON, R. & GIANNERINI, G. (1982) Le synclinal de Saint-Antonin (arc de Castellane, chaînes subalpines méridionales). Un exemple de bassin soumis à une déformation compressive permanente depuis l'Eocène supérieur. *Géologie Alpine*, t 58, p. 15-20.



- CHAUVEAU, J.C. & LEMOINE, M. 1961. Contribution à l'étude géologique du synclinal tertiaire de Barrême (moitié nord), feuille de Digne 1/50000. *Bull. Serv. Carte géol. Fr.*, 58, N° 264, p. 147-178.
- CLARK, J.D. & GARDINER, A.R. 2000. Outcrop Analogues for Deep-Water Channel and Levee Genetic Units from the Grès d'Annot Turbidite System, SE France. In: Weimer, P., Slatt, R.M., Coleman, J., Rosen, N.C., Nelson, H., Bouma, A.H., Styzen, M.J. & Lawrence, D.T. (eds). *Deep-Water Reservoirs of the World: Proceedings of the GCSSEPM Foundation 20<sup>th</sup> Annual Research Conference*, December 3-6, 2000, Houston, Texas., SEPM CD-ROM Sp. Publ. 28, 175-190.
- COLELLA, A. 1988. Gilbert-type fan deltas in the Crati basin (Pliocene-Holocene, Southern Italy). International workshop on fan deltas, Calabria, Italy. A. Colella ed., excursion guidebook. p. 17-78.
- COLEMAN, J. M. & WRIGHT, L. D. 1975. Modern river deltas : variability of processes and sand bodies. Deltas : Models for exploration. Ed. M. L. Broussard. Hous. Geol. Soc. p. 99-149.
- CRAMPTON, S. L. E. & ALLEN, P. A. 1995. Recognition of forebulge unconformities associated with early-stage foreland basin development : example from the north Alpine foreland basin. *Bull. AAPG*, 79, p. 1495-1514.
- CROSS, T.A. & LESSENGER, M.A. 1998. Sediment volume partitioning: rationale for stratigraphic model evaluation and high-resolution stratigraphic correlation. In: Gradstein, F.M., Sandvik, K.O. et Milton, N.J. (eds) *Sequence stratigraphy - Concepts and applications*. Norwegian Petroleum Society (NPF) Special Publication, Elsevier Science B.V., Amsterdam, 8, 171-195.
- CROSS, T.A., BAKER, M.R., CHAPIN, M.A., CLARK, M.S., GARDNER, M.H., HANSON, M.S., LESSENGER, M.A., LITTLE, L.D., McDONOUGH, K.J., SONNENFELD, M.D., VALASEK, D.W., WILLIAMS, M.R. & WITTER, D.N. 1993. Applications of high-resolution sequence stratigraphy to reservoir analysis. In: Eschard, R. & Doligez, B. (eds) *Subsurface reservoir characterization from outcrop observations*. Éditions Technip, Paris, 11-33.
- CRUMEYROLLE, P., RUBINO, J.L. & CLAUZON, G. 1991. Miocene depositional sequences within a tectonically controlled transgressive-regressive cycle. In: MACDONALD, D.I.M. (ed.) *Sedimentation, Tectonics and Eustasy: Sea level changes at active margins*. Special Publication of the International Association of Sedimentologists, 12, 373-390.
- DEPERET 1895. Note sur les fossiles oligocènes de Barrême. *Bull. Soc. Géol. de France*, (3), t. XXIII, p. 878-883.
- DICKENSON, W.R. 1974. Plate tectonics and sedimentation. In: Dickinson, W.R. (ed.) *Tectonics and sedimentation*. Society of Economic Paleontologists and Mineralogists Special Publication, Tulsa, 22, 1-27.
- DU FORNEL, E. 2003. *Reconstitution sédimentologique tridimensionnelle et simulation stratigraphique du système turbiditique éocène - oligocène des Grès d'Annot (Alpes méridionales)*. Thèse de doctorat en Sciences de la Terre de l'Université de Rennes 1, 243 p.
- DU FORNEL, E., JOSEPH, P., DESAUBLIAUX, G., ESCHARD, R., GUILLOCHEAU, F., LERAT, O., MULLER, C., RAVENNE, C. & SZTRAKOS, K. 2004. The southern Grès d'Annot Outcrops (French Alps): an attempt at regional correlation. In : Joseph P. & Lomas S.A. (eds). *Deep-Water Sedimentation in the Alpine Basin of SE France: New perspectives on the Grès d'Annot and related systems*, Geological Society, London, Special Publications, 221, p. 137-160.
- EDWARDS, D.A., LEEDER, M.R., BEST, J.L. & PANTIN, M.H. 1994. On experimental reflected density currents and the interpretation of certain turbidites. *Sedimentology*, 41, 437-461.
- ELLIOTT, T., APPS, G., DAVIES, H., EVANS, M., GHIBAUDO, G. & GRAHAM, R.H. 1985. A structural and sedimentological traverse through the Tertiary foreland basin of the external Alps of south-east France, in P.A. Allen, P. Homewood and G. William, (eds) *Int. Symposium on foreland Basins*, Excursion Guidebook, Fribourg, International Association of Sedimentologists, p. 39-73.
- ESPITALIÉ, J. & SIGAL, J. 1960. Microstratigraphie des "Marnes Bleues" des bassins tertiaires des Alpes méridionales. Le genre Caucasina (foraminifère). *Rev. Micropaléontol.*, vol.3, 4, p. 201-206.
- EUZEN, T., JOSEPH, P., DU FORNEL, E., LESUR, S., GRANJEON, D. & GUILLOCHEAU, F. 2004. Three-dimensional stratigraphic modelling of the Grès d'Annot system, Eocene-Oligocene, SE France. In : Joseph P. & Lomas S.A. (eds). *Deep-Water Sedimentation in the Alpine Basin of SE France: New perspectives on the Grès d'Annot and related systems*, Geological Society, London, Special Publications, 221, p. 161-180.
- EVANS, M & ELLIOT, T. 1999. Evolution of a thrust-sheet-top basin : The Tertiary Barrême basin, Alpes de Haute-provence, France. *Geol. Soc. of Am. Bull.* vol. 111, n°11, p. 1617-1643.
- EVANS, M. J. & MANGE-RAJETZKY, M. A. 1991. The provenance of sediments in the Barrême thrust-top basin, Haute-Provence, France. Developments in Sedimentary Provenance Studies, Morton A. C. Ed., *Geol. Soc. Spec. Publi. London*, 57, p. 323-342.
- EVANS, M. J., ELLIOTT, T., APPS, G. & MANGE-RAJETZKY, M. A. 1991. The Tertiary Grès de Ville of the Barrême Basin: feather edge equivalent to the Grès d'Annot ? In : Joseph P. & Lomas S.A. (eds). *Deep-Water Sedimentation in the Alpine Basin of SE France: New perspectives on the Grès d'Annot and related systems*, Geological Society, London, Special Publications, 221, p. 97-110.
- FAURE-MURET, A., KUENEN, PH., LANTEAUME, M. & FALLOT, P. 1956. Sur les flyschs des Alpes-Maritimes Françaises et Italiennes. *C. R. Ac. Sci.*, 243, 1697-1701.
- FAYOL, H. 1888. Résumé de la théorie des deltas et histoire de la formation du bassin de Commentery. *Bull. Soc. Géol. France*, série 3, t. XVI, p. 968-980.
- FLOOD, R.D. 1983. Classification of sedimentary furrows and a model for furrow initiation and evolution. *Geological Society of America Bulletin*, 94, 630-639
- FORD, M. 2004. The significance of growth structures in foreland basin development, *Basin Research*, 16, 361-375

- FORD, M., LICKORISH, W.H. & KUZNIR, N. 1999. Tertiary foreland sedimentation in the southern Subalpine chains, SE France: a geodynamic analysis. *Basin Research*, 11, 315-336.
- FORD, M. & LICKORISH, W.H. 2004. Foreland basin evolution around the western Alpine Arc. In : Joseph P. & Lomas S.A. (eds). *Deep-Water Sedimentation in the Alpine Basin of SE France: New perspectives on the Grès d'Annot and related systems*, Geological Society, London, Special Publications, 221, p. 39-63.
- GALLOWAY, W. E. 1975. Process framework for describing the morphology and stratigraphic evolution of the deltaic depositional systems. *Deltas : Models for exploration*. Ed. M. L. Broussard. Hous. Geol. Soc. p. 87-98.
- GARCIA, D., JOSEPH, P., MARECHAL, B. & MOUTTE, J. 2004. Patterns of geochemical variability in relation to turbidite facies in the Grès d'Annot Formation. In : Joseph P. & Lomas S.A. (eds). *Deep-Water Sedimentation in the Alpine Basin of SE France: New perspectives on the Grès d'Annot and related systems*, Geological Society, London, Special Publications, 221, p. 349-365.
- GARDNER, M.H & BORER, J.M. 2000. Submarine channel architecture along a slope to basin profile, Brushy Canyon Formation, West Texas. In: Bouma, A.H. et Stone, C.G. (eds) *Fine-grained turbidite systems*. American Association of Petroleum Geology, Memoir, 72 and SEPM (Society for Sedimentary Research), Special Publication, 68, 195-214.
- GAWTHORPE, R. L., HARDY, S., HUNT D. & RITCHIE, B. 1999. Controls on the variability of forced regressive/falling stage systems tract, insights from 3D numerical modelling of sedimentation and stratigraphy. Annual Meeting Expanded Abstracts, AAPG. Soc. of Econ. Paleo. Min., Tulsa, OK, US. p. A45-A46.
- GILBERT, G. K. 1885. The topographic features of lake shores. *U. S. Geol. Surv. 5th Ann. Rep.* p. 69-123.
- GOGUEL, J. 1936. Description tectonique de la bordure des Alpes de la Bléone au Var. *Mém. Serv. Carte. Géol. Fr.* 360 p..
- GRACIANSKY, P. C. 1972. Le bassin tertiaire de Barrême (Alpes de Haute-Provence) relation entre déformation et sédimentation ; chronologie des plissements. *C. R. Acad. Sc. Paris, Série D*, t. 275, p. 807-810.
- GRACIANSKY, P. C., DARDEAU, G., LEMOINE, M. & TRICART, P. 1988. De la distension à la compression : l'inversion structurale dans les Alpes. *Bull. Soc. Geol. Fr.*, (8), IV, n°5. p. 779-785.
- GRACIANSKY, P. C., DUROZOY, G. & GIGOT, P. 1982. Notice explicative de la feuille de Digne au 1:50000. *BRGM*. Orléans. 76 p.
- GRACIANSKY, P. C., LEMOINE, M. & SALIOT, P. 1971. Remarques sur la présence de minéraux et de paragenèses du métamorphisme alpin dans les galets des conglomérats oligocènes du synclinal de Barrême (Alpes de Haute-Provence). *C. R. Acad. Sc. Paris, Série D*, t. 272, p.3243-3245.
- GRAS, S. 1840. Statistique minéralogique du Département des Basses-Alpes. Prudhomme, imprimeur-libraire, Grenoble.
- GUBLER, Y. 1958. Étude critique des sources du matériel constituant certaines séries détritiques dans le Tertiaire des Alpes françaises du Sud: formations détritiques de Barrême, Flysch "Grès d'Annot". *Ecl. Geol. Helv.*, vol. 51, n°3, p.942-977.
- GUILLOCHEAU, F. 1990. Stratigraphie séquentielle des bassins de plate-forme : l'exemple dévonien armoricain. Thèse. Université de Strasbourg. 257 p.
- GUILLOCHEAU, F. 1995. Nature, rank and origin of Phanerozoic sedimentary cycles. *Comptes Rendus de l'Académie des Sciences, Paris, série IIa*, 320, 1141-1157.
- GUILLOCHEAU, F., QUÉMÈNER, J.M., ROBIN, C., JOSEPH, P. & BROUCKE, O. 2004. Genetic units / parasequences of the Annot turbidite system, SE France. In : Joseph P. & Lomas S.A. (eds). *Deep-Water Sedimentation in the Alpine Basin of SE France: New perspectives on the Grès d'Annot and related systems*, Geological Society, London, Special Publications, 221, p. 181-202.
- HAND, B.M. 1974. Supercritical flow in density currents. *Journal of Sedimentary Petrology*, 44, 637-648.
- HAND, B.M., MIDDLETON, G.V. & SKIPPER, K. 1972. Antidune cross-stratification in a turbidite sequence, Cloridorme Formation, Gaspé, Québec. *Sedimentology*, 18, 135-138.
- HAQ, B. U., HARDENBOL, J. & VAIL P. R. 1987. Chronology of fluctuating sea levels since the Triassic (250 million years ago to present). *Science*, vol. 235, p. 1156-1167.
- HARDENBOL, J., THIERRY, J., FARLEY, M. B., JACQUIN, T., GRACIANSKY, P. C. & VAIL, P. R. 1998. Mesozoic and Cenozoic sequence chronostratigraphic framework of european basins. Mesozoic and Cenozoic sequence chronostratigraphy of european basins. Ed. P. C. de Graciansky, J. Hardenbol, T. Jacquin & P. R. Vail. *SEPM Spe. Publ.*, n° 60. p.3-11.
- HARMS, J. C. 1975. Stratification and sequences in prograding shoreline deposits. In: Harms, J.C., Southard, J.B., Spearing, D.R., Walker, R.G. (eds) *Depositional environments as interpreted from primary sedimentary structures and stratification sequences*. Society of Economic Paleontologists and Mineralogists, Short Course, 2, 81-102.
- HILTON, V.C. 1995. Sandstone architecture and facies from the Annot Basin of the Tertiary SW Alpine foreland basin, SE France. In: *Atlas of deep water environments: Architectural style of turbidite systems: Pickering, K.T. ; Hiscott, R.N. ; Kenyon, N.H. ; Ricci Luchi, F. & Smith, R.D.A. eds Chapman & Hall, London : 227-235.*
- HOMWOOD, P.W., MAURIAUD, P. & LAFONT, F. 1999. Best practices in Sequences Stratigraphy for explorationists and reservoir engineers. *Bulletin du Centre de Recherche Elf Exploration Production, Mémoire*, 25, 81p.
- IVALDI, J.P. 1974. Origine du matériel détritique des séries "Grès d'Annot" d'après les données de la thermoluminescence (TLN et TLA). *Géol. Alpine*, 50 : 75-98.
- JEAN, S. 1985. Les Grès d'Annot au NW du massif de l'Argentera Mercantour. *Thèse Grenoble*.

- JEAN, S., KERCKHOVE, C., PERRIAUX, J., & RAVENNE, C. 1985. Un modèle paléogène de bassin à turbidites : les Grès d'Annot du NW du Massif de l'Argentera-Mercantour, *Géologie Alpine*, 61, 115-143.
- JOSEPH, P. & LOMAS, S.A. 2004. Deep-Water Sedimentation in the Alpine Foreland Basin of SE France: New perspectives on the Grès d'Annot and related systems – an introduction. In : Joseph P. & Lomas S.A. (eds). *Deep-Water Sedimentation in the Alpine Basin of SE France: New perspectives on the Grès d'Annot and related systems*, Geological Society, London, Special Publications, 221, p. 1-16.
- JOSEPH, P. & RAVENNE, C. 2001. Overview of the Grès d'Annot Basin. Guide Book for the Field Excursion of the Research Meeting “*Turbidite Sedimentation in Confined Systems*” held in Nice, 10-15 September 2001, by Joseph, Lomas, Broucke, Clark, Gardiner, Guillocheau, McCaffrey, Ravenne, Robin and Stanbrook.
- JOSEPH, P., BABONNEAU, N., BOURGEOIS, A., COTTERET, G., ESCHARD, R., GARIN, B., GOMES DE SOUZA, O., GRANJEON, D., GUILLOCHEAU, F., LERAT, O., QUEMENER, J.M. & RAVENNE, C. 2000. The Annot Sandstone outcrops (French Alps): architecture description as input for quantification and 3D reservoir modeling. In: Weimer, P., Slatt, R.M., Coleman, J., Rosen, N.C., Nelson, H., Bouma, A.H., Styzen, M.J. & Lawrence, D.T. (eds). *Deep-Water Reservoirs of the World: Proceedings of the GCSSEPM Foundation 20<sup>th</sup> Annual Research Conference*, December 3-6, 2000, Houston, Texas, SEPM CD-ROM Sp. Publ., 28, 422-449.
- KERCKHOVE, C. 1969. La "zone du Flysch" dans les nappes de l'Embrunais - Ubaye (Alpes Occidentales). *Géol. Alpine*, 45: 5-204.
- KNELLER, B.C. 1995. Beyond the turbidite paradigm: Physical models for deposition of turbidites and their implications for reservoir prediction. *Characterization of Deep Marine Clastic Systems*, Geol. Soc. of London Spec. Paper, v. 94, pp. 29-46.
- KNELLER, B., EDWARDS, D., MCCAFFREY, W. & MOORE, R. 1991. Oblique reflection of turbidity currents. *Geology*, 14, 250-252.
- KNELLER, B.C. & MCCAFFREY, W.D. 1999. Depositional effects of flow nonuniformity and stratification within turbidity currents approaching a bounding slope: deflection, reflection, and facies variation. *Journal of Sedimentary Research*, 69, 980-991.
- KNELLER, B.C., BENNETT, S.J. & MCCAFFREY, W.D. 1997. Velocity and turbulence structure of density currents and internal solitary waves: potential sediment transport and the formation of wave ripples in deep water. *Sedimentary Geology*, 112, 235-250.
- KUENEN, P.H., FAURE-MURET, A., LANTEAUME, M. & FALLOT, P. 1957. Observations sur les Flyschs des Alpes maritimes françaises et italiennes. *Bulletin de la Société Géologique de France*, (6) VII, 4-26.
- LABAUME, P., RITZ, J.F. & PHILIP, H. 1989. Failles normales récentes dans les Alpes sud-occidentales : leurs relations avec la tectonique compressive. *C.R. Acad. Sci. Paris*, t. 308, Série II, p. 1553-1560.
- LANTEAUME, M., BEAUDOIN, B. & CAMPREDON, R. 1967. Figures sédimentaires du Flysch "Grès d'Annot" du synclinal de Peira Cava. *CNRS ed.* : 99 p.
- LAPPARENT, A. F. 1938.-Études géologiques dans les régions provençales et alpines entre le Var et la Durance. *Bull. Serv. Carte Géol. Fr.*, n° 198, XL, p. 1-301.
- LAURENT, O., STEPHAN, J.F. & POPOFF, M. 2000. Modalités de la structuration miocène de la branche sud de l'arc de Castellane (chaînes subalpines méridionales). *Géologie de la France*, n° 3, p. 33-65.
- LAVAL, A., CREMER, M., BEGHIN, P. & RAVENNE, C. 1988. Density surges: two-dimensional experiments. *Sedimentology*, 35, 73-84.
- LIKORISCH W. H. & FORD M. 1998. Sequential restoration of the external Alpine Digne thrust system, SE France, constrained by kinematic data and synorogenic sediments. *Cenozoic Foreland Basins of Western Europe*. Ed. A. Mascle, C. Puigdefabregas, H. P. Luterbacher & M. Fernandez. *Geol. Soc. Spec. Publ.* 134. p. 189-211.
- LOWE, D.R. 1982. Sediment gravity flows: II. depositional models with special reference to the deposits of high-density turbidity currents. *Journal of Sedimentary Petrology*, 52, 279-297.
- MARTINI, E. 1971. Standard Tertiary and Quaternary calcareous nannoplankton zonation. *Proc. 6<sup>th</sup> Congr. Cof. Roma* 1970, 2:739-785.
- MCCAFFREY, W.D. & KNELLER, B.C. 2004. Scale effects of non-uniformity on deposition from turbidity currents with reference to the Grès d'Annot of SE France. In : Joseph P. & Lomas S.A. (eds). *Deep-Water Sedimentation in the Alpine Basin of SE France: New Perspectives on the Grès d'Annot and Related Systems*, Geological Society, London, Special Publications, 221, p. 301-310.
- MCPHERSON, J. G., SHANMUGAM, G. & MOIOLA, R. J. 1988. Fan deltas and braid deltas : conceptual problems. *Fan Deltas : Sedimentology and tectonic settings*. Ed. W. Nemec & R. J. Steel. *Blackie, Glasgow*. p. 14-22.
- MIDDLETON, G.V. & HAMPTON, M.A. 1973. Sediment gravity flows: mechanics of flow and deposition. In: G.V. Middleton & A.H. Bouma (eds.), *Turbidites and Deep-Water Sedimentation*, *Pacific. Section Soc. Econ. Paleont. Mineral.*, p.1-38.
- MITCHUM, JR., R.M. & VAN WAGONER, J.C. 1991. High-frequency sequences and their stacking patterns: sequence-stratigraphic evidence of high-frequency eustatic cycles. *Sedimentary Geology*, 70, 131-160.
- MONTENAT, C., LEYRIT, H., GILLOT, P.Y., JANIN, M.-C. & BARRIER, P. 1999. Extension du volcanisme oligocène de l'arc de Castellane. *Géologie de la France*, 1 : 43-48.
- MORAES, M.A.S., BECKER, M.R., MONTEIRO, M.C. & NETTO, S.L.A. 2000. Using outcrop analogs to improve 3D heterogeneity modeling of Brazilian sand-rich turbidite reservoirs. In: Weimer, P., Slatt, R.M., Coleman, J., Rosen, N.C., Nelson, H., Bouma, A.H., Styzen, M.J. & Lawrence, D.T. (eds). *Deep-Water Reservoirs of the*



- World: GCSSEPM Foundation 20<sup>th</sup> Annual Research Conference, December 3-6, 2000, Houston, Texas, SEPM CD-ROM Sp. Publ., 28, 587-605
- MORAES, M.A.S., BLASKOVSKI, P.R. & JOSEPH, P., 2004. The Grès d'Annot as an analog for Brazilian Cretaceous sandstone reservoirs: comparing convergent to passive-margin confined turbidites. In : Joseph P. & Lomas S.A.(eds). " *Deep-Water Sedimentation in the Alpine Basin of SE France: New perspectives on the Grès d'Annot and related systems* ", Geological Society, London, Special Publications, 221, p. 419-437.
- MULDER, T. & ALEXANDER, J. 2001. The physical character of subaqueous sedimentary density flows and their deposits. *Sedimentology*, 48, p. 269-299.
- MULDER, T. & SYVITSKI, J. P. M. 1995. Turbidity currents generated at river mouths during exceptional discharges to the world oceans. *Journal of Geology*, 103, 285-299.
- MUTTI, E. 1992. *Turbidites sandstones*. Agip - Istituto di Geologia, Università di Parma, Italy, 275 p.
- MUTTI, E. & NORMARK, W.L. 1987. Comparing examples of modern and ancient turbidite systems: problems and concepts. In: J.K. Legget & G.G. Zuffa (eds.), *Marine Clastic Sedimentology: Concepts and Case Studies*, Graham and Trotman, London, p.1-37.
- MUTTI, E., DAVOLI, G., TINTERRI, R. & ZAVALA, C. 1996. The importance of ancient fluvio-deltaic systems dominated by catastrophic flooding in tectonically active basins, *Memorie di Scienze Geologiche*, Padova, 48, p. 233 - 291.
- MUTTI, E., TINTERRI, R., REMACHA, E., MAVILLA, N., ANGELLA, S & FAVA, L. 1999. An introduction to the analysis of ancient turbidite basins from outcrop perspective. *AAPG Continuing Education Course Notes Series #39, American Association of Petroleum Geologists*, Tulsa, 61 p.
- MUTTI, E., TINTERRI, R., BENEVELLI, G., DI BIASE, D. & CAVANNA, G. 2003. Deltaic, mixed and turbidite sedimentation of ancient foreland basins. *Marine and Petroleum Geology*, 20, 733-755.
- NEMEC, W. & STEEL R. J. 1988. What is a fan delta and how do we recognize it ?. Fan Deltas : Sedimentology and tectonic settings. Ed. W. Nemec & R. J. Steel. *Blackie, Glasgow*. p. 1-13.
- PAIRIS, J.L. 1971. Tectonique et sédimentation tertiaire sur la marge orientale du bassin de Barrême. *Géologie Alpine*, 47, 203-214.
- PAIRIS, J. L. 1988. Paléogène marin et structuration des Alpes occidentales Françaises (domaine externe et confins sud-occidentaux du subbriançonnais). Thèse Doct. ès-Sci. Université Joseph Fournier, Grenoble.
- PANTIN, M.H. & LEEDER, M.R. 1987. Reverse flow in turbidity currents: the role of internal solitons. *Sedimentology*, 34, 1143-1155.
- PEMBERTON, S.G., McEACHERN, J.A. & FREY, R.W. 1992. Trace fossil facies models: environmental and allostratigraphic significance. In: Walker, R.G. & James, N.P. (eds) *Facies models: response to sea level change*. Geological Association of Canada, 47-72.
- PICKERING, K.T. & HILTON, V.C. 1998. *Turbidite systems of Southeast France*, Vallis Press, London, 229 p.
- PICKERING, K.T. & HISCOTT, R.N. 1985. Contained (reflected) turbidity currents from the Middle Ordovician Cloridorme Formation, Quebec, Canada: an alternative to the antidune hypothesis. *Sedimentology*, 32, 373-394.
- PLINK-BJÖRKLUND, P. & STEEL, R.J. 2002. Sea-level fall below the shelf edge, without basin floor fans. *Geology*, 30, 1115-1118.
- PLINK-BJÖRKLUND, P., MELLERE, D. & STEEL, R.J. 2001. Turbidite variability and architecture of sand-prone, deep-water slopes: Eocene clinoforms in the Central Basin, Spitsbergen. *Journal of Sedimentary Research*, 71, 895-912.
- POSAMENTIER, H. W., ALLEN, G. P., JAMES, D. P. & TESSON M. 1992. Forced regression in a sequence stratigraphic framework : Concepts, examples; and exploration significance. *Bull. AAPG*, vol. 76. p. 1687-1709.
- POSAMENTIER, H. W. & ALLEN, G. P. 1993. Siliciclastic sequence stratigraphic patterns in foreland ramp-type basin. *Geology*, vol. 21. p. 455-458.
- POSTMA, G. 1990. Depositional architecture and facies of river and fan-deltas: a synthesis. Coarse-Grained deltas. Ed. A. Colella & D. B. Prior. *Spec. Publs. int. Ass. Sediment*, 10, p.13-27.
- PRATHER, B.E., BOOTH, J.R., STEFFENS, G.S. & CRAIG, P.A. 1998. Classification, lithologic calibration, and stratigraphic succession of seismic facies of intraslope basins, deep-water Gulf of Mexico. *AAPG Bulletin*, 82, 701-728.
- PRAVE, A.R. & DUKE, W.L. 1990. Small-scale hummocky cross-stratification in turbidites: a form of antidune stratification? *Sedimentology*, 37, 531-539.
- PUIGDEFÀBREGAS, C., GJELBERG, J. & VAKSDAL, M. 2004. The Grès d'Annot in the Annot syncline: outer basin-margin onlap and associated soft-sediment deformation. In : Joseph P. & Lomas S.A. (eds). *Deep-Water Sedimentation in the Alpine Basin of SE France: New Perspectives on the Grès d'Annot and Related Systems*, Geological Society, London, Special Publications, 221, p. 367-388.
- RAVENNE, C., VIALLY, R., RICHE, P. & TRÉMOLIÈRES, P. 1987. Sédimentation et tectonique dans le bassin marin Eocène supérieur-Oligocène des Alpes du Sud, *Revue de l'IFP*, 42, 5, 529-553.
- READING, H.G. & RICHARDS, M. 1994. Turbidite Systems in Deep-Water Basin Margins Classified by Grain Size and Feeder System, *AAPG Bulletin*, 78, 5, 792-822.
- RITZ, J.F. 1991. Évolution du champ de contraintes dans les Alpes du Sud depuis la fin de l'Oligocène. Implications sismotectoniques. Thèse de doctorat de l'Université de Montpellier II, France.
- SALLES, L. 2010. Contrôles structuraux en 3 dimensions de la sédimentation turbiditique dans les chaînes plissées : exemple des Grès d'Annot (Sud Est de la France). Thèse de doctorat de l'Institut National Polytechnique de Lorraine, Nancy, France, 226 p.

- SALLES, L., FORD, M., JOSEPH, P., LE CARLIER DE VESLUD, C. & LE SOLLEUZ, A. (in revision). Progressive migration of a synclinal depocentre from turbidite growth strata: the Annot syncline, SE France. *Bull. Soc. Geol. France*.
- SCHLAGER, W. 1993. Accommodation and supply – a dual control on stratigraphic sequences. *Sedimentary Geology*, 86, 111-136.
- SERANNE, M. 1999. The Gulf of Lion continental margin (NW Mediterranean) revisited by IBS: An overview. In: Durand, B., Jolivet, L., Horvath, F. & Séranne, M. (eds) *The Mediterranean Basins: Tertiary Extension within the Alpine Orogen*. Geological Society, London, Special Publication, 156, 15-36.
- SERRA-KIEL, J., HOTTINGER, L., CAUS, E., DROBNE, K., FERRANDEZ, C., JAUHRI, A. K., LESS, G., PAVLOVEC, R., PIGNATTI, J., SAMSO, J. M., SCHAUB, H., SIREL, E., STROUGO, A., TAMBAREAU, Y., TOSQUELLA, J. & ZAKREVSKEYA, E. 1998. Larger foraminiferal biostratigraphy of the Tethyan Paleocene and Eocene. *Bull. Soc. Géol. de France*, t. 169, n°2. p.281-299.
- SHANMUGAN, G. 2000. 50 Years of the Turbidite Paradigm (1950s-1990s) : Deep-Water Processes and Facies Models – A Critical Perspective. *Mar. Petr. Geol.*, v.17, p.285-342.
- SINCLAIR, H.D. 1993. High resolution stratigraphy and facies differentiation of the shallow marine Annot Sandstones of SE France. *Sedimentology*, 40, 955-978.
- SINCLAIR, H.D. 1994. The influence of lateral basin slopes on turbidite sedimentation in the Annot Sandstones of SE France. *Journal of Sedimentary Research*, A64, 42-54.
- SINCLAIR, H.D. 1997. Tectonostratigraphic model for underfilled peripheral foreland basins: an Alpine perspective, *Geological Society of America Bulletin*, 109, 324-346.
- SINCLAIR, H.D. 2000. Delta-fed turbidites infilling topographically complex basins: a new depositional model for the Annot Sandstones, SE France, *Journal of Sedimentary Research*, 70, 3, 504-519.
- SMITH, R. & JOSEPH, P. 2004. Onlap stratal architectures in the Grès d'Annot: geometric models and controlling factors. In : Joseph P. & Lomas S.A. (eds). *Deep-Water Sedimentation in the Alpine Basin of SE France: New Perspectives on the Grès d'Annot and Related Systems*, Geological Society, London, Special Publications, 221, p. 389-399.
- STANLEY, D.J. 1961. Etudes sédimentologiques des Grès d'Annot et de leurs équivalents latéraux. *Thèse d'état Grenoble*, 1 vol. : 158 p. *Revue de l'IFP*, XVI, n°11. p. 1231-1254.
- STANLEY, D.J. 1975. Submarine canyon and slope sedimentation (Grès d'Annot) in the French Maritime Alps, *Proc. IX Intern. Cong. Sediment.*, Nice, 129 p.
- STANLEY, D.J. 1980. The Saint-Antonin conglomerate in the Maritime Alps: A model for coarse sedimentation on a submarine slope. *Smithsonian Contr. Marine Sciences*, 5, 25 p.
- STANLEY, D.J., PALMER, H.D. & DILL, R.F. 1978. Coarse sediment transport by mass flow and turbidity current processes and processes and down slope transformation in Annot Sandstone canyon-fan valley system. In: Sedimentation in submarine canyons, fans & trenches: Stanley & Kelling eds : 359 p.
- STOW, D.A.V. & SHANMUGAM, G. 1980. Sequence of structures in fine-grained turbidites; comparison of recent deep-sea and ancient flysch sediments. *Sedimentary Geology*, 25, 23-42.
- SZTRAKOS, K. & DU FORNEL, E. 2003. Stratigraphie, paléoécologie et foraminifères du paléogène des Alpes Maritimes et des Alpes de Haute-Provence (Sud-Est de la France). *Revue de micropaléontologie*, 46, 229-267.
- TERMIER, P. 1895. Sur les fossiles oligocènes de Barrême. In Depéret. Note sur les fossiles oligocènes de Barrême. *Bull. Soc. géol. de France*, (3), t. XXIII, p. 883-884.
- TOMASSO, M. & SINCLAIR, H.D. 2004. Deep-water sedimentation on an evolving fault-block: the Braux and St Benoît outcrops of the Grès d'Annot. In : Joseph P. & Lomas S.A. (eds). *Deep-Water Sedimentation in the Alpine Basin of SE France: New Perspectives on the Grès d'Annot and Related Systems*, Geological Society, London, Special Publications, 221, p. 267-283.
- TOURNOUER 1872. Note sur les fossiles tertiaires des Basses-Alpes recueillis par Mr Garnier. *Bull. Soc. Geol. Fr.*, (2), t. XXIX. p. 492-529.
- VANZON, F. 1973. Les modalités de la transgression nummulitique au synclinal de Blieux. Rapport d'option Géologie Générale. ENSMP, Paris.
- VON BLANCKENBURG, F. & DAVIES, J.H. 1995. Slab breakoff : a model for syncollisional magmatism and tectonics in the Alps. *Tectonics*, 14, 120-131. Weimer, P., Slatt, R.M., Coleman, J., Rosen, N.C., Nelson, H., Bouma, A.H., Styzen, M.J. & Lawrence, D.T. (eds). 2000. Deep-Water Reservoirs of the World: GCSSEPM Foundation 20<sup>th</sup> Annual Research Conference, December 3-6, 2000, Houston, Texas, SEPM CD-ROM Sp. Publ., 28.
- YAGISHITA, K. 1994. Antidunes and traction-carpet deposits in deep-water channel sandstones, Cretaceous, British Columbia, Canada. *Journal of Sedimentary Research*, A64, 34-41.
- ZURCHER, P. 1895. Compte rendu de la course du 24 septembre : de Barrême à Blieux et à Castellane. *Bull. Serv. C. G. F.*, Série 3, t. XXIII. p. 902-951.